Supporting Information

Expanding the Reactivity of Rosenthal's Reagent to Cyclopropenes and Allenes

*Marcel Eilers, Dennis Geik, Marc Schmidtmann, Sven Doye, Rüdiger Beckhaus**

Institut für Chemie, Carl von Ossietzky Universität Oldenburg, D-26111 Oldenburg, Germany

Table of Content

Experimental Section

General Considerations

Caution! Extreme care should be taken both in the handling of the cryogen liquid nitrogen and its use in the Schlenk line trap to avoid the condensation of oxygen from air. Reactions containing titanium complexes were performed under a dry oxygen-free nitrogen or argon atmosphere with rigorous exclusion of oxygen and moisture using standard Schlenk and glovebox techniques (< 0.5 ppm O_2, < 0.05 ppm H_2O). The glass equipment was stored in an oven at 120 °C, then evacuated and purged prior to use. Complex **1**,[1] methylcyclopropenes,[2] and allenes (**c-g**, **j-p**, **r**, **s** and **t**)[3] were prepared according to published procedures. Allenes **b** and **l**, and EtMgBr, were purchased from commercial suppliers. Silica gel from Grace (particle size = 40-63 µm) was used for flash chromatography. Silica gel 60 sheets with fluorescent indicator (254 nm) from Merck were used for thin layer chromatography; substances were detected with UV light. Solvents used exclusively in reactions under an inert atmosphere were dried according to standard procedures using a Na/K alloy and benzophenone as an indicator. They were then distilled and stored under a nitrogen atmosphere. Solid materials used in these reactions were dried under high vacuum prior to use. NMR spectra were recorded on a Bruker AVANCE III RMN 1Bay 500 MHz spectrometer or a JEOL JNM-ECZL 500 MHz spectrometer (^{1}H 500 MHz; ^{13}C 126 MHz; ^{19}F 470 MHz; ^{29}Si 99 MHz). ^{1}H NMR spectra are referenced to the residue solvent signals (^{1}H = 7.26 ppm for $CDCl_3$ and ^{1}H = 7.16 ppm for C_6D_6). ^{13}C NMR spectra are referenced to the central line of the solvent signal ($^{13}C\{^1H\}$ = 77.16 ppm for $CDCl_3$ and $^{13}C\{^1H\}$ = 128.06 ppm for C_6D_6). ^{19}F NMR spectra are referenced to the external standard ($^{19}F\{^1H\}$ = 0.00 ppm for $CFCl_3$). ^{29}Si NMR spectra are referenced to the external standard ($^{29}Si\{^1H\}$ = 0.00 ppm for $SiMe_4$). Absolute values of the coupling constants (δ) are provided in Hertz (Hz). Multiplicities of peaks are abbreviated as single (s), double (d), triplet (t) or multiplet (m). IR spectra were recorded on a Shimadzu IRSpirit QATR-S spectrometer or on a Bruker Tensor 27 spectrometer using the attenuated total reflection (ATR) method. Melting points were determined using a Mettler Toledo MP30. The samples were prepared in a glovebox, prior sealed with silicon grease and then fused before measurement. MS analyses were performed on a Thermo Scientific DFS (EI, 70 eV), Waters Q-TOF Premier (ESI^+, TOF), or Shimadzu GCMS-QP2020 (EI, 70 eV). High-resolution mass spectra were measured on a Thermo Fisher Scientific DFS™ Magnetic Sector HRMS System spectrometer (EI, 70 eV). Elemental analysis was performed on a Euro EA 3000 Elemental Analyzer. Because of the high sensitivity to moisture and air, sample preparation was performed in a glovebox. For this purpose, 0.5-2.5 mg of the samples together with a small amount of vanadium pentoxide as combustion aid were weighed into tin capsules before sealing and quickly measured in triplicate. Deviations in C and H values are due to the sensitivity of the compounds and possible incomplete combustion of titanium carbide.

Synthesis of 4,4'-(Penta-3,4-diene-1,1-diyl)bis(fluorobenzene) (h)

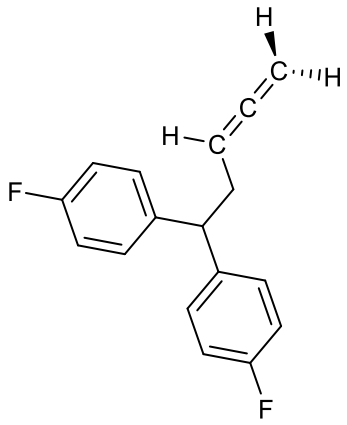

Under an atmosphere of argon, an oven-dried Schlenk flask was charged with 4,4'-(2-(2,2-dibromocyclopropyl)ethane-1,1-diyl)bis(fluorobenzene) (15.12 g, 36.33 mmol) and dry THF (40 mL). The solution was cooled to 0 °C with an ice bath and ethylmagnesium bromide (3.0 M in Et_2O, 18.2 mL, 54.50 mmol) was added slowly via a syringe through the septum under vigorous stirring. The reaction mixture was then allowed to warm to room temperature for 2 h, carefully quenched with aqueous HCl (1 M, 10 mL), diluted with water (10 mL) and extracted with Et_2O (3 x 60 mL). The combined organic layers were washed with brine (50 mL), dried with $MgSO_4$ and concentrated under reduced pressure. Flash chromatography (silica gel, hexane) afforded a colorless liquid of compound **h**.

Yield: 7.08 g (27.62 mmol, 76%).
IR (ATR): $\tilde{\nu}$ = 3042, 2918, 1956, 1603, 1505, 1443, 1415, 1299, 1220, 1157, 1100, 1015, 823, 787, 745, 716, 700, 668, 639, 565, 525, 496 cm^{-1}.
^{1}H NMR (500 MHz, $CDCl_3$): δ = 2.74 (tt, *J* = 7.9 Hz, 2.9 Hz, 2 H), 4.06 (t, *J* = 7.9 Hz, 1 H), 4.61 (dt, *J* = 6.2 Hz, 2.9 Hz, 2 H), 4.98-5.07 (m, 1 H), 6.97-7.03 (m, 4 H), 7.17-7.23 (m, 4 H) ppm.
^{13}C{^{1}H} NMR (125 MHz, DEPT, $CDCl_3$): δ = 35.0 (CH_2), 49.7 (CH), 75.1 (CH_2), 88.0 (CH), 115.4 (d, *J* = 21.2 Hz, CH), 129.5 (d, *J* = 7.9 Hz, CH), 140.0 (d, *J* = 3.3 Hz, C), 161.6 (d, *J* = 244.8 Hz, C), 209.4 (C) ppm.
^{19}F NMR (470 MHz, $CDCl_3$): δ = –116.7 ppm.
MS / HRMS (EI, 70 eV): In the determination of the molecular mass of the allene, only the trimerization product was detected.

Synthesis of 5-Vinylidene-10,11-dihydro-5*H*-dibenzo[*a*,*d*][*7*]annulene (q)

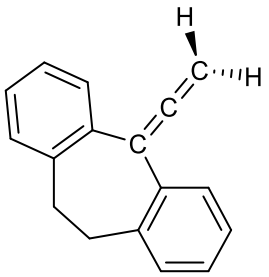

Under an atmosphere of argon, an oven-dried Schlenk flask was charged with 2,2-dibromo-10',11'-dihydrospiro[cyclopropane-1,5'-dibenzo[a,d][7]annulene] (11.60 g, 30.68 mmol) and dry THF (35 mL). The solution was cooled to 0 °C with an ice bath and ethylmagnesium bromide (3.0 M in Et_2O, 15.4 mL, 46.02 mmol) was added slowly via a syringe through the septum under vigorous stirring. The reaction mixture was then allowed to warm to room temperature for 2 h, carefully quenched with aqueous HCl (1 M, 10 mL), diluted with water (10 mL) and extracted with Et_2O (3 x 50 mL). The combined organic layers were washed with brine (50 mL), dried with $MgSO_4$ and concentrated under reduced pressure. Flash chromatography (silica gel, hexane) afforded a colorless liquid of compound **q**.

Yield: 5.97 g (27.34 mmol, 89%).

IR (ATR): $\tilde{\nu}$ = 3059, 3029, 2996, 2955, 2927, 2892, 2867, 1922, 1804, 1602, 1570, 1486, 1456, 1444, 1424, 1384, 1370, 1359, 1309, 1282, 1246, 1207, 1147, 1107, 1092, 1076, 1053, 1037, 1029, 1006, 973, 944, 926, 907, 897, 866, 852, 816, 769, 750, 736, 714, 674, 633, 589, 566, 536, 504, 482 cm^{-1}.

^{1}H NMR (500 MHz, $CDCl_3$): δ = 3.21 (s, 4 H), 5.21 (s, 2 H), 7.16-7.23 (m, 6 H), 7.44-7.51 (m, 2 H) ppm.

^{13}C{^{1}H} NMR (125 MHz, DEPT, $CDCl_3$): δ = 33.9 (CH_2), 76.2 (CH_2), 109.8 (C),126.3 (CH), 127.6 (CH), 129.4 (CH), 129.5 (CH), 135.7 (C), 139.5 (C), 211.4 (C) ppm.

MS (EI, 70 eV) m/z (%) = 218 (100) $[M]^+$, 203 (44), 202 (58), 84 (12).

HRMS (EI, 70 eV) calculated for $C_{17}H_{14}$: m/z = 218.1090; measured: m/z = 218.1087.

Synthesis of 2a

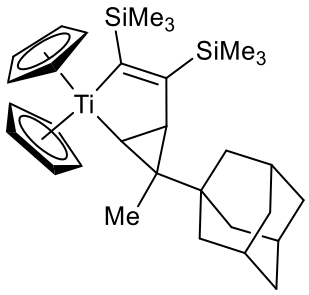

Complex **1** (139 mg, 0.400 mmol, 1.00 equiv.) was dissolved in 5 mL of *n*-hexane and then treated with 1-(1-methylcycloprop-2-en-1-yl)adamantane (75 mg, 0.400 mmol, 1.00 equiv.) at ambient temperature. An immediate color change of the solution from yellow to purple and the formation of a purple solid after a few minutes was observed. The reaction mixture was stirred for 1 h at ambient temperature. Afterwards, the mother liquor was decanted, the residue washed with 3 mL of *n*-hexane and dried under vacuum to yield **2a** as a purple solid.

Yield: 154 mg (0.287 mmol, 72%).
Melting point: 120 °C (dec.).
IR (ATR): $\tilde{\nu}$ = 2970 (w), 2929 (w), 2889 (m), 2837 (w), 1446 (w), 1366 (w), 1357 (w), 1342 (w), 1310 (w), 1275 (w), 1256 (w), 1245 (m), 1105 (w), 1054 (w), 1019 (m), 852 (m), 831 (m), 803 (s), 748 (m), 688 (m), 660 (m), 632 (m), 616 (w) cm^{-1}.
^{1}H NMR (500 MHz, C_6D_6, 298 K): δ = 0.09 (s, 9 H, $Si(CH_3)_3$), 0.24 (s, 9 H, $Si(CH_3)_3$), 1.14 (d, *J* = 8.4 Hz, 1 H, CH), 1.29 (s, 3 H, CH_3), 1.42 (d, *J* = 8.4 Hz, 1 H, CH), 1.47-1.51 (m, 3 H, Ad–H), 1.57-1.67 (m, 6 H, Ad–H), 1.68-1.73 (m, 3 H, Ad–H), 1.96-2.00 (m, 3 H, Ad–H), 5.94 (s, 5 H, Cp–H), 5.97 (s, 5 H, Cp–H) ppm.
^{13}C{^{1}H} NMR (126 MHz, C_6D_6, 298 K): δ = 2.3 ($Si(CH_3)_3$), 4.9 ($Si(CH_3)_3$), 14.7 (CH_3), 29.6 (3 x Ad–CH), 32.5 (CH), 37.5 (Ad–C_q), 37.7 (3 x Ad–CH_2), 39.5 (3 x Ad–CH_2), 53.7 ($\underline{C}_q$–CH_3), 75.9 (CH), 112.1 (C_5H_5), 114.3 (C_5H_5), 159.8 ($\underline{C}_q$–$Si(CH_3)_3$), 231.5 ($\underline{C}_q$–$Si(CH_3)_3$) ppm.
^{29}Si{^{1}H} INEPT NMR (99 MHz, C_6D_6, 298 K): δ = –20.3 ($Si(CH_3)_3$), –14.4 ($Si(CH_3)_3$) ppm.
EA: Anal. calcd. for $C_{32}H_{48}Si_2Ti$: C, 71.60; H, 9.01; Found: C, 72.05; H, 9.46.
HR/MS (EI, 40 eV) calculated for $C_{32}H_{48}Si_2Ti$: m/z = 536.2769; measured: m/z = 536.2770.

Synthesis of 2b

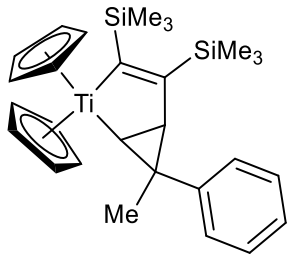

Complex **1** (139 mg, 0.400 mmol, 1.00 equiv.) was dissolved in 5 mL of *n*-hexane and then treated with (1-methylcycloprop-2-en-1-yl)benzene (52 mg, 0.400 mmol, 1.00 equiv.) at ambient temperature. An immediate color change of the solution from yellow to purple and the formation of a crystalline purple solid after a few minutes was observed. The reaction mixture was stirred for 1 h at ambient temperature. Afterwards, the mother liquor was decanted, the residue washed with 3 mL of *n*-hexane and dried under vacuum to yield **2b** as a purple crystalline solid.

Yield: 128 mg (0.267 mmol, 67%).

Melting point: 117 °C (dec.).

IR (ATR): $\tilde{\nu}$ = 3113 (w), 3016 (w), 2946 (w), 2894 (w), 1595 (w), 1495 (w), 1445 (w), 1370 (w), 1242 (m), 1019 (w), 964 (w), 856 (m), 837 (m), 804 (s), 746 (m), 697 (m), 680 (m), 661 (m), 629 (m), 609 (m), 556 (m) cm^{-1}.

^{1}H NMR (500 MHz, C_6D_6, 298 K): δ = 0.06 (s, 9 H, $Si(CH_3)_3$), 0.09 (s, 9 H, $Si(CH_3)_3$), 1.45 (d, *J* = 9.0 Hz, 1 H, CH), 1.65 (s, 3 H, CH_3), 1.73 (d, *J* = 9.0 Hz, 1 H, CH), 5.82 (s, 5 H, Cp–H), 5.90 (s, 5 H, Cp–H), 7.01-7.06 (m, 1 H, Ph–H), 7.12-7.15 (m, 2 H, Ph–H), 7.18-7.23 (m, 2 H, Ph–H) ppm.

^{13}C{^{1}H} NMR (126 MHz, C_6D_6, 298 K): δ = 1.8 ($Si(CH_3)_3$), 4.5 ($Si(CH_3)_3$), 18.1 (CH_3), 36.9 (CH), 47.8 ($\underline{C}_q$–CH_3), 84.4 (CH), 111.9 (C_5H_5), 114.1 (C_5H_5), 124.7 (Ph–CH), 124.8 (Ph–CH), 128.3 (Ph–CH), 151.8 (Ph–C_q), 155.0 ($\underline{C}_q$–$Si(CH_3)_3$), 231.3 ($\underline{C}_q$–$Si(CH_3)_3$) ppm.

^{29}Si{^{1}H} INEPT NMR (99 MHz, C_6D_6, 298 K): δ = –18.9 ($Si(CH_3)_3$), –12.3 ($Si(CH_3)_3$) ppm.

EA: Anal. calcd. for $C_{28}H_{38}Si_2Ti$: C, 70.26; H, 8.00; Found: C, 70.61; H, 8.65.

HR/MS (EI, 40 eV) calculated for $C_{28}H_{38}Si_2Ti$: m/z = 478.1986; measured: m/z = 478.1998.

Synthesis of 2c

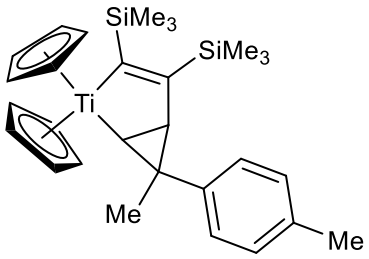

Complex **1** (500 mg, 1.435 mmol, 1.00 equiv.) was dissolved in 10 mL of *n*-hexane and then treated with 1-methyl-4-(1-methylcycloprop-2-en-1-yl)benzene (207 mg, 1.435 mmol, 1.00 equiv.) at ambient temperature. An immediate color change of the solution from yellow to purple and the formation of a crystalline purple solid after a few minutes was observed. The reaction mixture was stirred for 1 h at ambient temperature. Afterwards, the mother liquor was decanted, the residue washed with 3 mL of *n*-hexane and dried under vacuum to yield **2c** as a purple crystalline solid.

Yield: 613 mg (1.244 mmol, 87%).

Melting point: 116 °C (dec.).

IR (ATR): $\tilde{\nu}$ = 2929 (w), 2894 (w), 1510 (m), 1445 (w), 1244 (m), 1018 (m), 855 (m), 834 (m), 803 (s), 770 (m), 746 (m), 678 (m), 663 (m), 628 (m), 611 (m), 589 (m), 547 (m), 526 (m), 468 (m), 453 (m), 415 (m) cm^{-1}.

^{1}H NMR (500 MHz, C_6D_6, 298 K): δ = 0.10 (s, 9 H, $Si(CH_3)_3$), 0.14 (s, 9 H, $Si(CH_3)_3$), 1.54 (d, *J* = 8.9 Hz, 1 H, CH), 1.70 (s, 3 H, CH_3), 1.77 (d, *J* = 8.9 Hz, 1 H, CH), 2.19 (s, 3 H, CH_3), 5.86 (s, 5 H, Cp–H), 5.94 (s, 5 H, Cp–H), 7.08-7.11 (m, 2 H, Ph–H), 7.13-7.16 (m, 2 H, Ph–H) ppm.

^{13}C{^{1}H} NMR (126 MHz, C_6D_6, 298 K): δ = 1.8 ($Si(CH_3)_3$), 4.5 ($Si(CH_3)_3$), 18.1 (CH_3), 20.9 (Ph–CH_3), 36.8 (CH), 47.8 ($\underline{C}_q$–CH_3), 84.5 (CH), 111.9 (C_5H_5), 114.1 (C_5H_5), 124.7 (Ph–CH), 129.0 (Ph–CH), 133.8 (Ph–C_q), 149.0 (Ph–C_q), 154.9 ($\underline{C}_q$–$Si(CH_3)_3$), 231.0 ($\underline{C}_q$–$Si(CH_3)_3$) ppm.

^{29}Si{^{1}H} INEPT NMR (99 MHz, C_6D_6, 298 K): δ = –18.4 ($Si(CH_3)_3$), –11.8 ($Si(CH_3)_3$) ppm.

EA: Anal. calcd. for $C_{30}H_{44}Si_2Ti$: C, 70.83; H, 8.72; Found: C, 70.74; H, 8.61.

HR/MS (EI, 70 eV) calculated for $C_{29}H_{40}Si_2Ti$: m/z = 492.2143; measured: m/z = 492.2138.

Synthesis of 2d

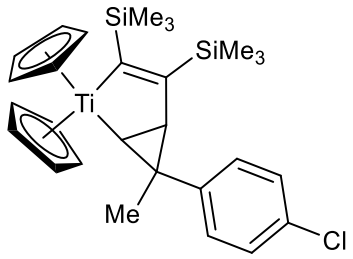

Complex **1** (500 mg, 1.435 mmol, 1.00 equiv.) was dissolved in 10 mL of *n*-hexane and then treated with 1-chloro-4-(1-methylcycloprop-2-en-1-yl)benzene (236 mg, 1.435 mmol, 1.00 equiv.) at ambient temperature. An immediate color change of the solution from yellow to purple and the formation of a purple crystalline solid after a few minutes was observed. The reaction mixture was stirred for 1 h at ambient temperature. Afterwards, the mother liquor was decanted, the residue washed with 3 mL of *n*-hexane and dried under vacuum to yield **2d** as a purple crystalline solid.

Yield: 619 mg (1.206 mmol, 84%).

Melting point: 128 °C (dec.).

IR (ATR): $\tilde{\nu}$ = 2948 (w), 2892 (w), 1489 (m), 1463 (w), 1446 (w), 1401 (m), 1243 (m), 1094 (w), 1018 (w), 1005 (w), 968 (w), 856 (m), 835 (m), 803 (s), 745 (m), 680 (m), 662 (m), 628 (m), 610 (m), 570 (w) cm^{-1}.

^{1}H NMR (500 MHz, C_6D_6, 298 K): δ = 0.08 (s, 9 H, $Si(CH_3)_3$), 0.10 (s, 9 H, $Si(CH_3)_3$), 1.30 (d, *J* = 8.9 Hz, 1 H, CH), 1.56 (s, 3 H, CH_3), 1.62 (d, *J* = 8.9 Hz, 1 H, CH), 5.84 (s, 5 H, Cp–H), 5.91 (s, 5 H, Cp–H), 6.88-6.92 (m, 2 H, Ph–H), 7.20-7.23 (m, 2 H, Ph–H) ppm.

^{13}C{^{1}H} NMR (126 MHz, C_6D_6, 298 K): δ = 1.7 ($Si(CH_3)_3$), 4.5 ($Si(CH_3)_3$), 17.7 (CH_3), 37.3 (CH), 46.7 ($\underline{C}_q$–CH_3), 83.5 (CH), 112.0 (C_5H_5), 114.2 (C_5H_5), 117.9 (Ph–CH), 126.1 (Ph–CH), 130.3 (Ph–C_q), 150.5 (Ph–C_q), 154.7 ($\underline{C}_q$–$Si(CH_3)_3$), 232.0 ($\underline{C}_q$–$Si(CH_3)_3$) ppm.

^{29}Si{^{1}H} INEPT NMR (99 MHz, C_6D_6, 298 K): δ = –18.3 ($Si(CH_3)_3$), –11.7 ($Si(CH_3)_3$) ppm.

EA: Anal. calcd. for $C_{29}H_{41}ClSi_2Ti$: C, 65.83; H, 7.81; Found: C, 66.01; H, 8.15.

HR/MS (EI, 70 eV) calculated for $C_{28}H_{37}ClSi_2Ti$: m/z = 512.1596; measured: m/z = 512.1601.

Synthesis of 3a

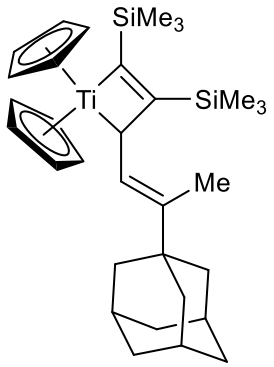

A solution of complex **2a** in benzene-d_6 was heated at 60°C for 24 h. The solution turned slightly orange during the heating process. **3a** was characterized through NMR experiments.

^{1}H NMR (500 MHz, C_6D_6, 298 K): δ = 0.29 (s, 9 H, $Si(CH_3)_3$), 0.36 (s, 9 H, $Si(CH_3)_3$), 1.66-1.73 (m, 6 H, Ad–H), 1.75 (s, 3 H, CH_3), 1.79-1.88 (m, 6 H, Ad–H), 2.00-2.04 (m, 3 H, Ad–H), 5.27 (s, 5 H, Cp–H), 5.32 (s, 5 H, Cp–H), 5.91 (d, *J* = 9.4 Hz, 1 H, CH), 6.07 (d, *J* = 9.4 Hz, 1 H, CH) ppm.

^{13}C{^{1}H} NMR (126 MHz, C_6D_6, 298 K): δ = 2.6 ($Si(CH_3)_3$), 3.1 ($Si(CH_3)_3$), 13.1 (CH_3), 29.4 (3 x Ad–CH), 37.5 (3 x Ad–CH_2, Ad–C_q), 42.2 (3 x Ad–CH_2), 107.0 ($\underline{C}_q$–$Si(CH_3)_3$), 108.0 (C_5H_5), 109.8 (C_5H_5), 123.8 (CH), 128.9 ($\underline{C}_q$–CH_3), 135.6 (CH), 250.9 ($\underline{C}_q$–$Si(CH_3)_3$) ppm.

^{29}Si{^{1}H} INEPT NMR (99 MHz, C_6D_6, 298 K): δ = –13.8 ($Si(CH_3)_3$), 1.1 ($Si(CH_3)_3$) ppm.

Synthesis of 3b

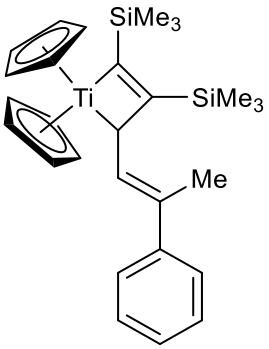

A solution of complex **2b** in benzene-d_6 was heated at 60°C for 24 h. The solution turned slightly orange during the heating process. **3b** was characterized through NMR experiments.

^{1}H NMR (500 MHz, C_6D_6, 298 K): δ = 0.23 (s, 9 H, $Si(CH_3)_3$), 0.33 (s, 9 H, $Si(CH_3)_3$), 2.13 (s, 3 H, CH_3), 5.29 (s, 5 H, Cp–H), 5.31 (s, 5 H, Cp–H), 6.14 (d, *J* = 10.0 Hz, 1 H, CH), 6.71 (d, *J* = 10.0 Hz, 1 H, CH), 7.06-7.11 (m, 1 H, Ph–H), 7.23-7.29 (m, 2 H, Ph–H), 7.56-7.59 (m, 2 H, Ph–H) ppm.

^{13}C{^{1}H} NMR (126 MHz, C_6D_6, 298 K): δ = 2.4 ($Si(CH_3)_3$), 3.1 ($Si(CH_3)_3$), 16.3 (CH_3), 105.7 ($\underline{C}_q$–$Si(CH_3)_3$), 108.4 (C_5H_5), 109.7 (C_5H_5), 119.4 ($\underline{C}_q$–CH_3), 121.7 (CH), 125.1 (Ph–CH), 125.6 (Ph–CH), 128.8 (Ph–CH), 142.3 (CH), 144.5 (Ph–C_q), 252.4 ($\underline{C}_q$–$Si(CH_3)_3$) ppm.

^{29}Si{^{1}H} INEPT NMR (99 MHz, C_6D_6, 298 K): δ = –13.7 ($Si(CH_3)_3$), 1.3 ($Si(CH_3)_3$) ppm.

Synthesis of 3c

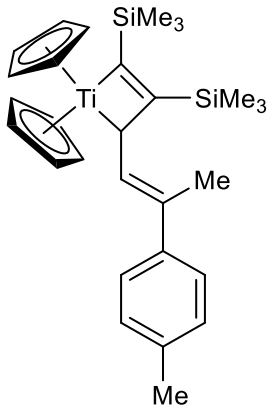

A solution of complex **2c** in benzene-d_6 was heated at 60°C for 24 h. The solution turned slightly orange during the heating process. **3c** was characterized through NMR experiments.

^{1}H NMR (500 MHz, C_6D_6, 298 K): δ = 0.25 (s, 9 H, $Si(CH_3)_3$), 0.33 (s, 9 H, $Si(CH_3)_3$), 2.16 (s, 3 H, CH_3), 2.20 (s, 3 H, Ph–CH_3), 5.31 (s, 5 H, Cp–H), 5.32 (s, 5 H, Cp–H), 6.18 (d, *J* = 10.1 Hz, 1 H, CH), 6.72 (d, *J* = 10.1 Hz, 1 H, CH), 7.09-7.12 (m, 2 H, Ph–H), 7.52-7.55 (m, 2 H, Ph–H) ppm.

^{13}C{^{1}H} NMR (126 MHz, C_6D_6, 298 K): δ = 2.4 ($Si(CH_3)_3$), 3.1 ($Si(CH_3)_3$), 16.3 (CH_3), 21.1 (Ph–CH_3), 105.8 ($\underline{C}_q$–$Si(CH_3)_3$), 108.3 (C_5H_5), 109.7 (C_5H_5), 119.4 ($\underline{C}_q$–CH_3), 122.1 (CH), 125.1 (Ph–CH), 129.5 (Ph–CH), 134.8 (Ph–C_q), 141.5 (CH), 141.7 (Ph–C_q), 252.2 ($\underline{C}_q$–$Si(CH_3)_3$) ppm.

^{29}Si{^{1}H} INEPT NMR (99 MHz, C_6D_6, 298 K): δ = –13.7 ($Si(CH_3)_3$), 1.4 ($Si(CH_3)_3$) ppm.

Synthesis of 3d

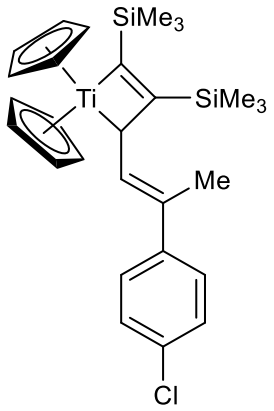

A solution of complex **2d** in benzene-d_6 was heated at 60°C for 24 h. The solution turned slightly orange during the heating process. **3d** was characterized through NMR experiments.

^{1}H NMR (500 MHz, C_6D_6, 298 K): δ = 0.21 (s, 9 H, $Si(CH_3)_3$), 0.32 (s, 9 H, $Si(CH_3)_3$), 2.00 (s, 3 H, CH_3), 5.27 (s, 5 H, Cp–H), 5.31 (s, 5 H, Cp–H), 6.06 (d, *J* = 10.1 Hz, 1 H, CH), 6.61 (d, *J* = 10.1 Hz, 1 H, CH), 7.19-7.22 (m, 2 H, Ph–H), 7.27-7.30 (m, 2 H, Ph–H) ppm.
^{13}C{^{1}H} NMR (126 MHz, C_6D_6, 298 K): δ = 2.3 ($Si(CH_3)_3$), 3.0 ($Si(CH_3)_3$), 16.0 (CH_3), 105.3 ($\underline{C}_q$–$Si(CH_3)_3$), 108.5 (C_5H_5), 109.7 (C_5H_5), 117.9 ($\underline{C}_q$–CH_3), 120.8 (CH), 126.1 (Ph–CH), 128.9 (Ph–CH), 131.1 (Ph–C_q), 142.8 (Ph–C_q), 142.9 (CH), 253.0 ($\underline{C}_q$–$Si(CH_3)_3$) ppm.
^{29}Si{^{1}H} INEPT NMR (99 MHz, C_6D_6, 298 K): δ = –13.1 ($Si(CH_3)_3$), 1.8 ($Si(CH_3)_3$) ppm.

Synthesis of 4c

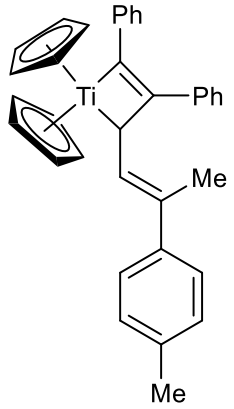

Complex **2c** (49.3 mg, 0.100 mmol, 1.00 equiv.) and diphenylacetylene (18 mg, 0.100 mmol, 1.00 equiv.) were dissolved in 5 mL of toluene and stirred at 60 °C overnight (16 h). A color change of the solution from pink over orange to green was observed. Afterwards, all volatile compounds were removed under reduced pressure, the residue washed with a small amount of *n*-hexane and dried under high vacuum to yield **4c** as a green solid.

Yield: 28 mg (0.056 mmol, 56%).
Melting point: 122 °C (dec.).
IR (ATR): $\tilde{\nu}$ = 3022 (w), 2963 (w), 2908 (w), 1591 (m), 1511 (m), 1489 (m), 1441 (m), 1261 (m), 1062 (m), 1018 (m), 841 (m), 806 (s), 777(s), 768 (s), 714 (s), 701 (s), 694 (s), 662 (m), 641 (m), 596 (m), 575 (m), 563 (m), 541 (m) cm^{-1}.
^{1}H NMR (500 MHz, C_6D_6, 298 K): δ = 1.96 (s, 3 H, CH_3), 2.15 (s, 3 H, Ph–CH_3), 5.47 (d, *J* = 9.7 Hz, 1 H, CH), 5.77 (s, 10 H, Cp–H), 6.83 (d, *J* = 9.7 Hz, 1 H, CH), 6.85-6.87 (m, 2 H, Ph–H), 6.92-6.96 (m, 2 H, Ph–H), 6.97-6.99 (m, 2 H, Ph–H), 7.03-7.06 (m, 2 H, Ph–H), 7.10-7.14 (m, 2 H, Ph–H), 7.25-7.28 (m, 2 H, Ph–H), 7.33-7.36 (m, 2 H, Ph–H) ppm.
^{13}C{^{1}H} NMR (126 MHz, C_6D_6, 298 K): δ = 16.5 (CH_3), 21.0 (Ph–CH_3), 88.2 (CH), 103.7 ($\underline{C}_q$–Ph), 113.7 (C_5H_5), 113.8 (C_5H_5), 121.1 ($\underline{C}_q$–CH_3), 124.8 (Ph–CH), 125.3 (Ph–CH), 126.3 (Ph–CH), 126.5 (Ph–CH), 128.4 (Ph–CH), 128.6 (Ph–CH), 129.3 (Ph–CH), 130.6 (Ph–CH), 134.7 (Ph–C_q), 137.8 (Ph–C_q), 141.6 (Ph–C_q), 141.9 (CH), 147.3 (Ph–C_q), 213.0 ($\underline{C}_q$–Ph) ppm.
HR/MS (EI, 70 eV) calculated for $C_{35}H_{32}Ti$: m/z = 500.1978; measured: m/z = 500.1967.

Synthesis of 4d

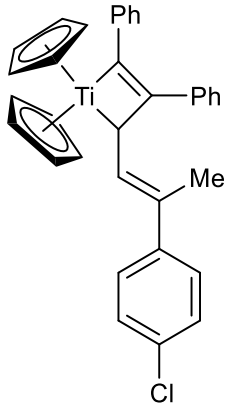

Complex **2d** (51.3 mg, 0.100 mmol, 1.00 equiv.) and diphenylacetylene (18 mg, 0.100 mmol, 1.00 equiv.) were dissolved in 5 mL of toluene and stirred at 60 °C overnight (16 h). A color change of the solution from pink over orange to green was observed. Afterwards, all volatile compounds were removed under reduced pressure, the residue washed with a small amount of *n*-hexane and dried under high vacuum to yield **4d** as a green solid.

Yield: 32 mg (0.061 mmol, 61%).
Melting point: 155 °C (dec.).
IR (ATR): $\tilde{\nu}$ = 3017 (w), 2924 (w), 1591 (m), 1548 (m), 1491 (m), 1475 (m), 1439 (m), 1403 (w), 1373 (w), 1144 (m), 1093 (m), 1069 (m), 1017 (m), 1008 (m), 930 (w), 840 (m), 810 (s), 787 (s), 771 (s), 766 (s), 704 (s), 697 (s), 640 (m), 591 (m), 534 (m) cm^{-1}.
^{1}H NMR (500 MHz, C_6D_6, 298 K): δ = 1.81 (s, 3 H, CH_3), 5.37 (d, *J* = 9.7 Hz, 1 H, CH), 5.75 (s, 10 H, Cp–H), 6.74 (d, *J* = 9.7 Hz, 1 H, CH), 6.84-6.87 (m, 2 H, Ph–H), 6.92-6.96 (m, 2 H, Ph–H), 7.03-7.06 (m, 2 H, Ph–H), 7.07-7.09 (m, 4 H, Ph–H), 7.11-7.14 (m, 2 H, Ph–H), 7.22-7.24 (m, 2 H, Ph–H) ppm.
^{13}C{^{1}H} NMR (126 MHz, C_6D_6, 298 K): δ = 16.1 (CH_3), 86.9 (CH), 103.2 ($\underline{C}_q$–Ph), 113.9 (C_5H_5), 119.8 ($\underline{C}_q$–CH_3), 125.0 (Ph–CH), 126.3 (Ph–CH), 126.3 (Ph–CH), 126.6 (Ph–CH), 128.6 (Ph–CH), 130.5 (Ph–CH), 131.0 (Ph–C_q), 137.6 (Ph–C_q), 142.6 (Ph–C_q), 143.4 (CH), 147.1 (Ph–C_q), 213.1 ($\underline{C}_q$–Ph) ppm.
HR/MS (EI, 70 eV) calculated for $C_{34}H_{29}Ti$: m/z = 520.1432; measured: m/z = 520.1435.

General Procedure for the Synthesis of Complexes 5

Complex **1** (139 mg, 0.400 mmol, 1.00 equiv.) was dissolved in 5 mL of *n*-hexane and then treated dropwise with the corresponding allene (0.820 mmol, 2.05 equiv.) via a syringe at ambient temperature. A distinct colour change of the reaction mixture from yellow to red and the formation of a red solid is observed. After stirring for 1 h at ambient temperature, the mother liquor was decanted, the residue washed with a small amount of *n*-hexane and the product dried under high vacuum.

Synthesis of 5a

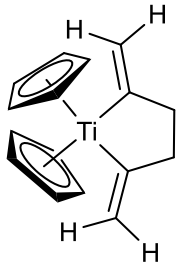

Following the general procedure using 1.33 mL of a toluene-solution of propa-1,3-diene (0.610 mol/L, 0.812 mmol, 2.03 equiv.), complex **5a** was obtained as a red solid.

Yield: 72 mg (0.279 mmol, 93%).

Melting point: 98 °C (dec.).

^{1}H NMR (500 MHz, C_6D_6, 305 K): δ = 2.48 (s, 4 H, CH_2-CH_2), 3.45 (s, 2 H, C=CH_2), 5.38 (s, 2 H, C=CH_2), 5.97 (s, 10 H, C_5H_5) ppm.

^{13}C{^{1}H} NMR (126 MHz, C_6D_6, 305 K): δ = 42.9 (*C*H_2-*C*H_2), 112.3 (C=*C*H_2), 115.6 (C_5H_5), 209.2 (Ti-C_q) ppm.

Synthesis of 5b and 5b'

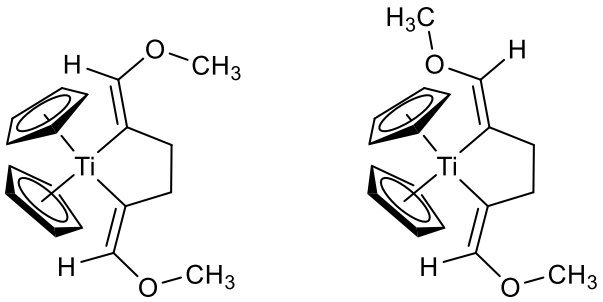

5b **5b'**

Following the general procedure, a mixture of complexes **5b** and **5b'** was obtained as a red-violet solid in a 5:1 ratio, as determined by integration of the corresponding signals in the NMR spectrum.

Yield: 102 mg (0.320 mmol, 80%).

Melting point: 127 °C (dec.).

^{1}H NMR (500 MHz, C_6D_6, 305 K, **5b**): δ = 2.76 (s, 4 H, CH_2-CH_2), 3.21 (s, 6 H, OCH_3), 3.95 (s, 2 H, C=C*H*), 6.00 (s, 10 H, C_5H_5) ppm.

^{13}C{^{1}H} NMR (126 MHz, C_6D_6, 305 K, **5b**): δ = 33.1 (*C*H_2-*C*H_2), 57.7 (O*C*H_3), 115.6 (*C*$_5$H$_5$), 138.9 (C=*C*H), 169.2 (Ti-*C*$_q$) ppm.

^{1}H NMR (500 MHz, C_6D_6, 305 K, **5b'**): δ = 2.33-2.37 (s, 2 H, CH_2-CH_2), δ = 2.77-2.80 (s, 2 H, CH_2-CH_2), 2.95 (s, 3 H, OCH_3), 3.23 (s, 3 H, OCH_3), 3.96 (s, 1 H, C=C*H*), 5.72 (s, 1 H, C=C*H*), 6.17 (s, 10 H, C_5H_5) ppm.

^{13}C{^{1}H} NMR (126 MHz, C_6D_6, 305 K, **5b'**): δ = 33.7 (*C*H_2-*C*H_2), 37.2 (*C*H_2-*C*H_2), 57.5 (O*C*H_3), 115.0 (*C*$_5$H$_5$), 138.6 (C=*C*H), 140.4 (C=*C*H), 168.1 (Ti-*C*$_q$), 170.2 (Ti-*C*$_q$) ppm.

Synthesis of 5c

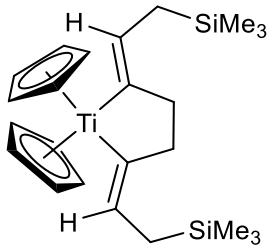

Following the general procedure, complex **5c** was obtained as an orange oil.

Yield: 49 mg (0.114 mmol, 28%).

Melting point: (-).

^{1}H NMR (500 MHz, C_6D_6, 305 K): δ = 0.10 (s, 18 H, Si(CH_3)$_3$), 1.38 (d, *J* = 8.0 Hz, 4 H, CH_2Si(CH$_3$)$_3$), 2.42 (s, 4 H, CH_2-CH_2), 3.63 (t, *J* = 8.0 Hz, 2 H, C=C*H*), 6.06 (s, 10 H, C_5H_5) ppm.

^{13}C{^{1}H} NMR (126 MHz, C_6D_6, 305 K): δ = –1.1 (Si(*C*H$_3$)$_3$), 20.4 (*C*H$_2$Si(CH$_3$)$_3$), 34.1 (*C*H_2-*C*H_2), 115.5 (*C*$_5$H$_5$), 120.7 (C=*C*H), 194.7 (Ti-*C*$_q$) ppm.

^{29}Si NMR (99 MHz, C_6D_6, 305 K): δ = 0.1 ppm.

Synthesis of 5d

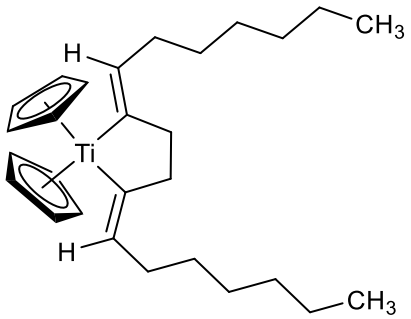

Following the general procedure, complex **5c** was obtained as a red oil.

Yield: 49 mg (0.114 mmol, 28%).

Melting point: (-).

^{1}H NMR (500 MHz, C_6D_6, 305 K): δ = 0.94 (t, *J* = 6.9 Hz, 6 H, C*H*$_3$), 1.33-1.38 (m, 4 H, C*H*$_2$), 1.89-1.94 (m, 4 H, C*H*$_2$), 2.49 (s, 4 H, C*H*$_2$-C*H*$_2$), 3.60 (t, *J* = 6.9 Hz, 2 H, C=C*H*), 6.04 (s, 10 H, C_5H_5) ppm.

^{13}C{^{1}H} NMR (126 MHz, C_6D_6, 305 K): δ = 14.4 (*C*H$_3$), 23.2 (*C*H$_2$), 29.4 (*C*H$_2$), 29.6 (*C*H$_2$), 30.6 (*C*H$_2$), 32.4 (*C*H$_2$), 34.3 (*C*H$_2$-*C*H$_2$), 115.6 (C_5H_5), 126.3 (C=*C*H), 196.9 (Ti-C_q) ppm.

Synthesis of 5e

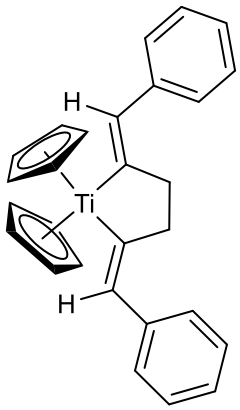

Following the general procedure, complex **5e** was obtained as a red solid.

Yield: 92 mg (0.224 mmol, 56%).

Melting point: 146 °C (dec.).

^{1}H NMR (500 MHz, C_6D_6, 305 K): δ = 2.66 (s, 4 H, C*H*$_2$-C*H*$_2$), 4.70 (s, 2 H, C=C*H*), 6.02 (s, 10 H, C_5H_5), 7.03-7.07 (m, 2 H, C*H*$_{ar}$), 7.09-7.12 (m, 4 H, C*H*$_{ar}$), 7.21-7.26 (m, C*H*$_{ar}$) ppm.

^{13}C{^{1}H} NMR (126 MHz, C_6D_6, 305 K): δ = 36.5 (*C*H$_2$-*C*H$_2$), 116.0 (C_5H_5), 125.1 (*C*H$_{ar}$), 126.2 (C=*C*H), 128.3 (*C*H$_{ar}$), 128.6 (*C*H$_{ar}$), 139.7 ($C_{q,ar}$), 205.0 (Ti-C_q) ppm.

Synthesis of 5f

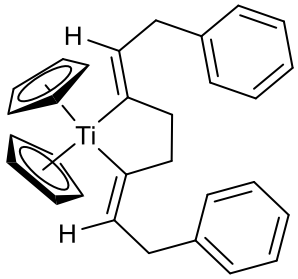

Following the general procedure, complex **5f** was obtained as a red solid.

Yield: 150 mg (0.342 mmol, 86%).

Melting point: 125 °C (dec.).

^{1}H NMR (500 MHz, C_6D_6, 305 K): δ = 2.51 (s, 4 H, CH_2-CH_2), 3.18 (d, *J* = 6.9 Hz, 4 H, CH-CH_2), 3.69 (t, *J* = 6.9 Hz, 2 H, CHCH$_2$), 5.91 (s, 10 H, C_5H_5), 7.08-7.13 (m, 2 H, CH_{ar}), 7.18-7.22 (m, 4 H, CH_{ar}), 7.23-7.27 (m, 4 H, CH_{ar}) ppm.

^{13}C{^{1}H} NMR (126 MHz, C_6D_6, 305 K): δ = 34.3 (CH$_2$-CH$_2$), 36.0 (CHCH$_2$), 115.7 (C_5H$_5$), 124.3 (CH$_{ar}$), 125.8 (CH-CH$_2$), 128.7 (CH$_{ar}$), 128.8 (CH$_{ar}$), 143.4 ($C_{q,ar}$), 196.8 (Ti-C_q) ppm.

Synthesis of 5g

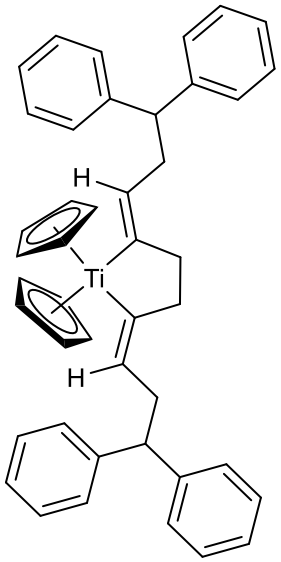

Following the general procedure, complex **5g** was obtained as a red solid.

Yield: 223 mg (0.360 mmol, 90%).

Melting point: 141 °C (dec.).

^{1}H NMR (500 MHz, C_6D_6, 305 K): δ = 2.36 (s, 4 H, CH_2-CH_2), 2.60 (dd, *J* = 8.0 Hz, 6.8 Hz, 4 H, CH_2), 3.39 (t, *J* = 6.8 Hz, 2 H, C=CH), 3.87 (t, *J* = 8.0 Hz, 2 H, CH), 5.74 (s, 10 H, C_5H_5), 7.04-7.10 (m, 4 H, CH_{ar}), 7.17-7.21 (m, 8 H, CH_{ar}), 7.22-7.25 (m, 8 H, CH_{ar}) ppm.

^{13}C{^{1}H} NMR (126 MHz, C_6D_6, 305 K): δ = 34.2 (CH$_2$-CH$_2$), 35.7 (CH$_2$), 52.5 (CH), 115.6 (C_5H$_5$), 124.2 (C=CH), 126.3 (CH$_{ar}$), 128.5 (CH$_{ar}$), 128.6 (CH$_{ar}$), 145.9 ($C_{q,ar}$), 197.3 (Ti-C_q) ppm.

Synthesis of 5h

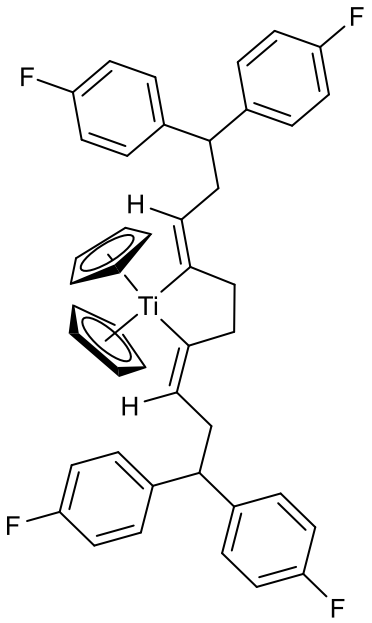

Following the general procedure, complex **5h** was obtained as an orange solid.

Yield: 260 mg (0.376 mmol, 94%).

Melting point: 162-164 °C (dec.).

^{1}H NMR (500 MHz, C_6D_6, 305 K): δ = 2.31 (s, 4 H, CH_2-CH_2), 2.40 (dd, *J* = 8.0 Hz, 6.8 Hz, 4 H, CH_2), 3.29 (t, *J* = 6.8 Hz, 2 H, C=C*H*), 3.65 (t, *J* = 8.0 Hz, 2 H, C*H*), 5.75 (s, 10 H, C_5H_5), 6.83-6.88 (m, 10 H, CH_{ar}), 6.89-6.94 (m, 8 H, CH_{ar}) ppm.

^{13}C{^{1}H} NMR (126 MHz, C_6D_6, 305 K): δ = 34.2 (*C*H_2-*C*H_2), 35.8 (*C*H_2), 50.7 (*C*H), 115.4 (d, *J* = 20.7 Hz, *C*H_{ar}), 115.6 (C_5H_5), 123.8 (C=*C*H), 129.7 (d, *J* = 7.4 Hz, *C*H_{ar}), 141.3 (d, *J* = 3.7 Hz, $C_{q,ar}$), 161.9 (d, *J* = 244.2 Hz, $C_{q,ar}$), 197.4 (Ti-C_q) ppm.

^{19}F NMR (470 MHz, C_6D_6, 305 K): –116.83 ppm.

Synthesis of 5j

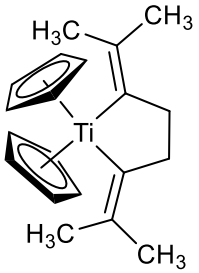

Following the general procedure, complex **5j** was obtained as a red solid.

Yield: 121 mg (0.385 mmol, 96%).

Melting point: 172-174 °C (dec.).

^{1}H NMR (500 MHz, C_6D_6, 305 K): δ = 0.77 (s, 6 H, CH_3), 1.48 (s, 6 H, CH_3), 2.23 (s, 4 H, CH_2-CH_2), 6.07 (s, 10 H, C_5H_5) ppm.

^{13}C{^{1}H} NMR (126 MHz, C_6D_6, 305 K): δ = 21.0 (*C*H_3), 25.5 (*C*H_3), 30.9 (*C*H_2-*C*H_2), 113.7 (C_5H_5), 124.1 ($C_q(Me)_2$), 209.2 (Ti-C_q) ppm.

Synthesis of 5i

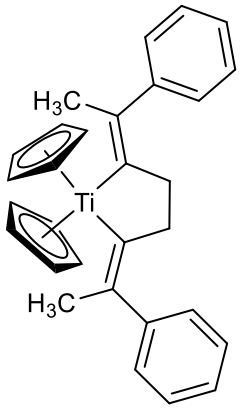

Following the general procedure, complex **5i** was obtained as an orange solid.

Yield: 124 mg (0.283 mmol, 71%).

Melting point: 151 °C (dec.).

^{1}H NMR (500 MHz, C_6D_6, 305 K): δ = 0.91 (s, 6 H, CH_3), 1.78 (s, 4 H, CH_2-CH_2), 5.99 (s, 10 H, C_5H_5), 6.81-6.84 (m, 4 H, CH_{ar}), 6.87-6.92 (m, 2 H, CH_{ar}), 7.02-7.07 (m, CH_{ar}) ppm.

^{13}C{^{1}H} NMR (126 MHz, C_6D_6, 305 K): δ = 25.2 (CH_3), 33.2 (CH_2-CH_2), 114.1 (C_5H_5), 125.4 (CH_{ar}), 128.11 (CH_{ar}), 128.24 (CH_{ar}), 131.5 (C_q), 147.3 ($C_{q,ar}$), 190.7 (Ti-C_q) ppm.

Synthesis of 5k

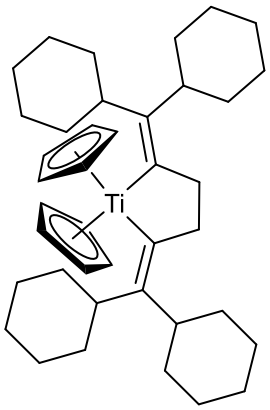

Following the general procedure, complex **5k** was obtained as an orange solid.

Yield: 80 mg (0.136 mmol, 34%).

Melting point: 119 °C (dec.).

^{1}H NMR (500 MHz, C_6D_6, 305 K): δ = 0.21-0.25 (m, 1 H, Cy-CH), 0.40-0.50 (m, 1 H, Cy-CH_2), 1.09-1.15 (m, 6 H, Cy-CH/CH_2), 1.23-1.29 (m, 6 H, Cy-CH_2), 1.55-1.80 (m, 30 H, Cy-CH/CH_2), 2.46 (s, 4 H, CH_2-CH_2), 6.18 (s, 10 H, C_5H_5) ppm.

^{13}C{^{1}H} NMR (126 MHz, C_6D_6, 305 K): δ = 10.5 (Cy-CH_2), 26.8 (Cy-CH_2), 27.1 (Cy-CH_2), 27.2 (Cy-CH_2), 28.2 (Cy-CH_2), 31.1 (CH_2-CH_2), 31.9 (Cy-CH_2), 33.2 (Cy-CH_2), 42.1 (Cy-CH), 47.9 (Cy-CH), 113.2 (C_5H_5), 142.5 (C_q), 189.2 (Ti-C_q) ppm.

Synthesis of 5l

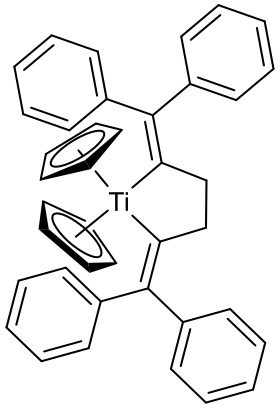

Following the general procedure, complex **5l** was obtained as a red solid.

Yield: 185 mg (0.329 mmol, 82%).

Melting point: 147 °C (dec.).

^{1}H NMR (500 MHz, C_6D_6, 305 K): δ = 2.39 (s, 4 H, CH_2-CH_2), 5.84 (s, 10 H, C_5H_5), 6.90-6.96 (m, 2 H, CH_{ar}), 6.98-7.05 (m, 4 H, CH_{ar}), 7.08-7.12 (m, CH_{ar}), 7.13-7.18 (m, CH_{ar}) ppm.

^{13}C{^{1}H} NMR (126 MHz, C_6D_6, 305 K): δ = 35.6 (CH_2-CH_2), 114.2 (C_5H_5), 125.6 (CH_{ar}), 125.9 (CH_{ar}), 128.3 (CH_{ar}), 129.3 (CH_{ar}), 130.0 (CH_{ar}), 141.7 (C_q), 146.8 ($C_{q,ar}$), 147.6 ($C_{q,ar}$), 197.5 (Ti-C_q) ppm.

Synthesis of 5m

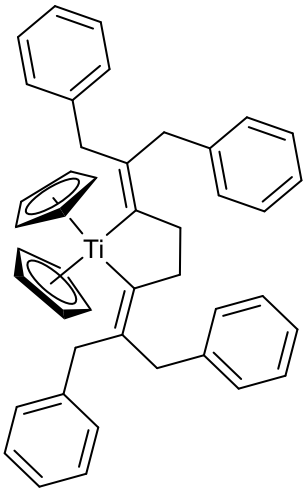

Following the general procedure, complex **5m** was obtained as a red solid.

Yield: 208 mg (0.336 mmol, 84%).

Melting point: 152 °C (dec.).

^{1}H NMR (500 MHz, C_6D_6, 305 K): δ = 2.24 (s, 4 H, CH_2), 2.46 (s, 4 H, CH_2-CH_2), 3.20 (s, 4 H, CH_2), 6.03 (s, 10 H, C_5H_5), 7.07-7.15 (m, 7 H, CH_{ar}), 7.21-7.31 (m, 13 H, CH_{ar}) ppm.

^{13}C{^{1}H} NMR (126 MHz, C_6D_6, 305 K): δ = 31.2 (CH_2), 37.6 (CH_2-CH_2), 42.4 (CH_2), 114.0 (C_5H_5), 125.9 (CH_{ar}), 126.3 (CH_{ar}), 128.7 (CH_{ar}), 128.9 (CH_{ar}), 129.0 (CH_{ar}), 129.4 (CH_{ar}), 131.2 (C_q), 141.5 ($C_{q,ar}$), 142.5 ($C_{q,ar}$), 191.0 (Ti-C_q) ppm.

Synthesis of 5n

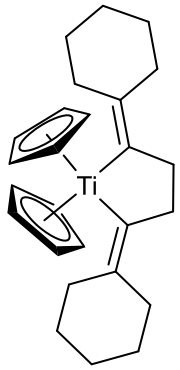

Following the general procedure, complex **5n** was obtained as a red solid.

Yield: 142 mg (0.360 mmol, 90%).

Melting point: 147 °C (dec.).

^{1}H NMR (500 MHz, C_6D_6, 305 K): δ = 0.83-1.00 (m, 4 H, CH_2), 1.35-1.57 (m, 10 H, CH_2), 1.89-2.08 (m, 4 H, CH_2), 2.27 (s, 4 H, CH_2-CH_2), 6.11 (s, 10 H, C_5H_5) ppm.

^{13}C{^{1}H} NMR (126 MHz, C_6D_6, 305 K): δ = 27.7 (CH_2), 28.3 (CH_2), 28.6 (CH_2), 29.5 (CH_2-CH_2), 31.4 (CH_2), 36.0 (CH_2), 113.6 (C_5H_5), 133.1 (C_q), 183.8 (Ti-C_q) ppm.

Synthesis of 5o

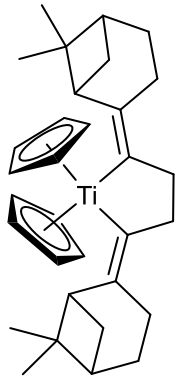

Following the general procedure, complex **5o** was obtained as a red solid.

Yield: 87 mg (0.183 mmol, 46%).

Melting point: 162 °C (dec.).

^{1}H NMR (500 MHz, C_6D_6, 305 K): δ = 0.40-0.45 (m, 2 H, CH_2), 0.89 (s, 6 H, CH_3), 1.22 (s, 6 H, CH_3) 1.49-1.52 (m, 2 H, CH_2), 1.66-1.69 (m, 2 H, CH_2), 1.72-1.78 (m, 2 H, CH_2), 1.93-1.98 (m, 4 H, CH_2/CH), 2.06-2.09 (m, 2 H, CH_2), 2.17-2.22 (m, 2 H, CH_2), 2.32-2.33 (m, 2 H, CH_2), 2.75-2.78 (t, J = 5.6 Hz, 2 H, CH), 6.19 (s, 10 H, C_5H_5) ppm.

^{13}C{^{1}H} NMR (126 MHz, C_6D_6, 305 K): δ = 27.7 (CH_2), 28.3 (CH_2), 28.6 (CH_2), 29.5 (CH_2-CH_2), 31.4 (CH_2), 36.0 (CH_2), 113.6 (C_5H_5), 133.1 (C_q), 183.8 (Ti-C_q) ppm.

Synthesis of 5p

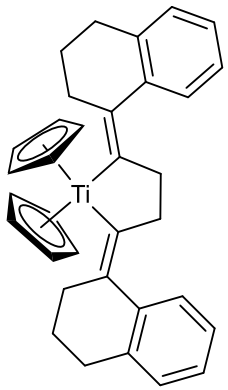

Following the general procedure, complex **5p** was obtained as a red solid.

Yield: 76 mg (0.155 mmol, 39%).

Melting point: 179 °C (dec.).

^{1}H NMR (500 MHz, C_6D_6, 305 K): δ = 1.08 (t, *J* = 6.8 Hz, 4 H, CH_2), 1.69 (pent, *J* = 6.8 Hz, 4 H, CH_2), 2.49 (s, 4 H, CH_2-CH_2), 2.62 (t, *J* = 6.8 Hz, 4 H, CH_2), 6.12 (s, 10 H, C_5H_5), 7.05-7.08 (m, 4 H, CH_{ar}), 7.10-7.14 (m, 2 H, CH_{ar}), 7.17-7.20 (m, 2 H, CH_{ar}) ppm.

^{13}C{^{1}H} NMR (126 MHz, C_6D_6, 305 K): δ = 23.5 (CH_2), 29.6 (CH_2), 32.1 (CH_2), 33.5 (CH_2-CH_2), 114.0 (C_5H_5), 124.9 (CH_{ar}), 125.5 (CH_{ar}), 128.3, (CH_{ar}), 128.9 (CH_{ar}), 132.3 (C_q), 138.0 ($C_{q,ar}$), 140.3 ($C_{q,ar}$), 192.6 (Ti-C_q) ppm.

Synthesis of 5q

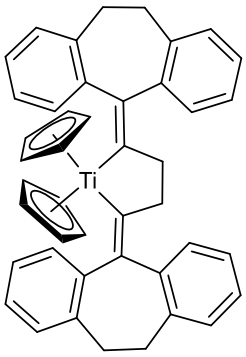

Following the general procedure, complex **5q** was obtained as an orange solid.

Yield: 91 mg (0.148 mmol, 37%).

Melting point: 146 °C (dec.).

^{1}H NMR (500 MHz, C_6D_6, 305 K): δ = 2.08 (d, *J* = 9.7 Hz, 2 H, CH_2-CH_2), 2.19 (d, *J* = 9.7 Hz, 2 H, CH_2-CH_2), 2.68-2.80 (m, 4 H, CH_2), 3.44-3.49 (m, 2 H, CH_2), 3.70-3.74 (m, 2 H, CH_2), 5.81 (s, 10 H, C_5H_5), 6.54-6.58 (m, 2 H, Ph-*H*), 6.78-6.83 (m, 2 H, Ph-*H*), 6.87-6.92 (m, 2 H, Ph-*H*), 6.97-7.03 (m, 10 H, Ph-*H*) ppm.

^{13}C{^{1}H} NMR (126 MHz, C_6D_6, 305 K): δ = 33.0 (CH_2), 33.5 (CH_2), 34.7 (CH_2), 113.7 (C_5H_5), 125.3 (Ph-*C*H), 125.4 (Ph-*C*H), 126.1 (Ph-*C*H), 126.5 (Ph-*C*H), 128.1 (Ph-*C*H), 129.0 (Ph-*C*H), 129.6 (Ph-*C*H), 129.8 (Ph-*C*H), 137.0 (C_q), 138.6 (Ph-C_q), 138.6 (Ph-C_q), 145.1 (Ph-C_q), 146.8 (Ph-C_q), 195.7 (Ti-C_q) ppm.

Synthesis of 5r

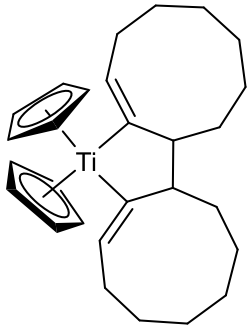

Following the general procedure, complex **5r** was obtained as an orange solid.

Yield: 120 mg (0.284 mmol, 71%).

Melting point: 161 °C (dec.).

^{1}H NMR (500 MHz, C_6D_6, 305 K): δ = 1.18-1.30 (m, 2 H, CH_2), 1.39-1.84 (m, 18 H, CH_2), 2.10-2.20 (m, 2 H, CH_2), 2.29-2.39 (m, 2 H, CH_2), 2.53-2.60 (m, 2 H, C*H*-C*H*), 3.49 (ddd, *J* = 9.0 Hz, 7.1 Hz, 1.7 Hz, 2 H, C=C*H*), 6.12 (s, 10 H, C_5H_5) ppm.

^{13}C{^{1}H} NMR (126 MHz, C_6D_6, 305 K): δ = 24.5 (*C*H_2), 25.4 (*C*H_2), 25.7 (*C*H_2), 26.5 (*C*H_2), 27.5 (*C*H_2), 36.5 (*C*H_2), 54.6 (*C*H-*C*H), 116.1 (C_5H_5), 129.6 (C=*C*H), 198.1 (Ti-C_q) ppm.

Synthesis of 5s

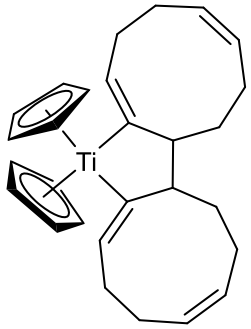

Following the general procedure, complex **5s** was obtained as an orange solid.

Yield: 136 mg (0.325 mmol, 81%).

Melting point: 168 °C (dec.).

^{1}H NMR (500 MHz, C_6D_6, 305 K): δ = 1.36-1.45 (m, 2 H, CH_2), 1.80-1.95 (m, 6 H, CH_2), 1.97-2.06 (m, 2 H, CH_2), 2.08-2.14 (m, 2 H, CH_2), 2.18-2.25 (m, 2 H, C*H*-C*H*), 2.33-2.44 (m, 2 H, CH_2), 2.45-2.53 (m, 2 H, CH_2), 3.55 (td, *J* = 7.9 Hz, 1.6 Hz, 2 H, C=C*H*), 5.57-5.63 (m, 2 H, C*H*=C*H*), 5.72-5.78 (m, 2 H, C*H*=C*H*), 6.10 (s, 10 H, C_5H_5) ppm.

^{13}C{^{1}H} NMR (126 MHz, C_6D_6, 305 K): δ = 26.3 (*C*H_2), 27.1 (*C*H_2), 29.8 (*C*H_2), 37.8 (*C*H_2), 53.4 (*C*H-*C*H), 116.4 (C_5H_5), 129.6 (C=*C*H), 130.4 (*C*H=*C*H), 131.2 (*C*H=*C*H), 197.8 (Ti-C_q) ppm.

Synthesis of 5t and 5t'

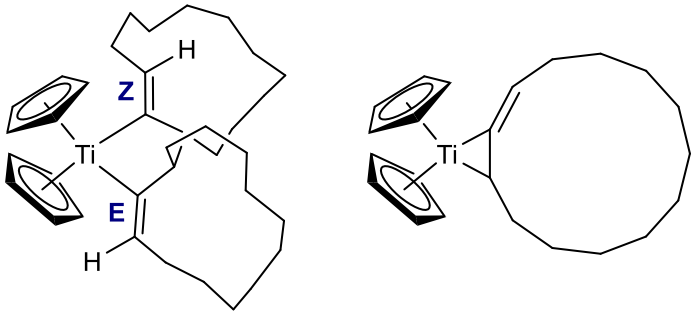

5t **5t'**

Complex **1** (139 mg, 0.400 mmol, 1.00 equiv.) was directly treated with cyclotrideca-1,2-diene (285 mg, 1.600 mmol, 4.00 equiv.) at ambient temperature. A colour change from yellow to red is observed. After 24 h at ambient temperature, a red solid formed, which was washed with *n*-hexane and dried under high vacuum to yield **5t** and **5t'** in a product mixture as a red solid.

Yield: 35 mg (0.065 mmol, 16%).

Melting point: 134 °C (dec.).

^{1}H NMR of **5t** (500 MHz, C_6D_6, 305 K): δ = –0.10 (dtd, *J* = 14.0 Hz, 10.3 Hz, 1.8 Hz, 1 H, C*H*$_2$), 1.10-2.35 (m, 39 H, C*H*$_2$), 2.20 (dd, *J* = 11.1, 3.6 Hz, 1 H, C*H*), 3.16-3.21 (m, 2 H, C*H*), 5.48 (ddd, *J* = 10.6, 3.1, 1.3 Hz, 1 H, C*H*), 6.18 (s, 5 H, Cp–*H*), 6.20 (s, 5 H, Cp–*H*) ppm.

^{13}C{^{1}H} NMR of **5t** (126 MHz, C_6D_6, 305 K): δ = 25.3-29.3 (18 x *C*H$_2$), 31.2 (*C*H$_2$), 36.3 (*C*H$_2$), 54.4 (*C*H), 57.7 (*C*H), 115.5 (5 x Cp–*C*H), 115.6 (5 x Cp–*C*H), 127.5 (*C*H), 133.3 (*C*H), 197.1 (*C*$_q$), 200.7 (*C*$_q$) ppm.

^{1}H NMR of **5t'** (500 MHz, C_6D_6, 305 K): δ = 1.25-2.35 (m, 20 H, C*H*$_2$), 2.55 (dt, *J* = 10.6 Hz, 2.2 Hz, 1 H, C*H*), 3.15-3.17 (m, 1 H, C*H*), 6.12 (s, 10 H, Cp–*H*) ppm.

^{13}C{^{1}H} NMR of **5t'** (126 MHz, C_6D_6, 305 K): δ = 25.3-29.3 (8 x *C*H$_2$), 36.8 (*C*H$_2$), 39.4 (*C*H$_2$), 51.2 (*C*H), 116.1 (10 x Cp–*C*H), 127.3 (*C*H), 201.1 (*C*$_q$) ppm.

NMR Spectra

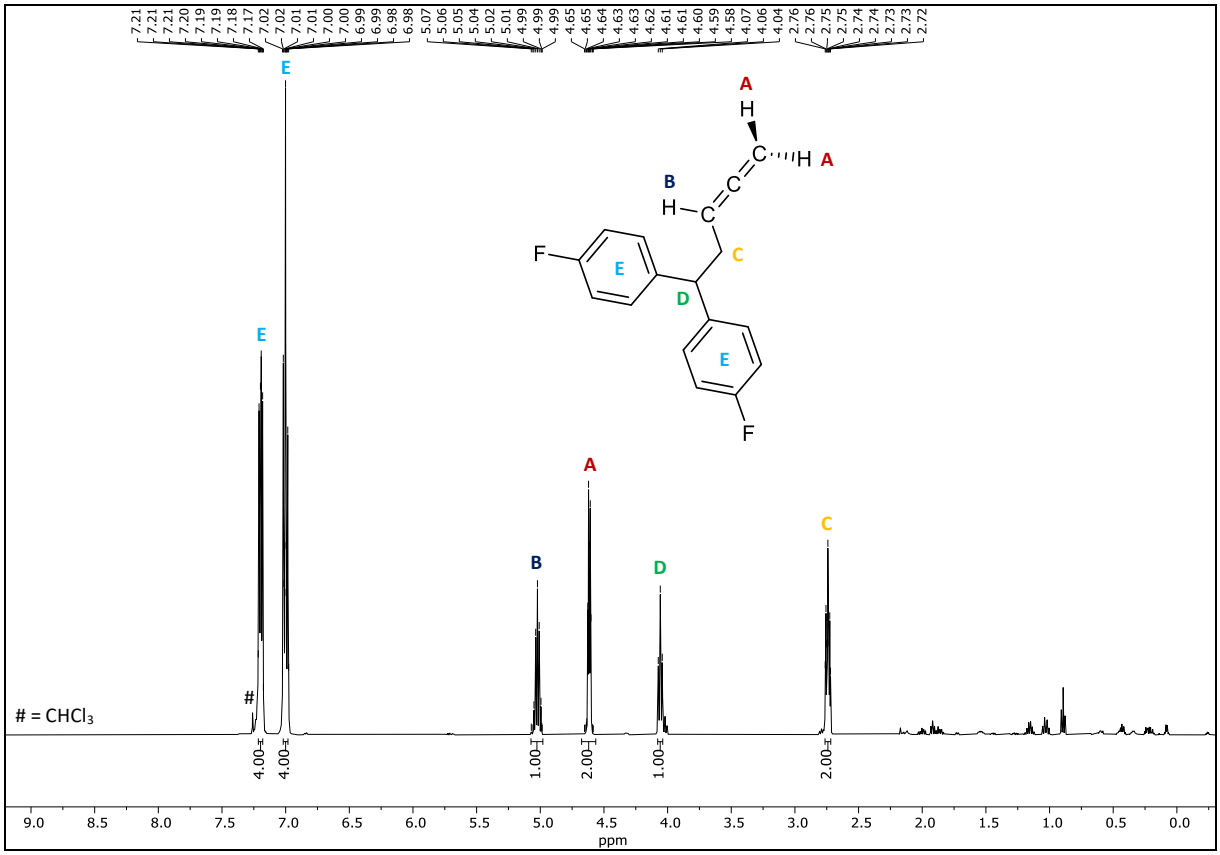

Figure S1: ^{1}H NMR spectrum of **h** (500 MHz, $CDCl_3$, 305 K).

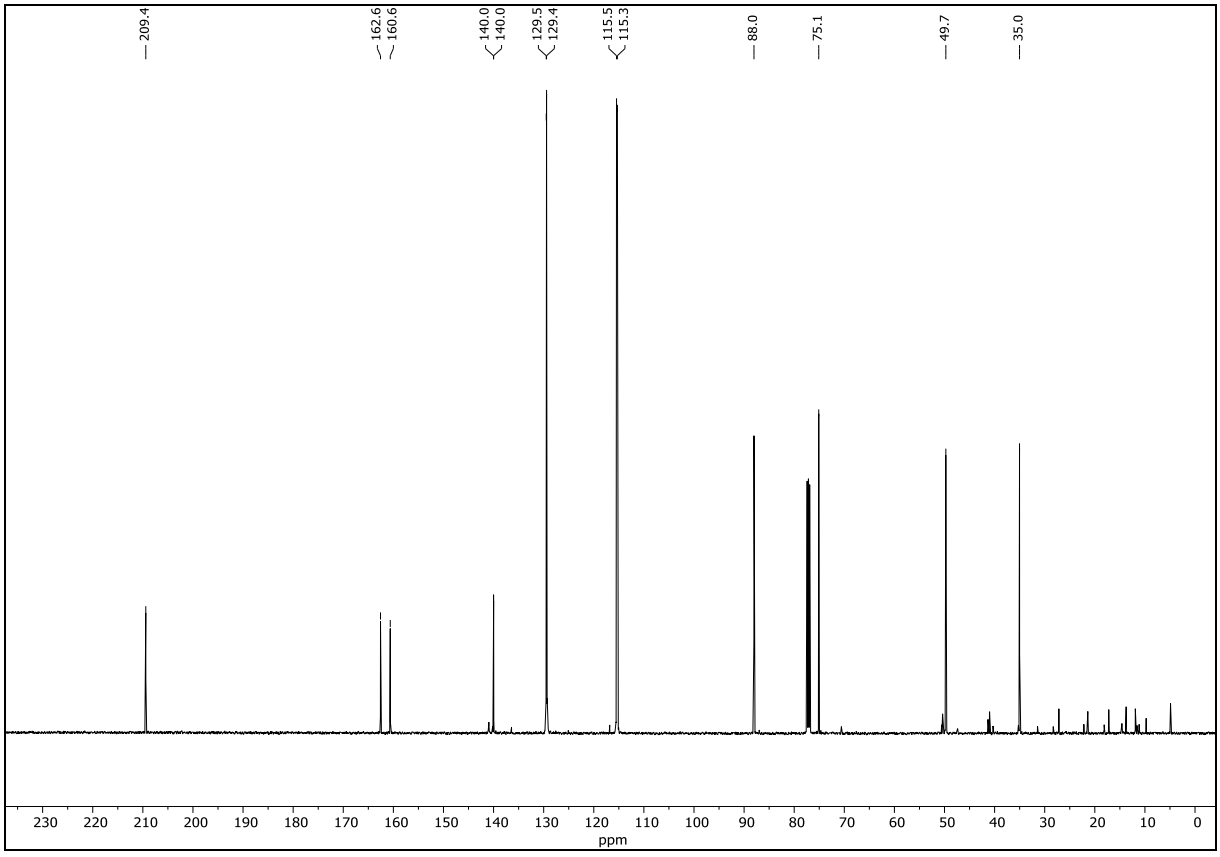

Figure S2: $^{13}C\{^{1}H\}$ NMR spectrum of **h** (126 MHz, $CDCl_3$, 305 K).

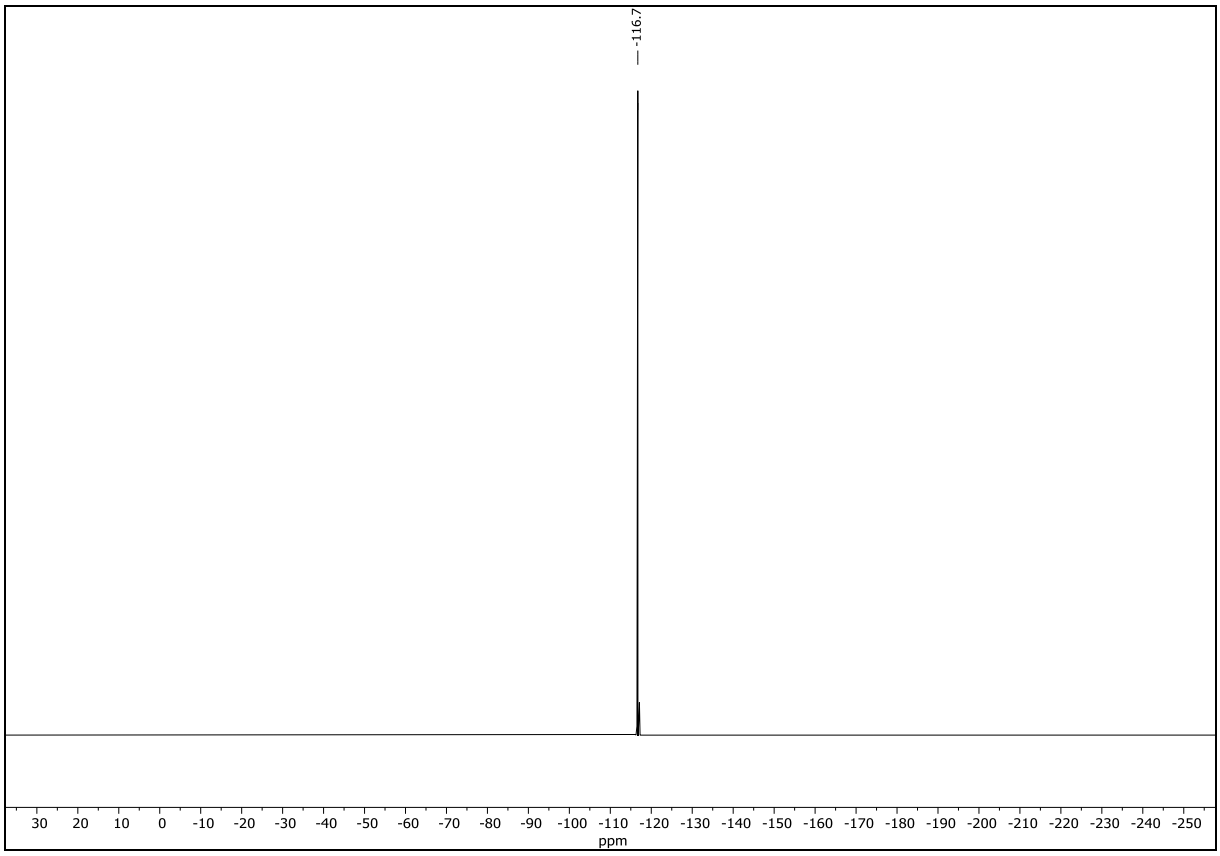

Figure S3: $^{19}F\{^{1}H\}$ NMR spectrum of **h** (470 MHz, $CDCl_3$, 305 K).

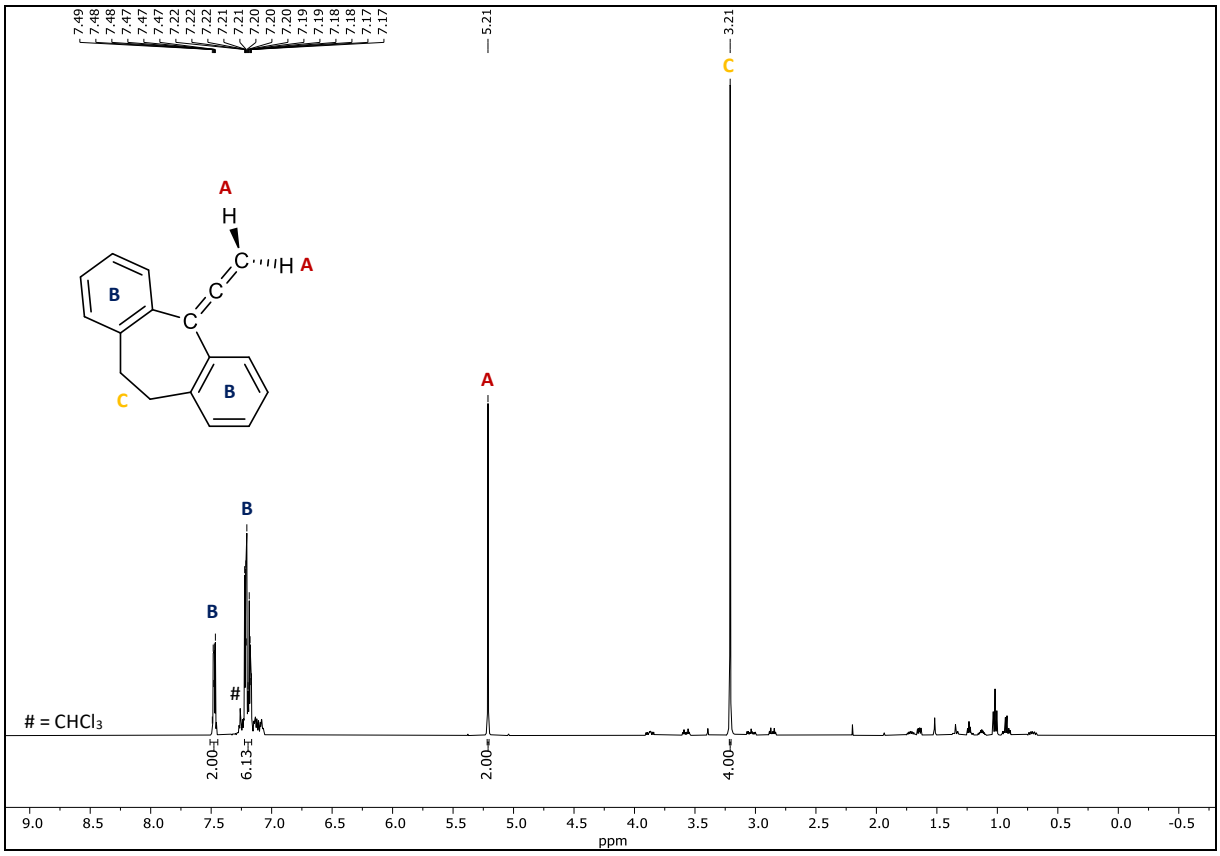

Figure S4: ^{1}H NMR spectrum of **q** (500 MHz, $CDCl_3$, 305 K).

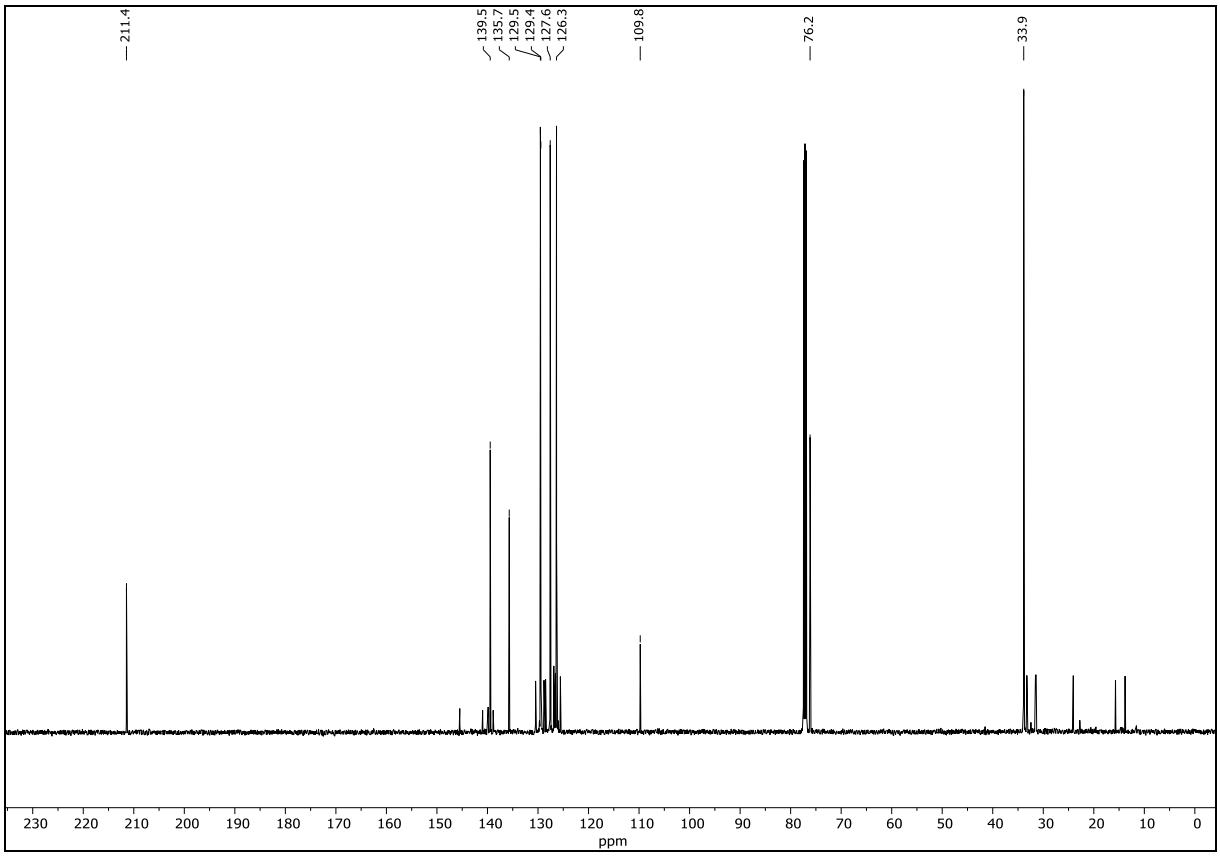

Figure S5: $^{13}C\{^{1}H\}$ NMR spectrum of **h** (126 MHz, $CDCl_3$, 305 K).

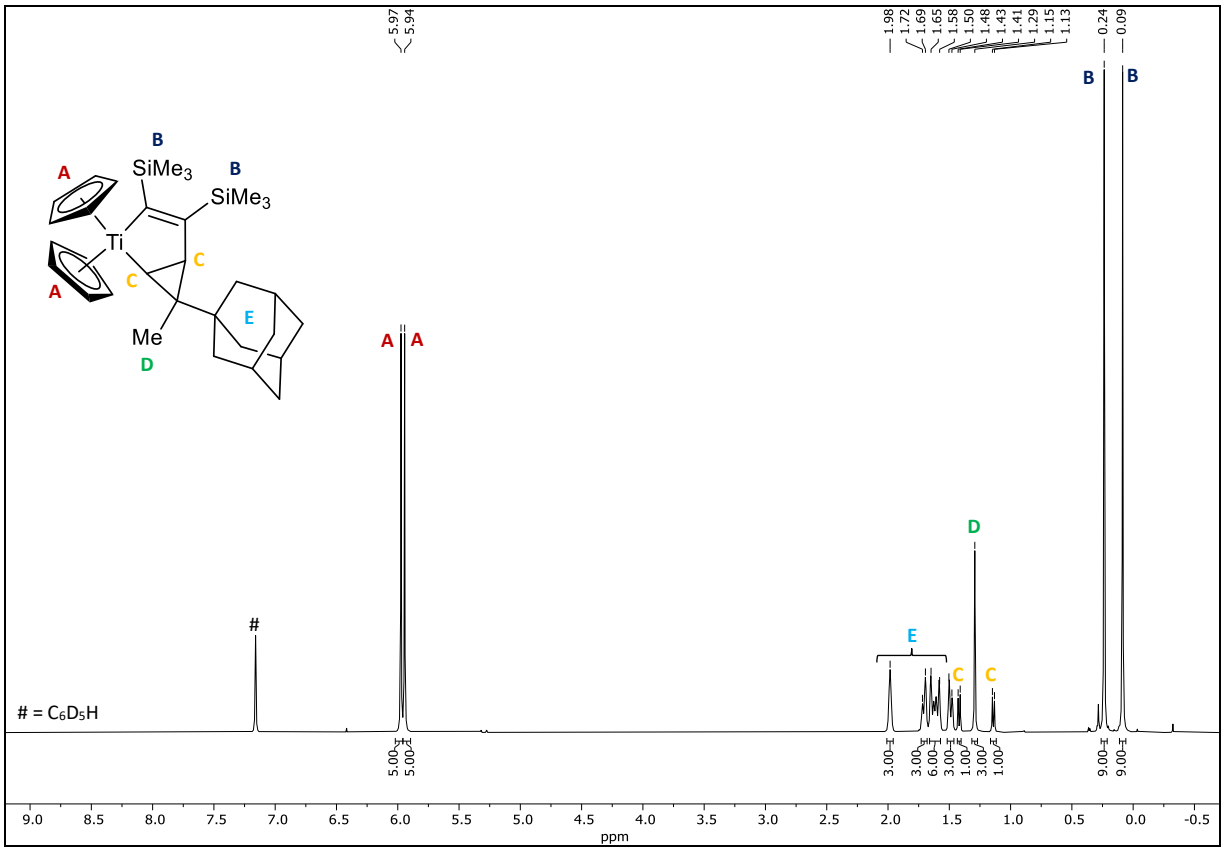

Figure S6: ^{1}H NMR spectrum of **2a** (500 MHz, C_6D_6, 298 K).

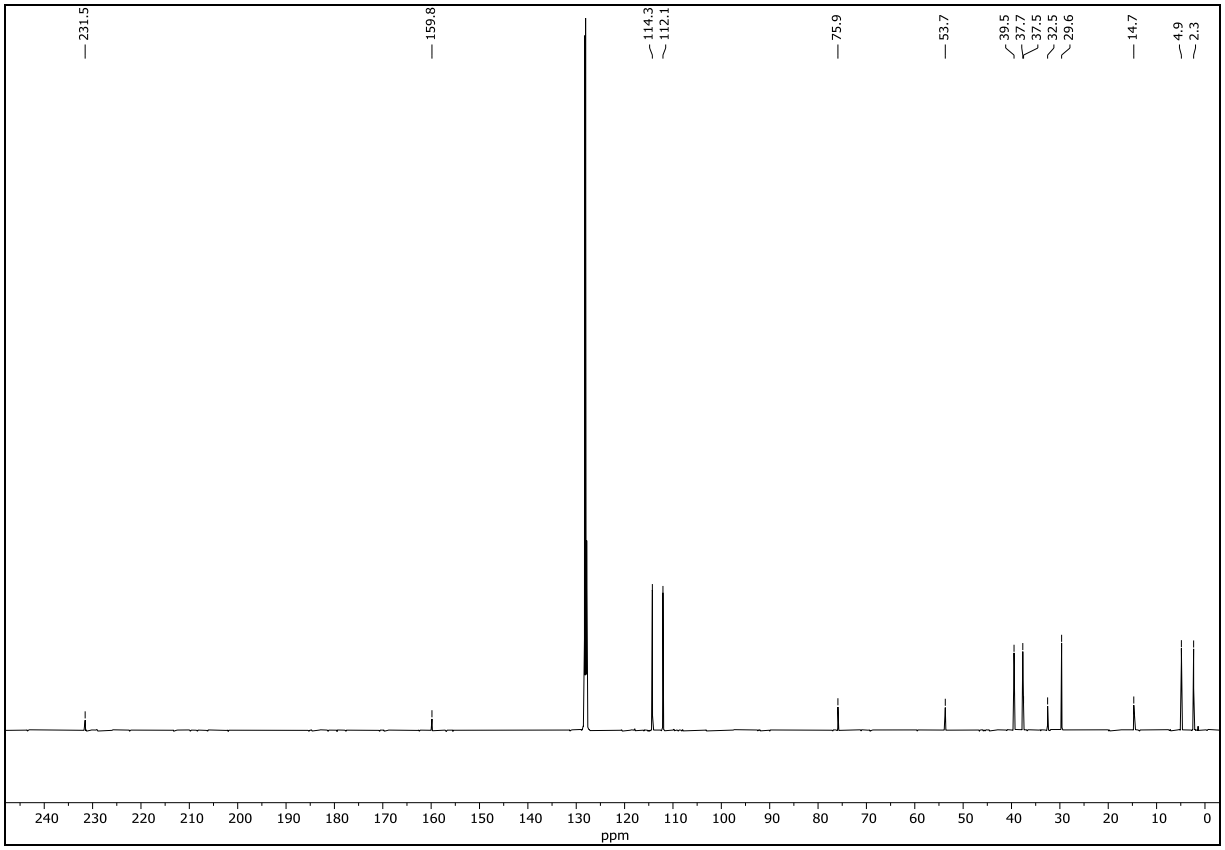

Figure S7: ^{13}C{^{1}H} NMR spectrum of **2a** (126 MHz, C_6D_6, 298 K).

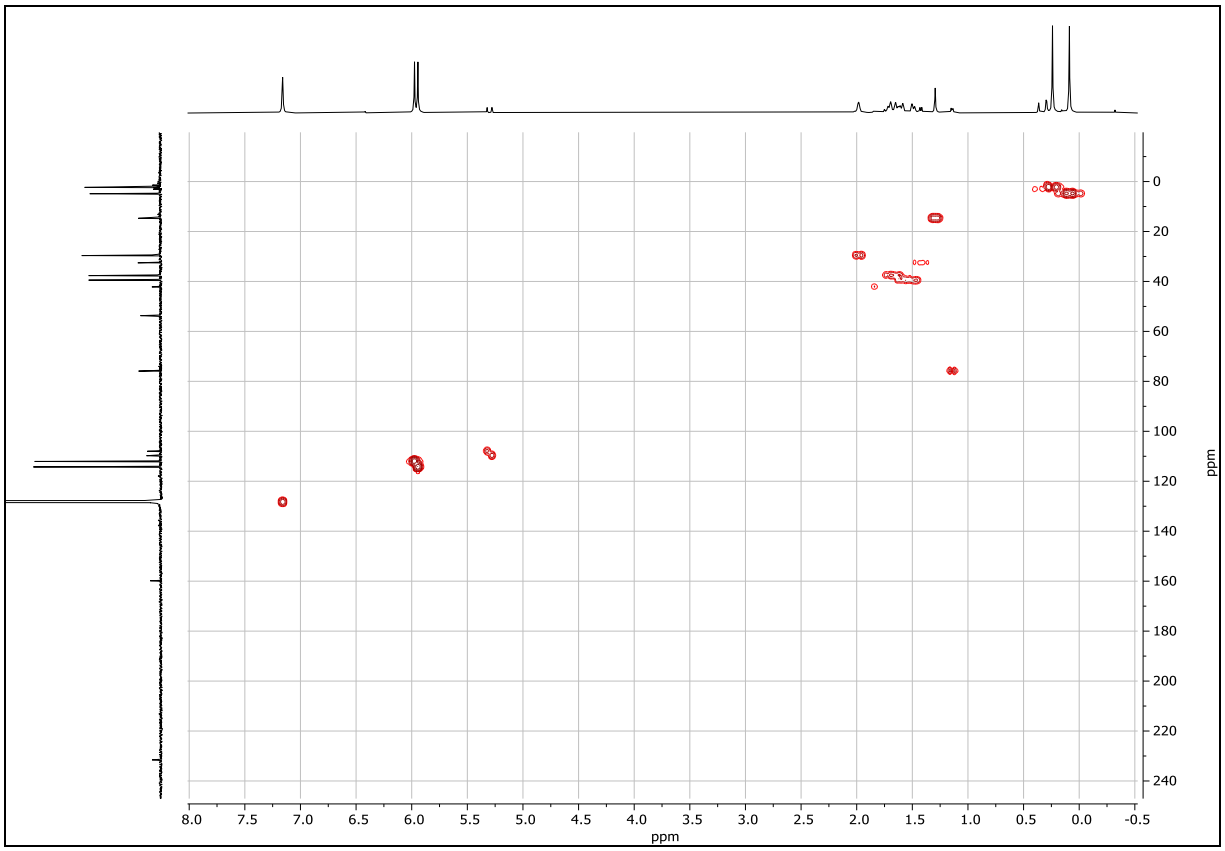

Figure S8: $^{1}H,^{13}C$ HMQC NMR spectrum of **2a** (500MHz, 126 MHz, C_6D_6, 298 K).

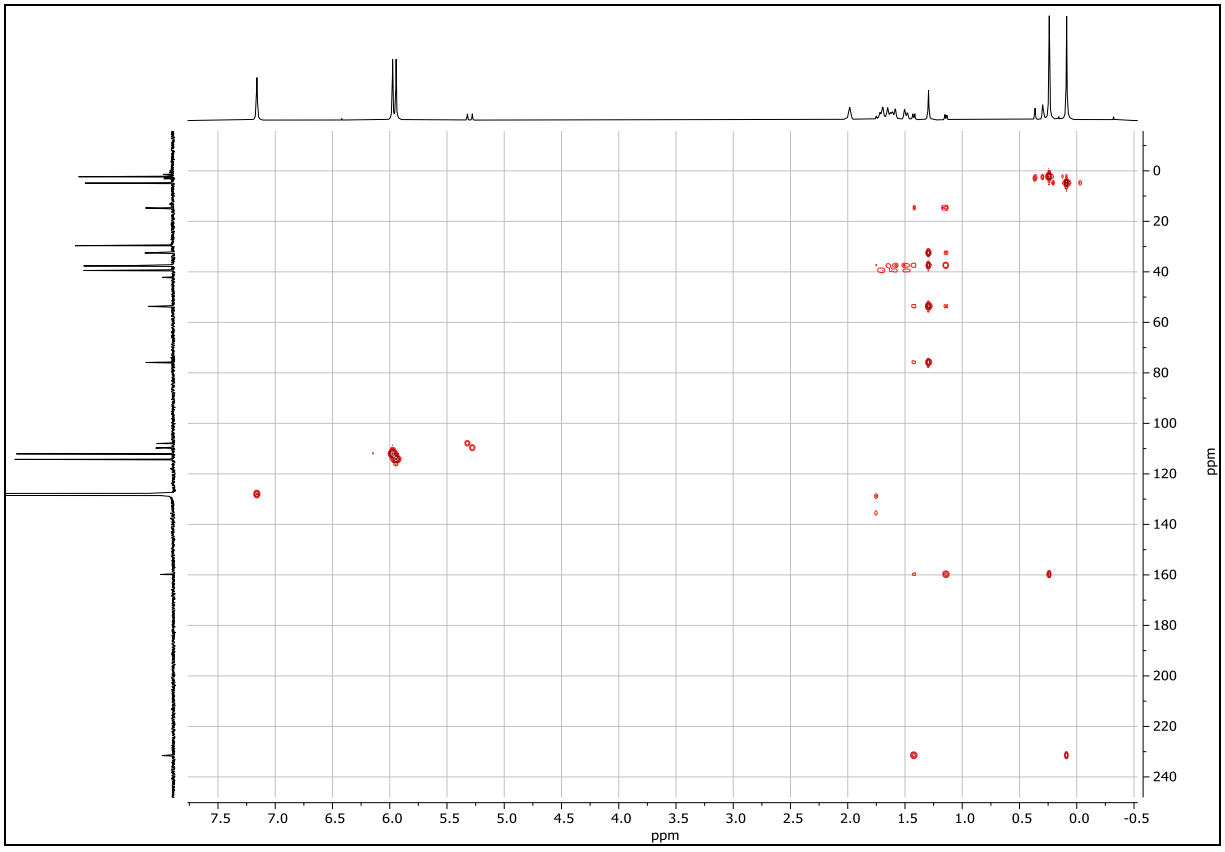

Figure S9: $^{1}H,^{13}C$ HMBC NMR spectrum of **2a** (500MHz, 126 MHz, C_6D_6, 298 K).

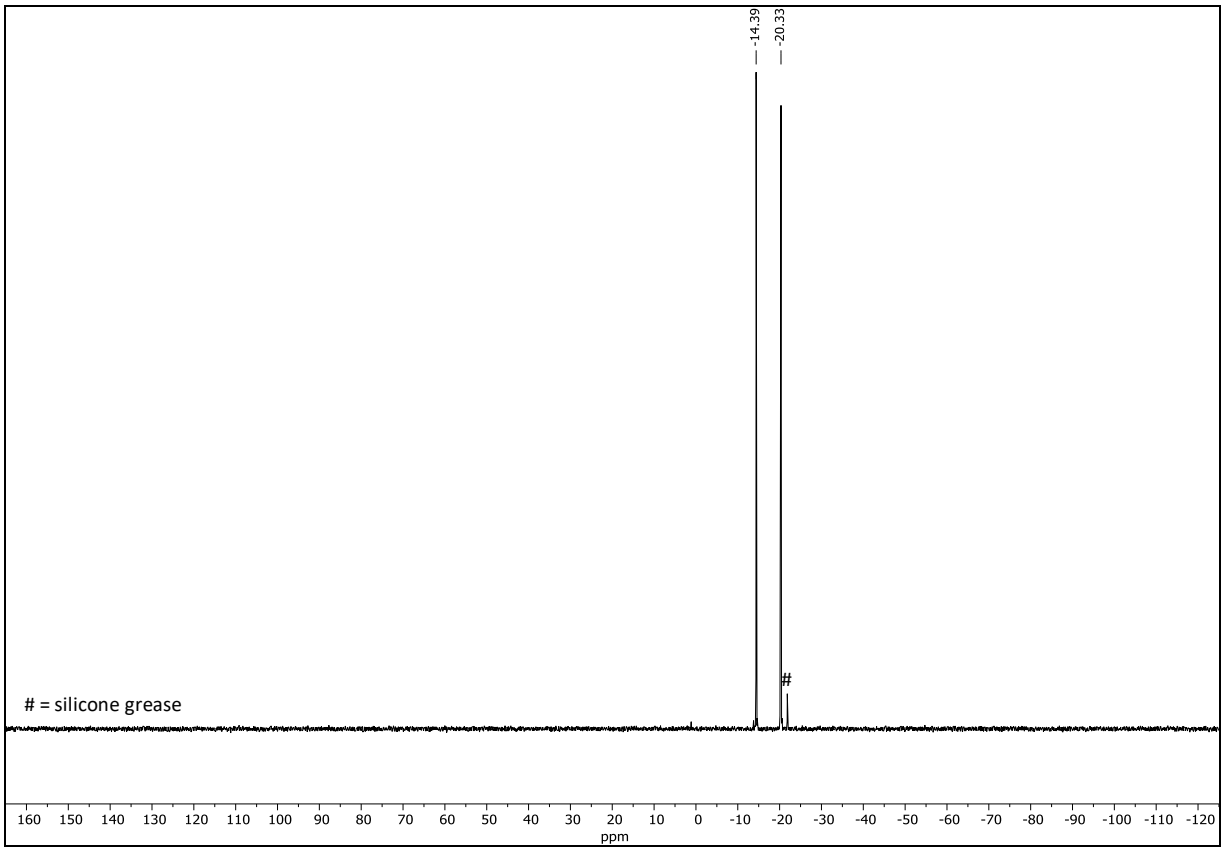

Figure S10: $^{29}Si\{^{1}H\}$ INEPT NMR spectrum of **2a** (99 MHz, C_6D_6, 298 K).

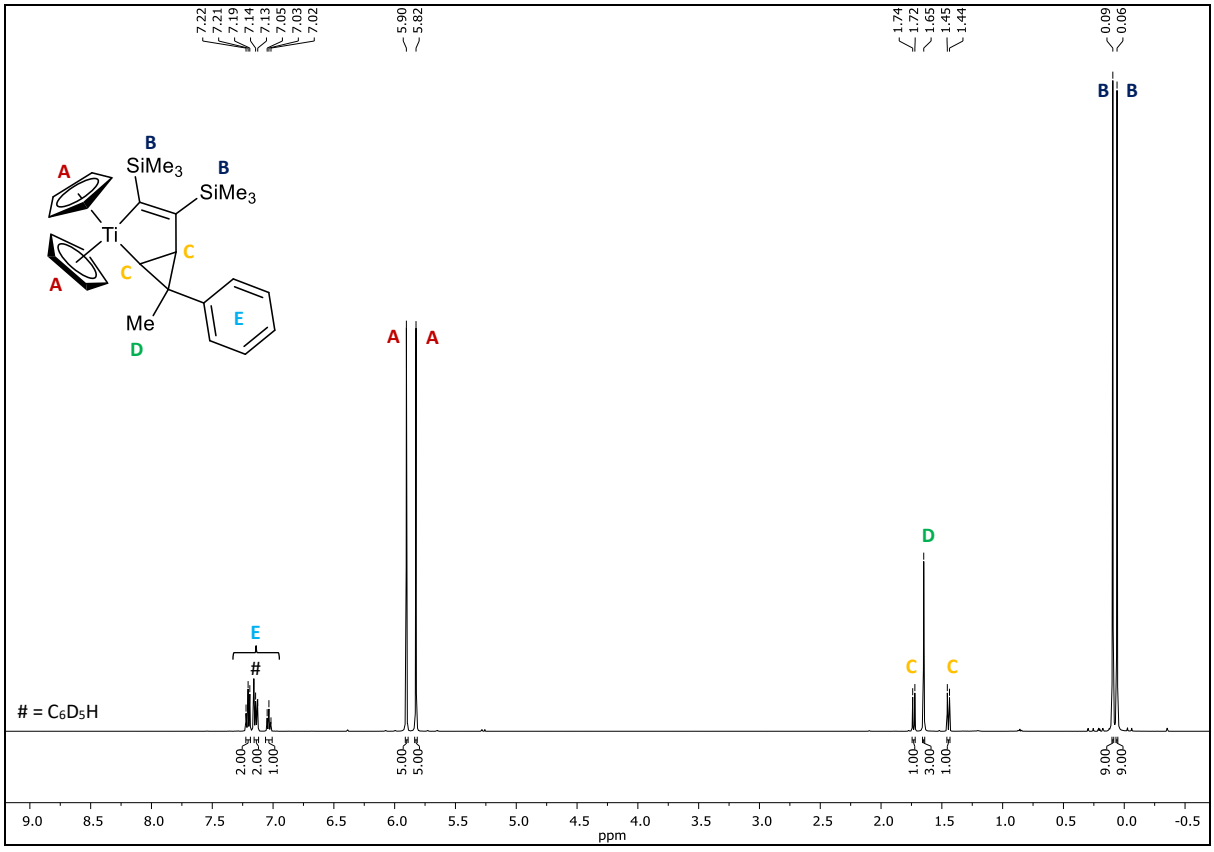

Figure S11: ^{1}H NMR spectrum of **2b** (500 MHz, C_6D_6, 298 K).

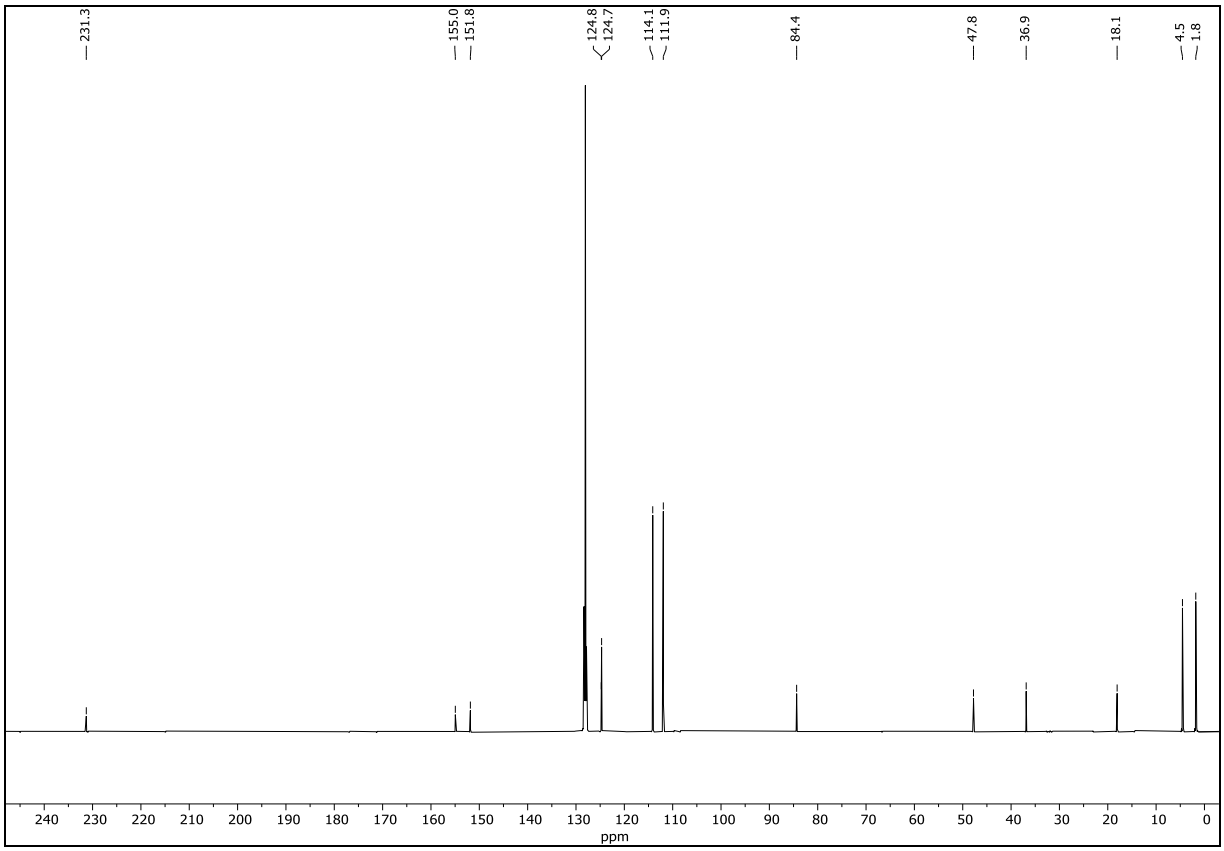

Figure S12: $^{13}C\{^{1}H\}$ NMR spectrum of **2b** (126 MHz, C_6D_6, 298 K).

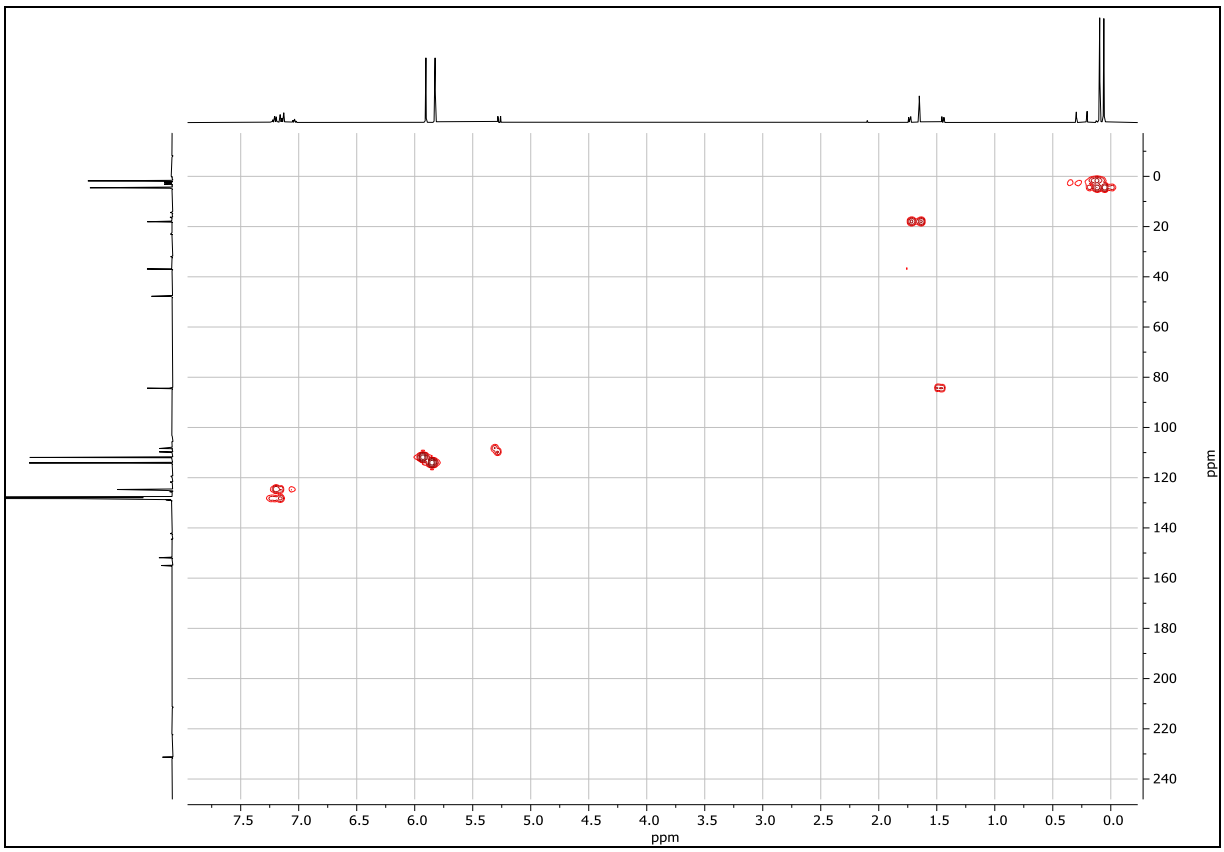

Figure S13: $^{1}H,^{13}C$ HMQC NMR spectrum of **2b** (500MHz, 126 MHz, C_6D_6, 298 K).

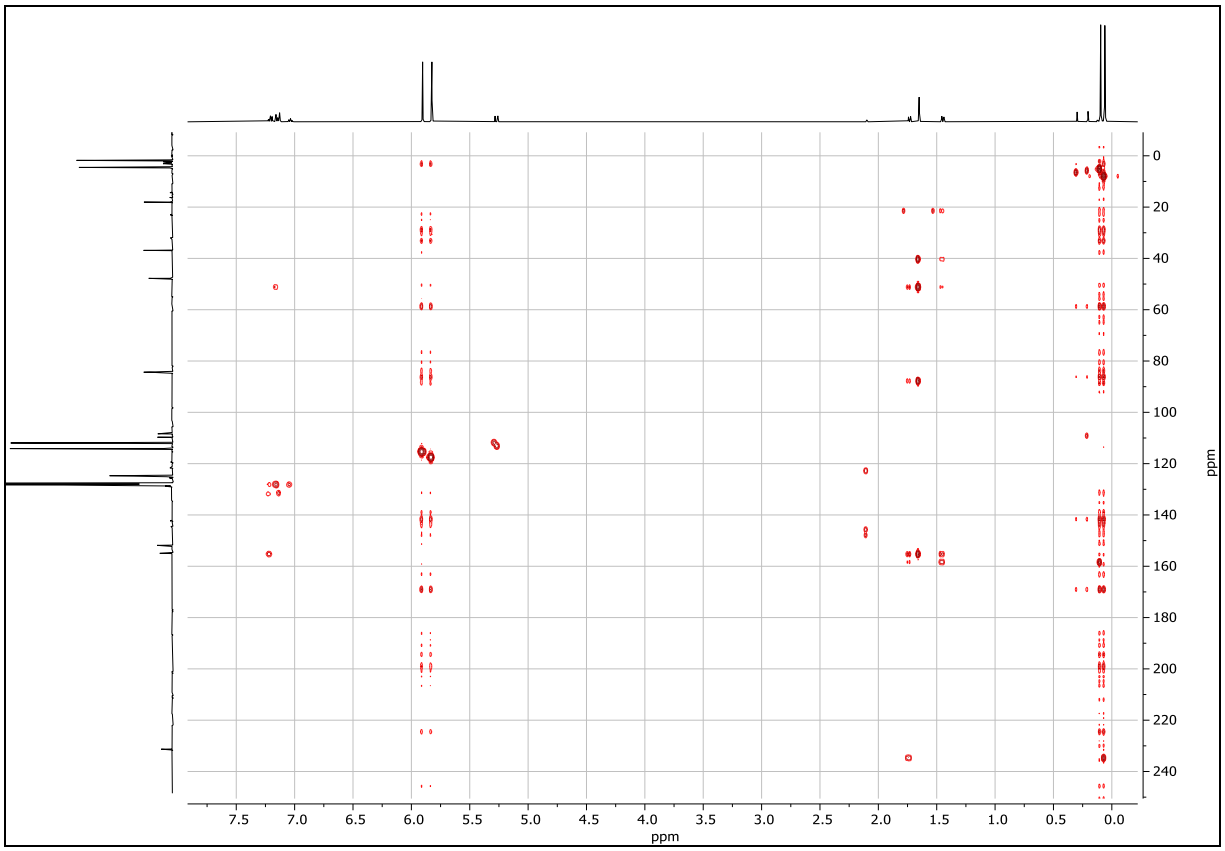

Figure S14: $^{1}H,^{13}C$ HMBC NMR spectrum of **2b** (500MHz, 126 MHz, C_6D_6, 298 K).

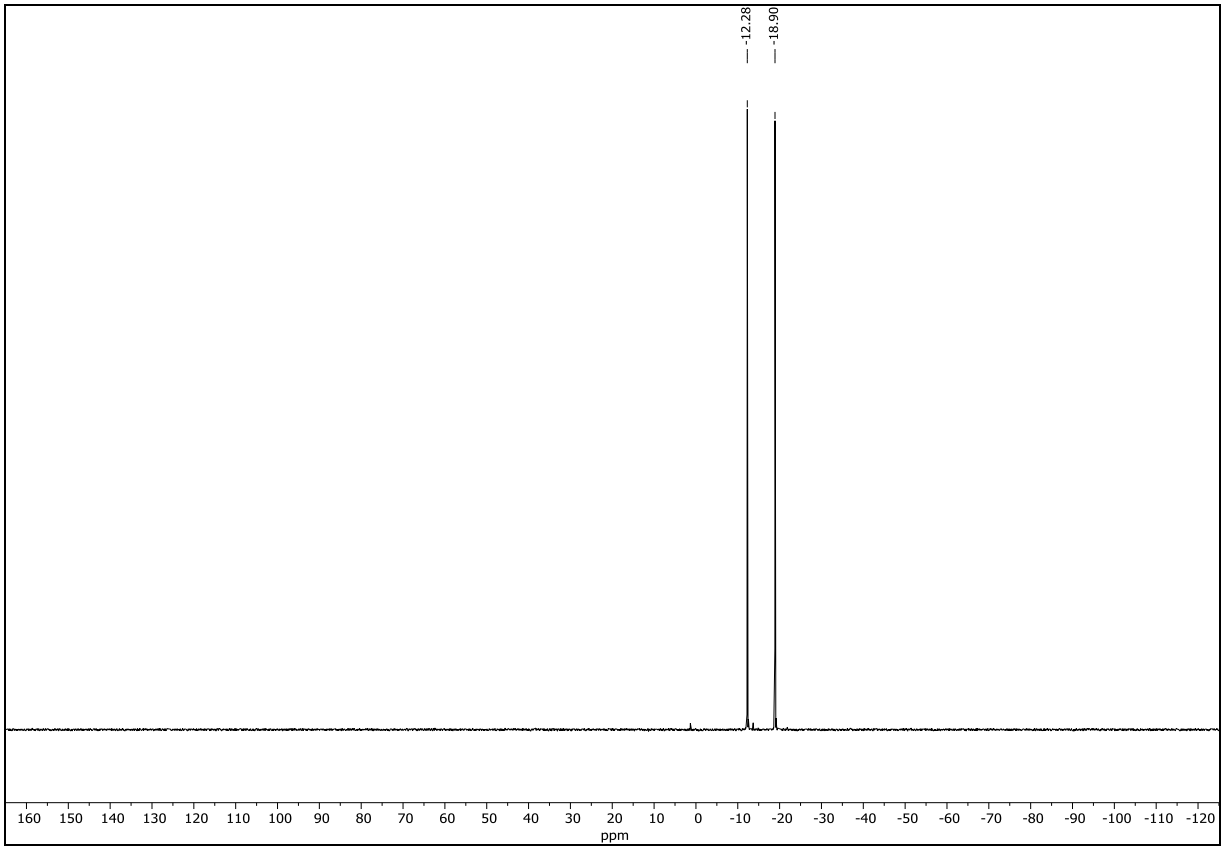

Figure S15: $^{29}Si\{^{1}H\}$ INEPT NMR spectrum of **2b** (99 MHz, C_6D_6, 298 K).

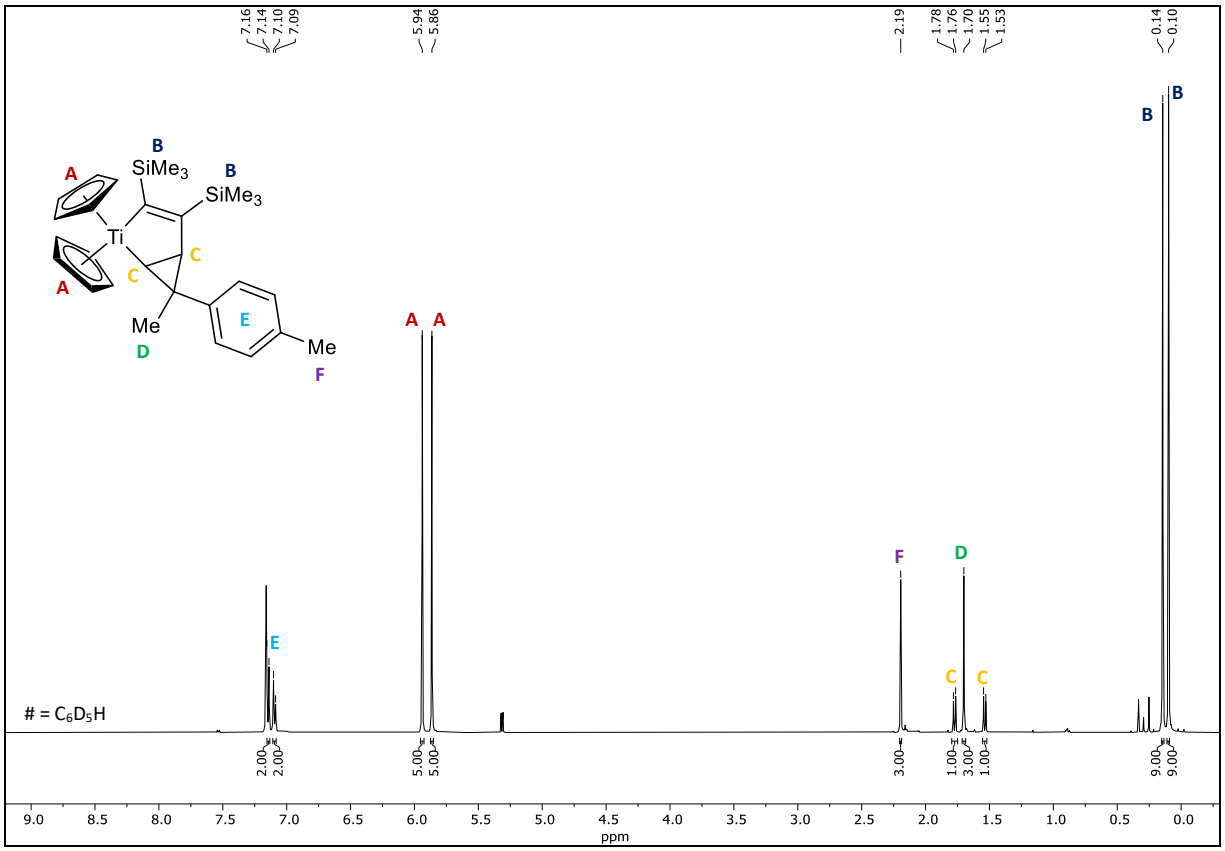

Figure S16: ^{1}H NMR spectrum of **2c** (500 MHz, C_6D_6, 298 K).

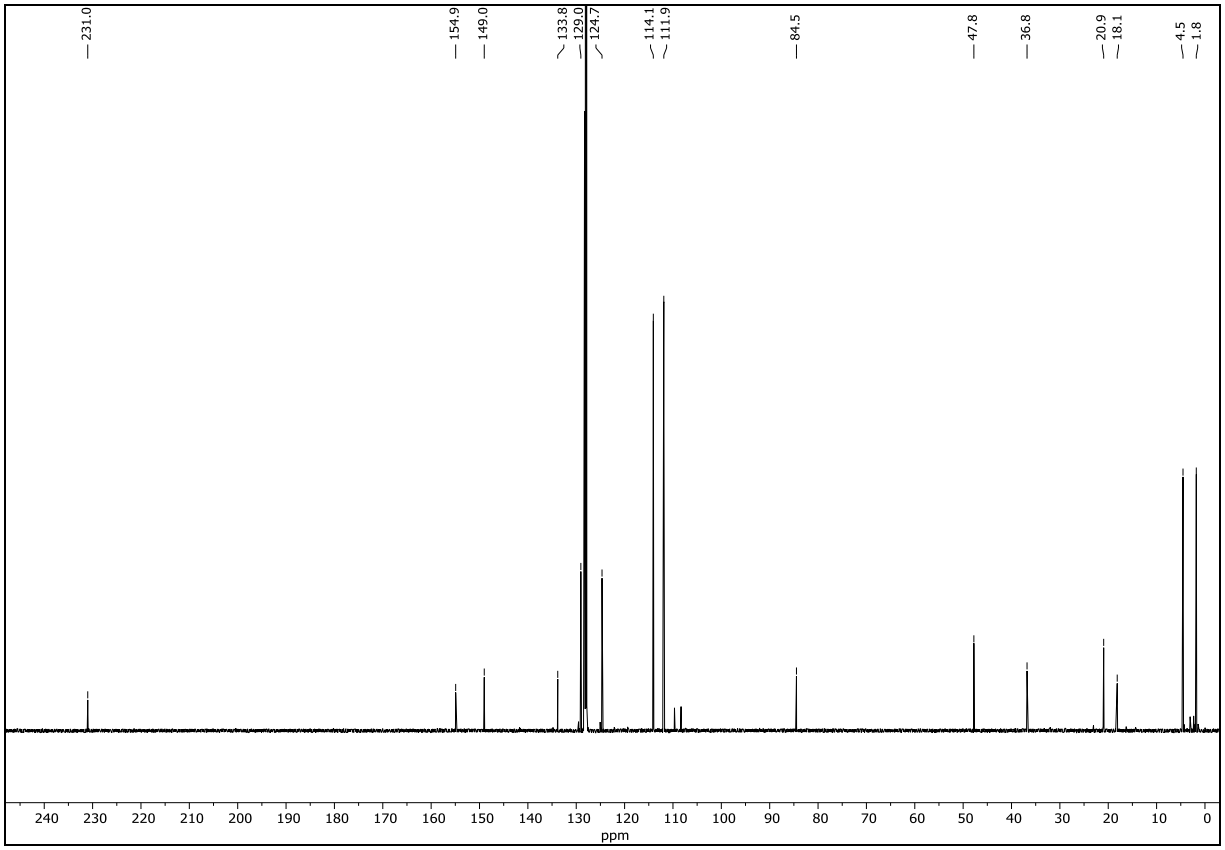

Figure S17: ^{13}C{^{1}H} NMR spectrum of **2c** (126 MHz, C_6D_6, 298 K).

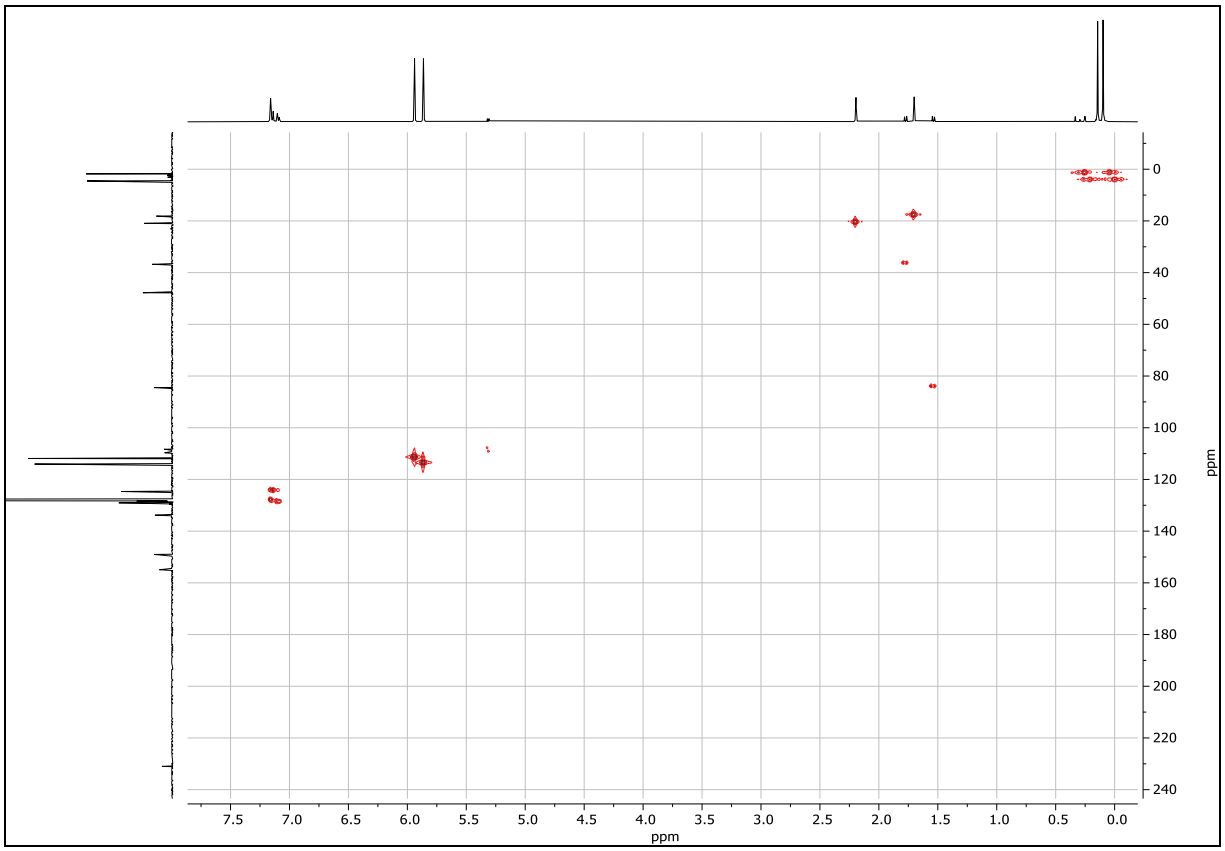

Figure S18: $^{1}H,^{13}C$ HMQC NMR spectrum of **2c** (500MHz, 126 MHz, C_6D_6, 298 K).

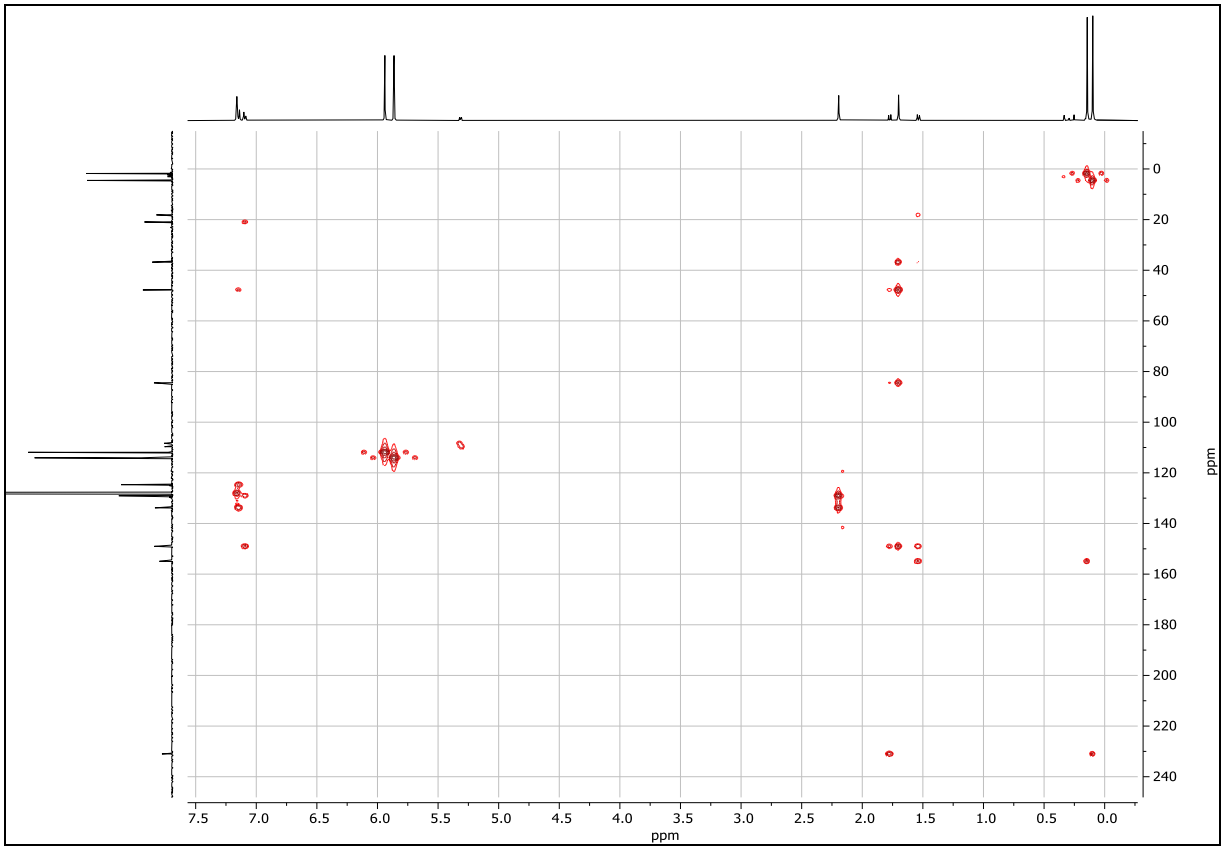

Figure S19: $^{1}H,^{13}C$ HMBC NMR spectrum of **2c** (500MHz, 126 MHz, C_6D_6, 298 K).

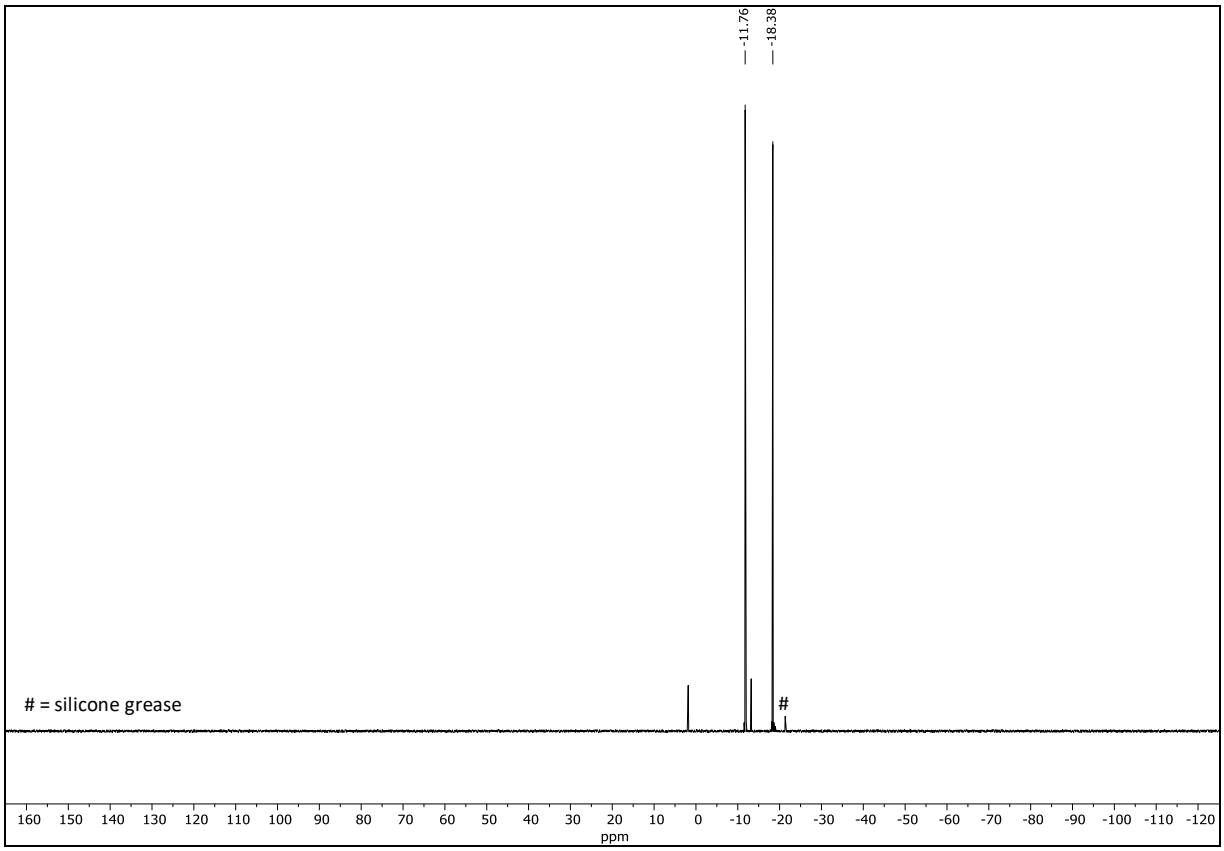

Figure S20: $^{29}Si\{^{1}H\}$ INEPT NMR spectrum of **2c** (99 MHz, C_6D_6, 298 K).

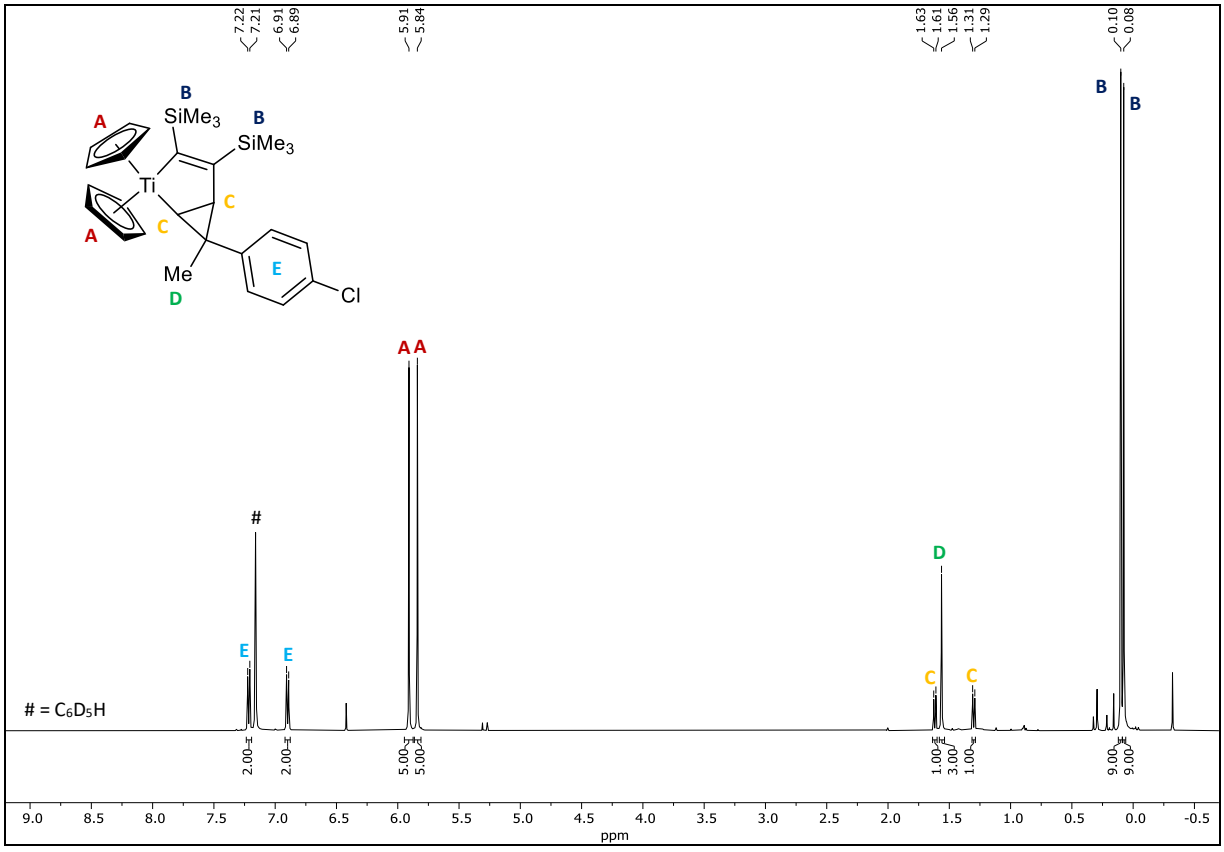

Figure S21: ^{1}H NMR spectrum of **2d** (500 MHz, C_6D_6, 298 K).

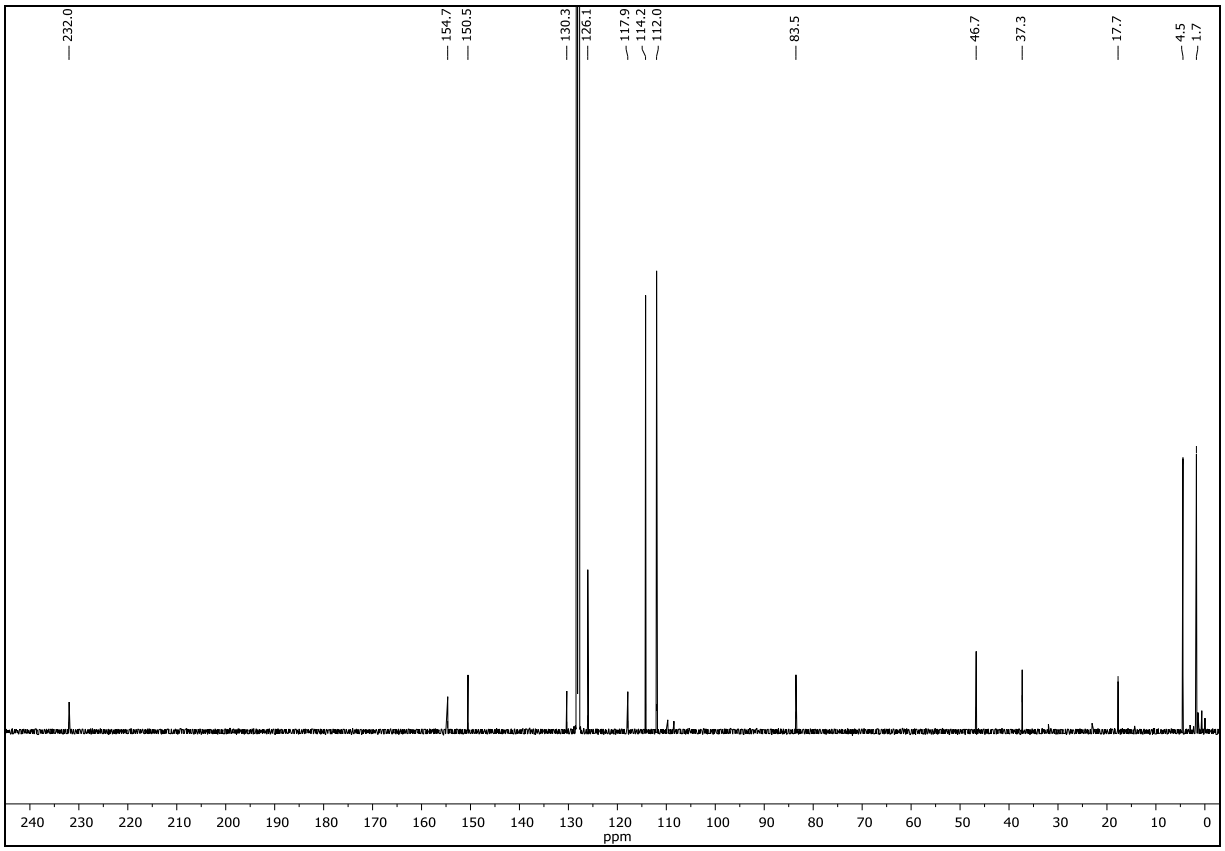

Figure S22: $^{13}C\{^{1}H\}$ NMR spectrum of **2d** (126 MHz, C_6D_6, 298 K).

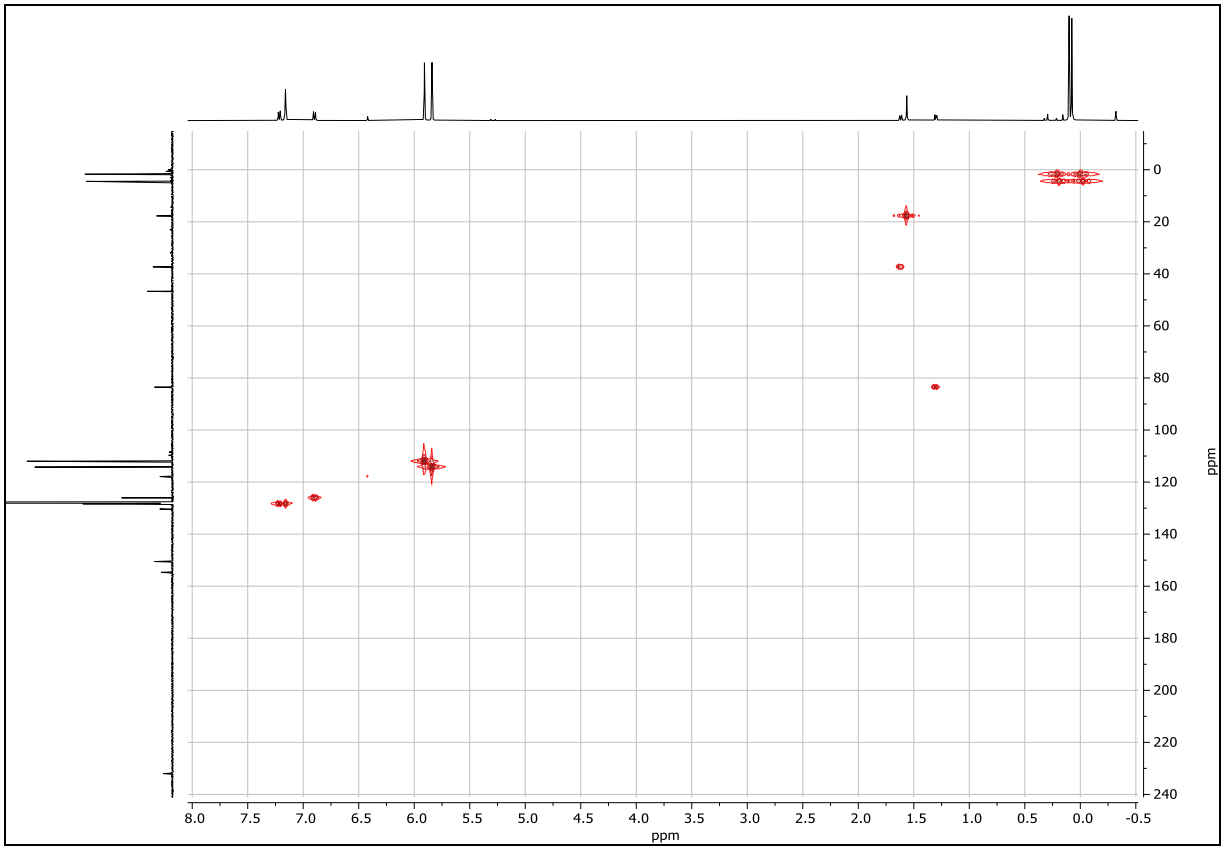

Figure S23: $^{1}H,^{13}C$ HMQC NMR spectrum of **2d** (500MHz, 126 MHz, C_6D_6, 298 K).

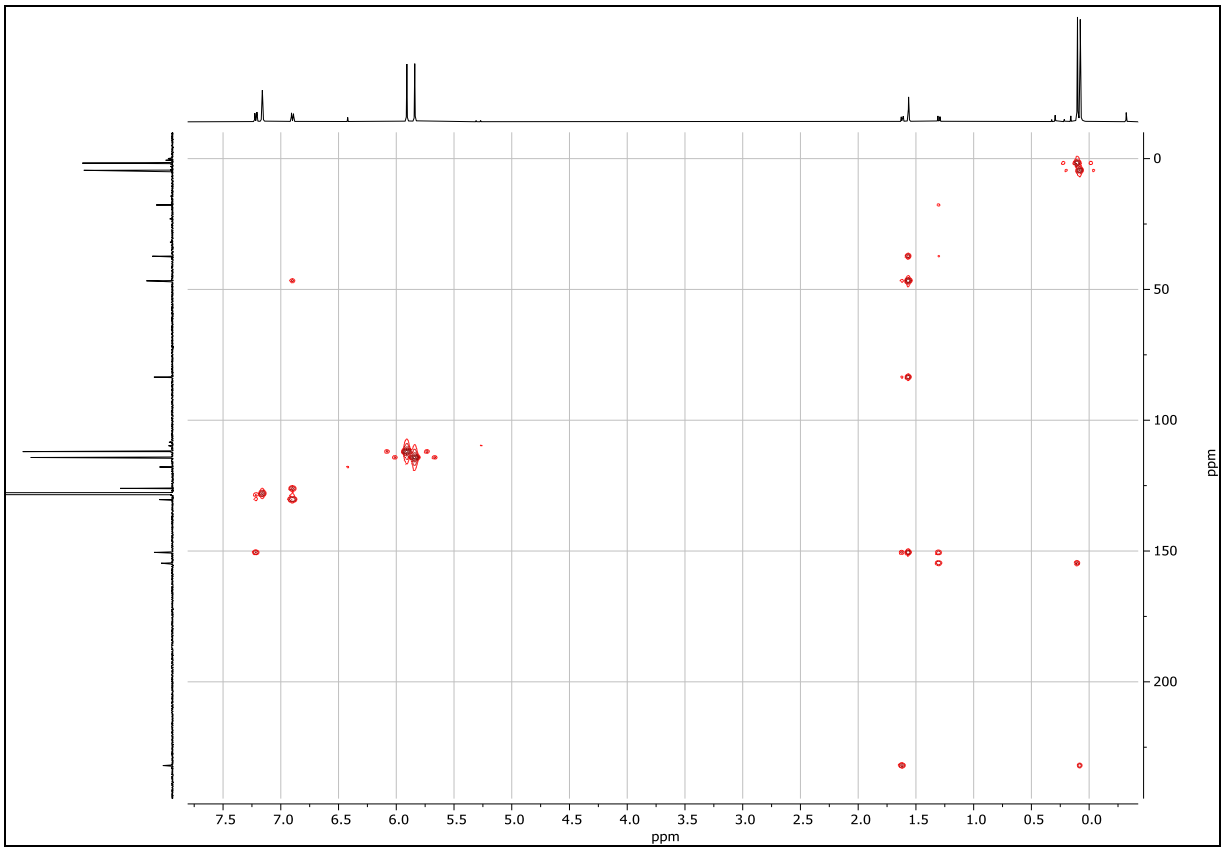

Figure S24: $^{1}H,^{13}C$ HMBC NMR spectrum of **2d** (500MHz, 126 MHz, C_6D_6, 298 K).

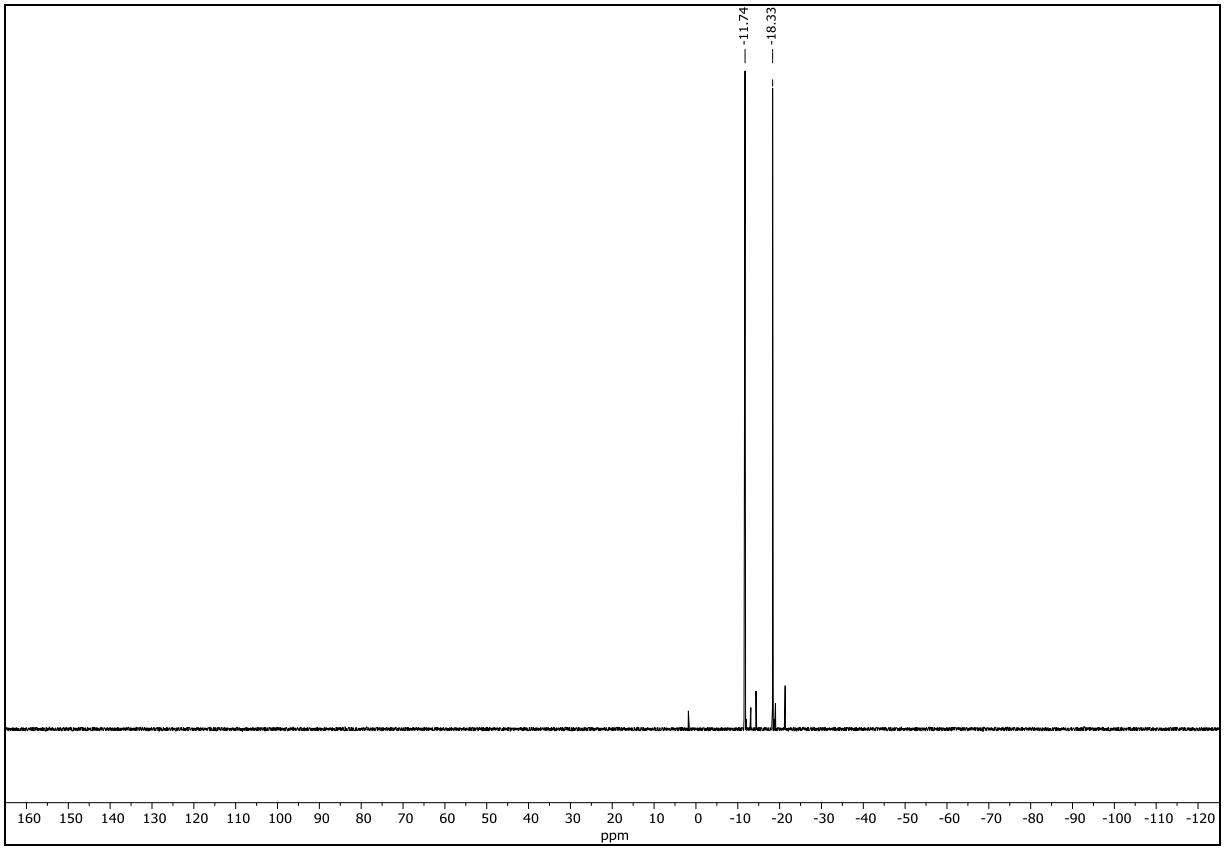

Figure S25: $^{29}Si\{^{1}H\}$ INEPT NMR spectrum of **2d** (99 MHz, C_6D_6, 298 K).

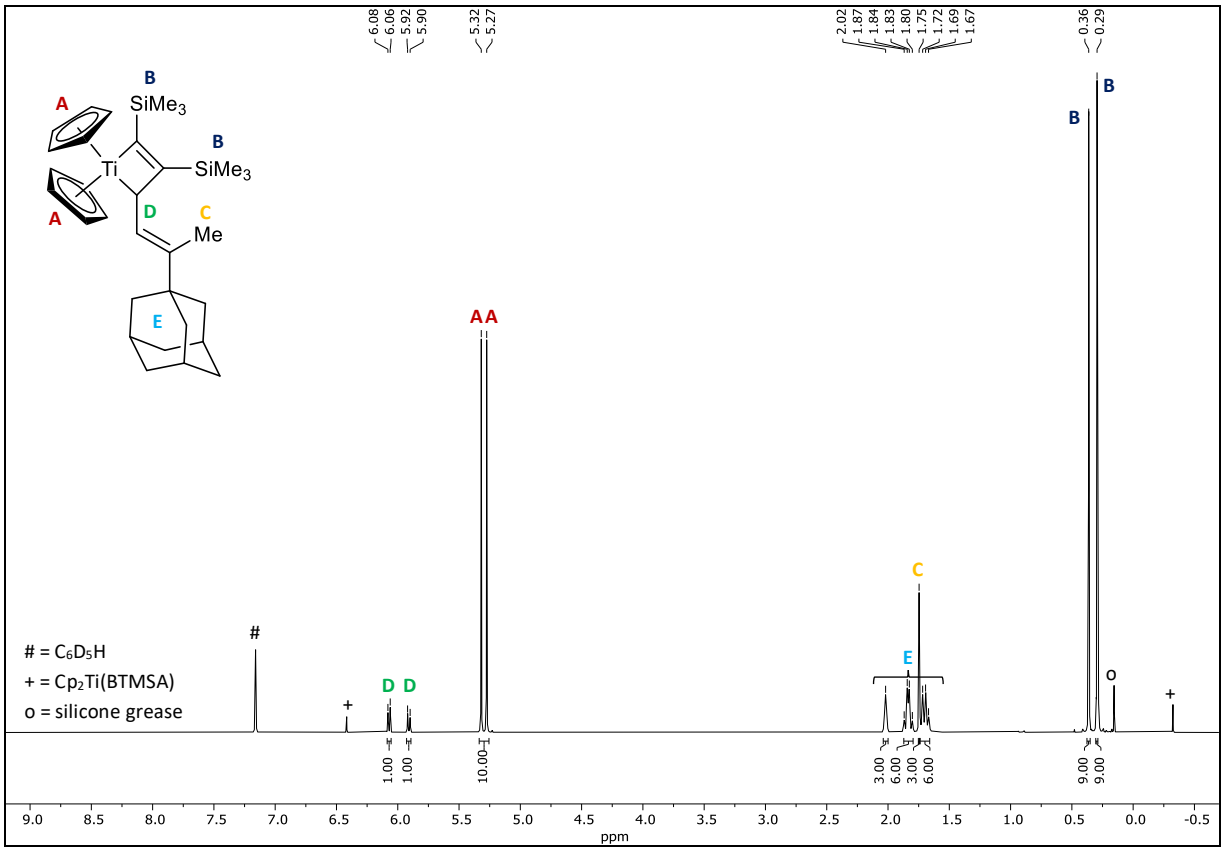

Figure S26: ^{1}H NMR spectrum of **3a** (500 MHz, C_6D_6, 298 K).

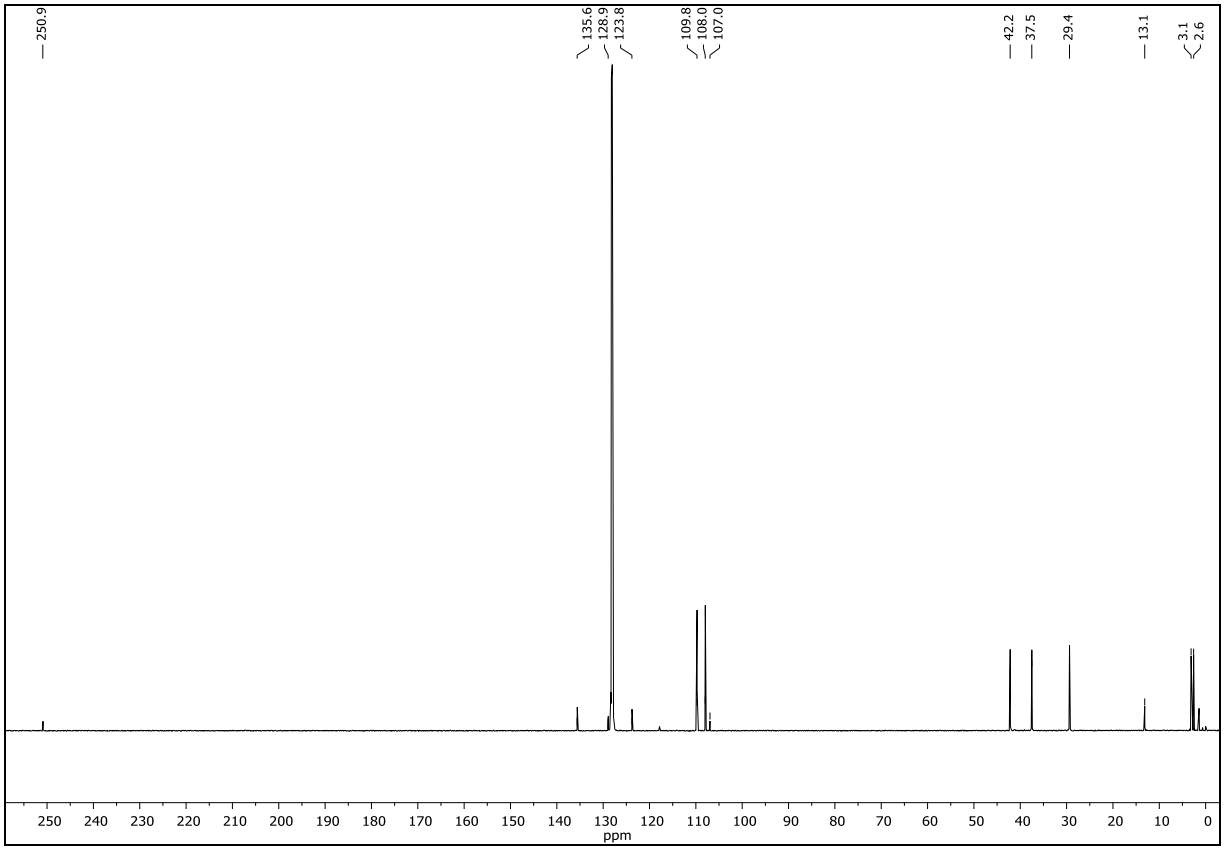

Figure S27: ^{13}C{^{1}H} NMR spectrum of **3a** (126 MHz, C_6D_6, 298 K).

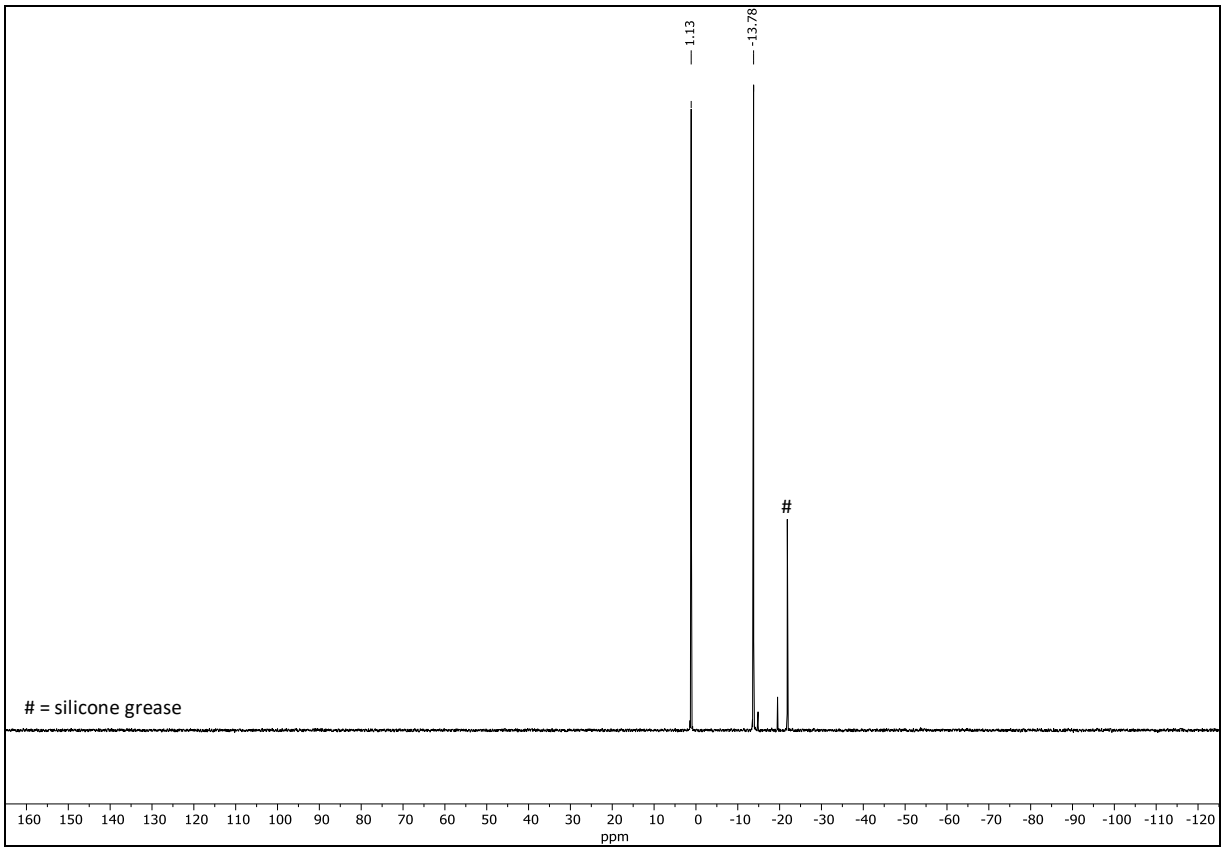

Figure S28: $^{29}Si\{^{1}H\}$ INEPT NMR spectrum of **3a** (99 MHz, C_6D_6, 298 K).

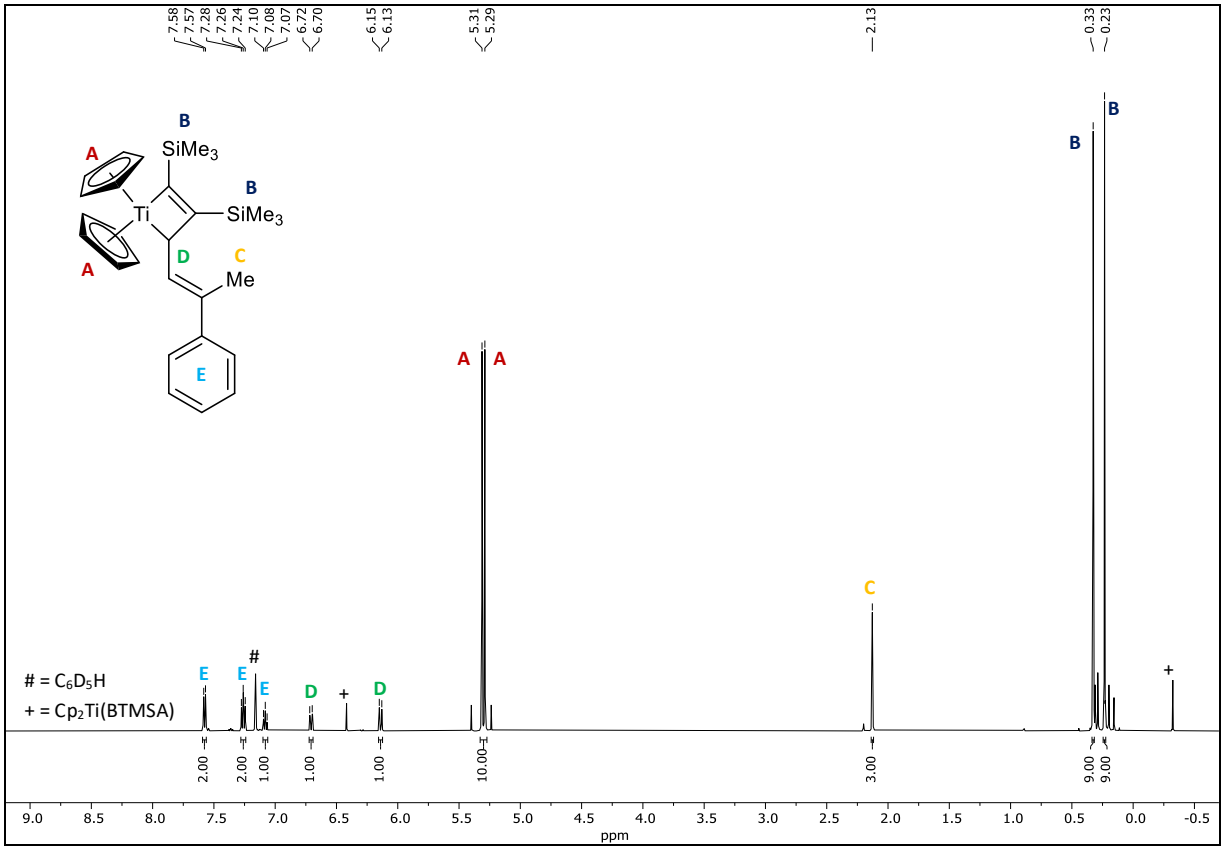

Figure S29: ^{1}H NMR spectrum of **3b** (500 MHz, C_6D_6, 298 K).

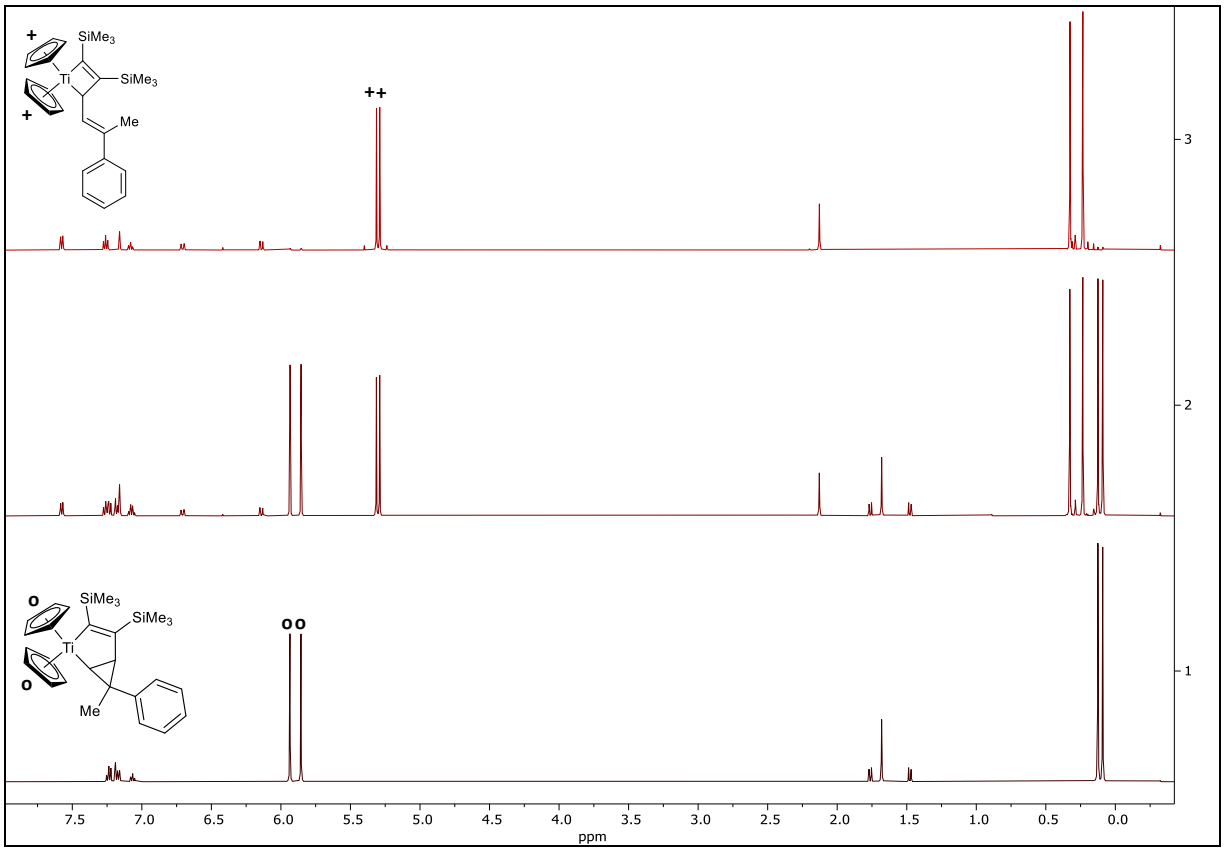

Figure S30: Stacked ^{1}H NMR spectra of **3b** (500 MHz, C_6D_6, 298 K) after heating the NMR sample at 60 °C for 1 = 0 h, 2 = 8 h, 3 = 24 h.

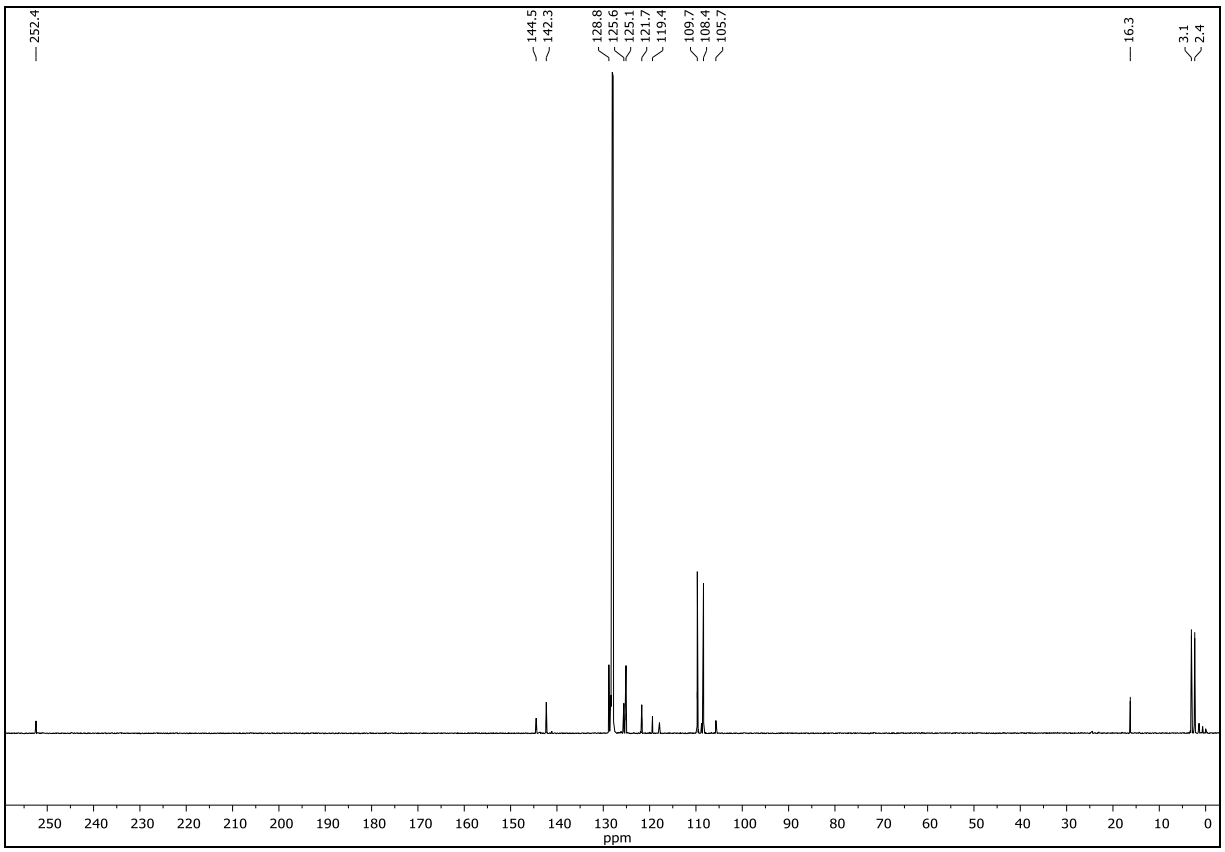

Figure S31: $^{13}C\{^{1}H\}$ NMR spectrum of **3b** (126 MHz, C_6D_6, 298 K).

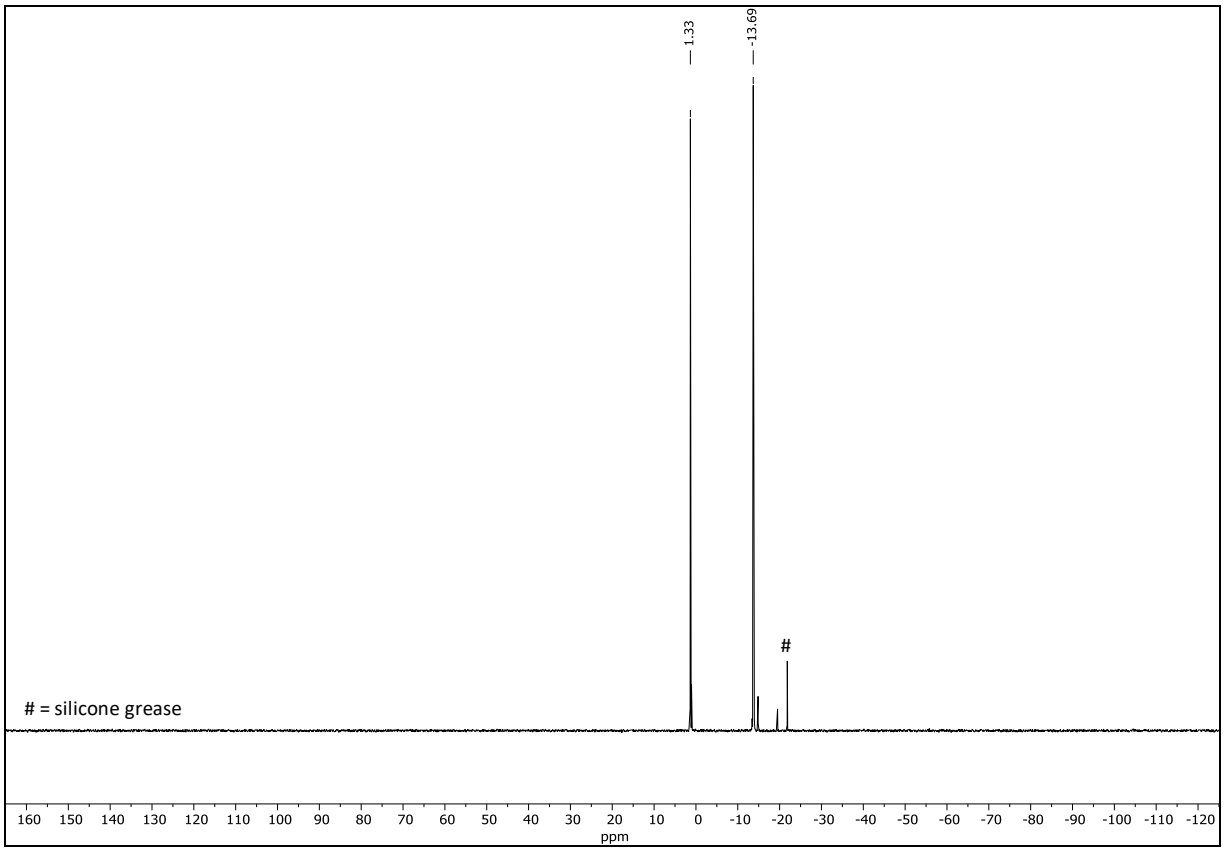

Figure S32: $^{29}Si\{^{1}H\}$ INEPT NMR spectrum of **3b** (99 MHz, C_6D_6, 298 K).

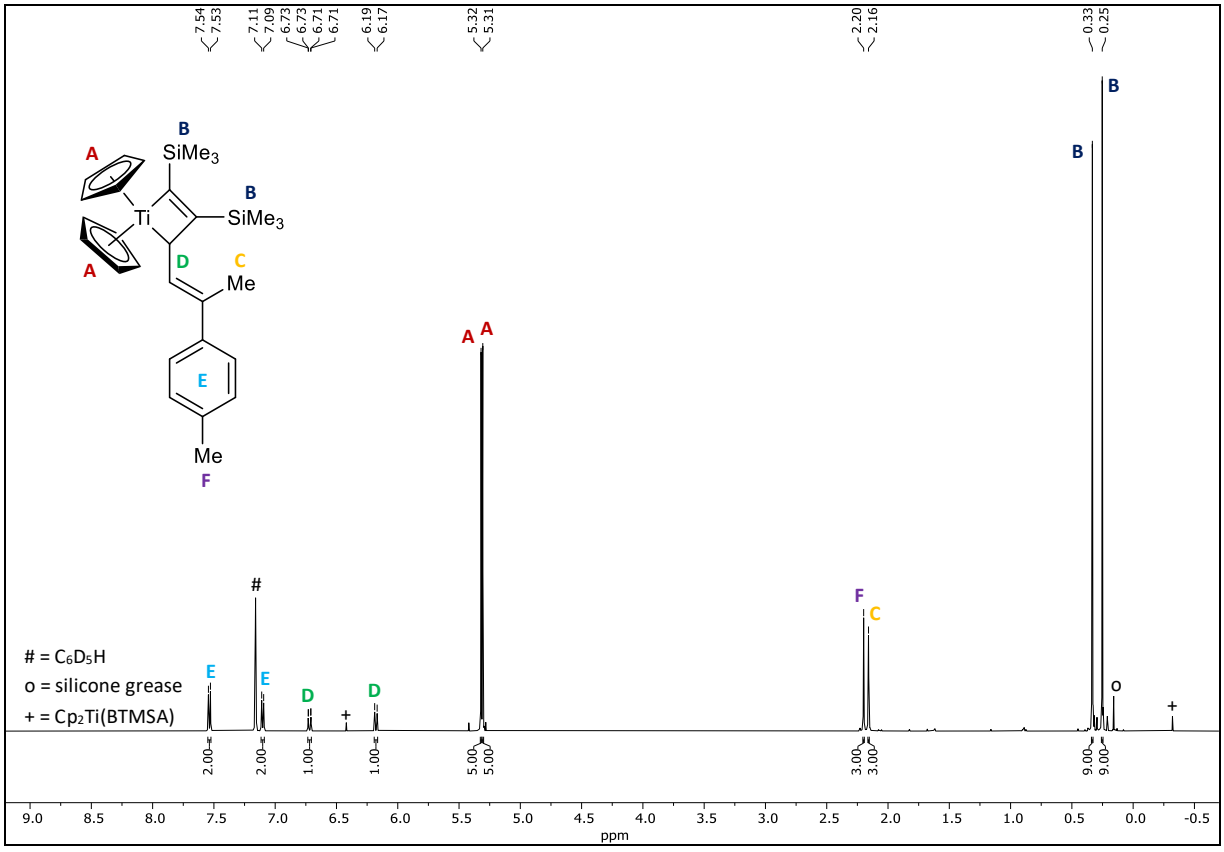

Figure S33: ^{1}H NMR spectrum of **3c** (500 MHz, C_6D_6, 298 K).

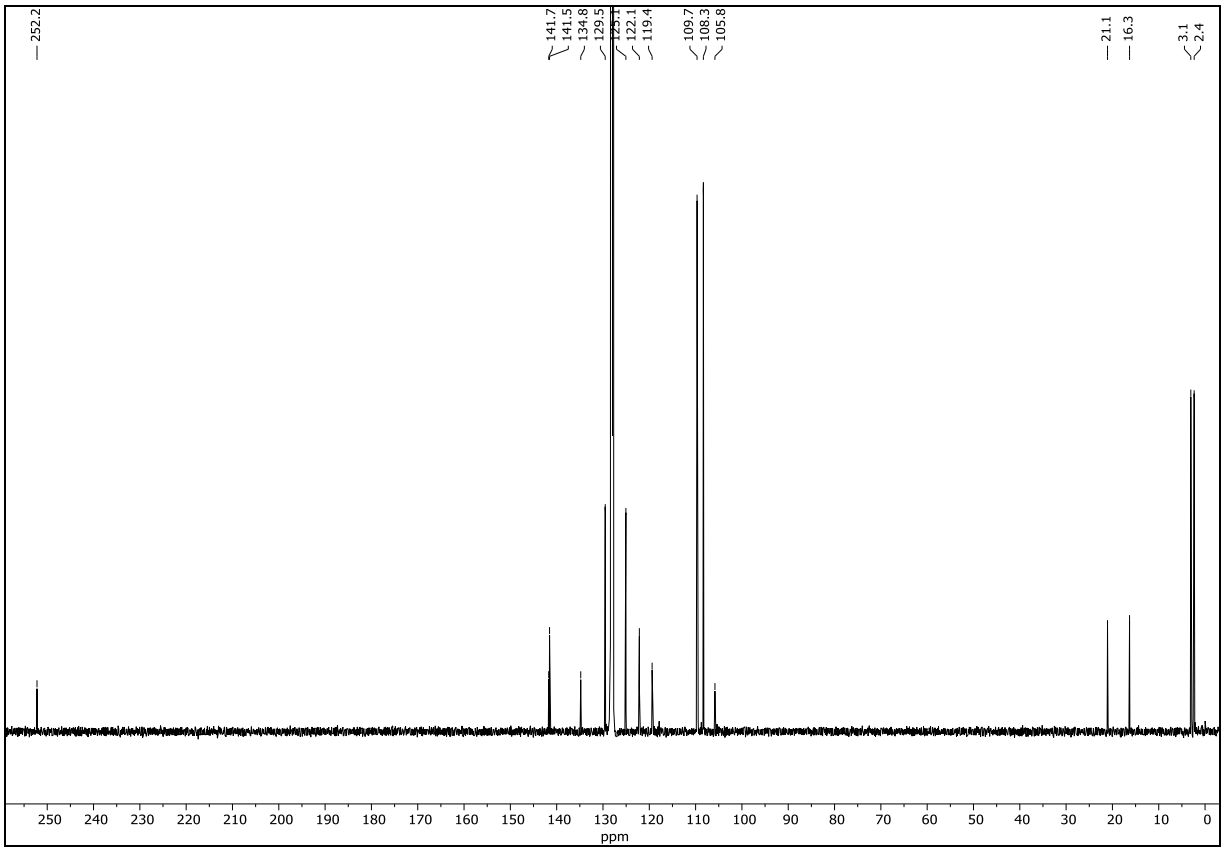

Figure S34: $^{13}C\{^{1}H\}$ NMR spectrum of **3c** (126 MHz, C_6D_6, 298 K).

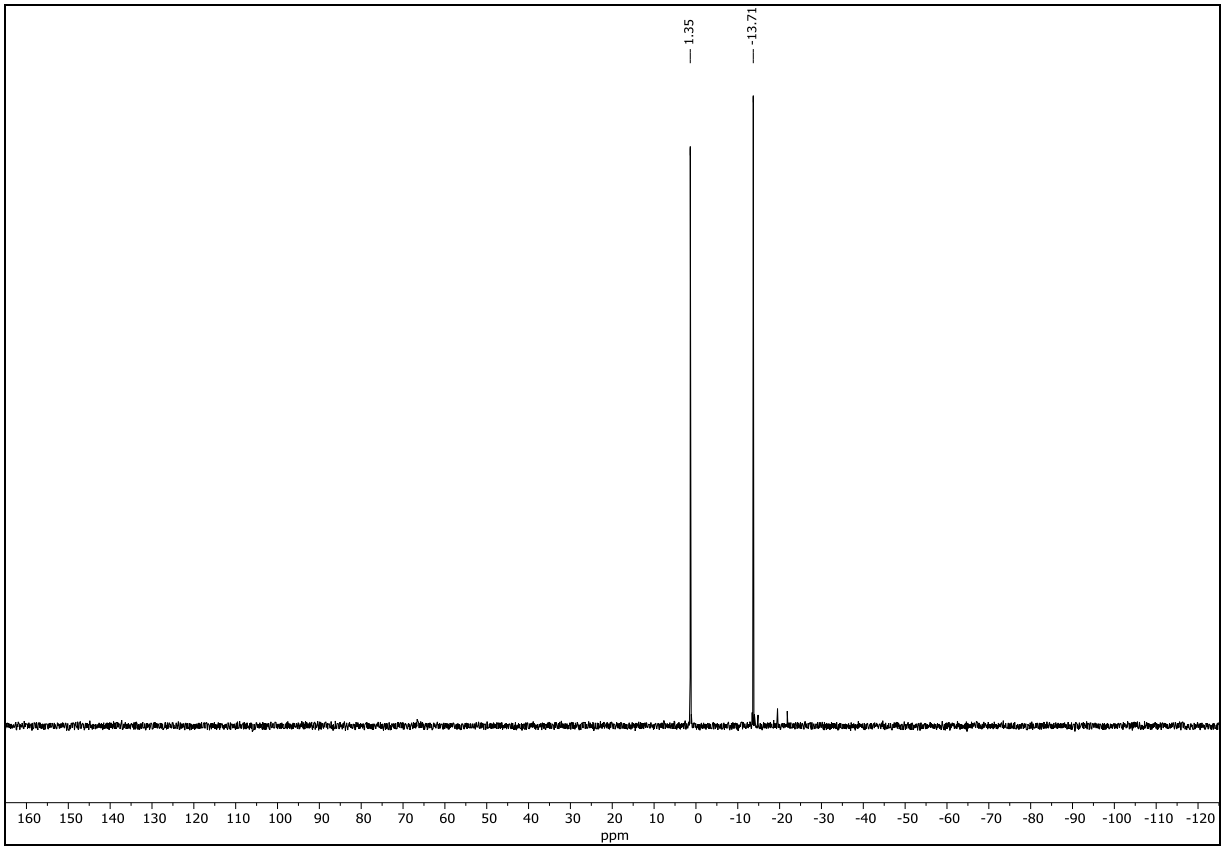

Figure S35: $^{29}Si\{^{1}H\}$ INEPT NMR spectrum of **3c** (99 MHz, C_6D_6, 298 K).

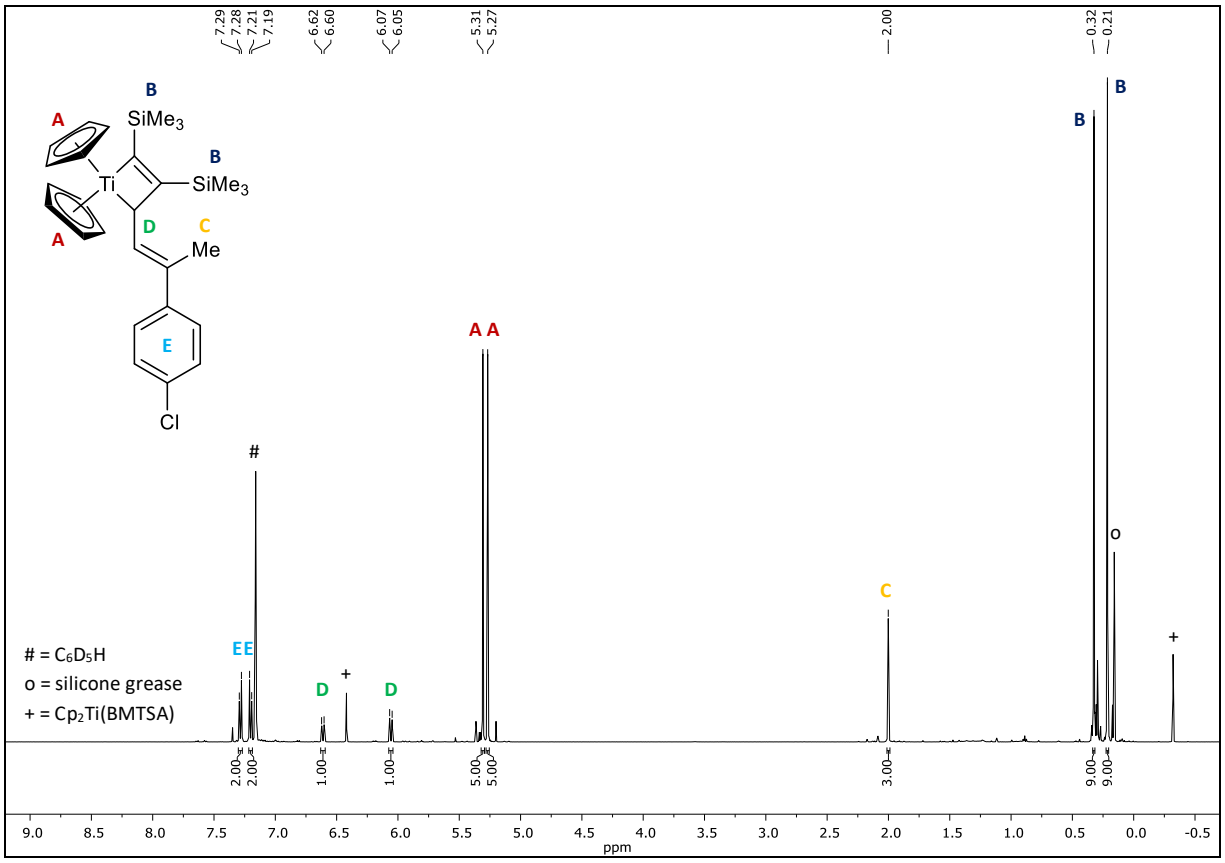

Figure S36: ^{1}H NMR spectrum of **3d** (500 MHz, C_6D_6, 298 K).

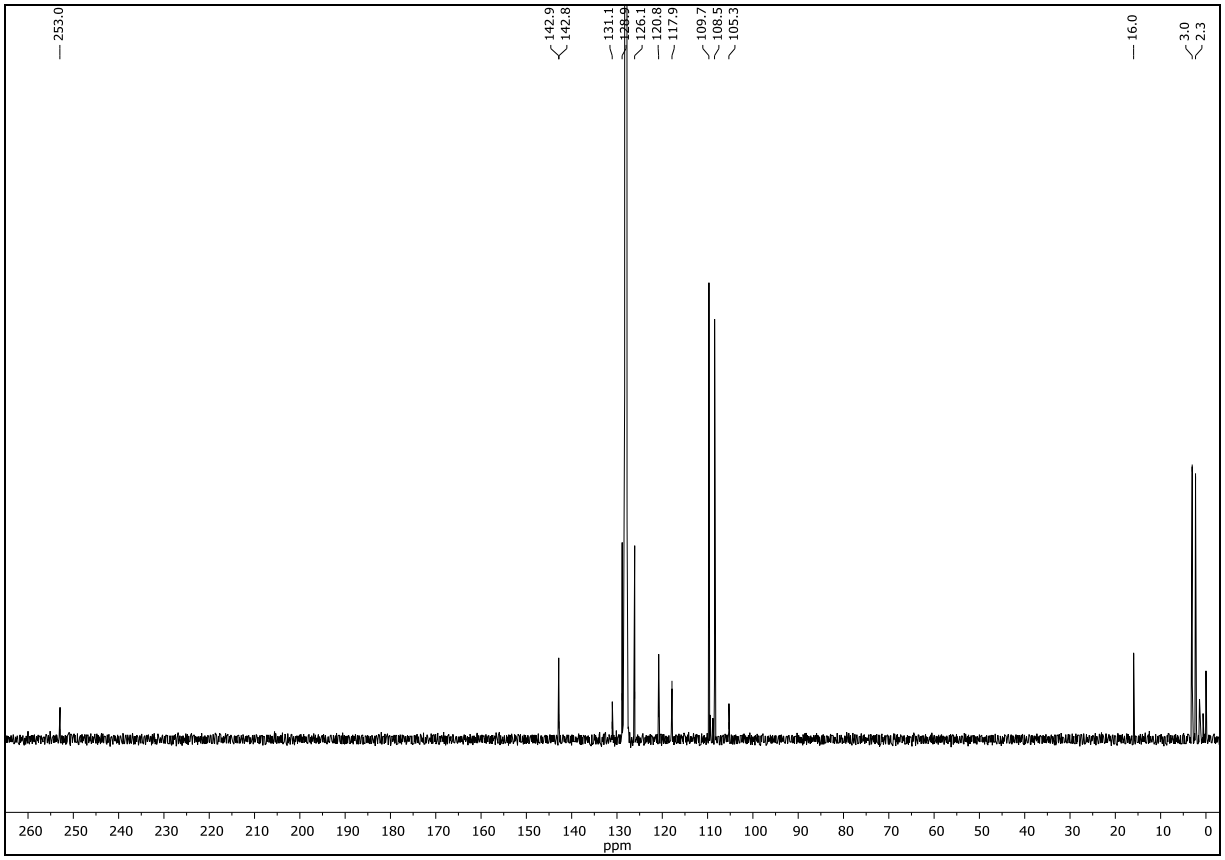

Figure S37: $^{13}C\{^{1}H\}$ NMR spectrum of **3d** (126 MHz, C_6D_6, 298 K).

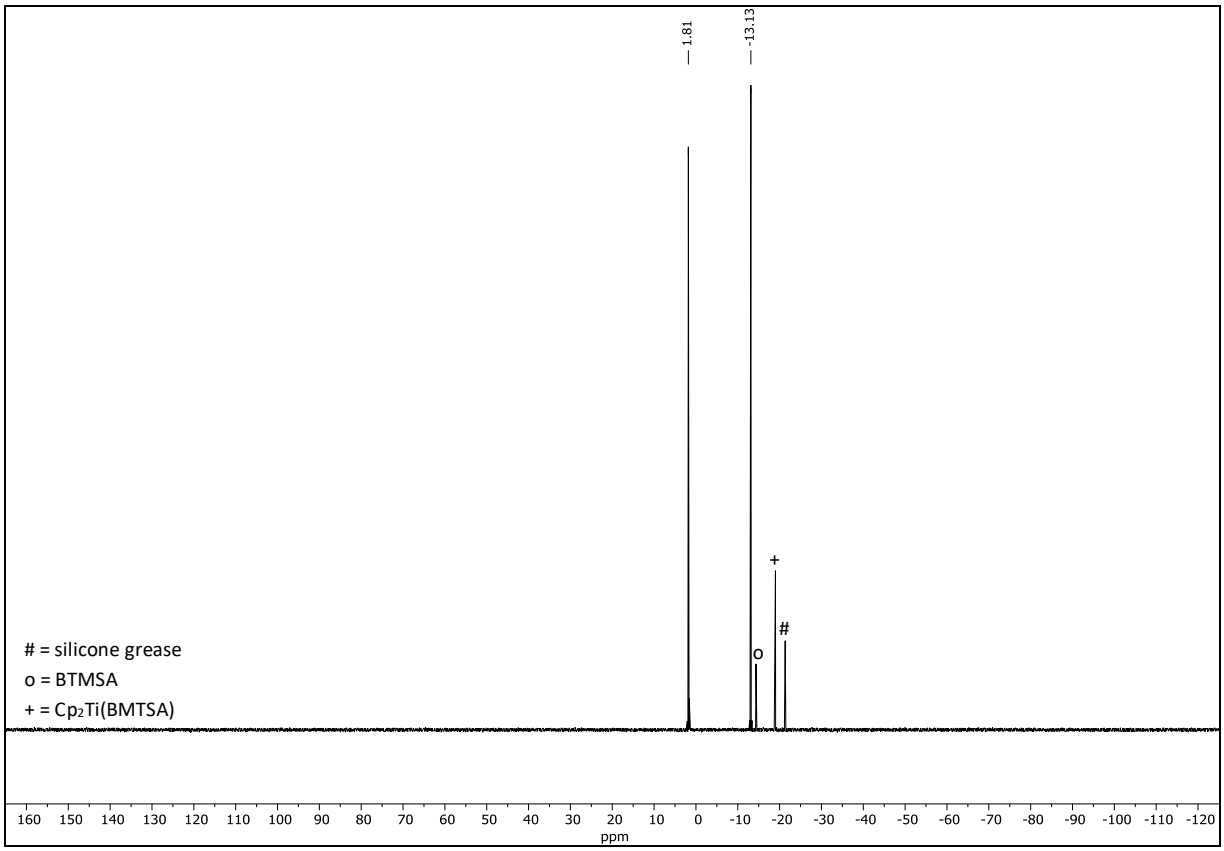

Figure S38: $^{29}Si\{^{1}H\}$ INEPT NMR spectrum of **3d** (99 MHz, C_6D_6, 298 K).

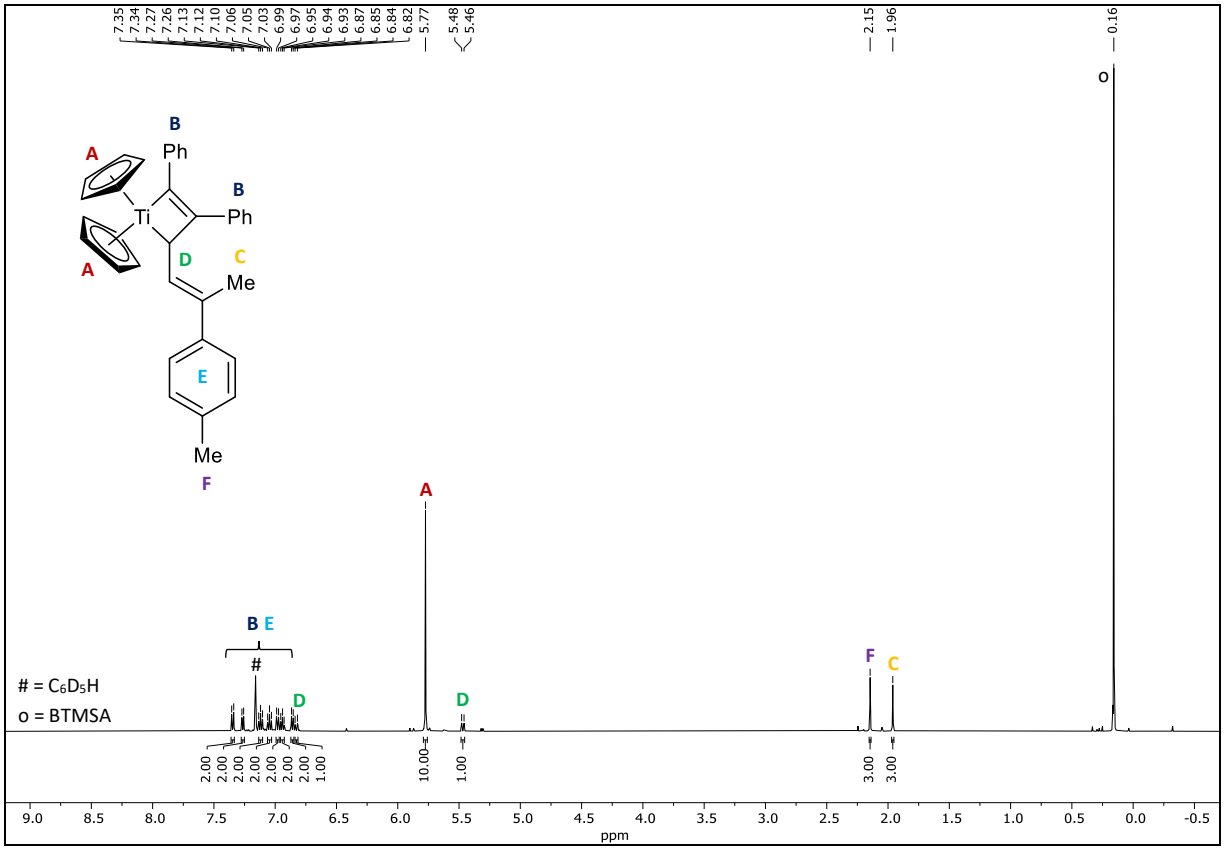

Figure S39: ^{1}H NMR spectrum of **4c** (500 MHz, C_6D_6, 298 K), NMR experiment (n = 0.050 mmol).

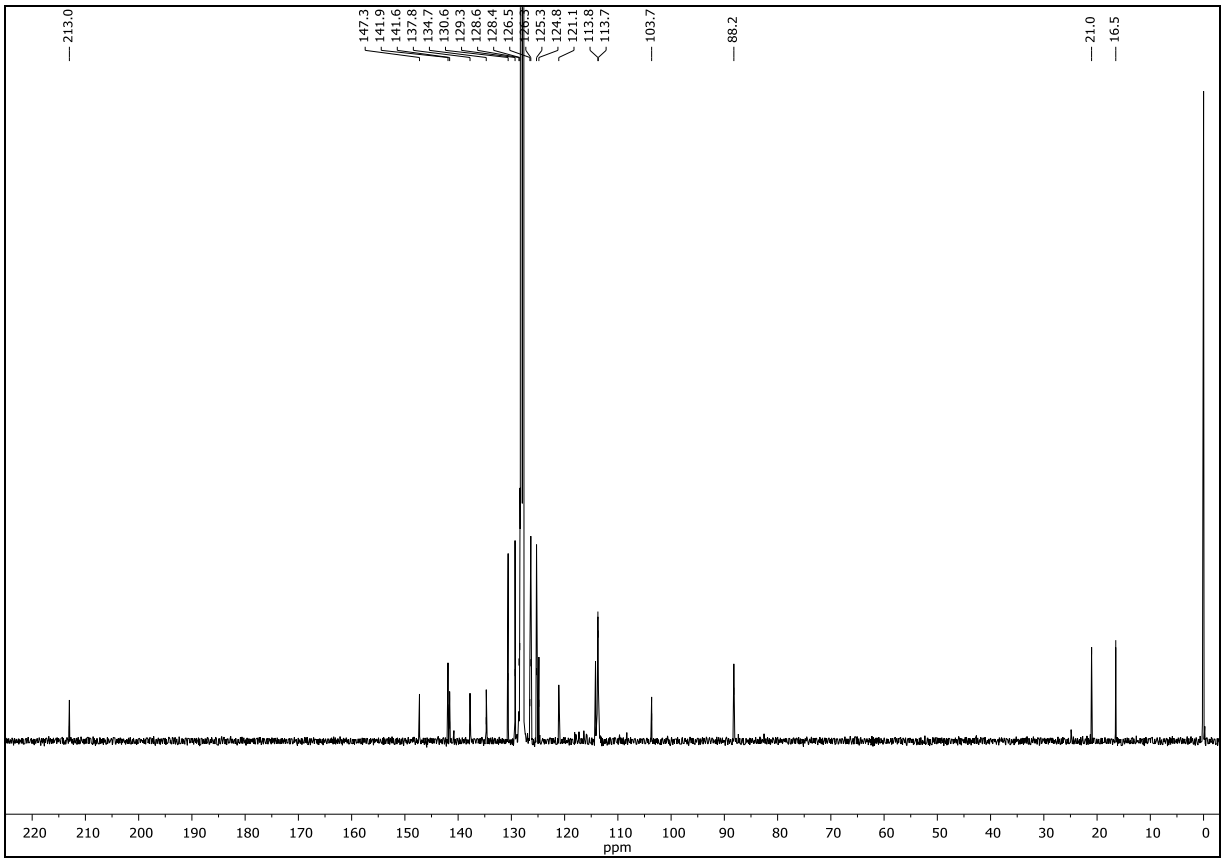

Figure S40: $^{13}C\{^{1}H\}$ NMR spectrum of **4c** (126 MHz, C_6D_6, 298 K), NMR experiment (n = 0.050 mmol).

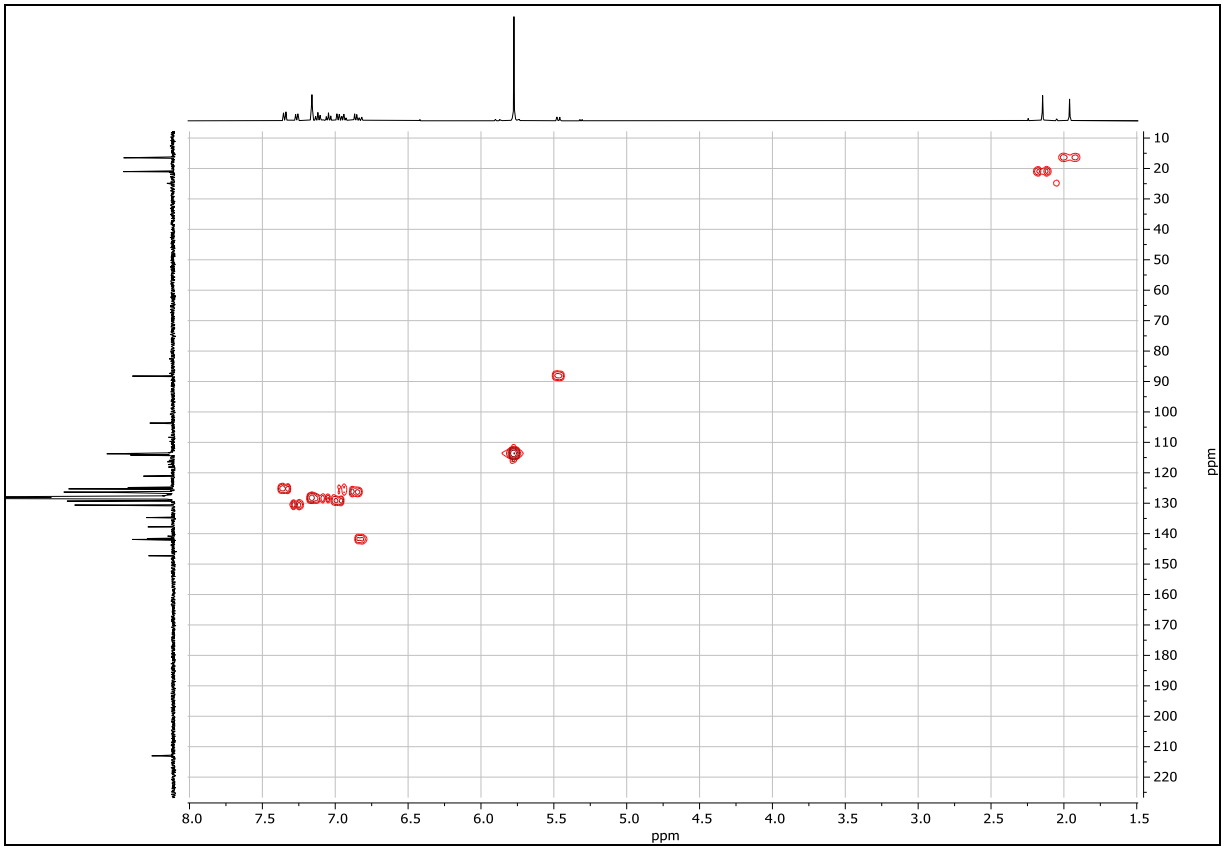

Figure S41: $^{1}H,^{13}C$ HMQC NMR spectrum of **4c** (500 MHz, 126 MHz, C_6D_6, 298 K), NMR experiment (n = 0.050 mmol).

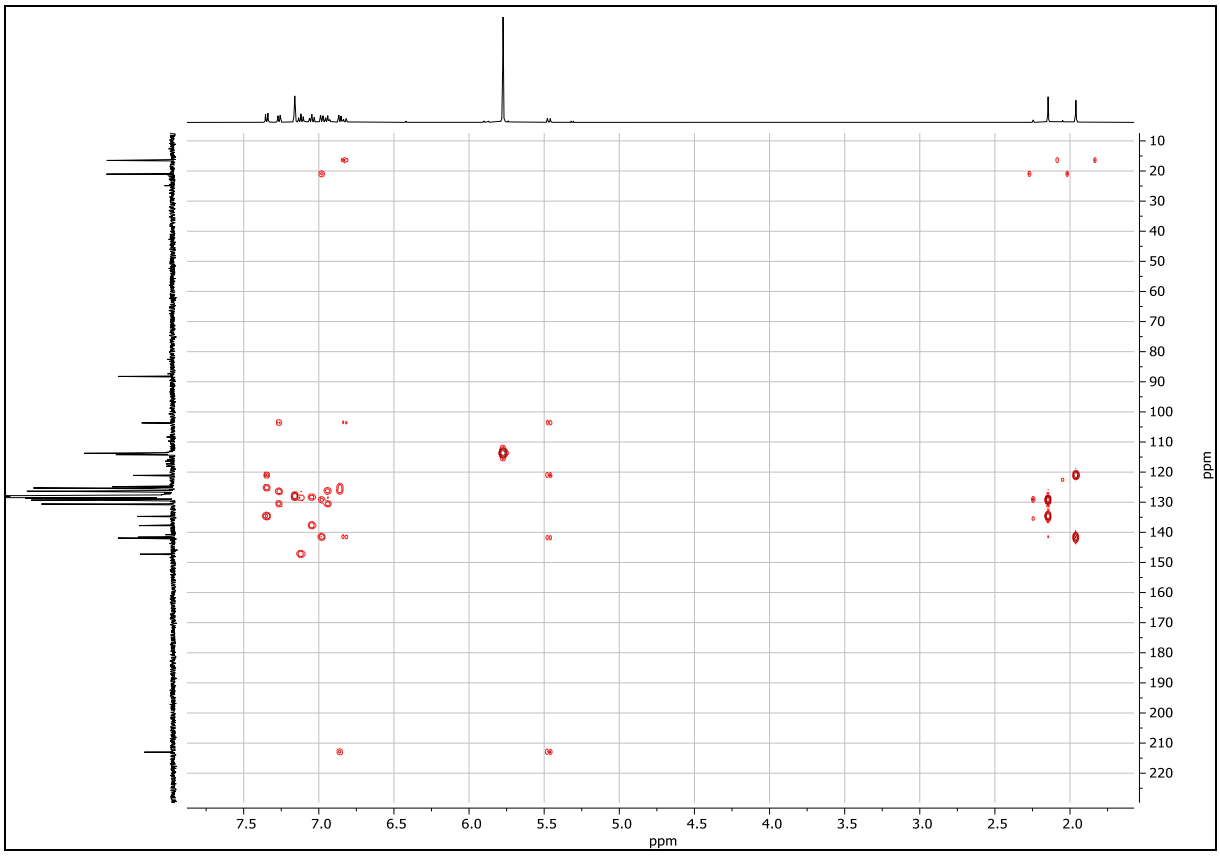

Figure S42: $^{1}H,^{13}C$ HMBC NMR spectrum of **4c** (500 MHz, 126 MHz, C_6D_6, 298 K), NMR experiment (n = 0.050 mmol).

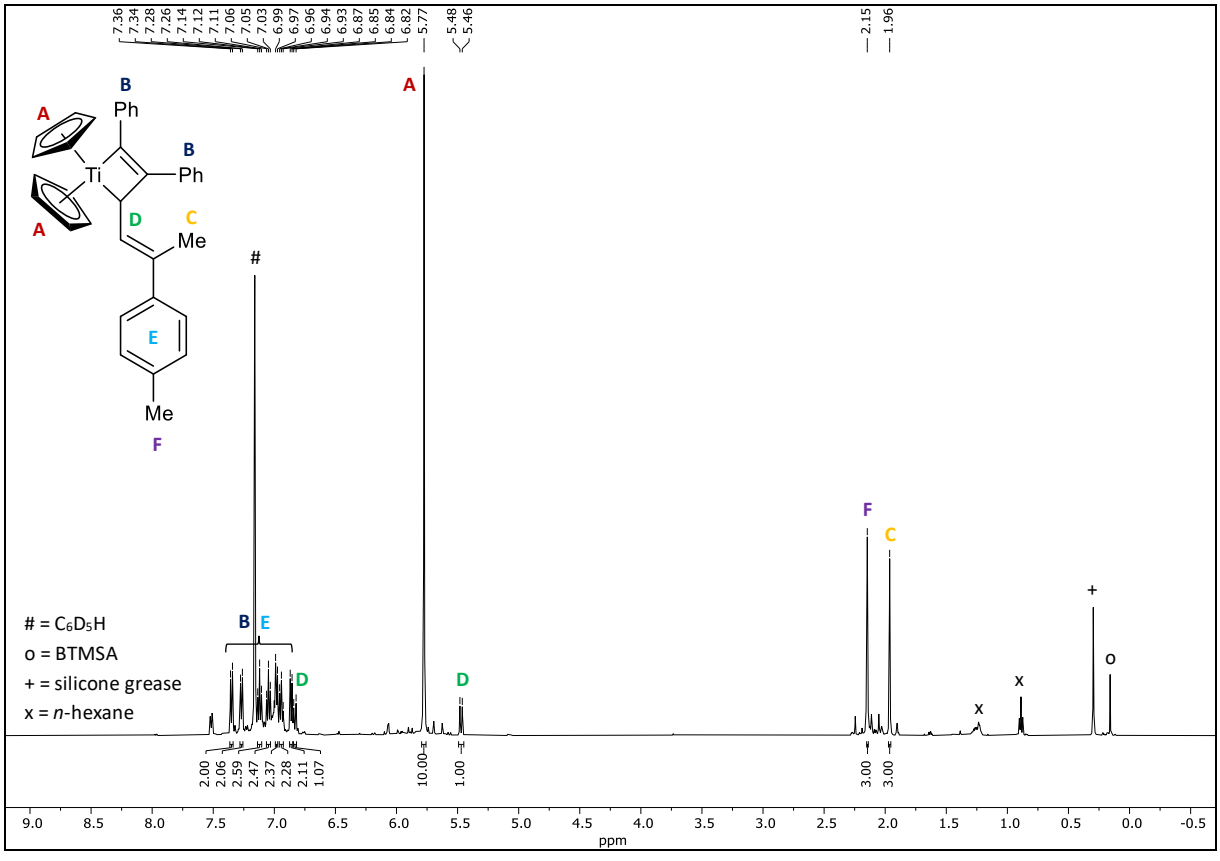

Figure S43: ^{1}H NMR spectrum of isolated **4c** (500 MHz, C_6D_6, 298 K).

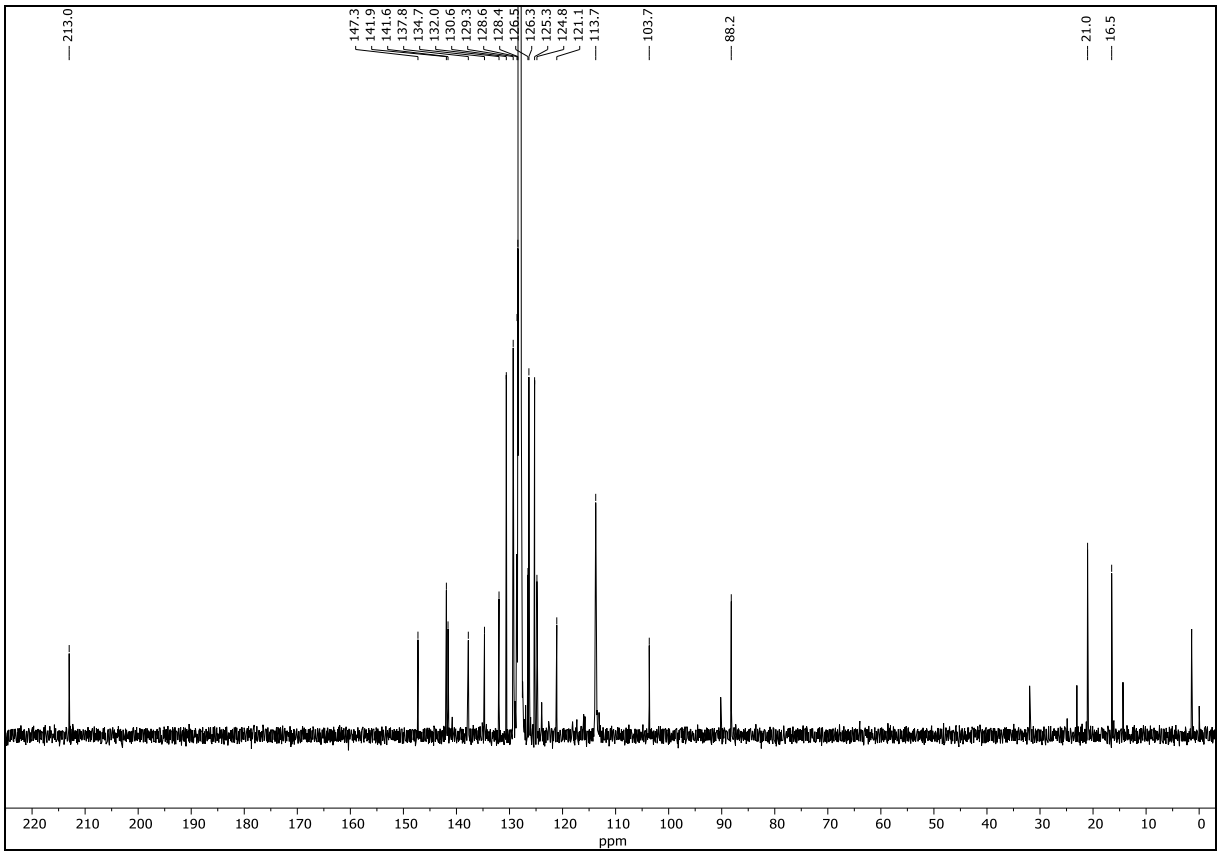

Figure S44: $^{13}C\{^{1}H\}$ NMR spectrum of isolated **4c** (126 MHz, C_6D_6, 298 K).

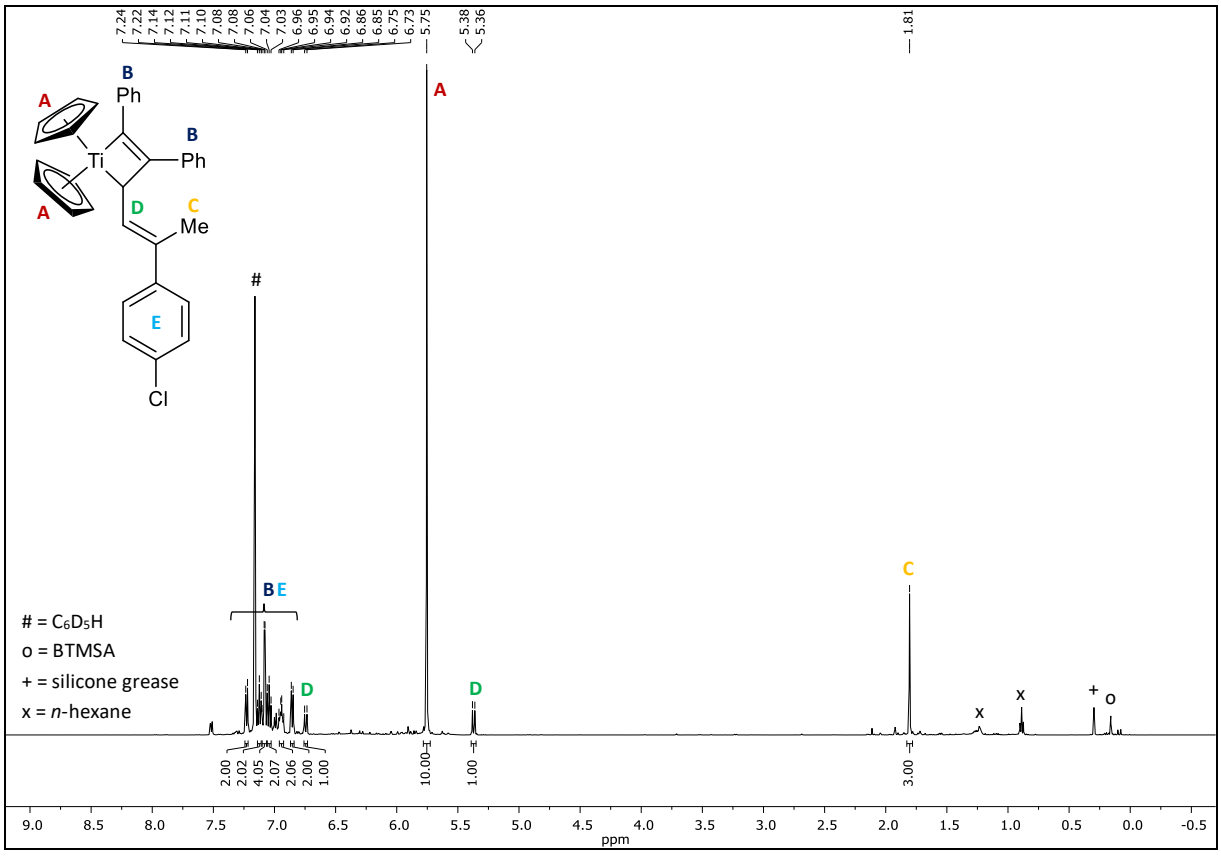

Figure S45: ^{1}H NMR spectrum of **4d** (500 MHz, C_6D_6, 298 K).

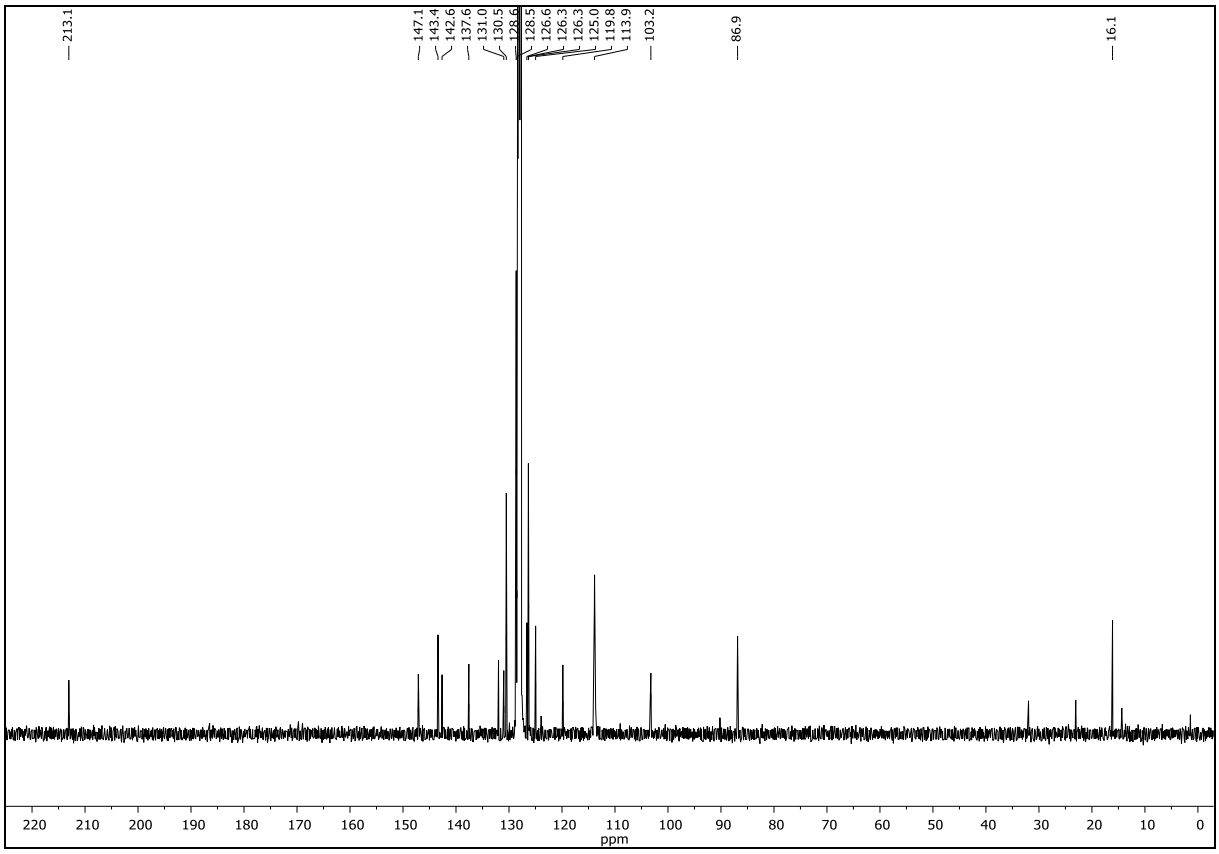

Figure S46: $^{13}C\{^{1}H\}$ NMR spectrum of **4d** (126 MHz, C_6D_6, 298 K).

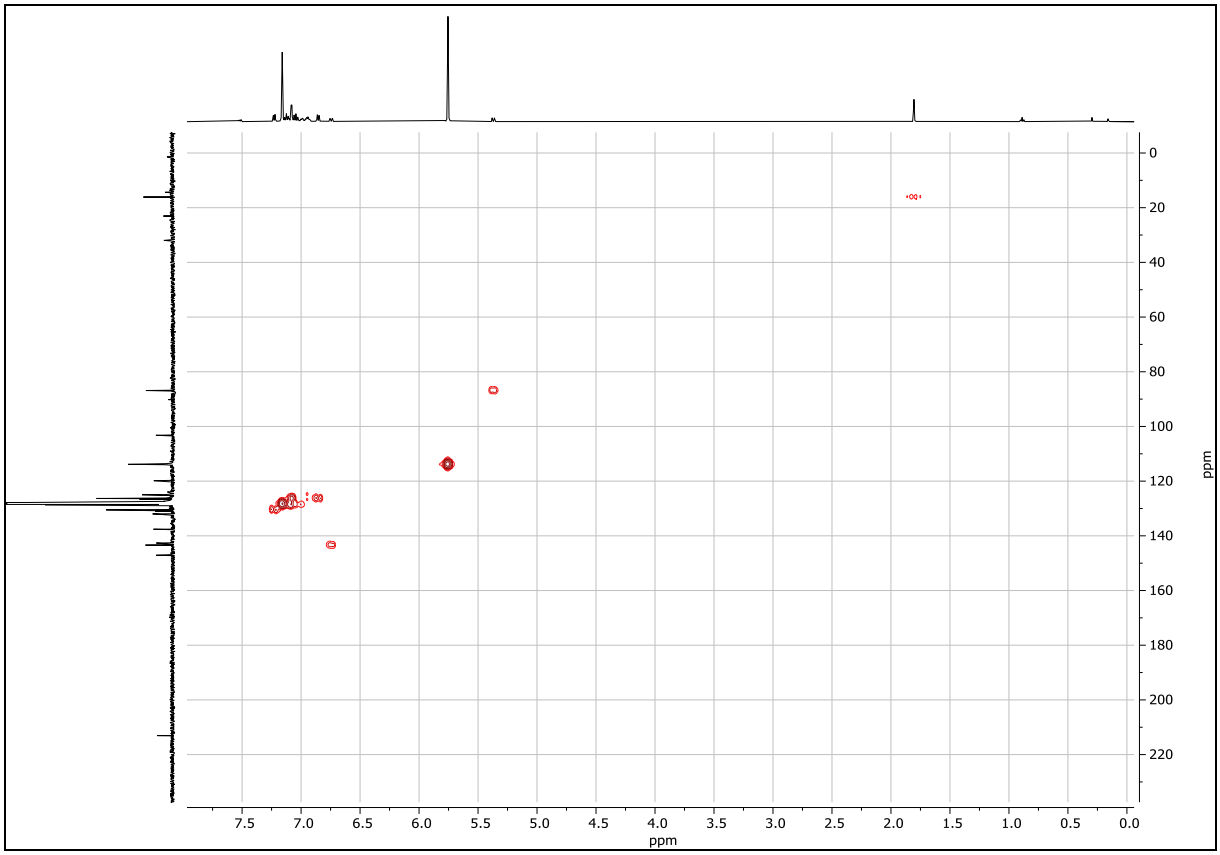

Figure S47: $^{1}H,^{13}C$ HMQC NMR spectrum of **4d** (500 MHz, 126 MHz, C_6D_6, 298 K).

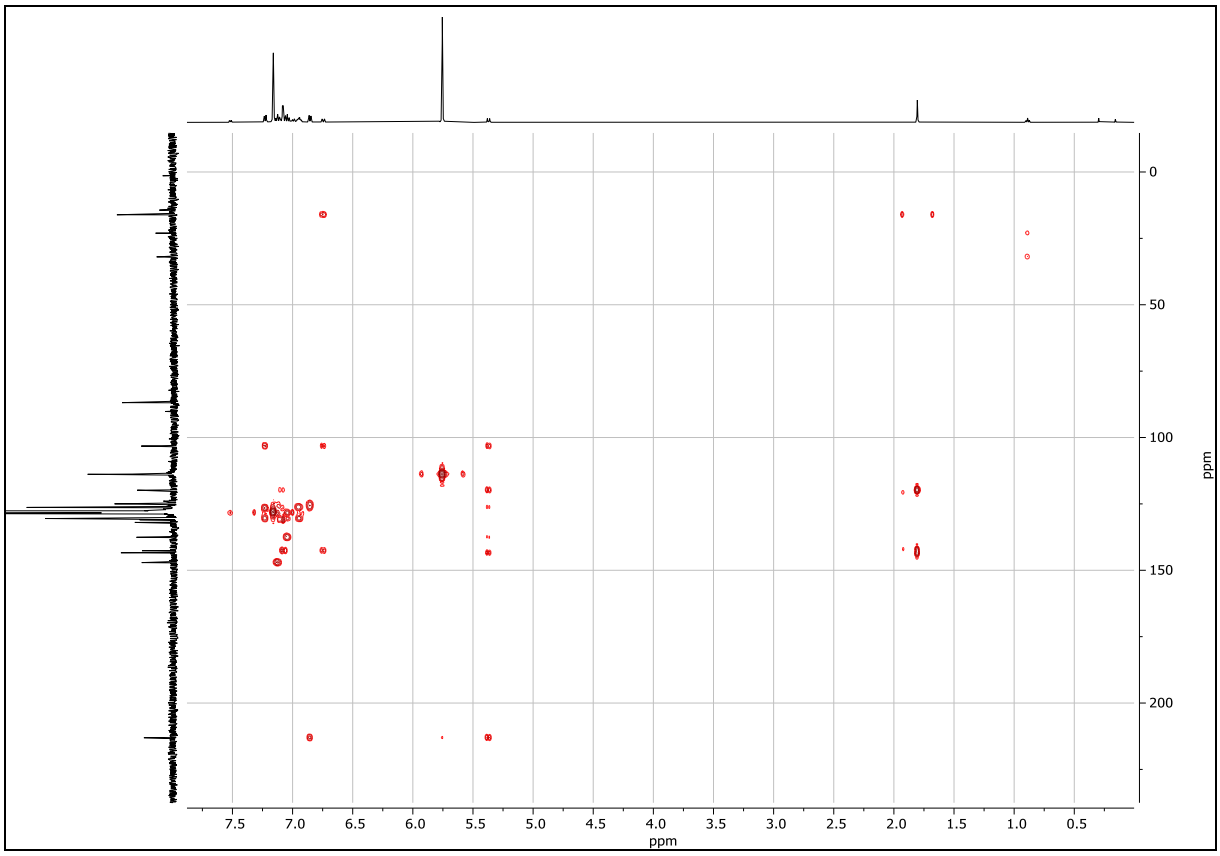

Figure S48: $^{1}H,^{13}C$ HMBC NMR spectrum of **4d** (500 MHz, 126 MHz, C_6D_6, 298 K).

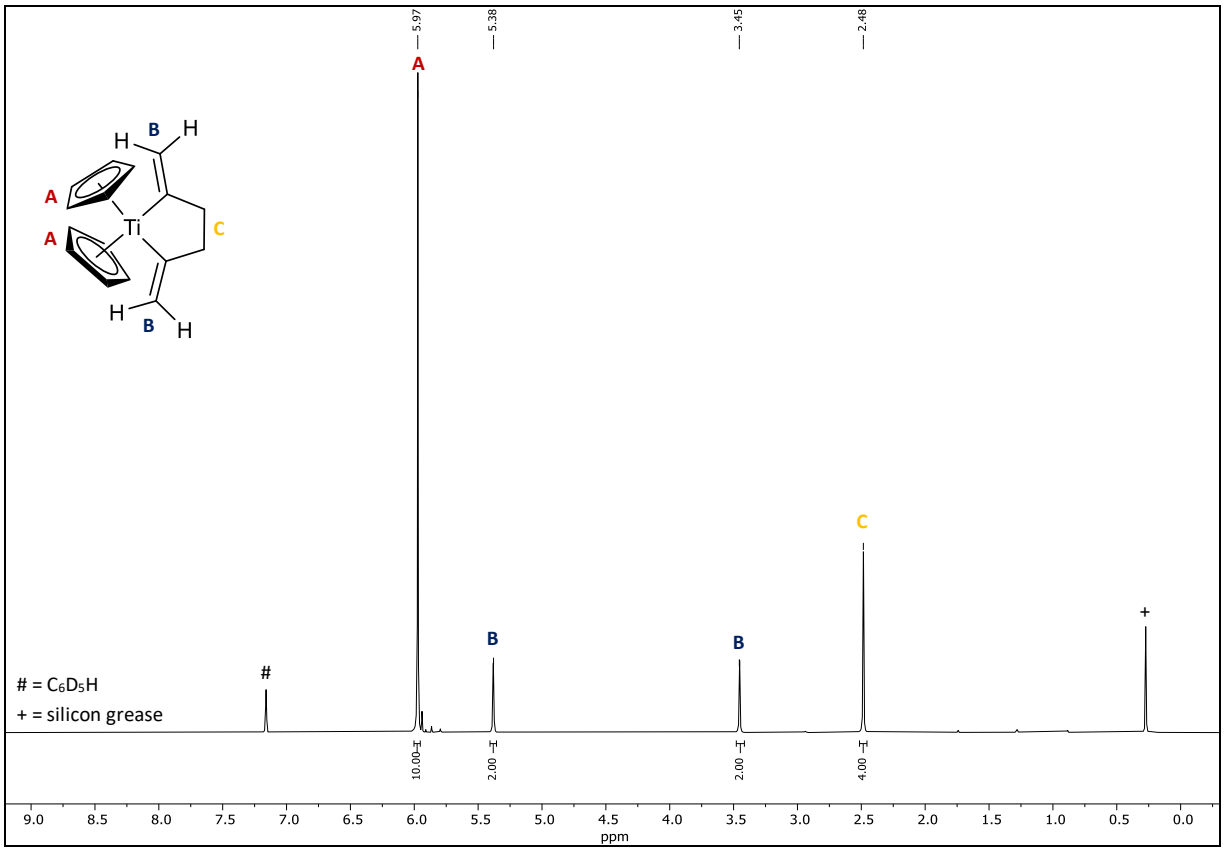

Figure S49: ^{1}H NMR spectrum of **5a** (500 MHz, C_6D_6, 305 K).

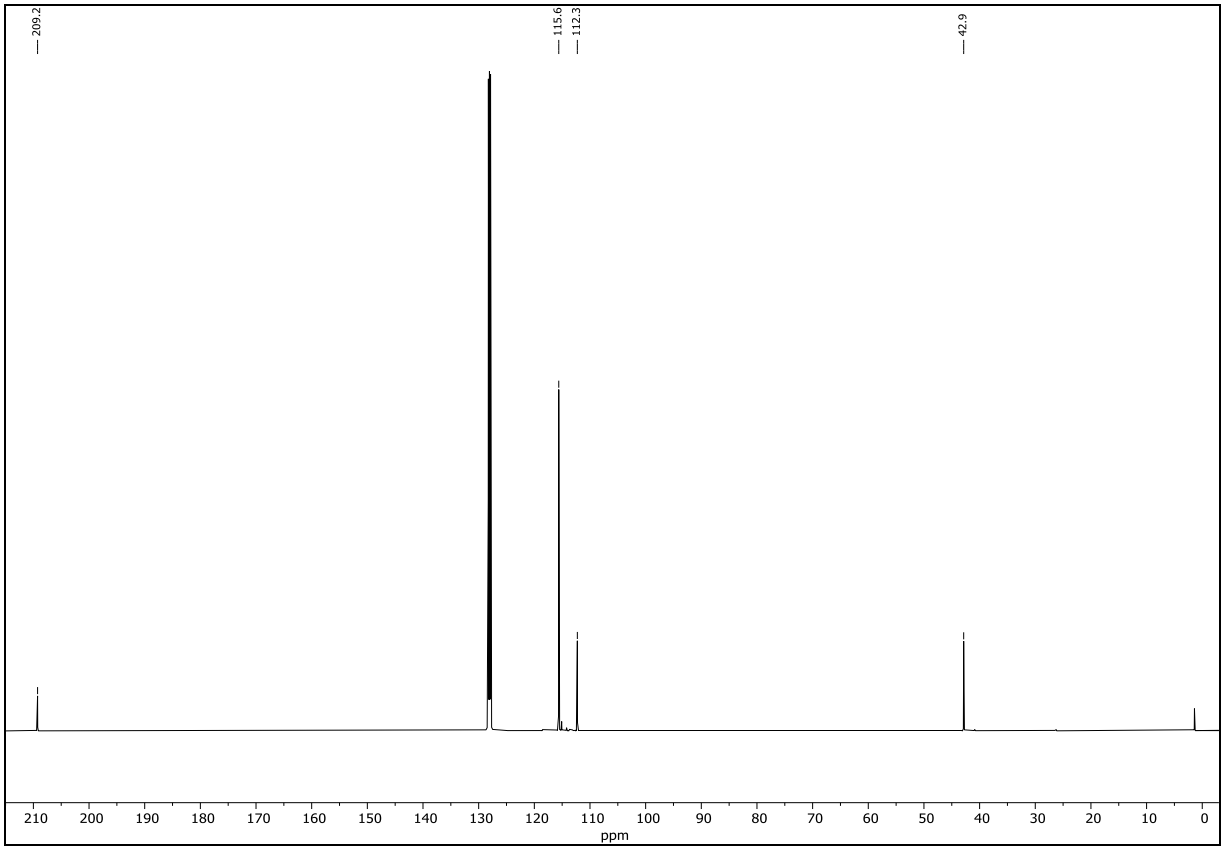

Figure S50: ^{13}C{^{1}H} NMR spectrum of **5a** (126 MHz, C_6D_6, 305 K).

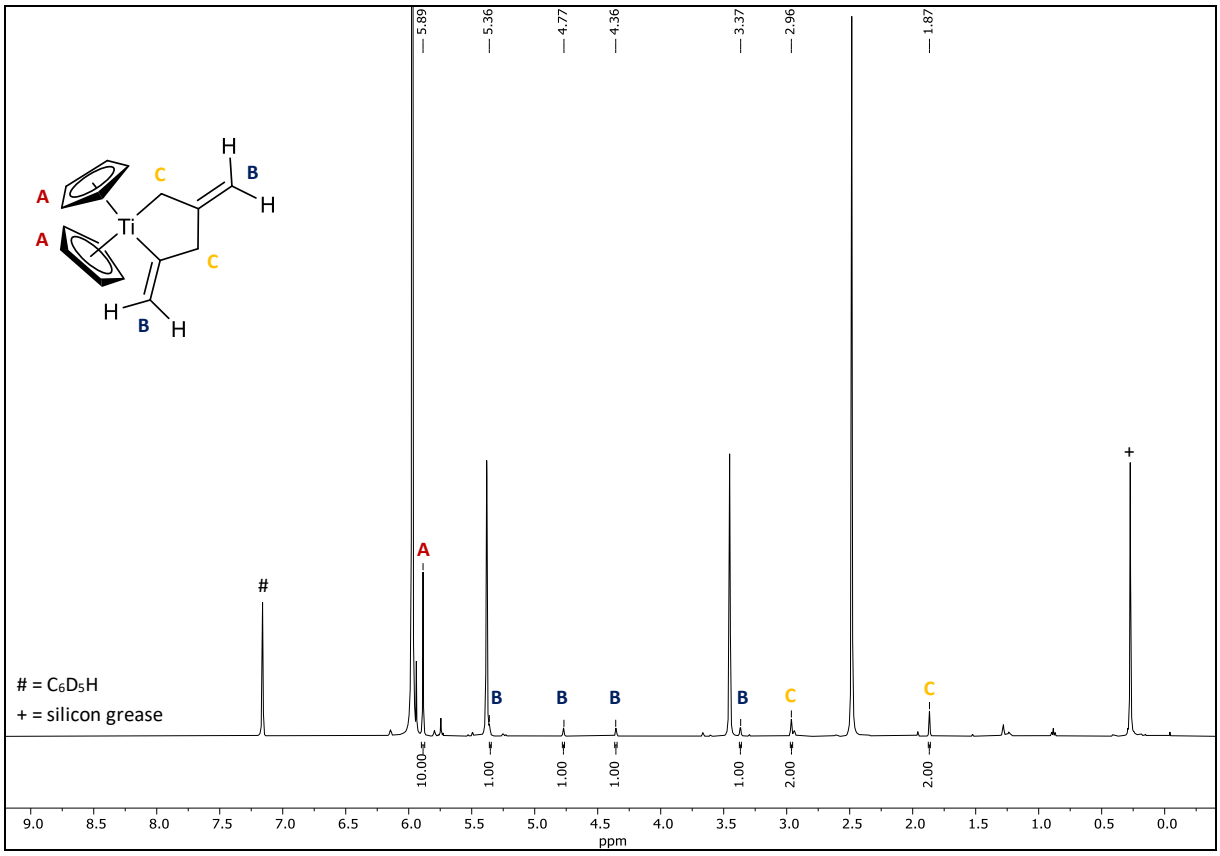

Figure S51: ^{1}H NMR spectrum of **5a'** (500 MHz, C_6D_6, 305 K).

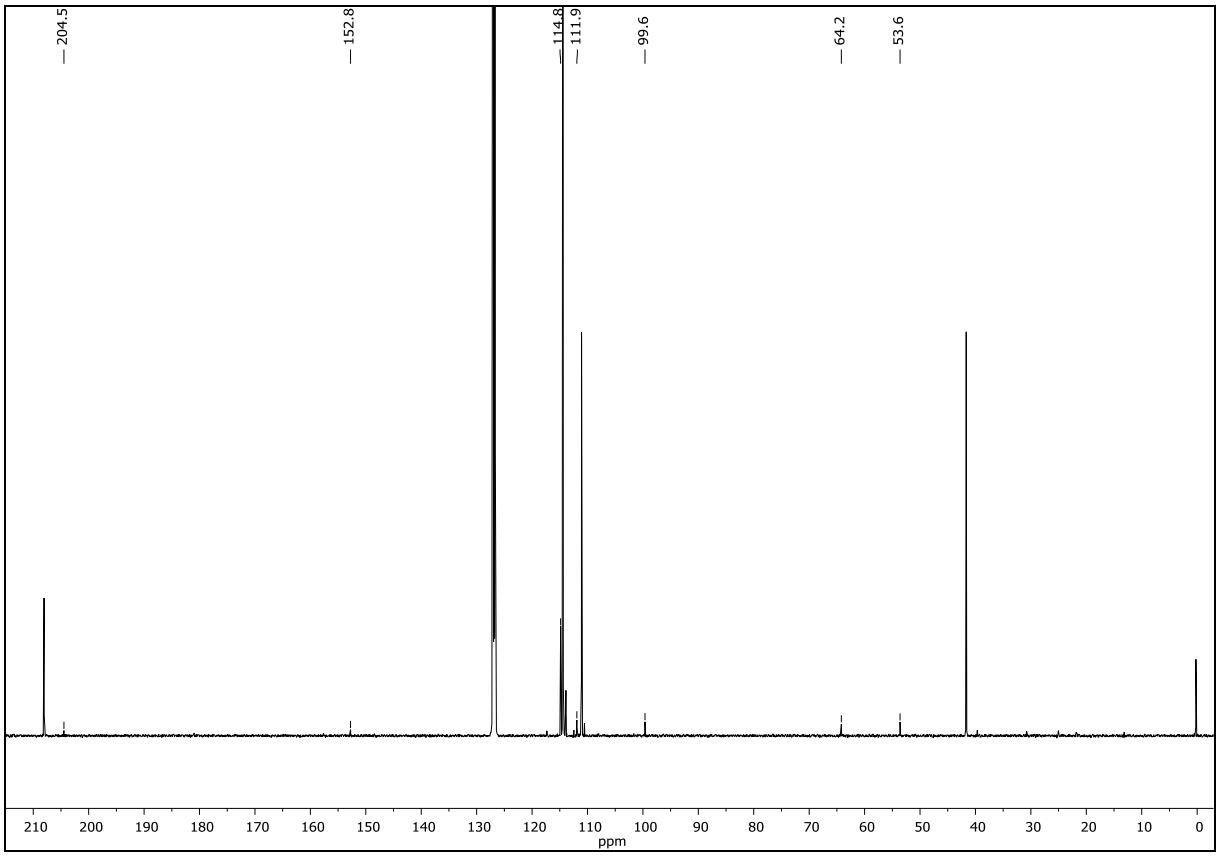

Figure S52: $^{13}C\{^{1}H\}$ NMR spectrum of **5a'** (126 MHz, C_6D_6, 305 K).

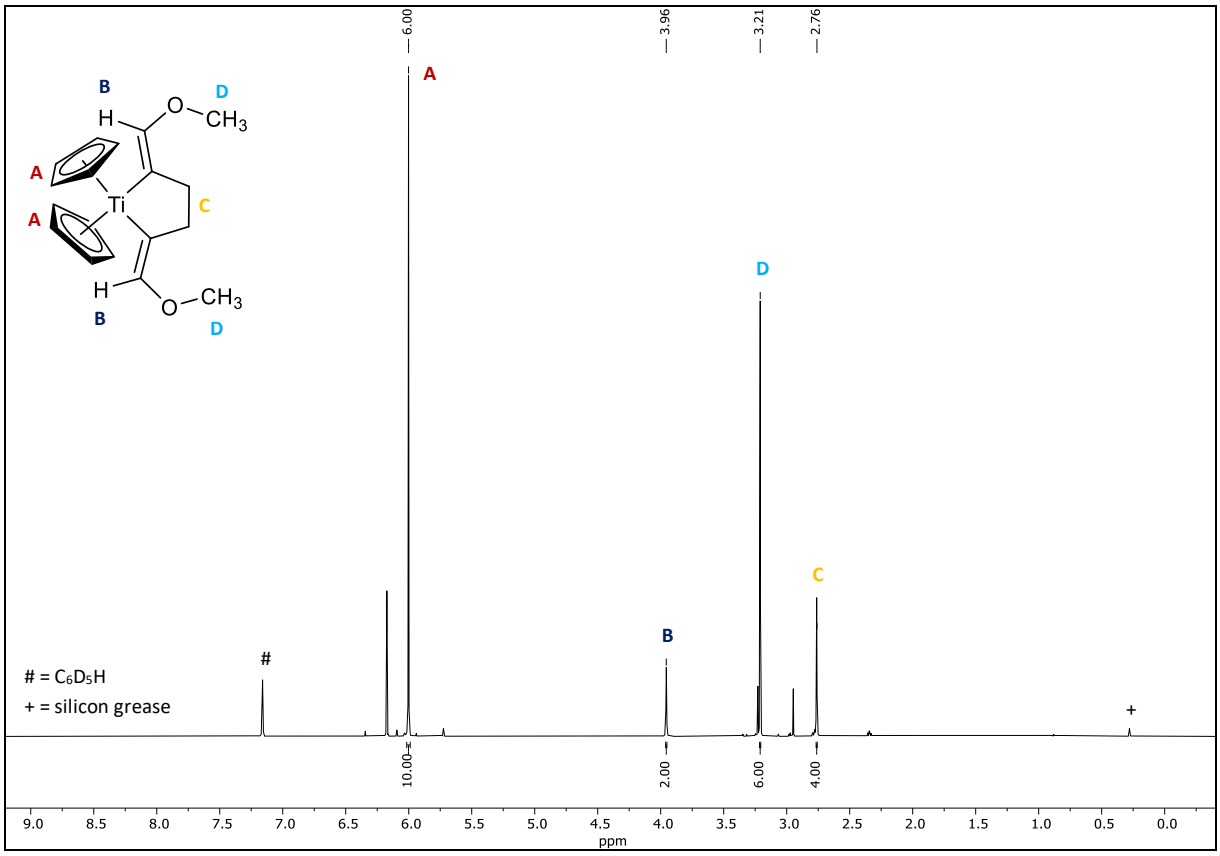

Figure S53: ^{1}H NMR spectrum of **5b** (500 MHz, C_6D_6, 305 K).

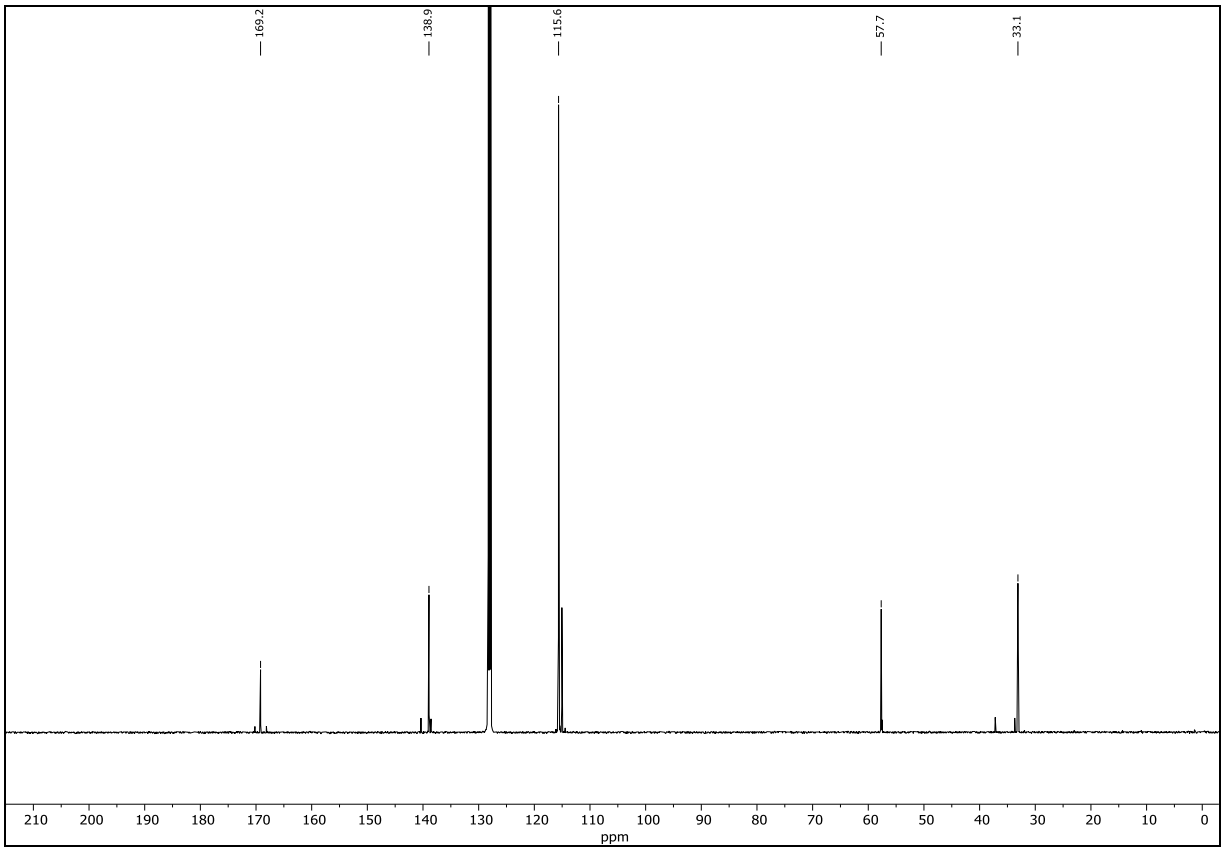

Figure S54: ^{13}C{^{1}H} NMR spectrum of **5b** (126 MHz, C_6D_6, 305 K).

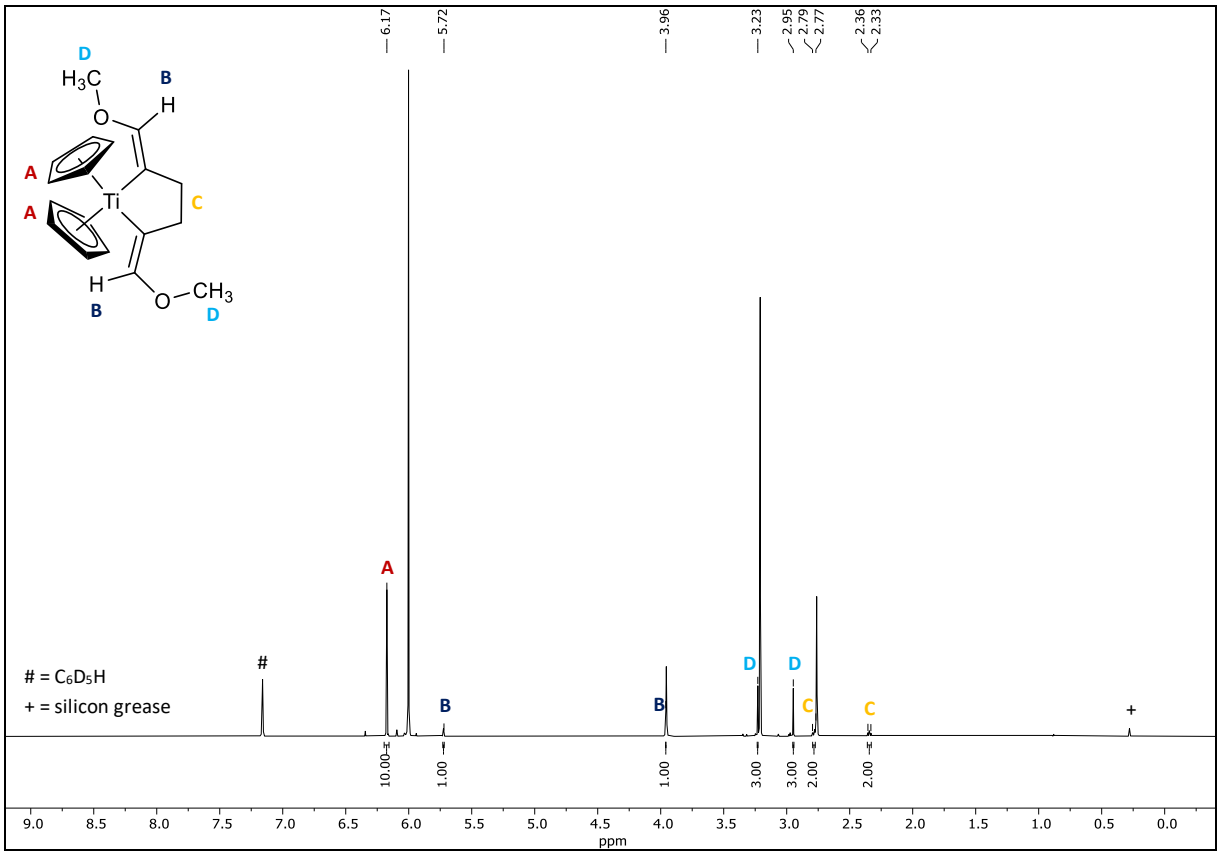

Figure S55: ^{1}H NMR spectrum of **5b'** (500 MHz, C_6D_6, 305 K).

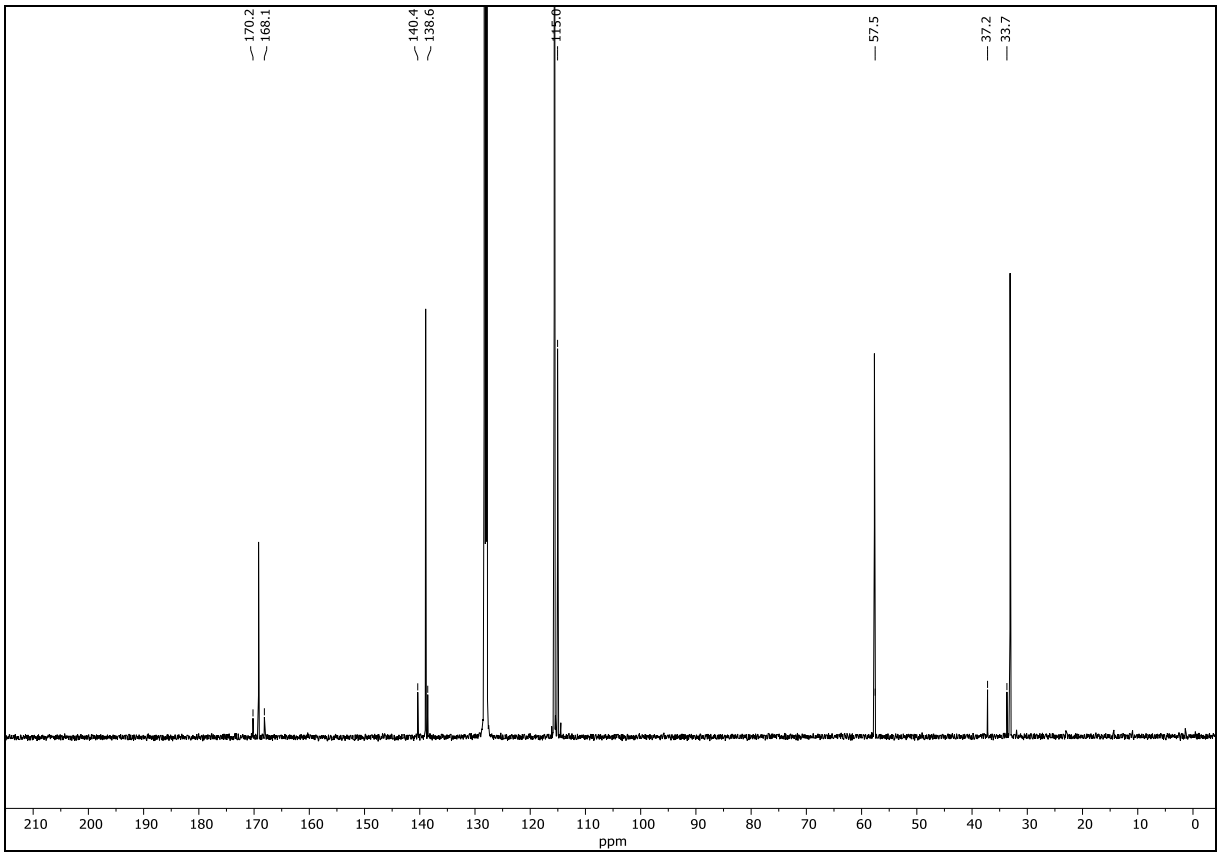

Figure S56: $^{13}C\{^{1}H\}$ NMR spectrum of **5b'** (126 MHz, C_6D_6, 305 K).

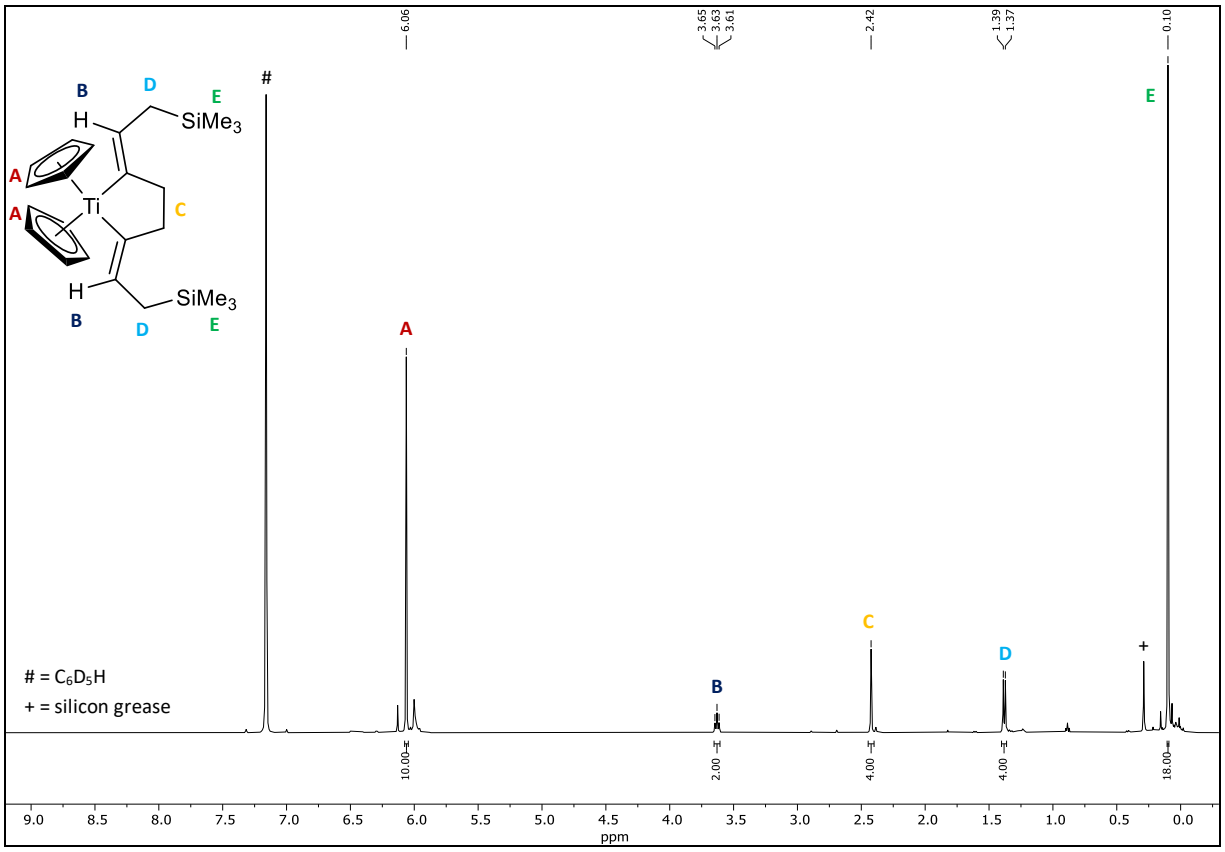

Figure S57: ^{1}H NMR spectrum of **5c** (500 MHz, C_6D_6, 305 K).

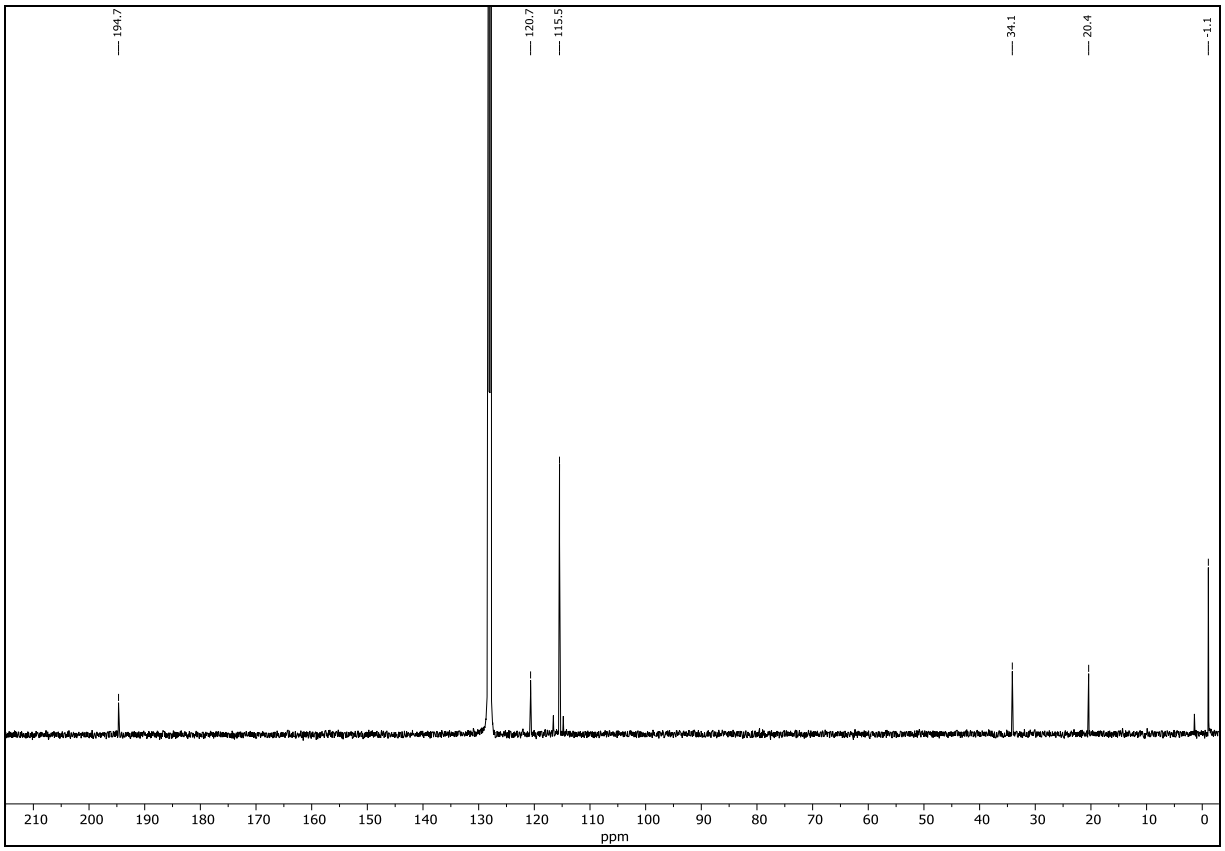

Figure S58: $^{13}C\{^{1}H\}$ NMR spectrum of **5c** (126 MHz, C_6D_6, 305 K).

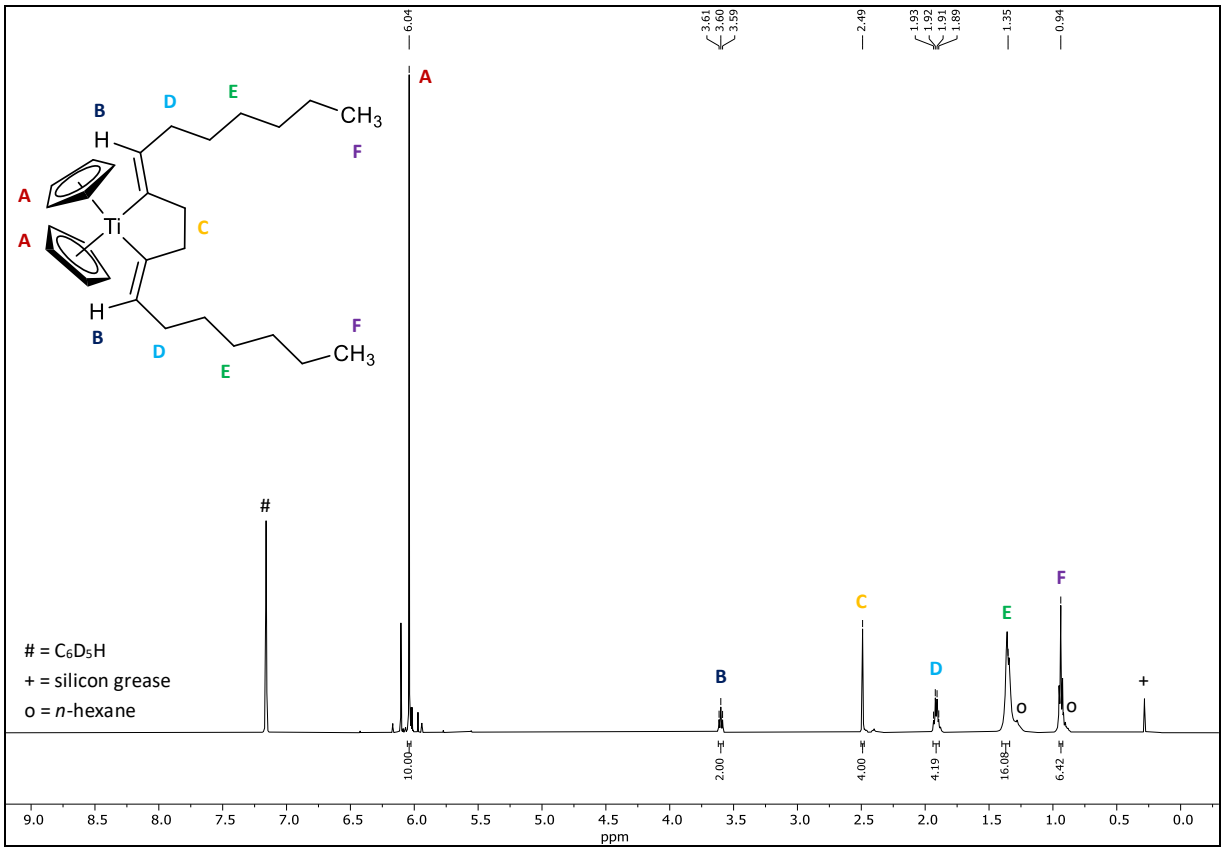

Figure S59: ^{1}H NMR spectrum of **5d** (500 MHz, C_6D_6, 305 K).

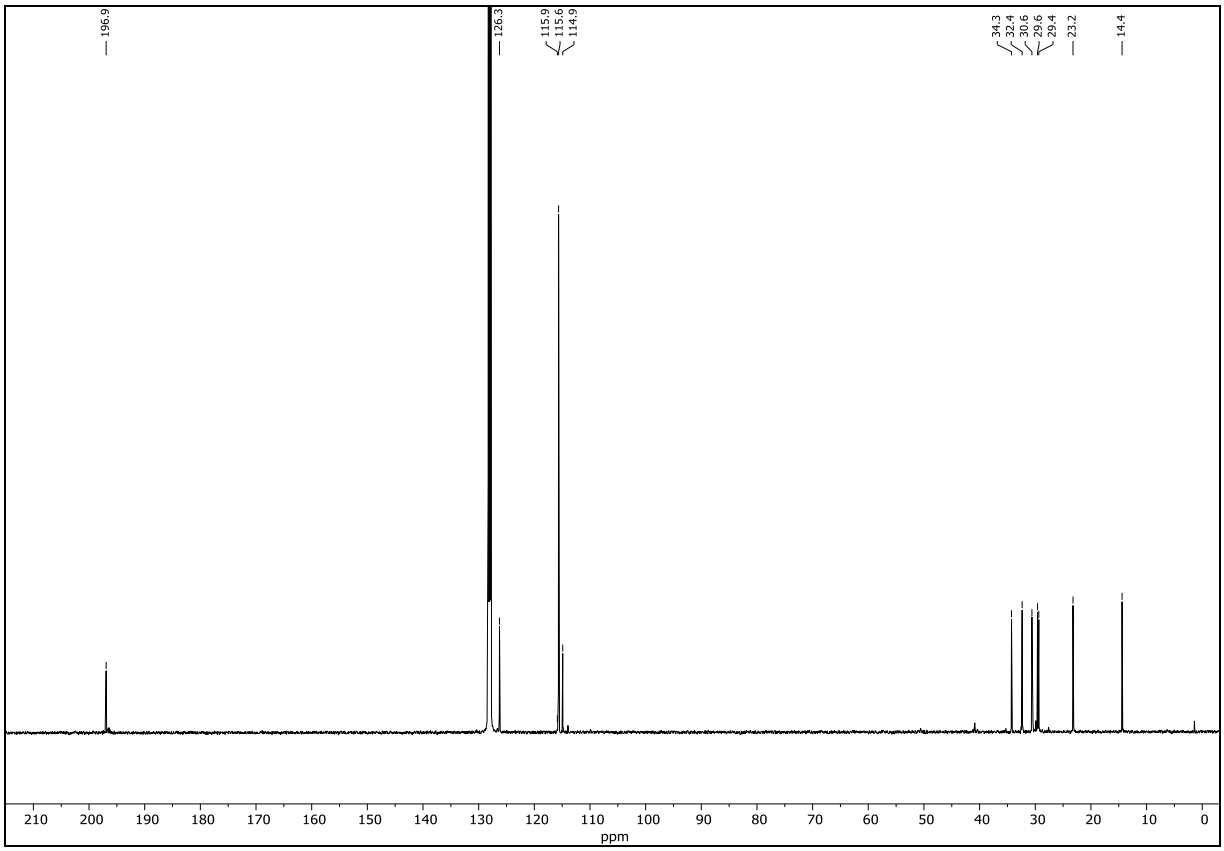

Figure S60: $^{13}C\{^{1}H\}$ NMR spectrum of **5d** (126 MHz, C_6D_6, 305 K).

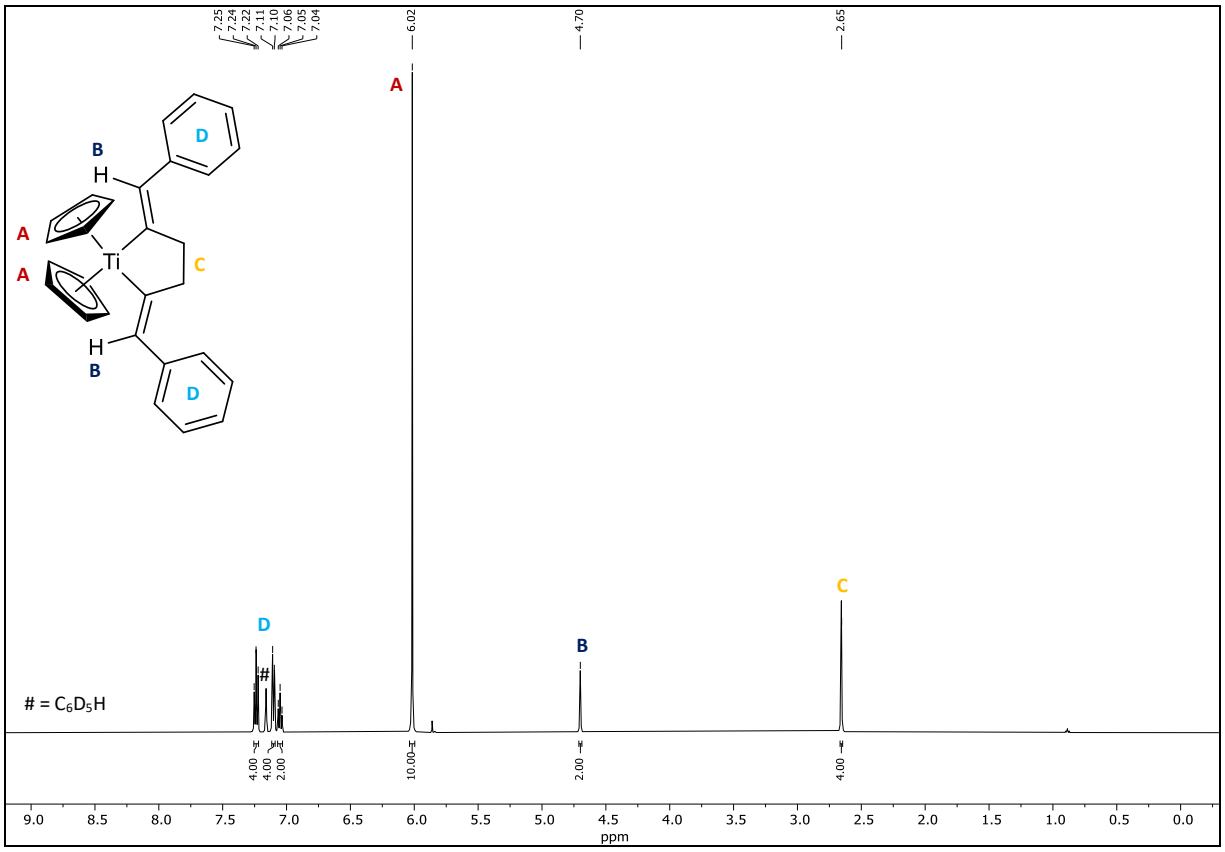

Figure S61: ^{1}H NMR spectrum of **5e** (500 MHz, C_6D_6, 305 K).

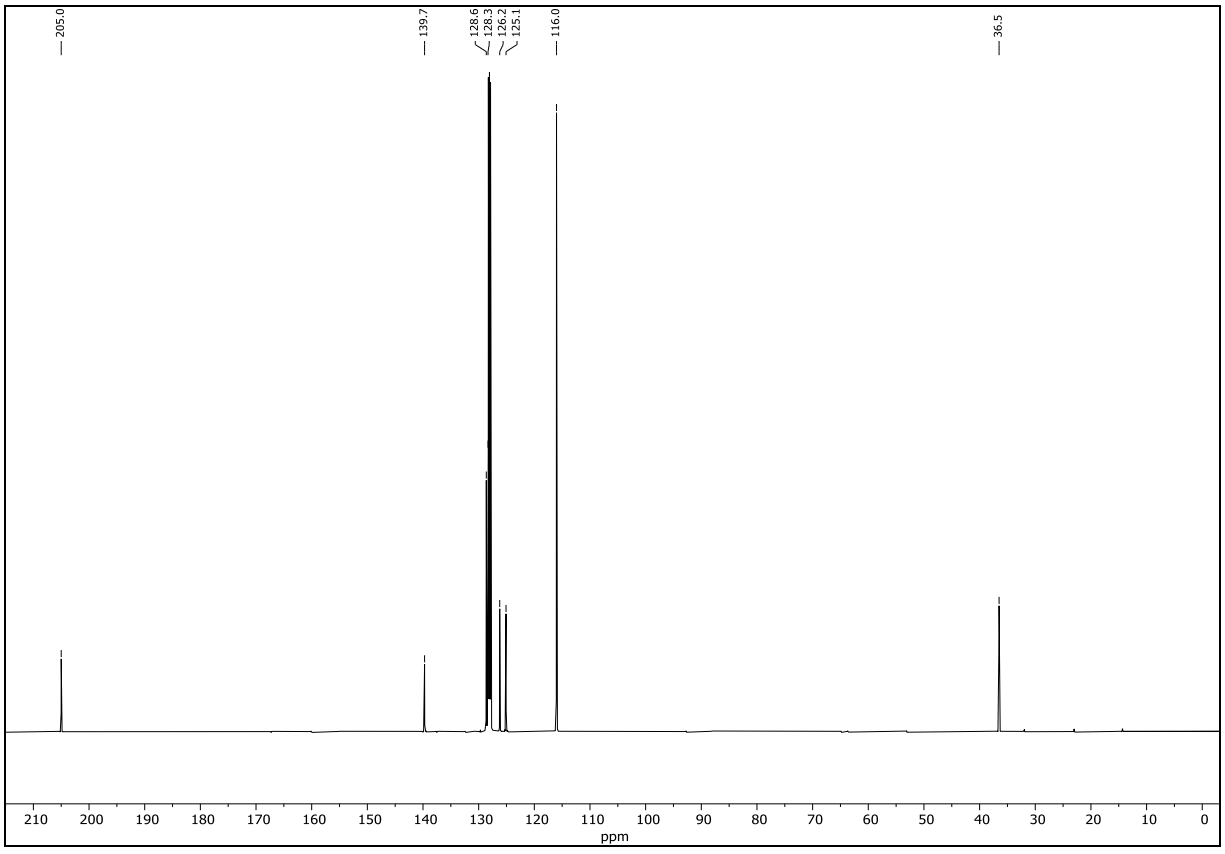

Figure S62: ^{13}C{^{1}H} NMR spectrum of **5e** (126 MHz, C_6D_6, 305 K).

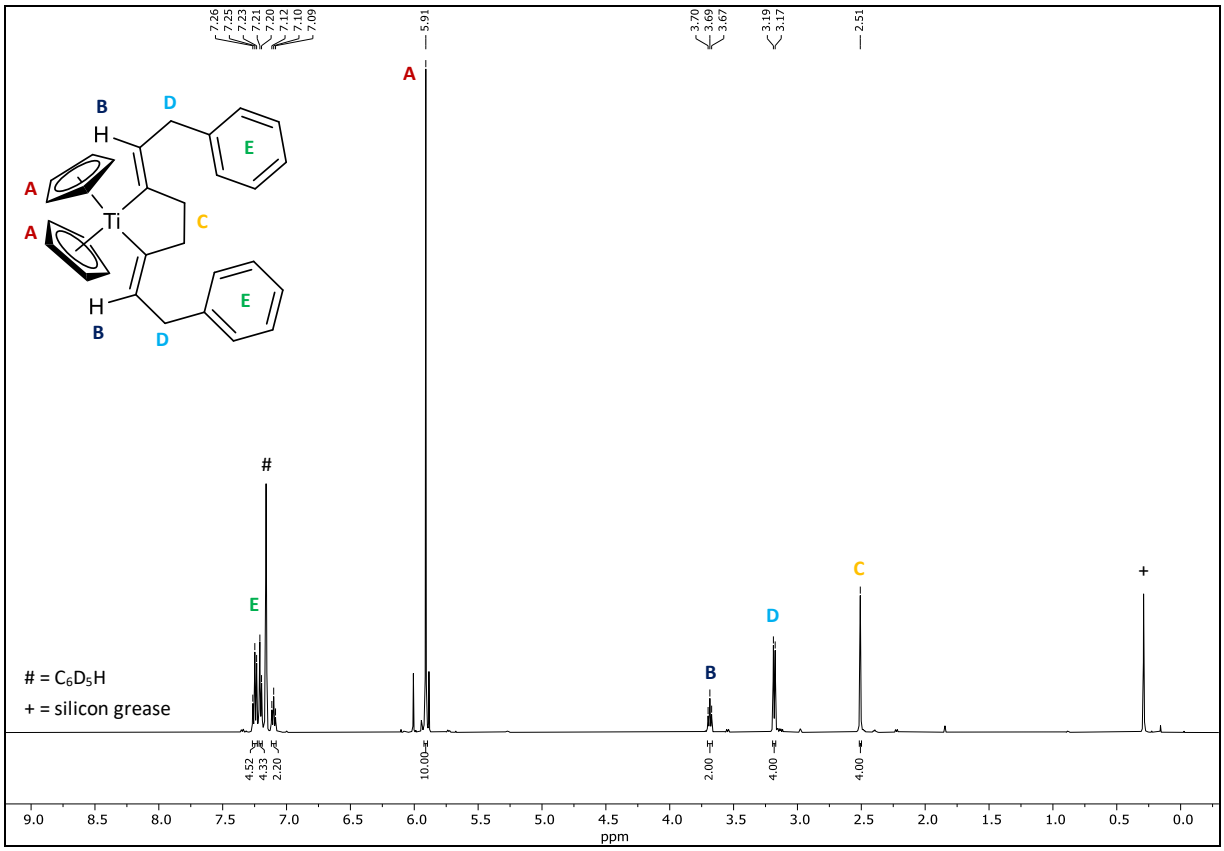

Figure S63: ^{1}H NMR spectrum of **5f** (500 MHz, C_6D_6, 305 K).

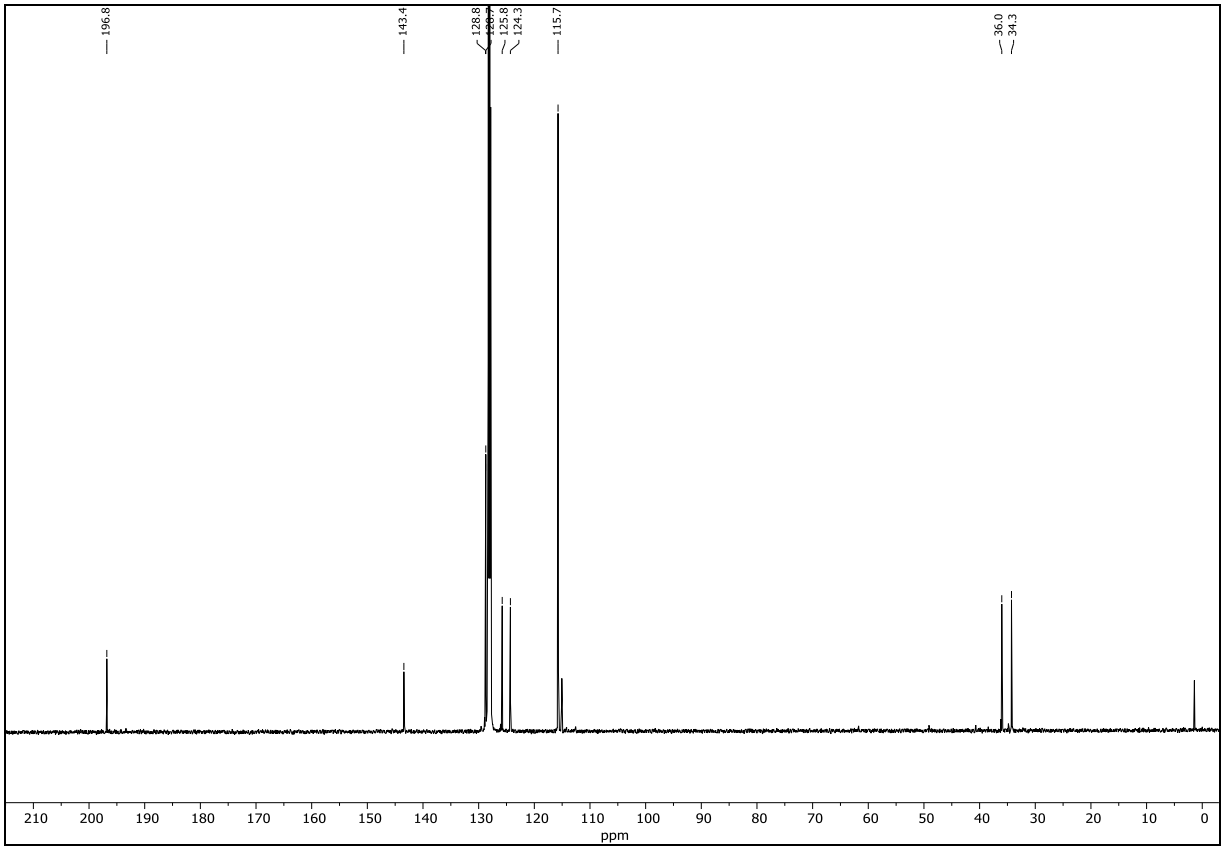

Figure S64: ^{13}C{^{1}H} NMR spectrum of **5f** (126 MHz, C_6D_6, 305 K).

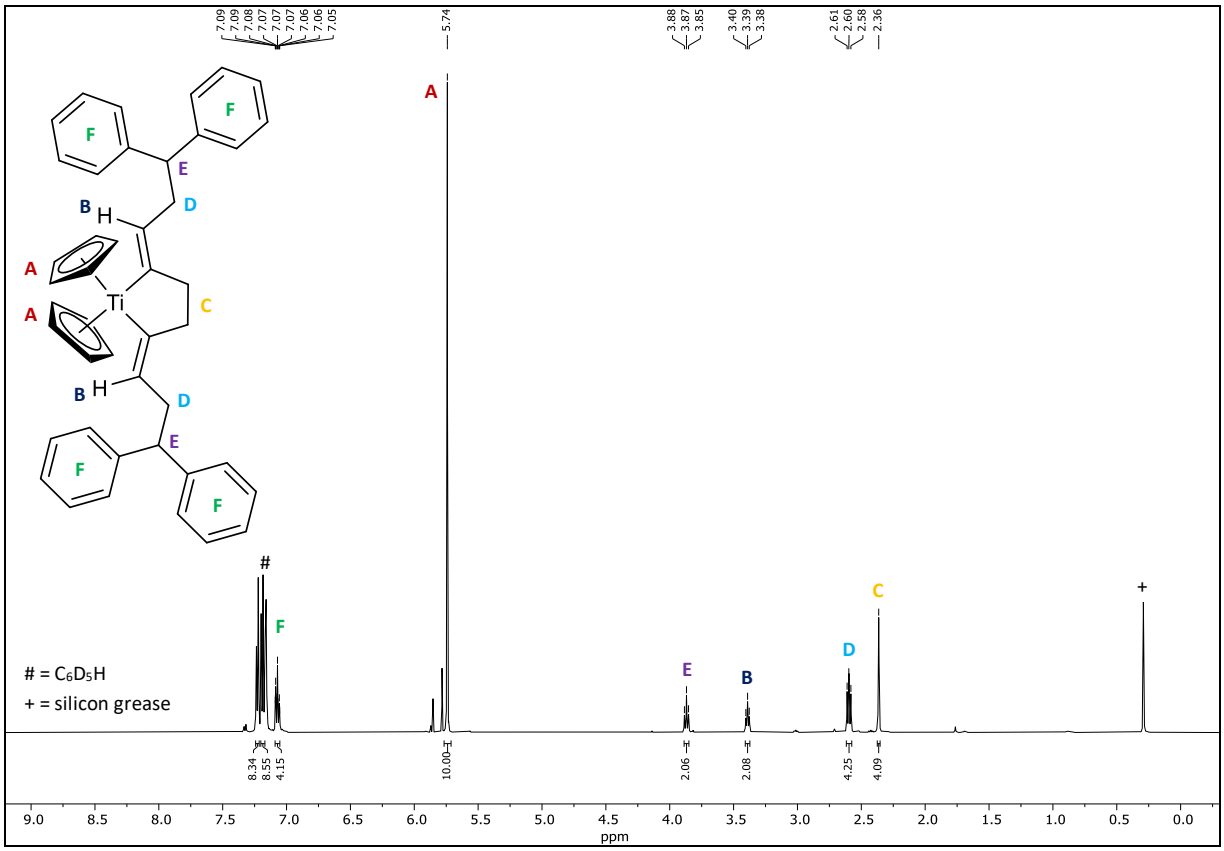

Figure S65: ^{1}H NMR spectrum of **5g** (500 MHz, C_6D_6, 305 K).

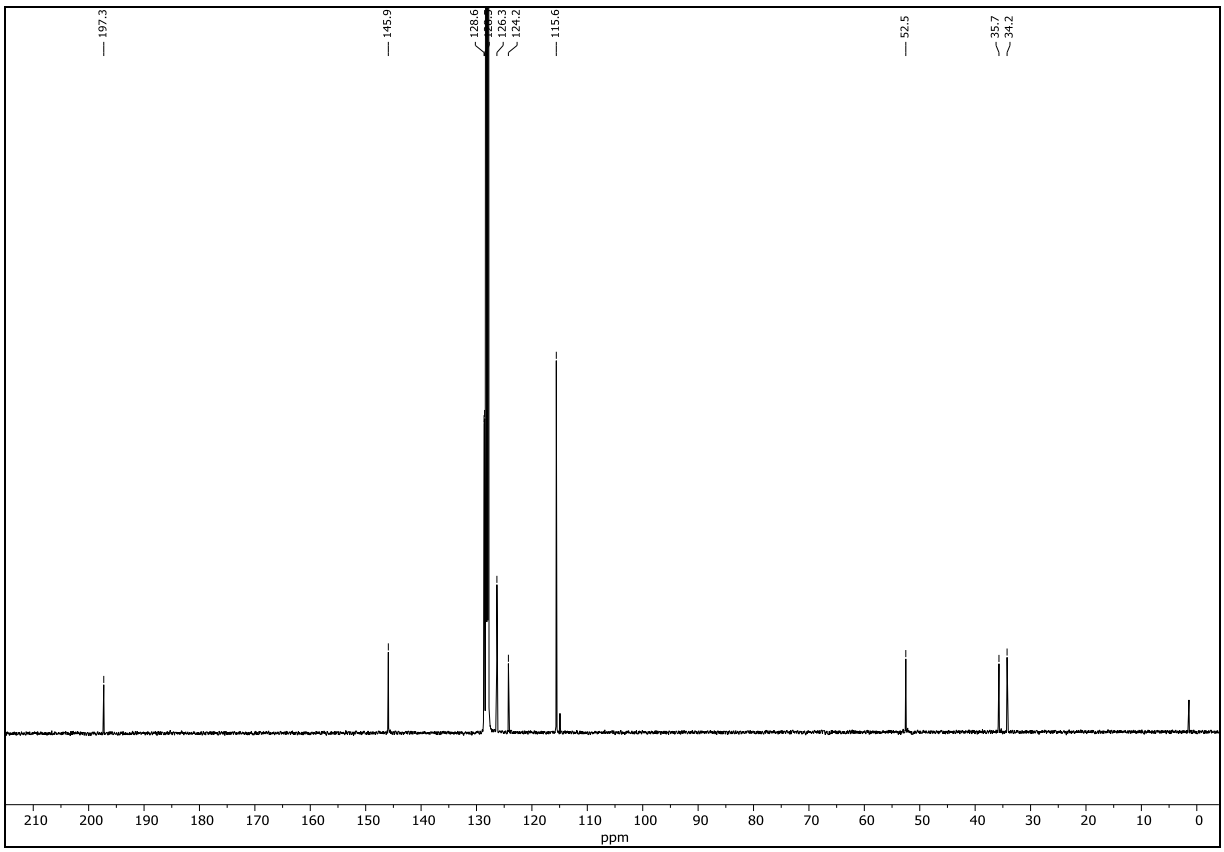

Figure S66: $^{13}C\{^{1}H\}$ NMR spectrum of **5g** (126 MHz, C_6D_6, 305 K).

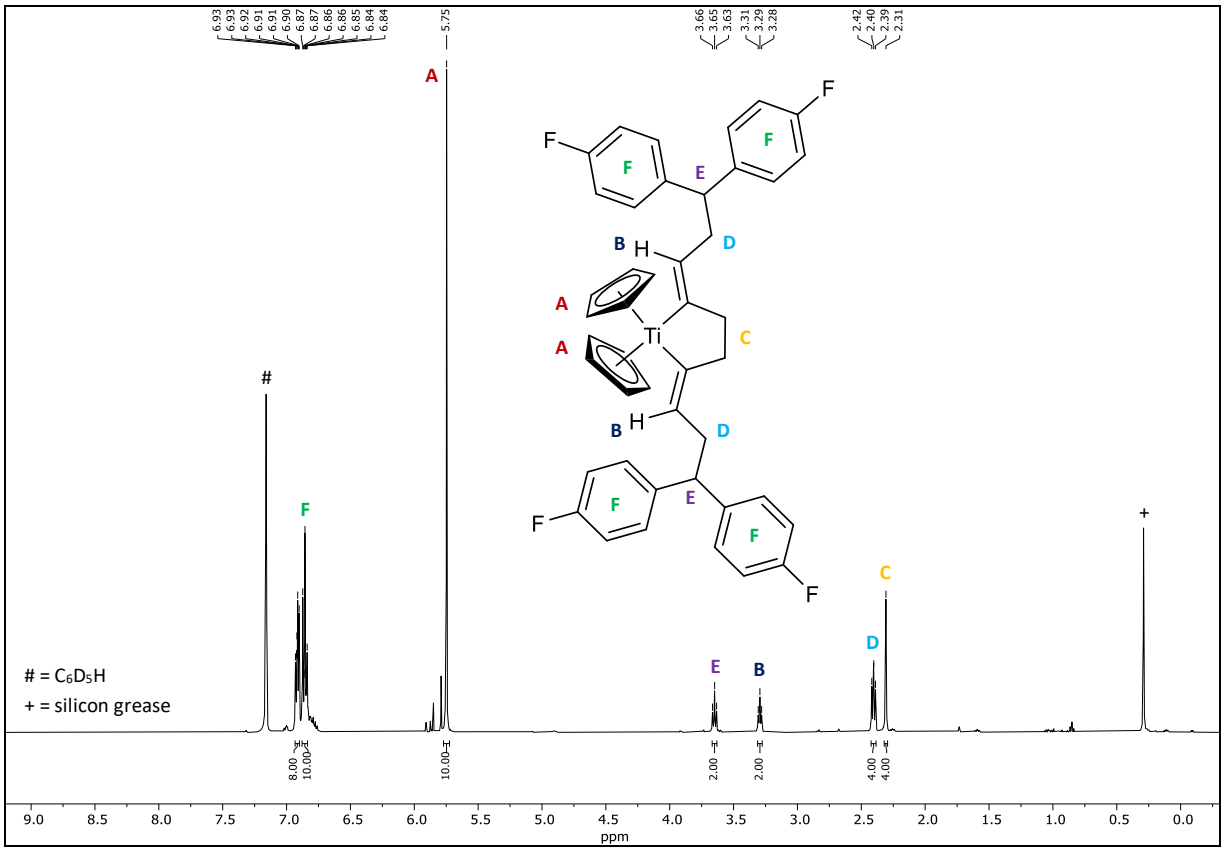

Figure S67: ^{1}H NMR spectrum of **5h** (500 MHz, C_6D_6, 305 K).

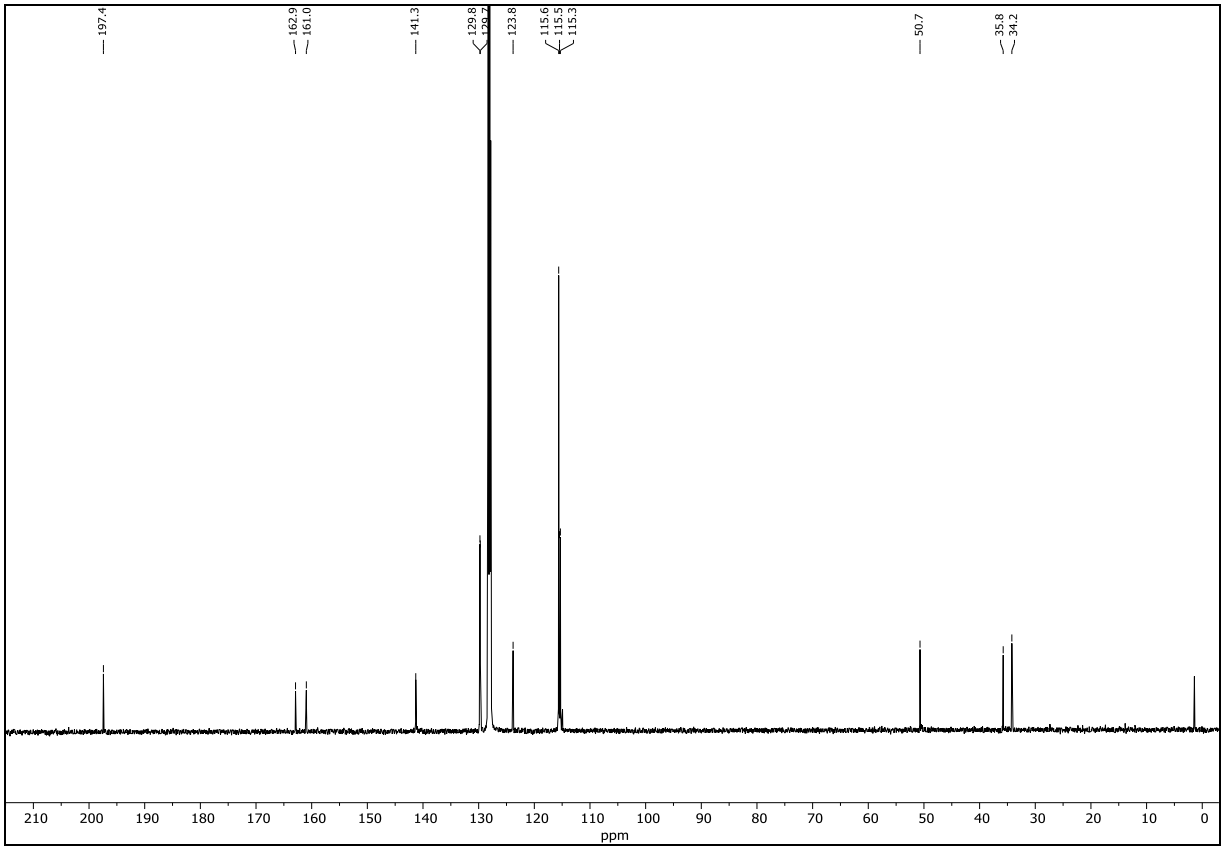

Figure S68: ^{13}C{^{1}H} NMR spectrum of **5h** (126 MHz, C_6D_6, 305 K).

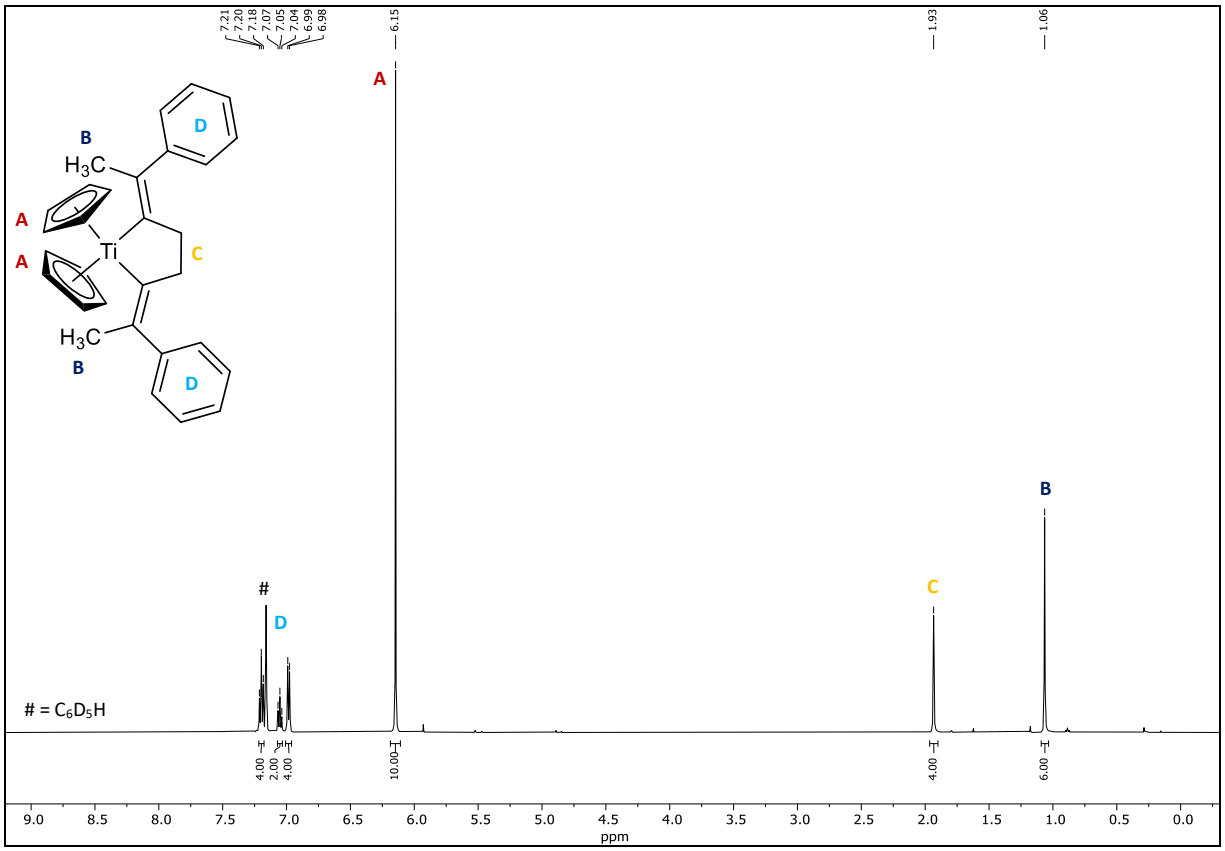

Figure S69: ^{1}H NMR spectrum of **5i** (500 MHz, C_6D_6, 305 K).

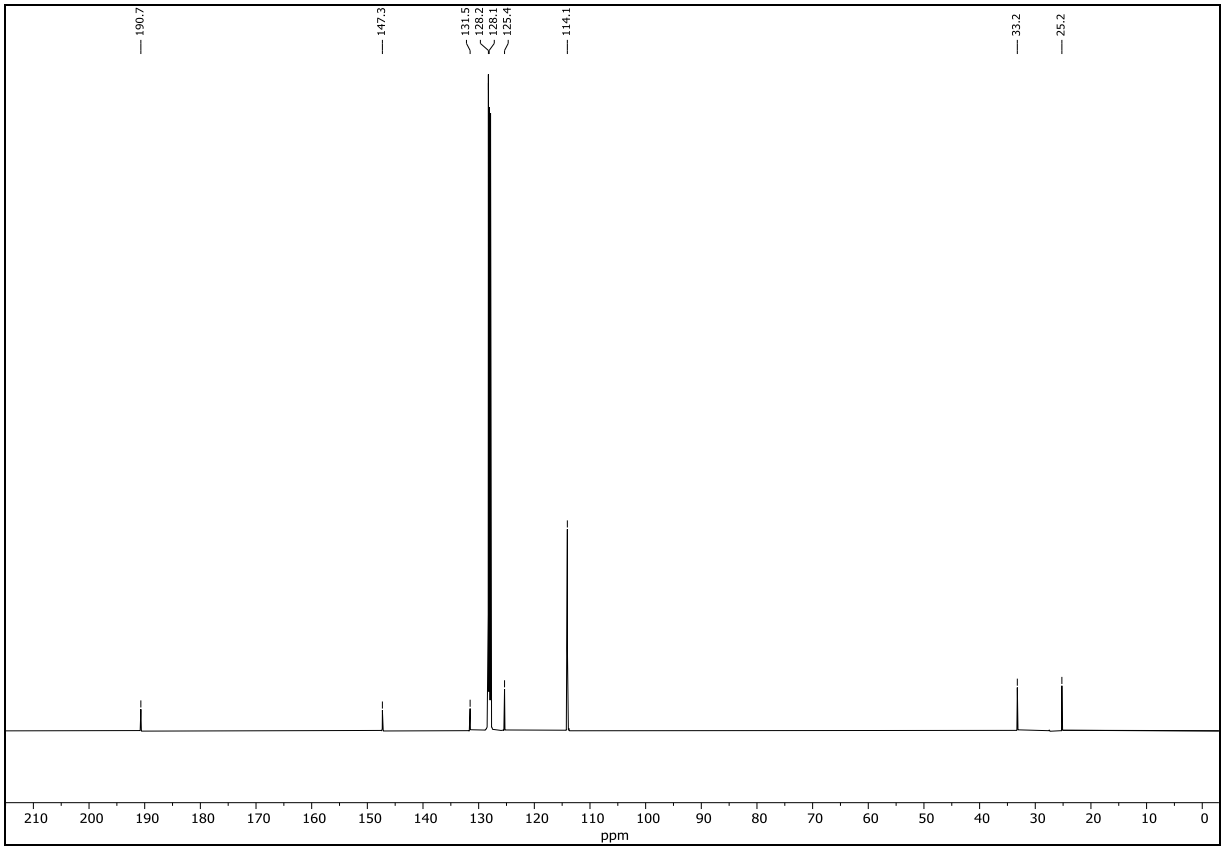

Figure S70: ^{13}C{^{1}H} NMR spectrum of **5i** (126 MHz, C_6D_6, 305 K).

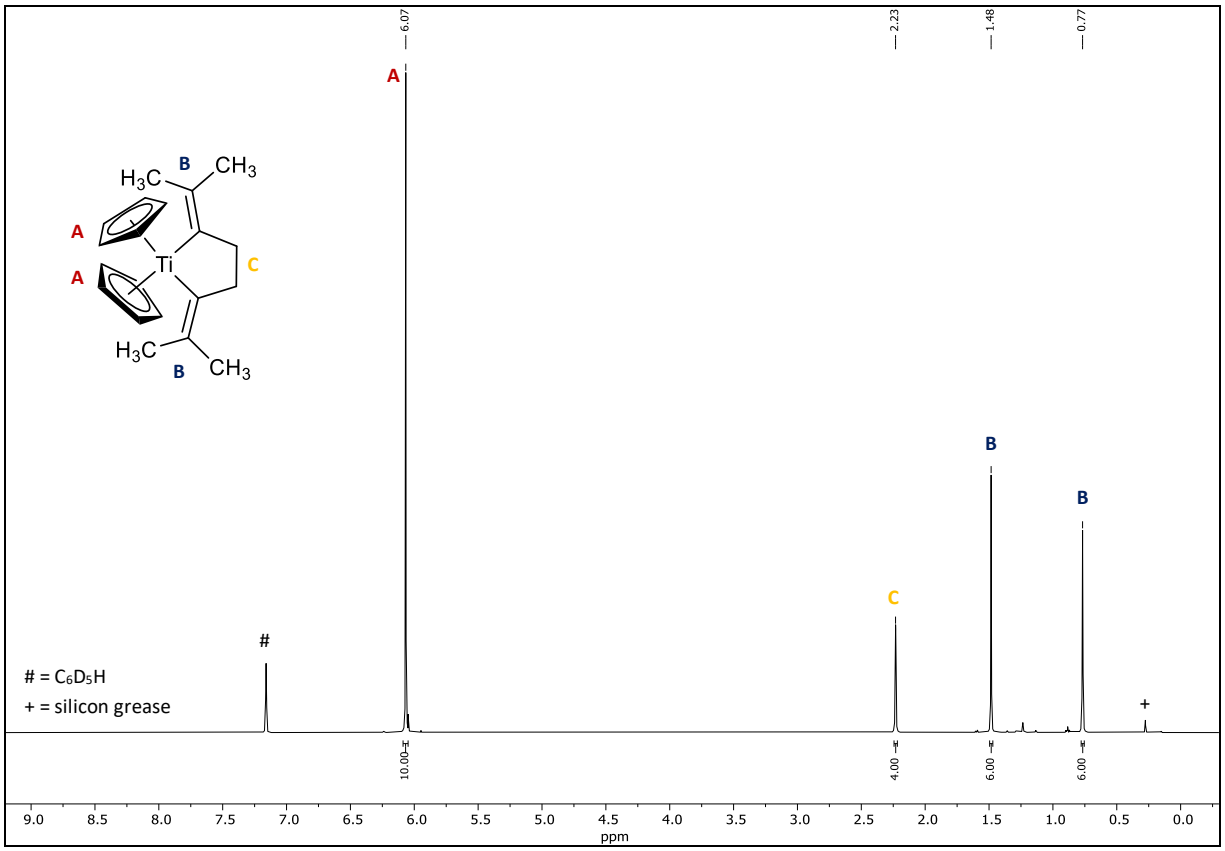

Figure S71: ^{1}H NMR spectrum of **5j** (500 MHz, C_6D_6, 305 K).

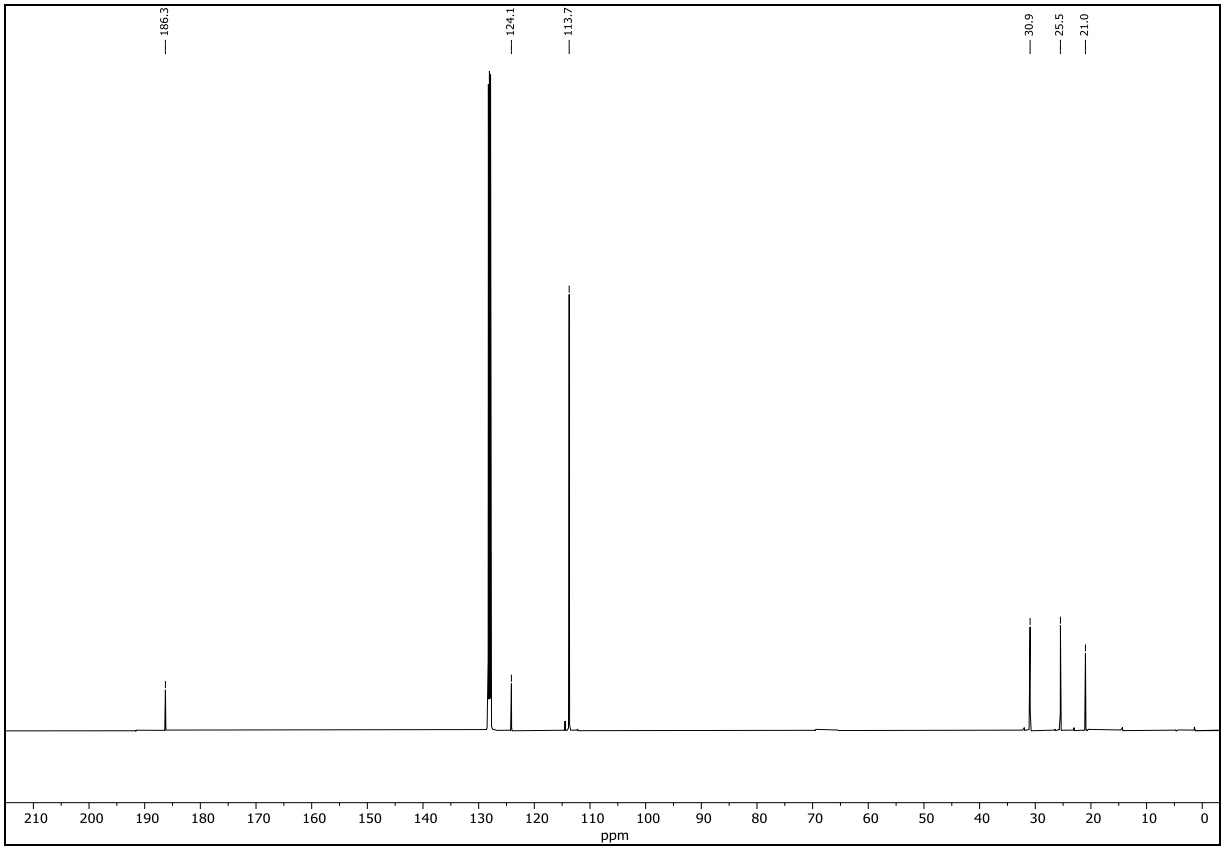

Figure S72: ^{13}C{^{1}H} NMR spectrum of **5j** (126 MHz, C_6D_6, 305 K).

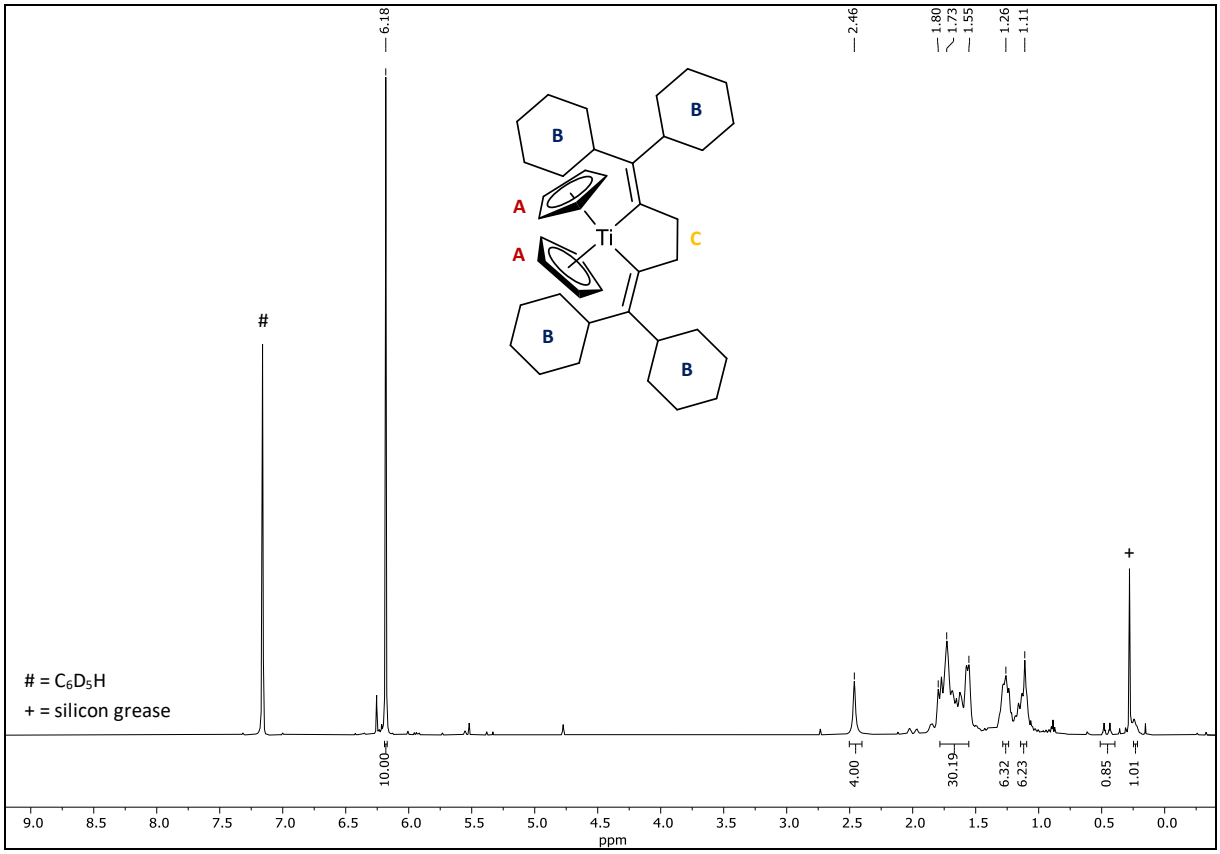

Figure S73: $^{13}C\{^{1}H\}$ NMR spectrum of **5k** (126 MHz, C_6D_6, 305 K).

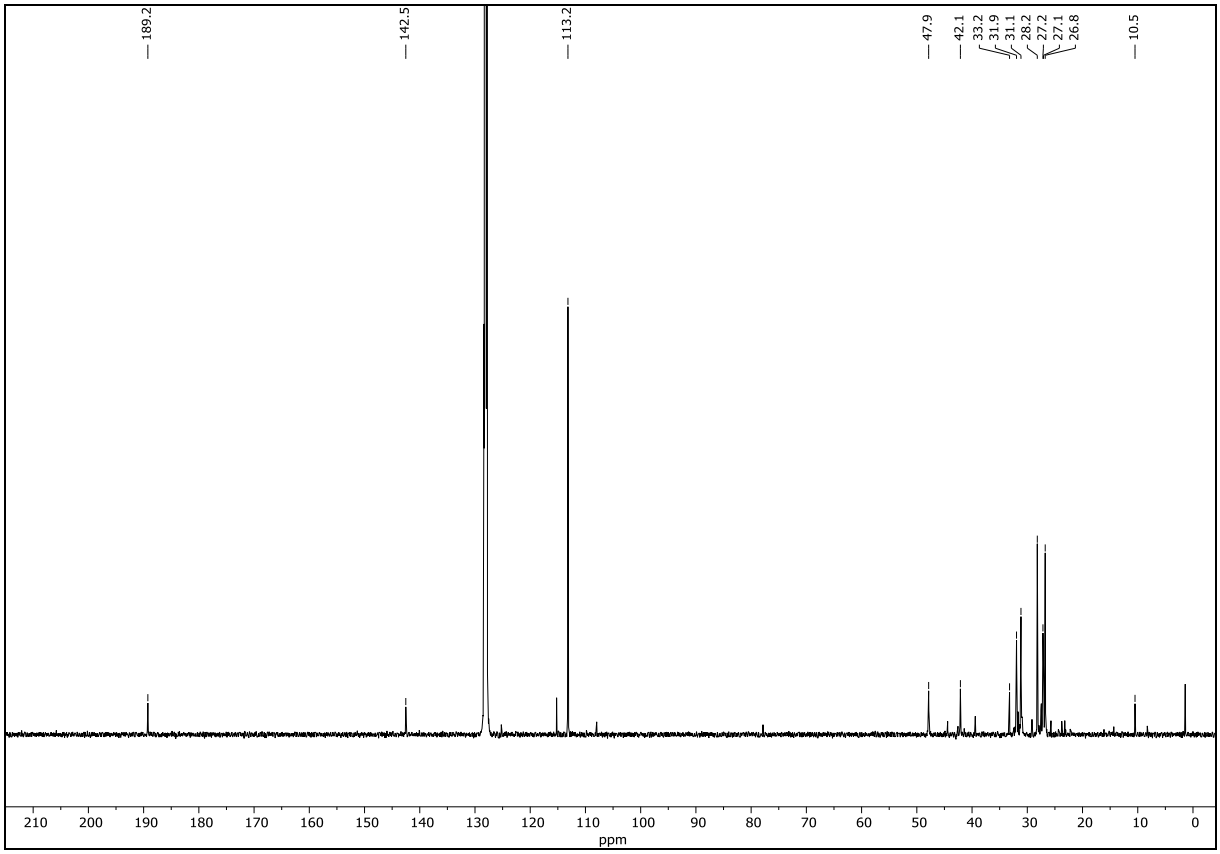

Figure S74: $^{13}C\{^{1}H\}$ NMR spectrum of **5k** (126 MHz, C_6D_6, 305 K).

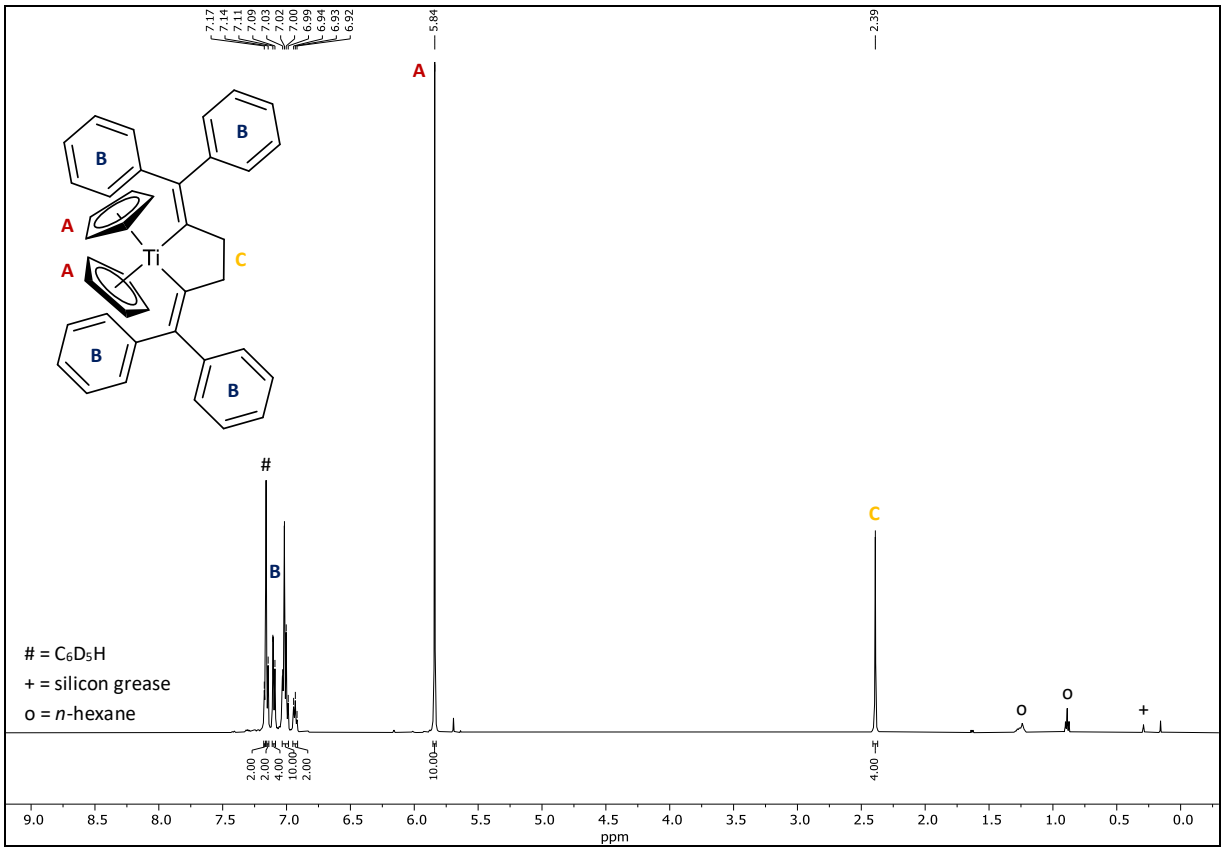

Figure S75: ^{1}H NMR spectrum of **5l** (500 MHz, C_6D_6, 305 K).

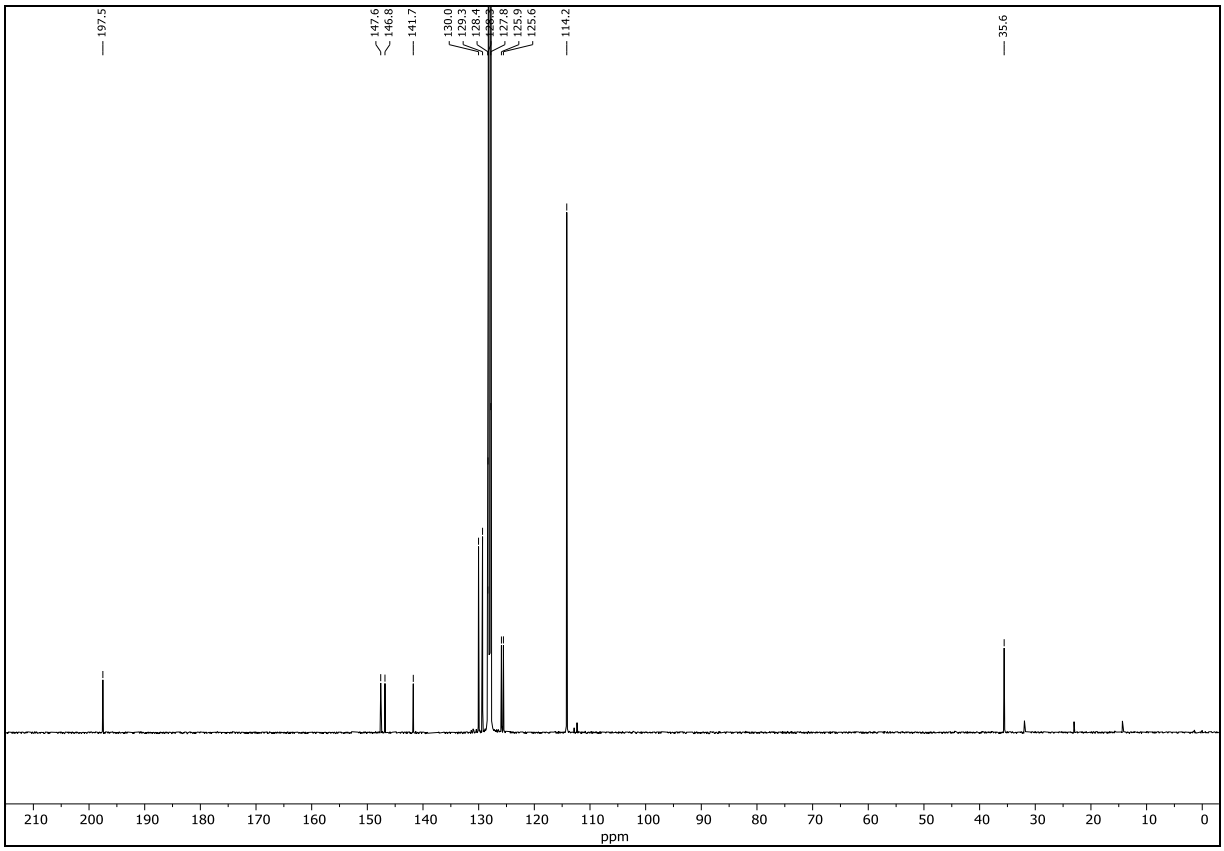

Figure S76: $^{13}C\{^{1}H\}$ NMR spectrum of **5l** (126 MHz, C_6D_6, 305 K).

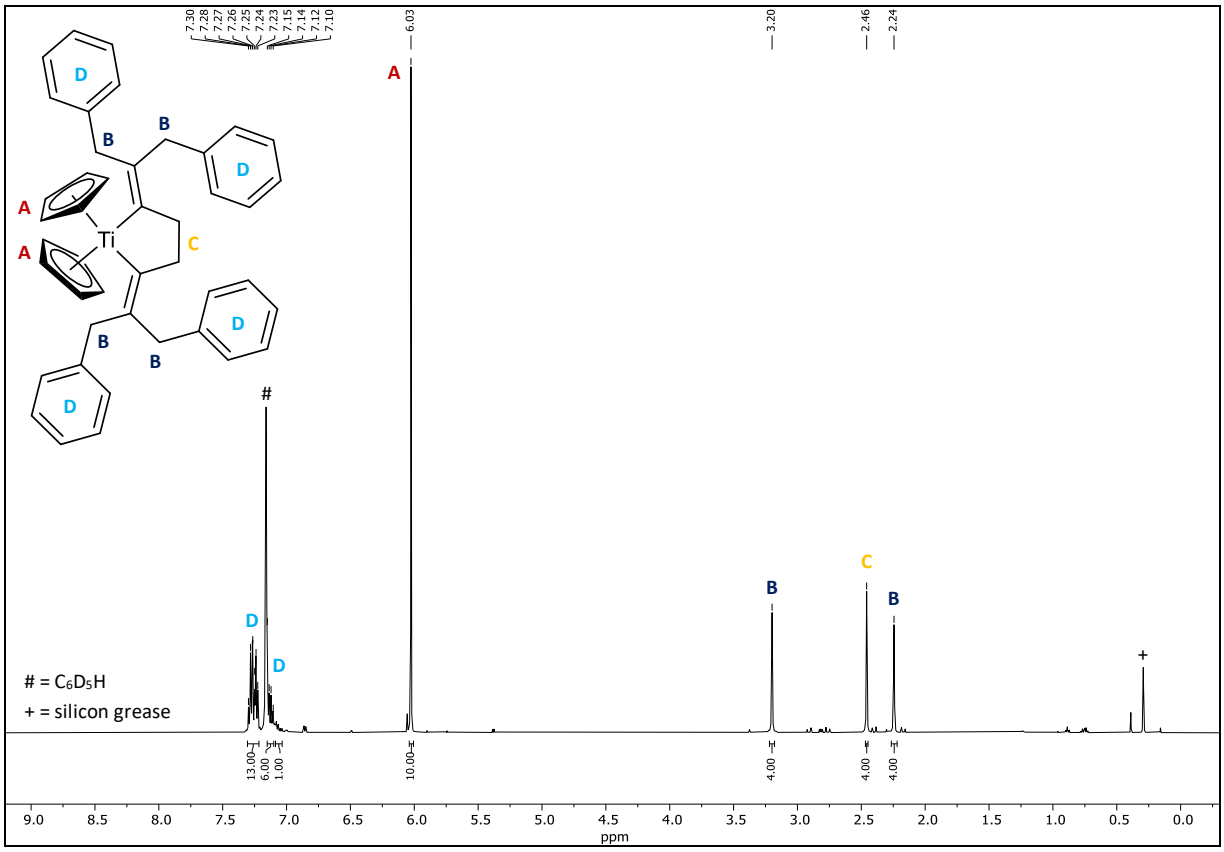

Figure S77: ^{1}H NMR spectrum of **5m** (500 MHz, C_6D_6, 305 K).

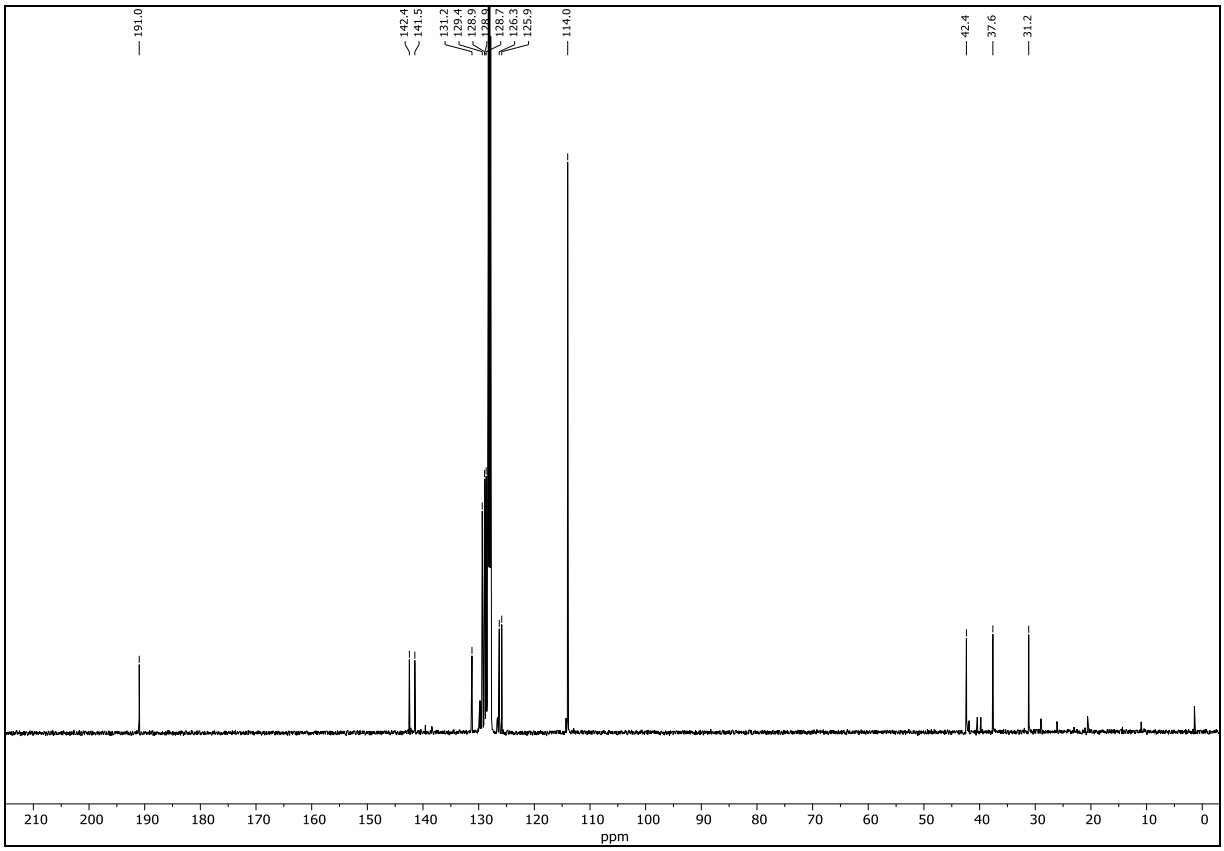

Figure S78: ^{13}C{^{1}H} NMR spectrum of **5m** (126 MHz, C_6D_6, 305 K).

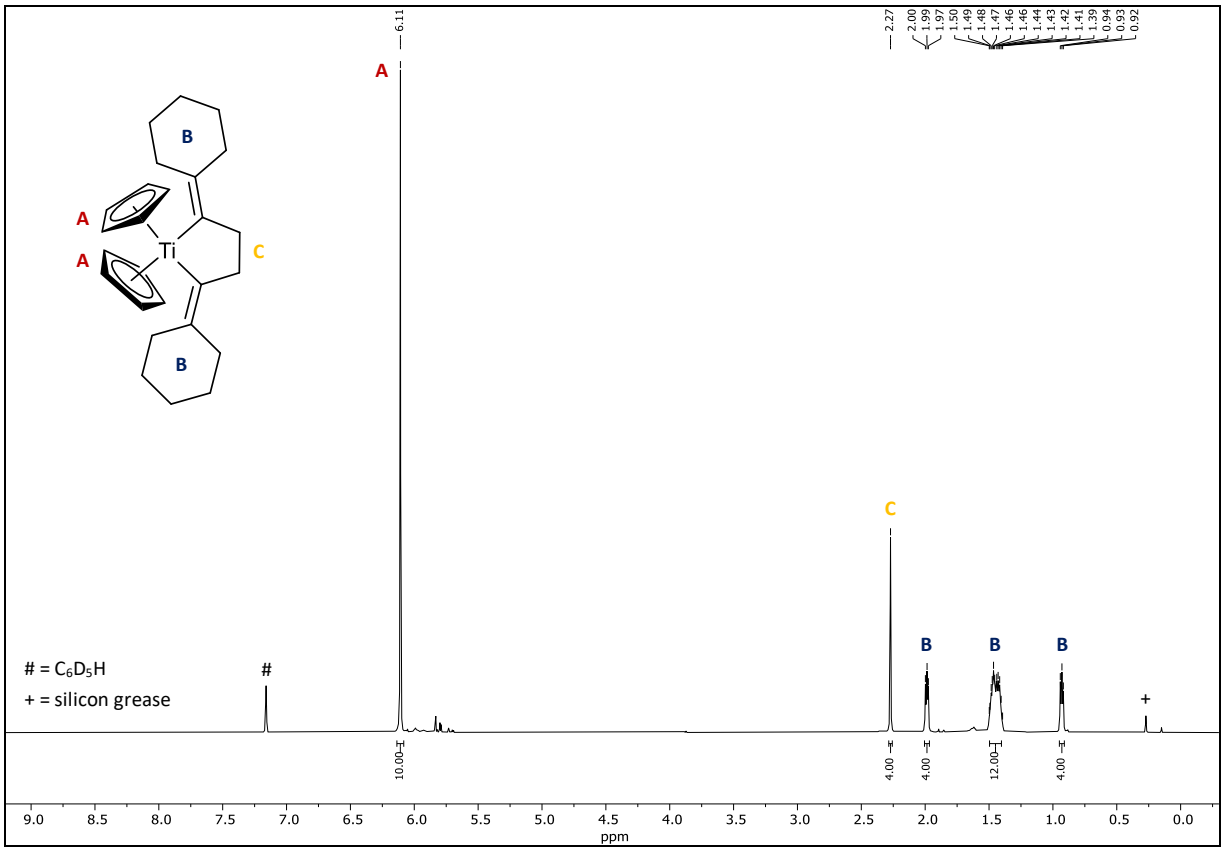

Figure S79: ^{1}H NMR spectrum of **5n** (500 MHz, C_6D_6, 305 K).

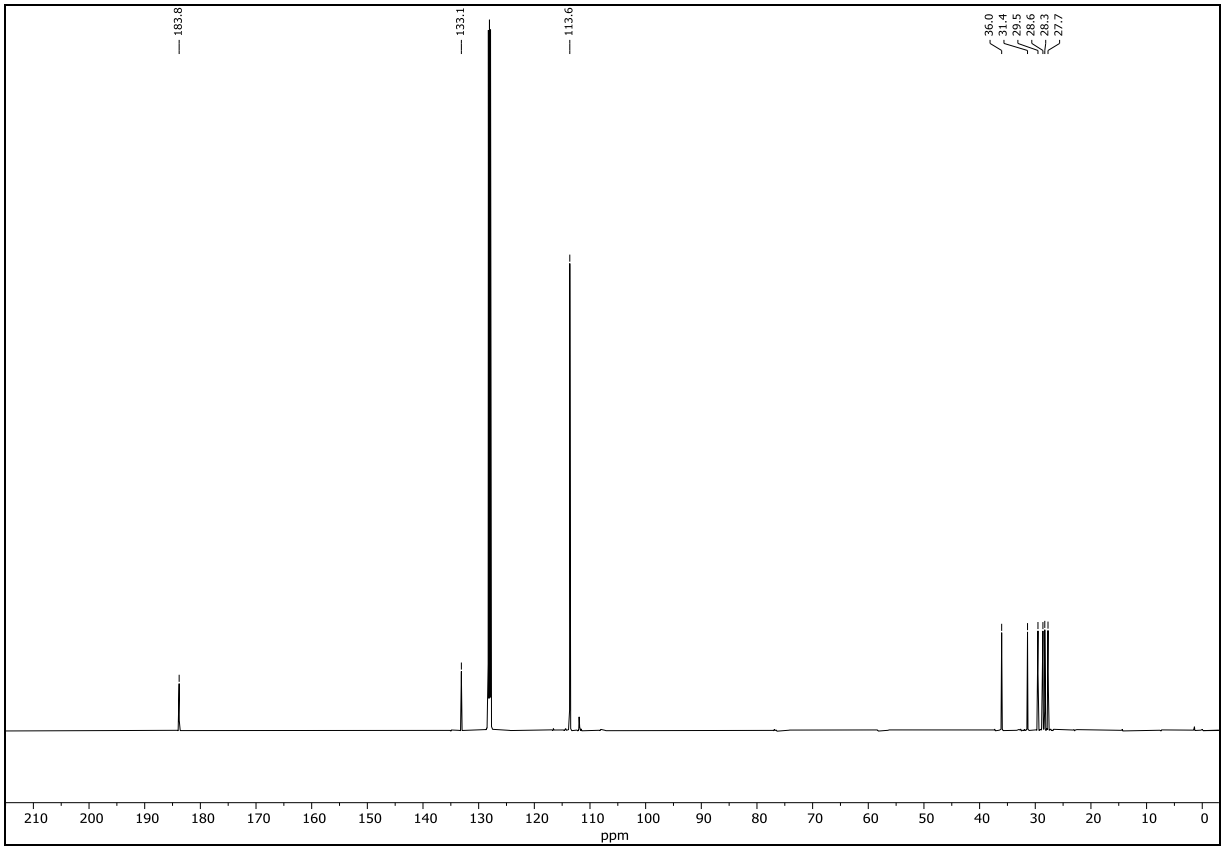

Figure S80: $^{13}C\{^{1}H\}$ NMR spectrum of **5n** (126 MHz, C_6D_6, 305 K).

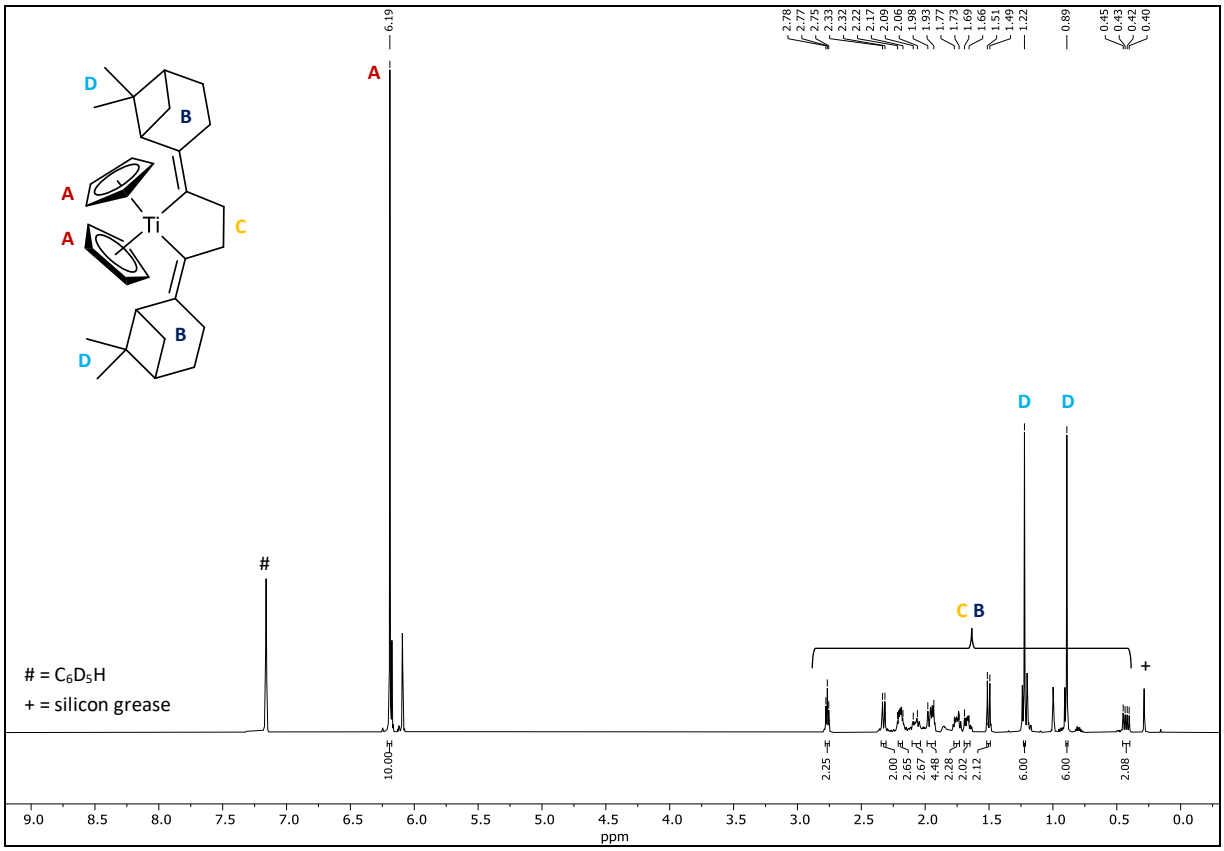

Figure S81: ^{1}H NMR spectrum of **5o** (500 MHz, C_6D_6, 305 K).

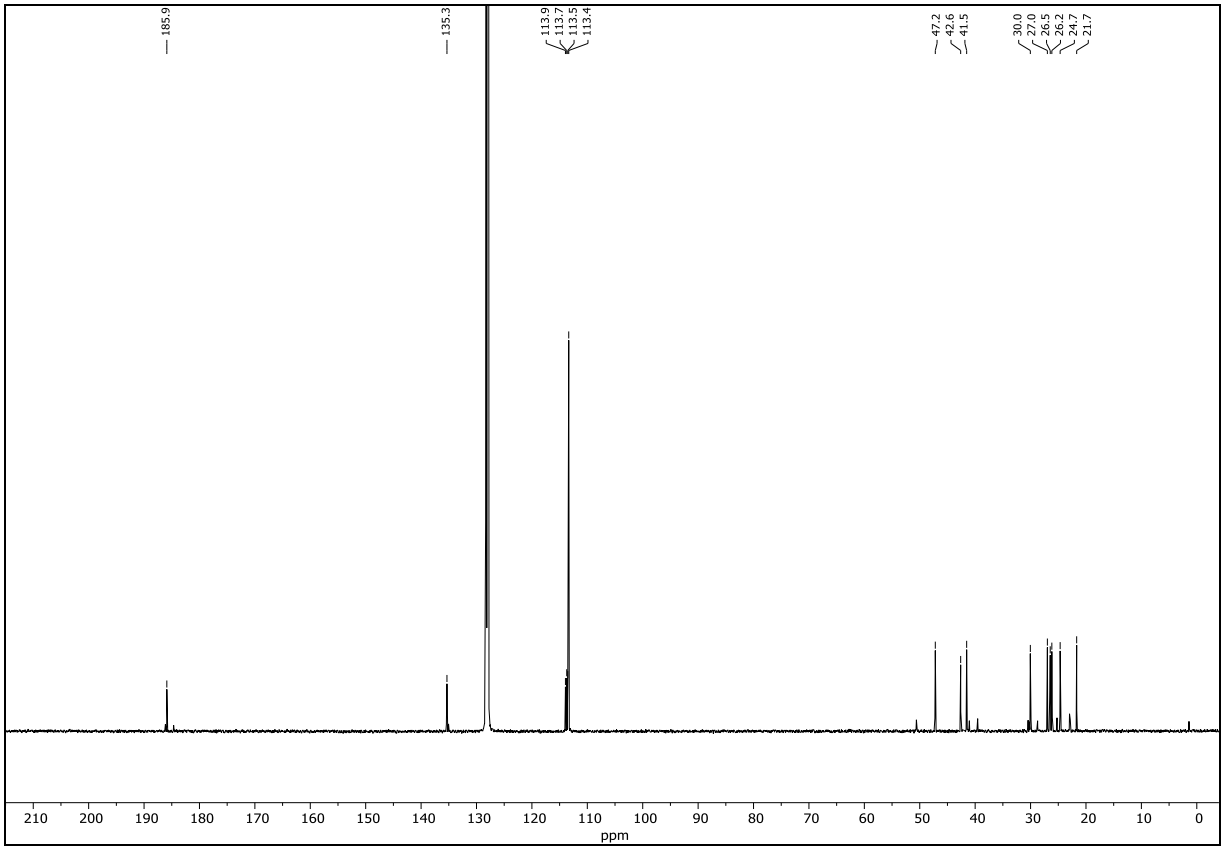

Figure S82: $^{13}C\{^{1}H\}$ NMR spectrum of **5o** (126 MHz, C_6D_6, 305 K).

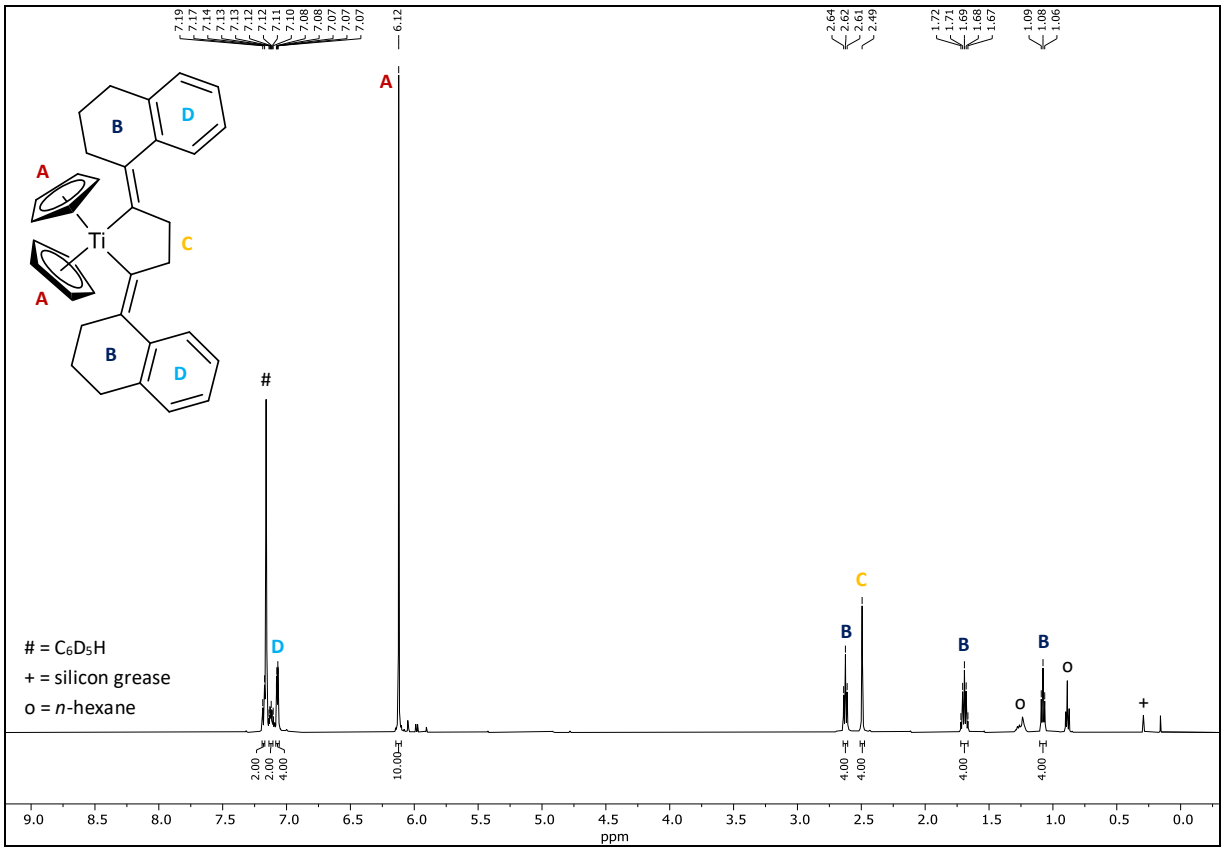

Figure S83: ^{1}H NMR spectrum of **5p** (500 MHz, C_6D_6, 305 K).

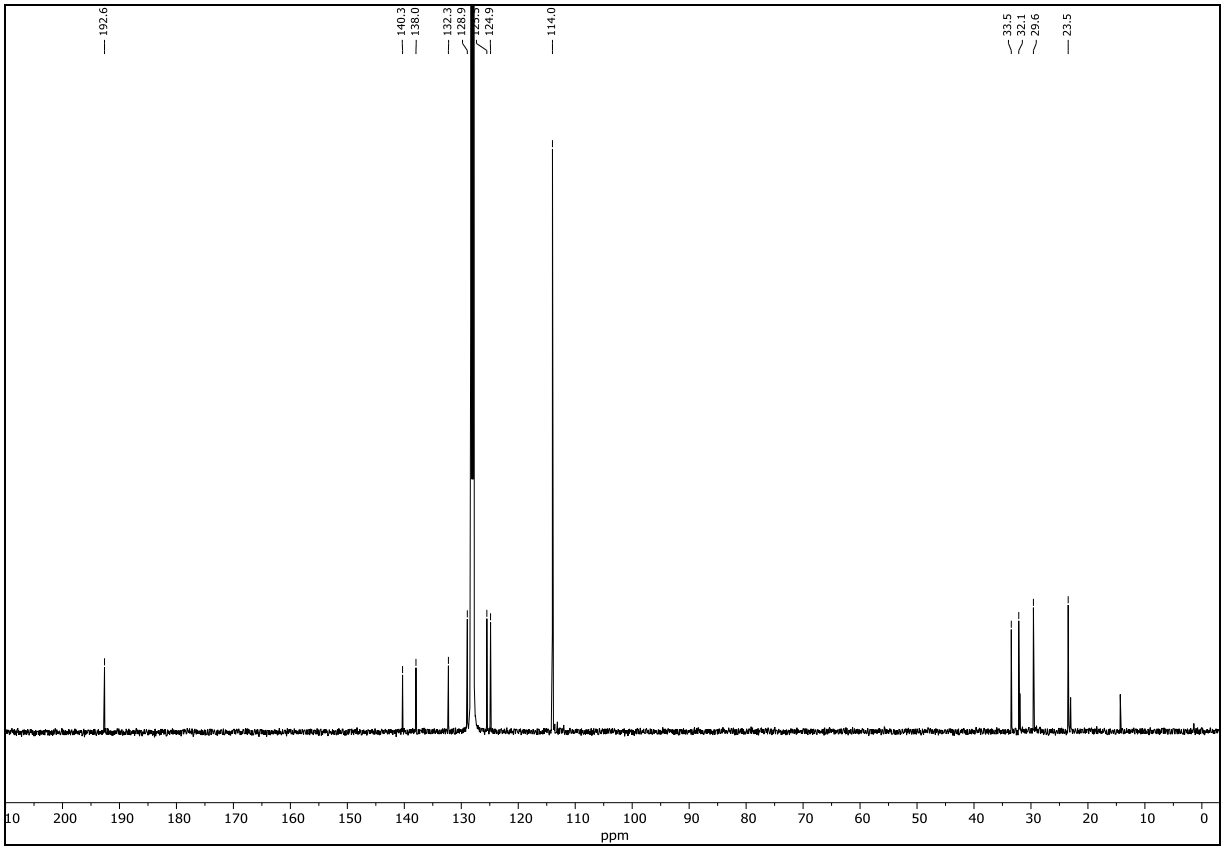

Figure S84: ^{13}C{^{1}H} NMR spectrum of **5p** (126 MHz, C_6D_6, 305 K).

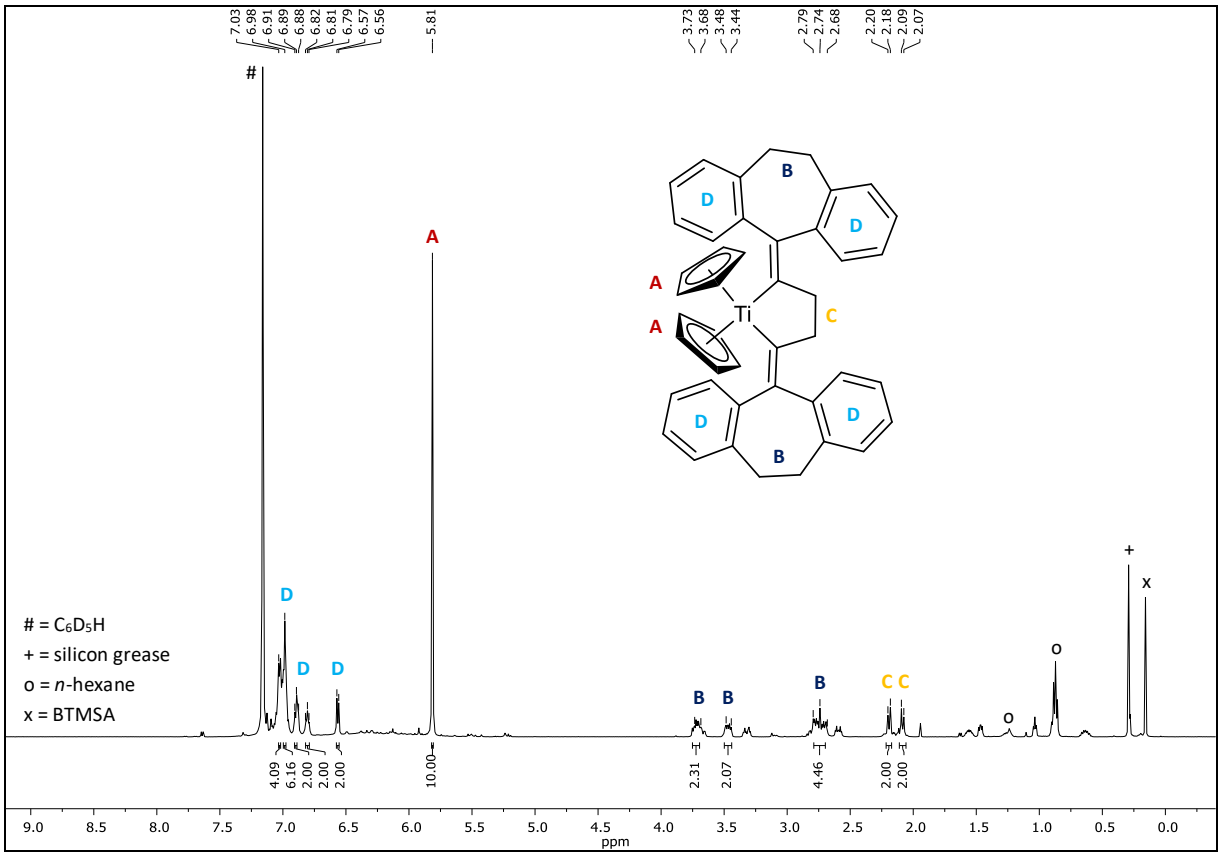

Figure S85: ^{1}H NMR spectrum of **5q** (500 MHz, C_6D_6, 305 K).

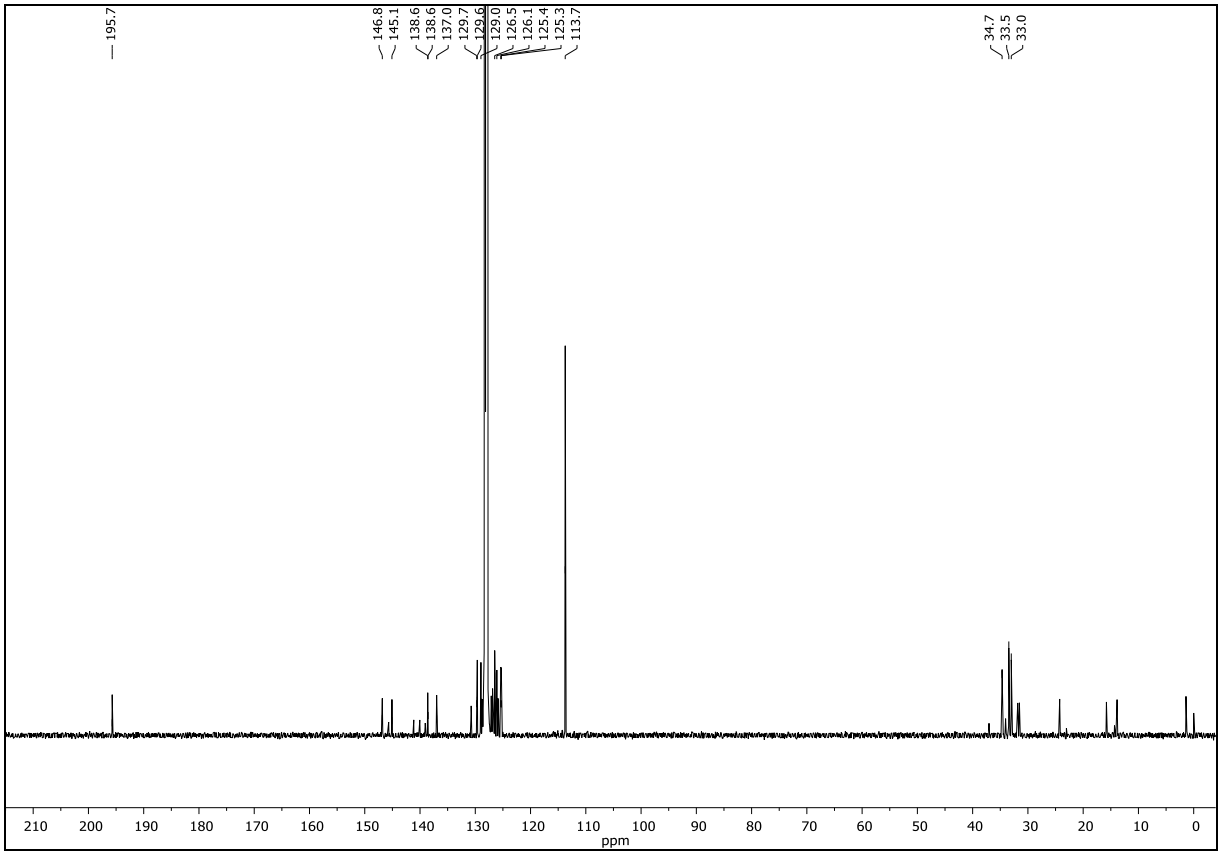

Figure S86: $^{13}C\{^{1}H\}$ NMR spectrum of **5q** (126 MHz, C_6D_6, 305 K).

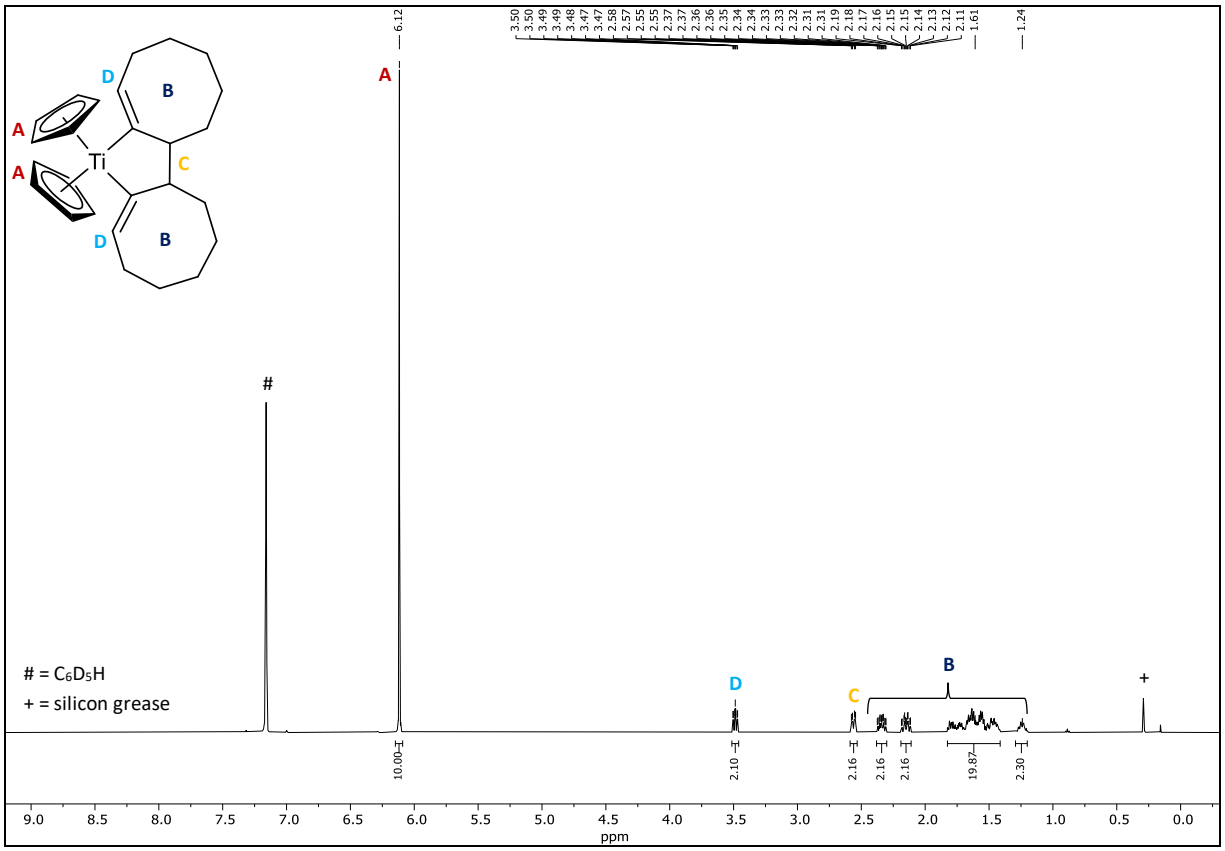

Figure S87: ^{1}H NMR spectrum of **5r** (500 MHz, C_6D_6, 305 K).

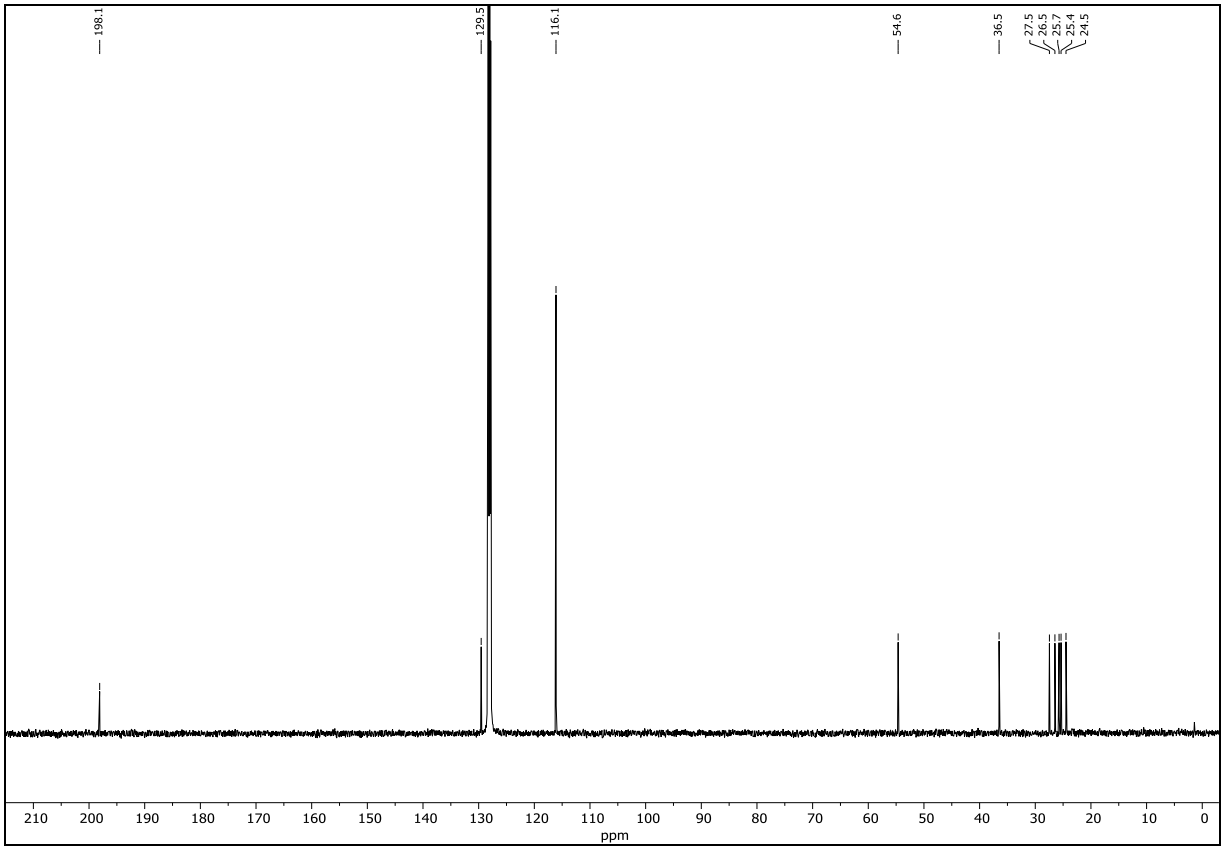

Figure S88: $^{13}C\{^{1}H\}$ NMR spectrum of **5r** (126 MHz, C_6D_6, 305 K).

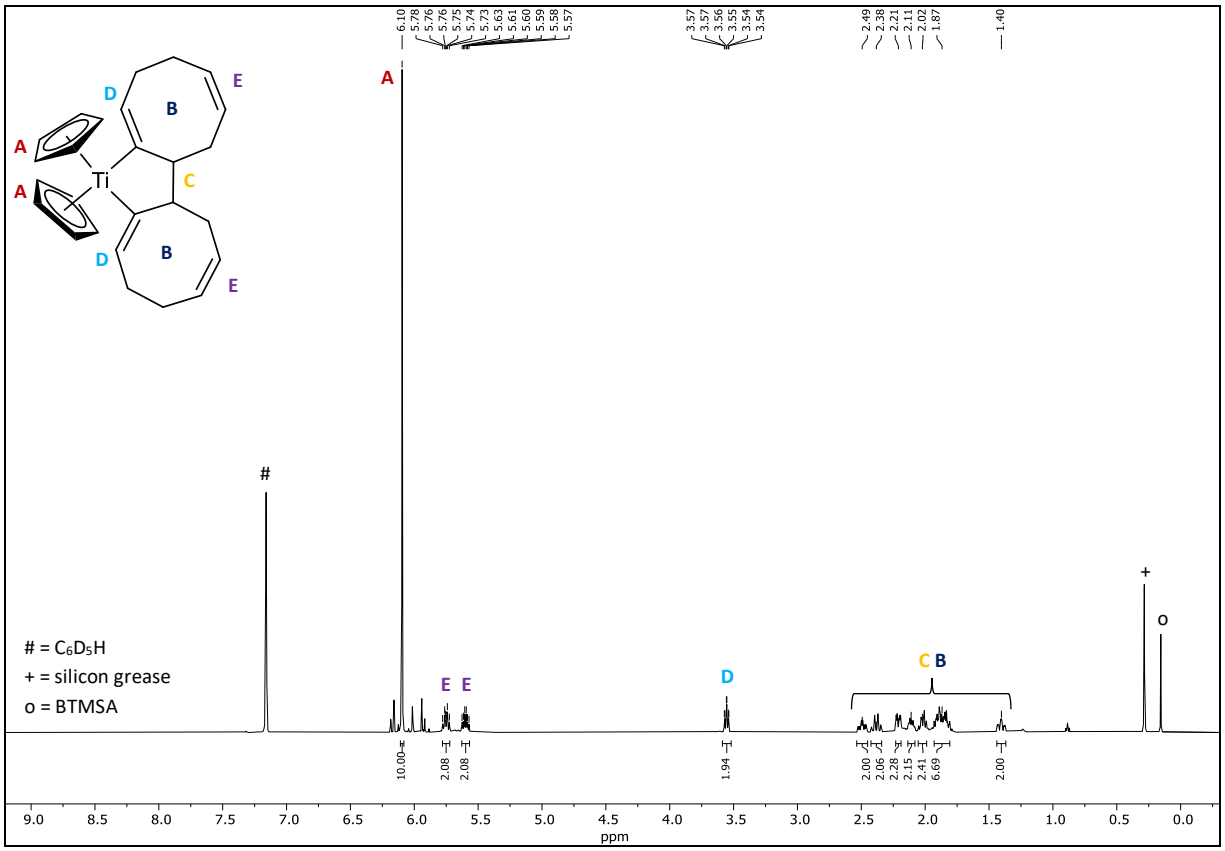

Figure S89: ^{1}H NMR spectrum of **5s** (500 MHz, C_6D_6, 305 K).

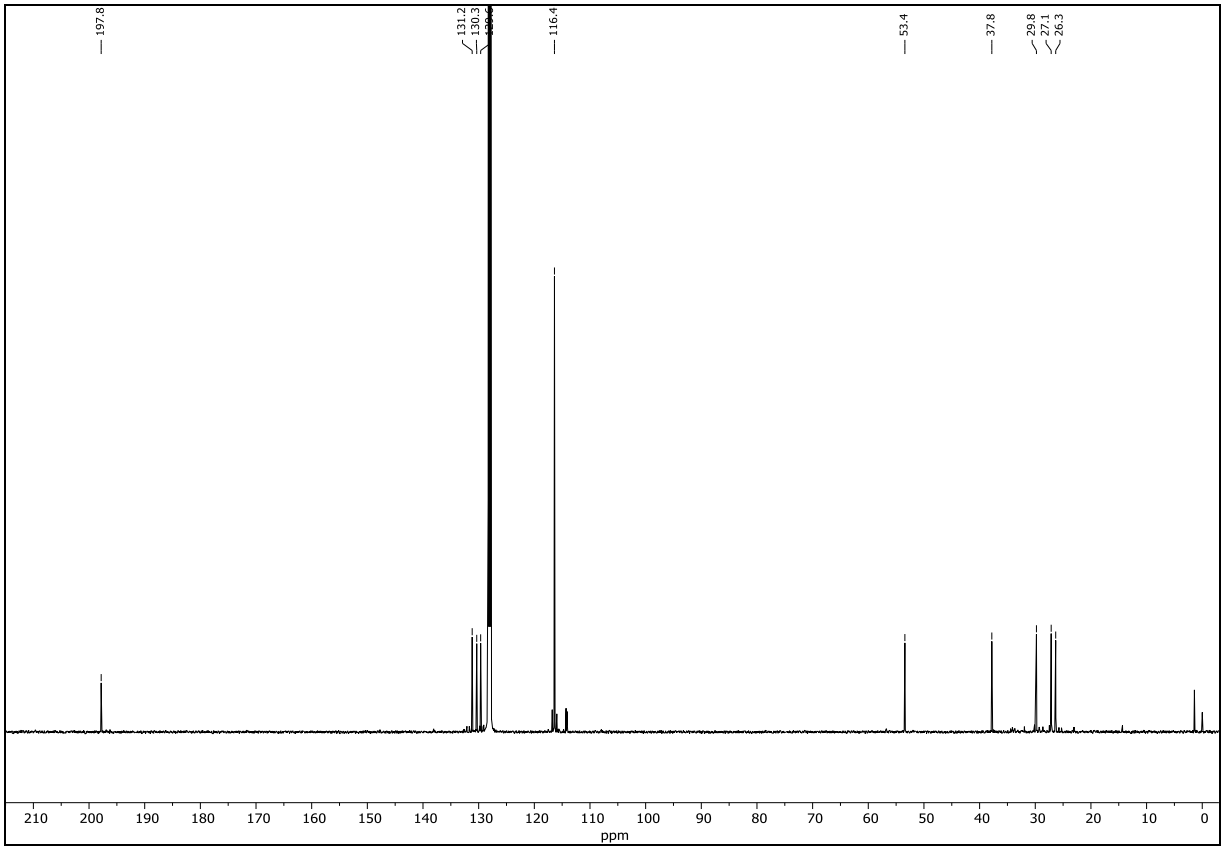

Figure S90: $^{13}C\{^{1}H\}$ NMR spectrum of **5s** (126 MHz, C_6D_6, 305 K).

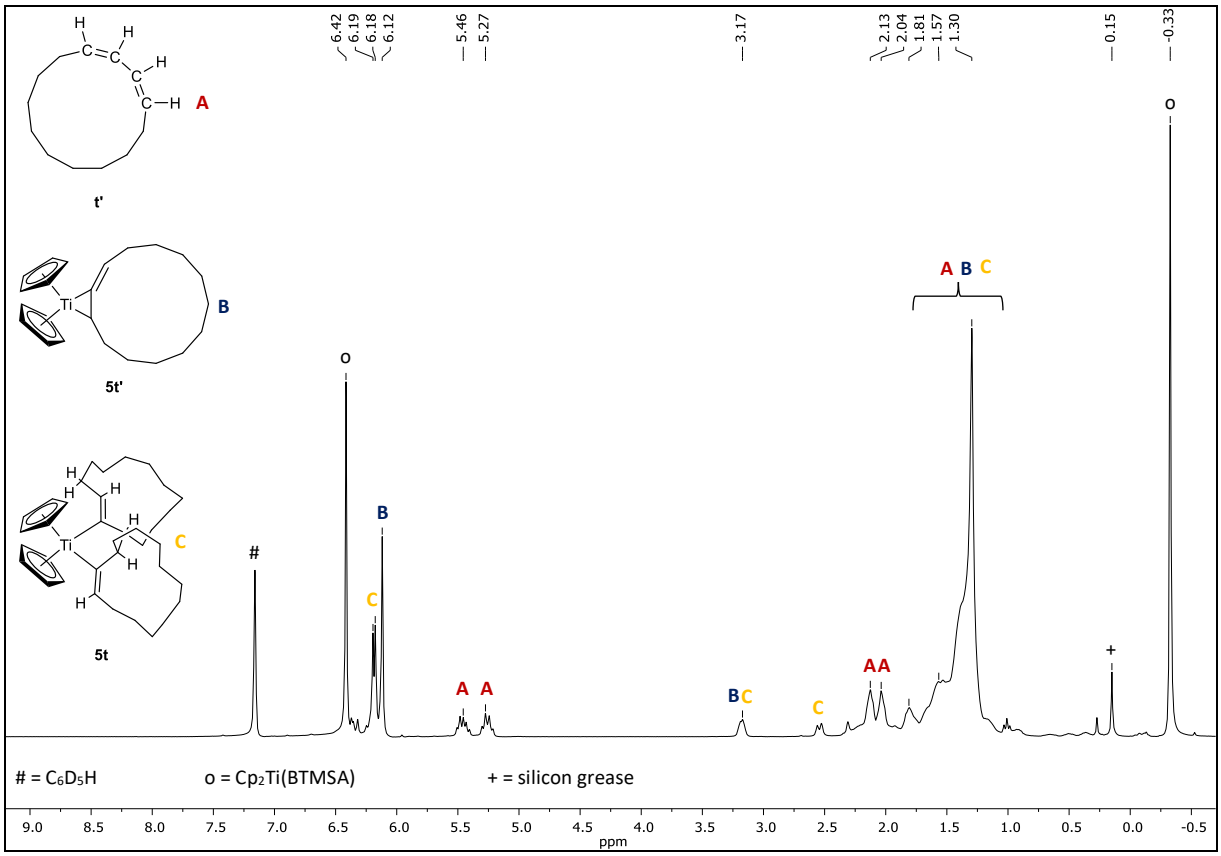

Figure S91: ^{1}H NMR spectrum of the products from the reaction of complex **1** with allene **t** (300 MHz, C_6D_6, 298 K).

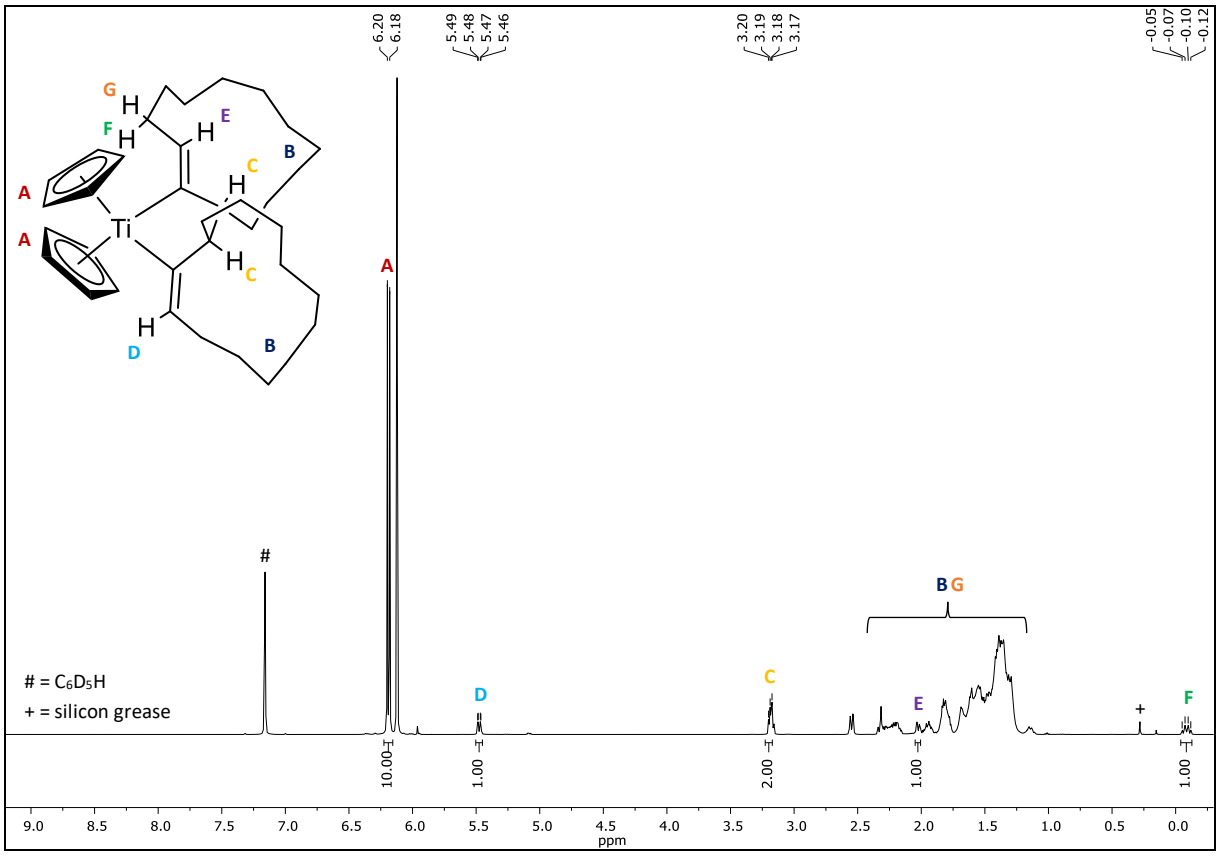

Figure S92: ^{1}H NMR spectrum of **5t** (500 MHz, C_6D_6, 305 K).

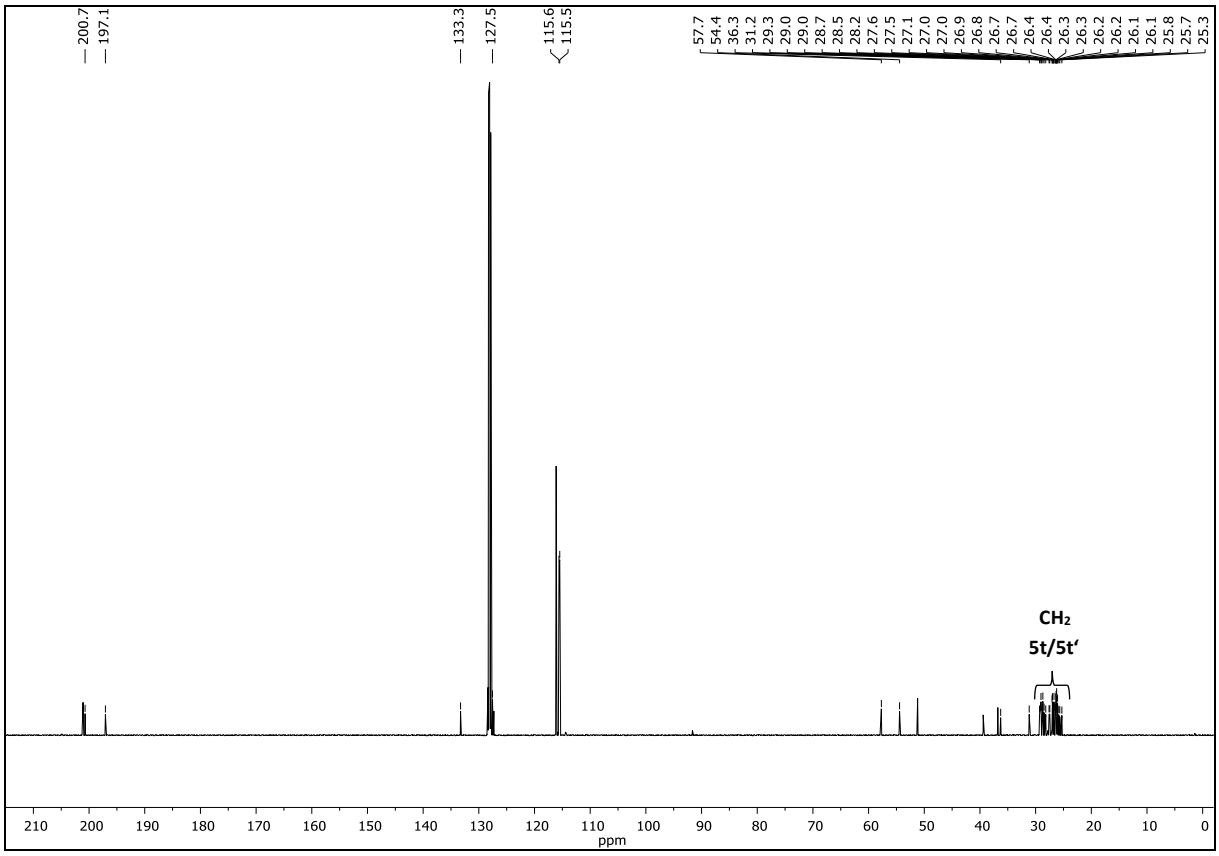

Figure S93: $^{13}C\{^{1}H\}$ NMR spectrum of **5t** (126 MHz, C_6D_6, 305 K).

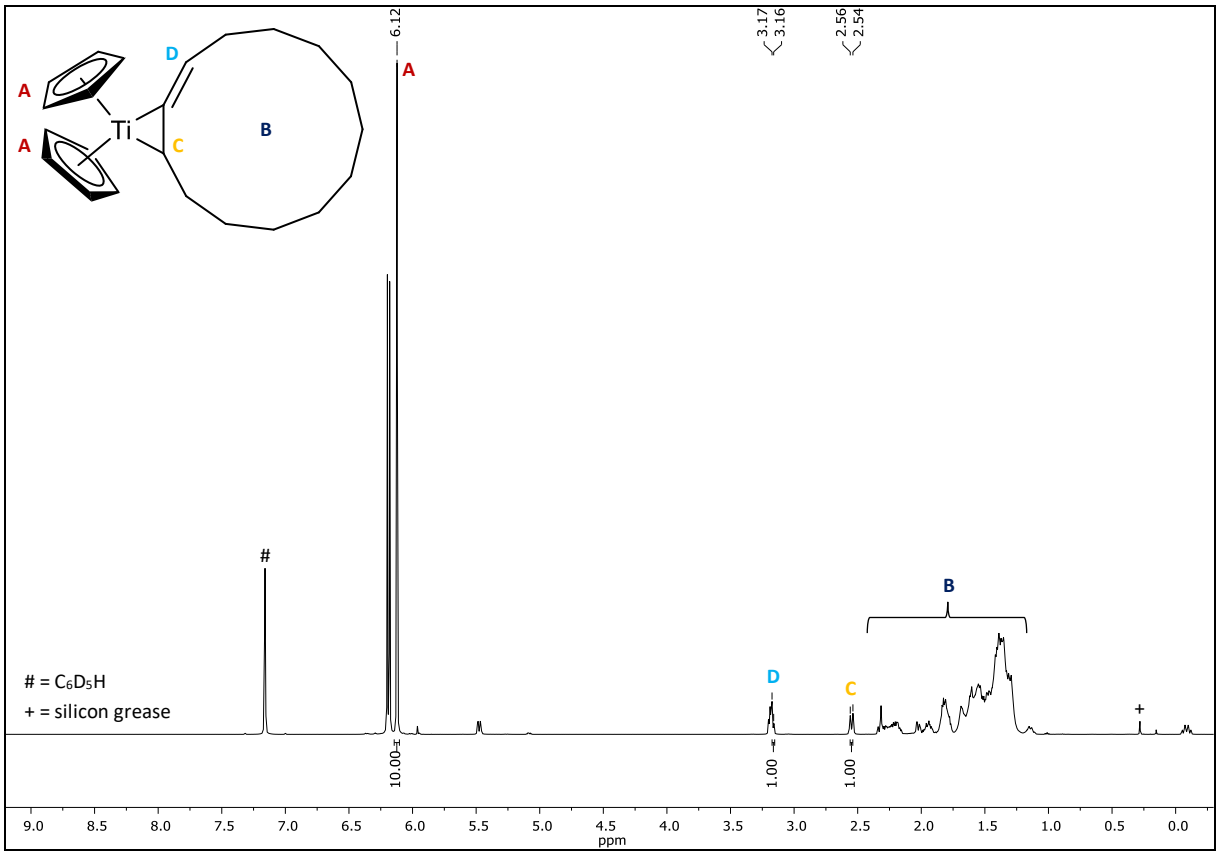

Figure S94: ^{1}H NMR spectrum of **5t'** (500 MHz, C_6D_6, 305 K).

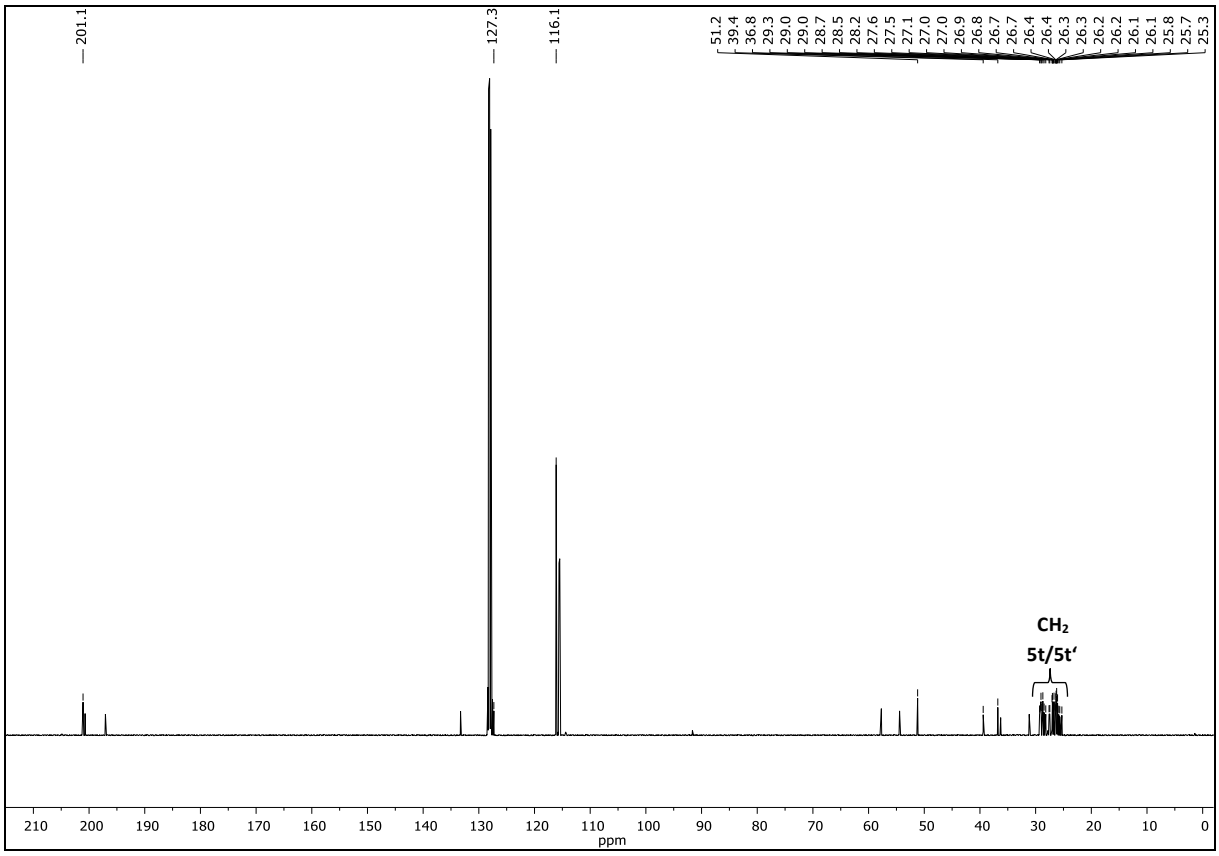

Figure S95: $^{13}C\{^{1}H\}$ NMR spectrum of **5t'** (126 MHz, C_6D_6, 305 K).

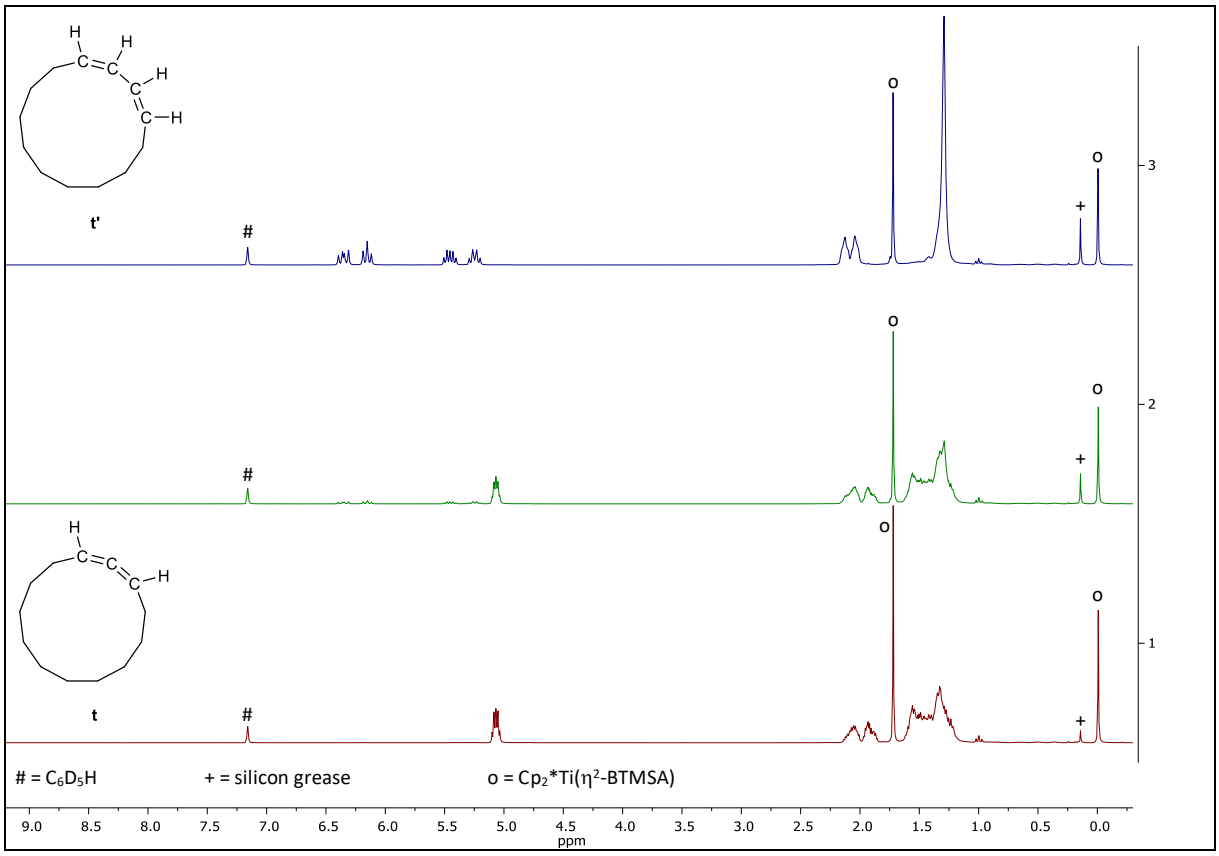

Figure S96: Stacked ^{1}H NMR spectra of the isomerization reaction of allene **t** (bottom) by $Cp^*_2Ti(\eta^2\text{-BTMSA})$ to give cyclotrideca-1,3-diene **t'** (top) (500 MHz, C_6D_6, 305 K); 1 = 0 h, 2 = 3 h, 3 = 16 h.

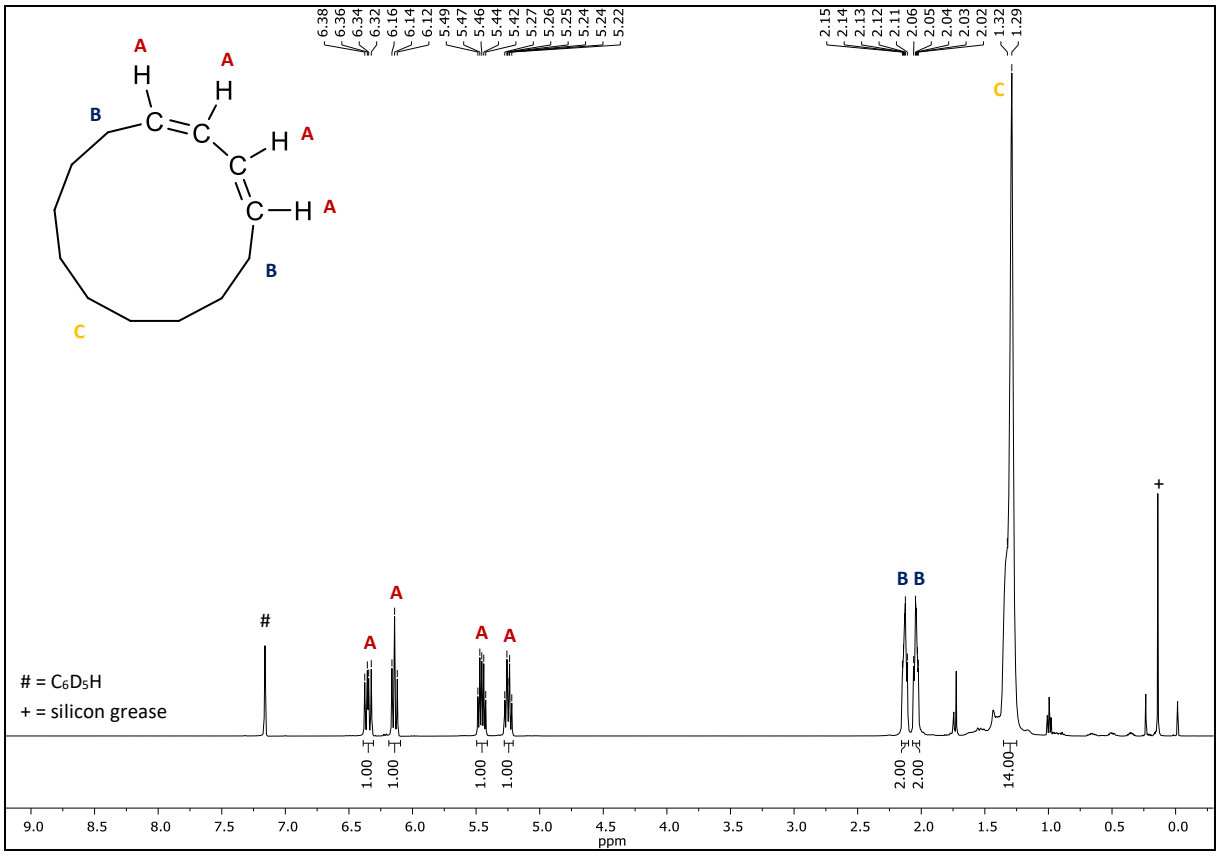

Figure S97: ^{1}H NMR spectrum of **t'** (500 MHz, C_6D_6, 305 K).

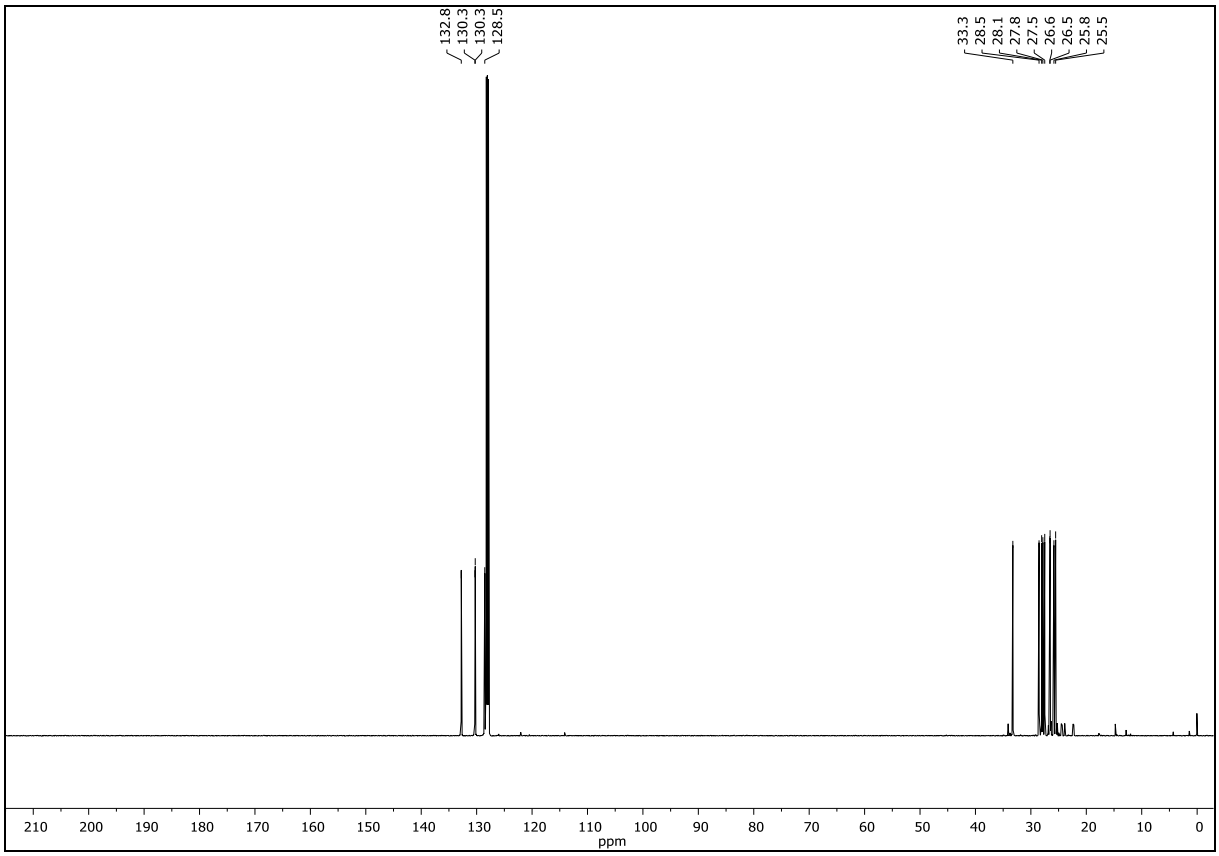

Figure S98: $^{13}C\{^{1}H\}$ NMR spectrum of **t'** (126 MHz, C_6D_6, 305 K).

Crystallographic Data

Single crystal X-ray data measured on a Bruker AXS D8 Venture diffractometer (multilayer optics, Mo-Kα and Cu-Kα radiation with λ = 0.71073 Å and 1.54178 Å respectively, Kappa 4-circle goniometer, Photon III C14 CPAD detector).

All crystals were measured at a temperature of 100 K. Absorption corrections using equivalent reflections were performed with the program SADABS.[4] All structures were solved with the program SHELXS[5] and refined with SHELXL[6] using the OLEX2[7] GUI.

All non-H atoms were refined with anisotropic atomic displacement parameters (ADPs); in case of disorder some minor sites were refined with isotropic ADPs instead. H atoms bonded to C were located in the difference Fourier maps and placed on idealized geometric positions with idealized ADPs using the riding model.

In **5b** all ligands are disordered. The site occupancies of the 1,6-dimethoxyhexene ligand and one Cp ligand refine to approximately 0.93 : 0.07; the site occupancies of the other Cp ligand refine to 0.80 : 0.20. The minor site of 1,6-dimethoxyhexene was restrained to have the same geometry as the respective major site (SAME instruction of SHELXL), and the isotropic ADPs were constrained to be the same (EADP). The Cp ligand with an occupancy of 0.07 was constrained to have ideal geometry (AFIX 56).

In **5o** both Cp ligands are disordered with refined site occupancies of approximately 0.93 : 0.07. The Cp ligands of the minor sites were constrained to have ideal geometry (AFIX 56), and the isotropic ADPs were constrained to be the same (EADP).

The crystal of **5t** was of poor quality, showed diffuse scattering, and radiation damage during the measurement, hence, the structure is of comparatively poor quality, too. One cyclotridecene ligand is disordered (0.50 : 0.50) and was refined using restraints on the anisotropic ADPs (RIGU).

The crystallographic data can be obtained free of charge from https://www.ccdc.cam.ac.uk/structures/ quoting the CCDC numbers 2463910-2463915 and 2470638-2470649.

Table S1: Crystal Structure Data for Compounds **2a**, **2b**, **2c** and **2d**.

Complex	**2a**	**2b**	**2c**	**2d**
Lab ID	MAP359	MAP358	MAP393	MAP394
CCDC	2463915	2463914	2463911	2463912
empirical formula	$C_{38}H_{48}D_6Si_2Ti$	$C_{28}H_{38}Si_2Ti$	$C_{29}H_{40}Si_2Ti$	$C_{28}H_{37}ClSi_2Ti$
fw	620.93	478.66	492.69	513.10
colour	brown	red brown	red	red brown
Habit	block	block	block	block
cryst dimens, mm	0.12 x 0.06 x 0.04	0.14 x 0.10 x 0.04	0.15 x 0.13 x 0.10	0.12 x 0.10 x 0.06
cryst syst	monoclinic	triclinic	triclinic	triclinic
space group	$P2_1/n$	P-1	P-1	P-1
a, Å	13.1108(6)	9.7843(7)	9.9598(4)	10.0789(5)
b, Å	10.2423(5)	10.6241(7)	10.8054(5)	10.7767(5)
c, Å	25.2436(11)	12.5157(8)	13.1951(6)	12.9427(6)
α, deg	90	95.663(3)	110.0916(14)	109.0461(17)
β, deg	95.6324(16)	95.294(3)	91.8127(15)	91.4751(17)
γ, deg	90	90.890(3)	92.8264(15)	94.0174(17)
V, Å³	3373.5(3)	1288.73(15)	1330.22(10)	1323.81(11)
Z	4	2	2	2
ρ_{caclcd}, g cm^{-3}	1.223	1.234	1.230	1.287
μ, mm^{-1}	0.350	0.439	0.427	0.529
T, K	100(2)	100(2)	100(2)	100(2)
λ, Å	0.71073	0.71073	0.71073	0.71073
θ range, deg	1.621 – 34.970	1.642 – 40.248	1.645 – 40.248	1.667 – 40.249
no. of rflns collected	149944	212769	105567	145728
no. of indep rflns (R(int))	14814 0.0505	16226 0.0492	16740 0.0303	16674 0.0356
no. of rflns with $I>2\sigma(I)$	13073	14442	15614	15056
abs cor	semi-empirical	semi-empirical	semi-empirical	semi-empirical
max, min transmission	1.0000, 0.9244	1.0000, 0.9198	1.0000, 0.9390	1.0000, 0.9225
final R indices [$I>2\sigma(I)$]	R1 = 0.0401 wR2 = 0.0954	R1 = 0.0377 wR2 = 0.0988	R1 = 0.0262 wR2 = 0.0787	R1 = 0.0312 wR2 = 0.0903
R indices (all data)	R1 = 0.0478 wR2 = 0.0990	R1 = 0.0440 wR2 = 0.1022	R1 = 0.0284 wR2 = 0.0800	R1 = 0.0352 wR2 = 0.0931
GOF on F^2	1.127	1.137	1.095	1.045
largest diff peak / hole (e.Å^{-3})	1.052 / -0.526	1.058 / -0.407	0.722 / -0.335	1.797 / -0.812

Table S2: Crystal Structure Data for Compounds **4c**, **4d**, **5a**, and **5b**.

Complex	**4c**	**4d**	**5a**	**5b**
Lab ID	MAP441	MAP442	MAP346	MAP75
CCDC	2463913	2463910	2470641	2470638
empirical formula	$C_{35}H_{32}Ti$	$C_{34}H_{29}ClTi$	$C_{16}H_{18}Ti$	$C_{18}H_{22}O_2Ti$
fw	500.50	520.92	258.20	318.25
colour	dark green	dark red	orange	red
Habit	block	plate	plate	plate
cryst dimens, mm	0.08 x 0.08 x 0.05	0.11 x 0.07 x 0.02	0.12 x 0.12 x 0.025	0.10 x 0.08 x 0.03
cryst syst	monoclinic	monoclinic	orthorhombic	monoclinic
space group	$P2_1/c$	$P2_1/c$	*Pbcn*	$P2_1/c$
a, Å	8.2256(4)	18.8218(5)	7.2500(2)	8.5677(4)
b, Å	15.7546(8)	16.4998(5)	15.4970(4)	12.2738(6)
c, Å	20.0225(9)	8.2891(2)	11.7203(3)	15.0541(7)
α, deg	90	90	90	90
β, deg	91.1451(18)	94.2446(12)	90	101.2368(16)
γ, deg	90	90	90	90
V, Å³	2594.2(2)	2567.17(12)	1316.81(6)	1552.72(13)
Z	4	4	4	4
ρ_{caclcd}, g cm^{-3}	1.281	1.348	1.302	1.361
μ, mm^{-1}	0.352	3.929	0.624	0.553
T, K	100(2)	100(2)	100(2)	100(2)
λ, Å	0.71073	1.54178	0.71073	0.71073
θ range, deg	1.645 – 36.318	2.354 – 74.479	2.629 – 40.246	2.158 – 34.967
no. of rflns collected	145565	39685	120273	92395
no. of indep rflns (R(int))	12583 0.0471	5255 0.0480	4149 0.0363	6812 0.0513
no. of rflns with $I>2\sigma(I)$	11134	5005	3771	6042
abs cor	semi-empirical	semi-empirical	semi-empirical	semi-empirical
max, min transmission	1.0000, 0.9267	1.0000, 0.7564	1.0000, 0.8968	1.0000, 0.9143
final R indices [$I>2\sigma(I)$]	R1 = 0.0378 wR2 = 0.0968	R1 = 0.0330 wR2 = 0.0889	R1 = 0.0293 wR2 = 0.0750	R1 = 0.0578 wR2 = 0.1433
R indices (all data)	R1 = 0.0442 wR2 = 0.1004	R1 = 0.0346 wR2 = 0.0902	R1 = 0.0334 wR2 = 0.0777	R1 = 0.0652 wR2 = 0.1479
GOF on F^2	1.061	1.084	1.081	1.094
largest diff peak / hole (e.Å^{-3})	0.610 / -0.362	0.311 / -0.432	0.539 / -0.393	1.400 / -0.692

Table S3: Crystal Structure Data for Compounds **5e**, **5f**, **5i**, and **5j**.

Complex	**5e**	**5i**	**5j**
Lab ID	MAP373	MAP153	MAP128
CCDC	2470644	2470649	2470648
empirical formula	$C_{28}H_{26}Ti$	$C_{30}H_{30}Ti$	$C_{20}H_{26}Ti$
fw	410.39	438.44	314.31
colour	orange	red orange	red orange
Habit	block	block	block
cryst dimens, mm	0.14 x 0.14 x 0.07	0.15 x 0.13 x 0.09	0.11 x 0.08 x 0.05
cryst syst	tetragonal	monoclinic	monoclinic
space group	*I*-42*d*	$P2_1/c$	$P2_1/c$
a, Å	14.2020(3)	16.1429(7)	8.1816(3)
b, Å	14.2020(3)	16.6373(7)	23.8056(11)
c, Å	22.6244(6)	16.9216(7)	25.5009(11)
α, deg	90	90	90
β, deg	90	93.3760(16)	94.4182(16)
γ, deg	90	90	90
V, Å³	4563.2(2)	4536.8(3)	4952.0(4)
Z	8	8	12
ρ_{caclcd}, g cm^{-3}	1.195	1.284	1.265
μ, mm^{-1}	0.385	0.392	0.510
T, K	100(2)	100(2)	100(2)
λ, Å	0.71073	0.71073	0.71073
θ range, deg	2.71 – 40.09	1.694 – 40.249	1.602 – 34.971
no. of rflns collected	178071	376079	248449
no. of indep rflns (R(int))	7192 0.0411	28554 0.0448	21768 0.0655
no. of rflns with $I>2\sigma(I)$	7032	24318	18968
abs cor	semi-empirical	semi-empirical	semi-empirical
max, min transmission	1.0000, 0.9224	1.0000, 0.9081	1.0000, 0.9120
final R indices [$I>2\sigma(I)$]	R1 = 0.0208 wR2 = 0.0586	R1 = 0.0374 wR2 = 0.0990	R1 = 0.0485 wR2 = 0.0989
R indices (all data)	R1 = 0.0215 wR2 = 0.0590	R1 = 0.0462 wR2 = 0.1043	R1 = 0.0589 wR2 = 0.1027
GOF on F^2	1.114	1.051	1.137
largest diff peak / hole (e.Å^{-3})	0.358 / -0.291	0.772 / -0.735	1.118 / -0.509

Table S4: Crystal Structure Data for Compounds **5k**, **5l**, **5n**, and **5o**.

Complex	**5k**	**5l**	**5n**	**5o**
Lab ID	MAP154	MAP158	MAP73	MAP181
CCDC	2470643	2470646	2470642	2470639
empirical formula	$C_{40}H_{58}Ti$	$C_{40}H_{34}Ti$	$C_{26}H_{34}Ti$	$C_{32}H_{42}Ti$
fw	586.76	562.57	394.43	474.55
colour	red	red	orange	red
Habit	block	block	plate	block
cryst dimens, mm	0.16 x 0.10 x 0.06	0.08 x 0.05 x 0.05	0.20 x 0.18 x 0.03	0.14 x 0.09 x 0.07
cryst syst	monoclinic	Tetragonal	monoclinic	monoclinic
space group	$P2_1/n$	$P4_3$	$P2_1/c$	$P2_1$
a, Å	15.1717(7)	22.1525(4)	15.8813(5)	10.1447(2)
b, Å	13.7665(6)	22.1525(4)	16.4133(5)	10.1649(2)
c, Å	16.4988(7)	24.1648(8)	7.9404(3)	13.2164(3)
α, deg	90	90	90	90
β, deg	103.5396(17)	90	96.9409(13)	111.2741(8)
γ, deg	90	90	90	90
V, Å³	3350.2(3)	11858.5(6)	2054.61(12)	1270.00(5)
Z	4	16	4	2
ρ_{caclcd}, g cm^{-3}	1.163	1.260	1.275	1.241
μ, mm^{-1}	0.281	2.633	0.424	0.355
T, K	100(2)	100(2)	100(2)	100(2)
λ, Å	0.71073	1.54178	0.71073	0.71073
θ range, deg	1.642 – 34.970	2.706 – 74.493	1.292 – 40.248	1.653 – 34.971
no. of rflns collected	168000	200918	138760	81114
no. of indep rflns (R(int))	14727 0.0503	24181 0.1046	12942 0.0453	11163 0.0339
no. of rflns with $I>2\sigma(I)$	12730	20445	11661	10625
abs cor	semi-empirical	semi-empirical	semi-empirical	semi-empirical
max, min transmission	1.0000, 0.9506	1.0000, 0.8740	1.0000, 0.9099	1.0000, 0.9197
final R indices [$I>2\sigma(I)$]	R1 = 0.0463 wR2 = 0.1089	R1 = 0.0681 wR2 = 0.1675	R1 = 0.0358 wR2 = 0.0839	R1 = 0.0324 wR2 = 0.0798
R indices (all data)	R1 = 0.0559 wR2 = 0.1131	R1 = 0.0822 wR2 = 0.1787	R1 = 0.0415 wR2 = 0.0863	R1 = 0.0352 wR2 = 0.0813
GOF on F^2	1.133	1.097	1.097	1.065
largest diff peak / hole (e.Å^{-3})	0.471 / -0.360	1.763 / -0.454	0.624 / -0.547	0.433 / -0.256

Table S5: Crystal Structure Data for Compounds **5p**, **5r**, and **5t**.

Complex	**5p**	**5r**	**5t**
Lab ID	MAP155	MAP378	MAP77
CCDC	2470645	2470647	2470640
empirical formula	$C_{37}H_{34}D_3Ti$	$C_{28}H_{38}Ti$	$C_{55}H_{40}D_{12}Ti$
fw	532.58	422.48	772.94
colour	red	red	orange
Habit	block	block	rod
cryst dimens, mm	0.14 x 0.09 x 0.08	0.15 x 0.10 x 0.09	0.13 x 0.04 x 0.04
cryst syst	monoclinic	monoclinic	orthorhombic
space group	$P2_1/n$	$P2_1/n$	$Pna2_1$
a, Å	11.2225(4)	13.9824(5)	16.2420(14)
b, Å	16.2455(6)	9.1041(3)	11.5573(11)
c, Å	15.1819(5)	17.9064(7)	32.294(3)
α, deg	90	90	90
β, deg	95.0952(12)	108.5728(12)	90
γ, deg	90	90	90
V, Å³	2756.95(17)	2160.72(14)	6062.0(9)
Z	4	4	8
ρ_{caclcd}, g cm^{-3}	1.283	1.299	1.172
μ, mm^{-1}	0.335	0.408	2.530
T, K	100(2)	100(2)	100(2)
λ, Å	0.71073	0.71073	1.54178
θ range, deg	1.840 – 40.249	1.536 – 40.249	2.736 – 74.473
no. of rflns collected	213152	208497	101119
no. of indep rflns (R(int))	17364 0.0397	13620 0.0364	12277 0.0800
no. of rflns with $I>2\sigma(I)$	15507	12124	10941
abs cor	semi-empirical	semi-empirical	semi-empirical
max, min transmission	1.0000, 0.9170	1.0000, 0.9196	1.0000, 0.8381
final R indices [$I>2\sigma(I)$]	R1 = 0.0333 wR2 = 0.0907	R1 = 0.0277 wR2 = 0.0818	R1 = 0.0870 wR2 = 0.2104
R indices (all data)	R1 = 0.0386 wR2 = 0.0941	R1 = 0.0322 wR2 = 0.0849	R1 = 0.0941 wR2 = 0.2163
GOF on F^2	1.054	1.053	1.160
largest diff peak / hole (e.Å^{-3})	0.674 / -0.464	0.600 / -0.541	2.515 / -0.415

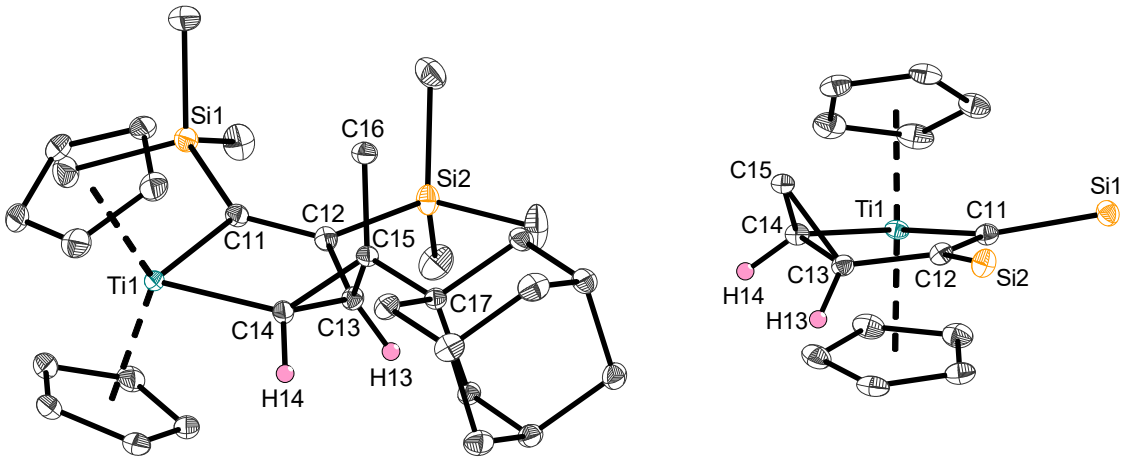

Figure S99: Molecular structure of complex **2a** (supine isomer). Hydrogen atoms and co-crystalized benzene-d_6 are omitted for clarity. Thermal ellipsoids are drawn at the 50% probability level. Selected bond lengths (Å) and angles (deg): Ti1–C11 2.2037(9), Ti1–C14 2.1392(9), C11–C12 1.3662(13), C11–Si1 1.8733(10), C12–Si2 1.9006(9), C12–C13 1.5099(13), C13–C14 1.5267(13), C14–C15 1.5204(12), C13–C15 1.5442(12), C15–C16 1.5172(13), C15–C17 1.5585(12); C11–Ti1–C14 83.72(3), Ti1–C11–Si1 122.21(5), Ti1–C11–C12 109.92(6), Ti1–C14–C13 105.87(6), C11–C12–C13 119.06(8), C12–C13–C15 119.50(7), C13–C15–C14 59.75(6).

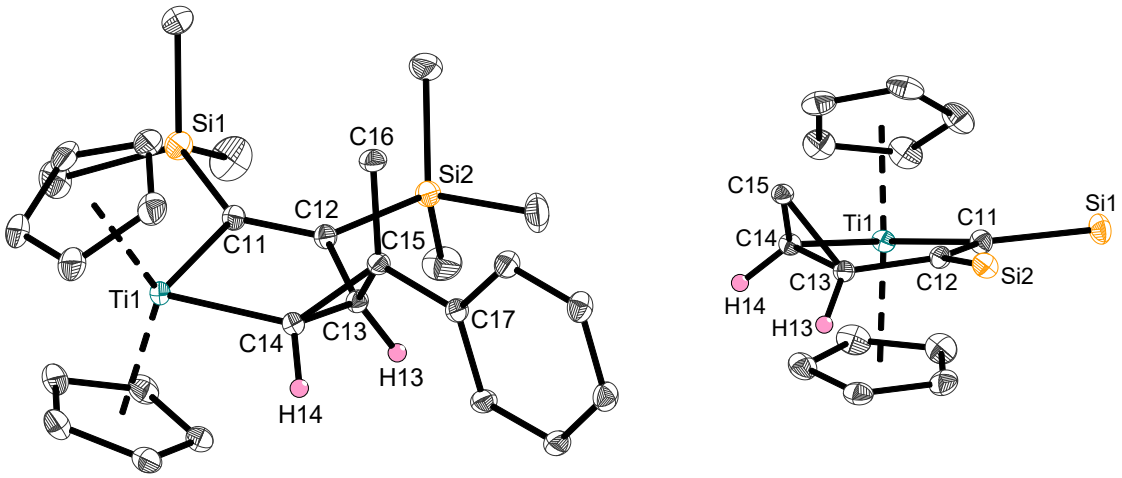

Figure S100: Molecular structure of complex **2b** (supine isomer). Hydrogen atoms are omitted for clarity. Thermal ellipsoids are drawn at the 50% probability level. Selected bond lengths (Å) and angles (deg): Ti1–C11 2.1920(7), Ti1–C14 2.1495(7), C11–C12 1.3640(9), C11–Si1 1.8767(7), C12–Si2 1.9004(7), C12–C13 1.5117(9), C13–C14 1.5192(9), C14–C15 1.5349(9), C13–C15 1.5416(9), C15–C16 1.5143(9), C15–C17 1.5056(9); C11–Ti1–C14 86.49(3), Ti1–C11–Si1 125.47(3), Ti1–C11–C12 107.50(5), Ti1–C14–C13 102.14(4), C11–C12–C13 119.79(6), C12–C13–C15 120.12(5), C13–C15–C14 59.18(4).

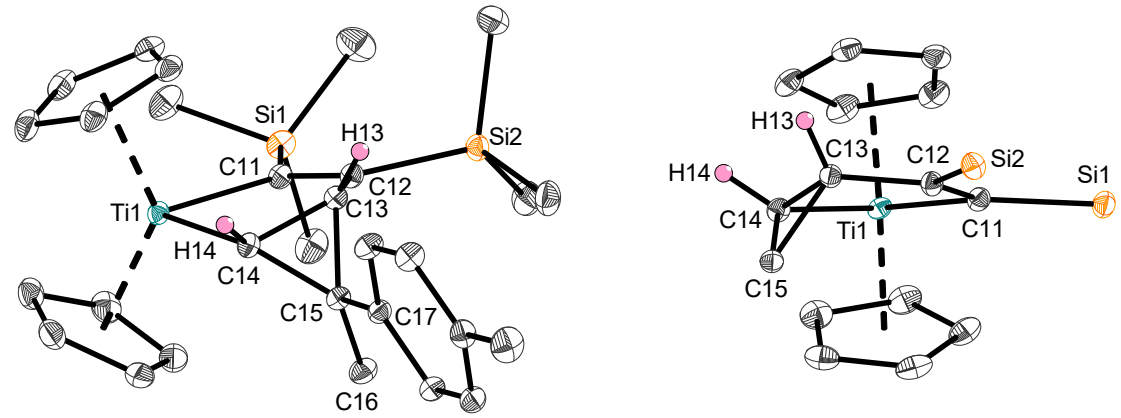

Figure S101: Molecular structure of complex **2c** (prone isomer). Hydrogen atoms are omitted for clarity. Thermal ellipsoids are drawn at the 50% probability level. Selected bond lengths (Å) and angles (deg): Ti1–C11 2.1911(5), Ti1–C14 2.1423(5), C11–C12 1.3645(7), C11–Si1 1.8757(5), C12–Si2 1.9017(5), C12–C13 1.5120(6), C13–C14 1.5186(7), C14–C15 1.5291(7), C13–C15 1.5469(7), C15–C16 1.5144(7), C15–C17 1.5051(7); C11–Ti1–C14 87.048(18), Ti1–C11–Si1 125.11(2), Ti1–C11–C12 106.81(3), Ti1–C14–C13 101.60(3), C11–C12–C13 119.98(4), C12–C13–C15 120.04(4), C13–C15–C14 59.16(3).

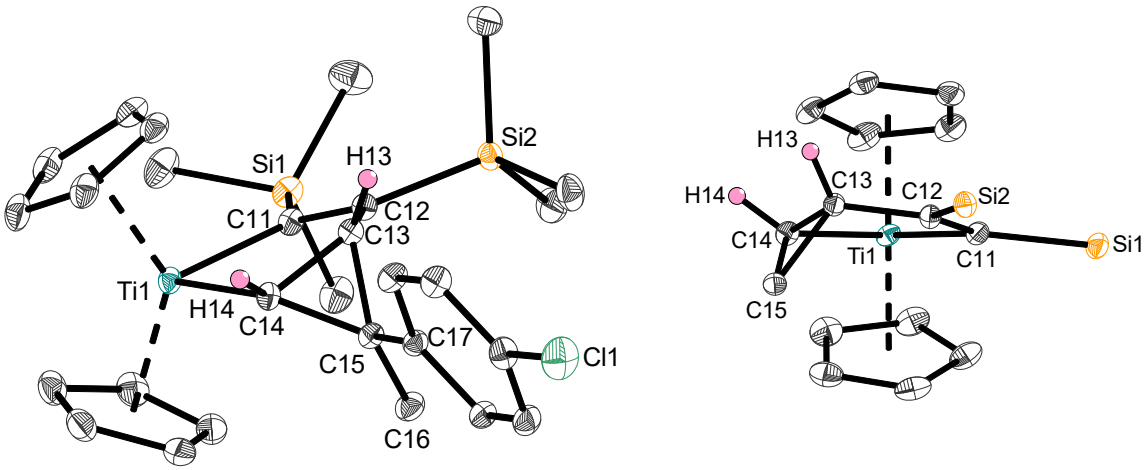

Figure S102: Molecular structure of complex **2d** (prone isomer). Hydrogen atoms are omitted for clarity. Thermal ellipsoids are drawn at the 50% probability level. Selected bond lengths (Å) and angles (deg): Ti1–C11 2.1903(6), Ti1–C14 2.1445(6), C11–C12 1.3667(8), C11–Si1 1.8785(6), C12–Si2 1.9022(6), C12–C13 1.5134(8), C13–C14 1.5159(8), C14–C15 1.5299(8), C13–C15 1.5469(8), C15–C16 1.5132(9), C15–C17 1.5038(8); C11–Ti1–C14 86.58(2), Ti1–C11–Si1 124.68(3), Ti1–C11–C12 107.19(4), Ti1–C14–C13 102.22(4), C11–C12–C13 119.89(5), C12–C13–C15 119.37(5), C13–C15–C14 59.03(4).

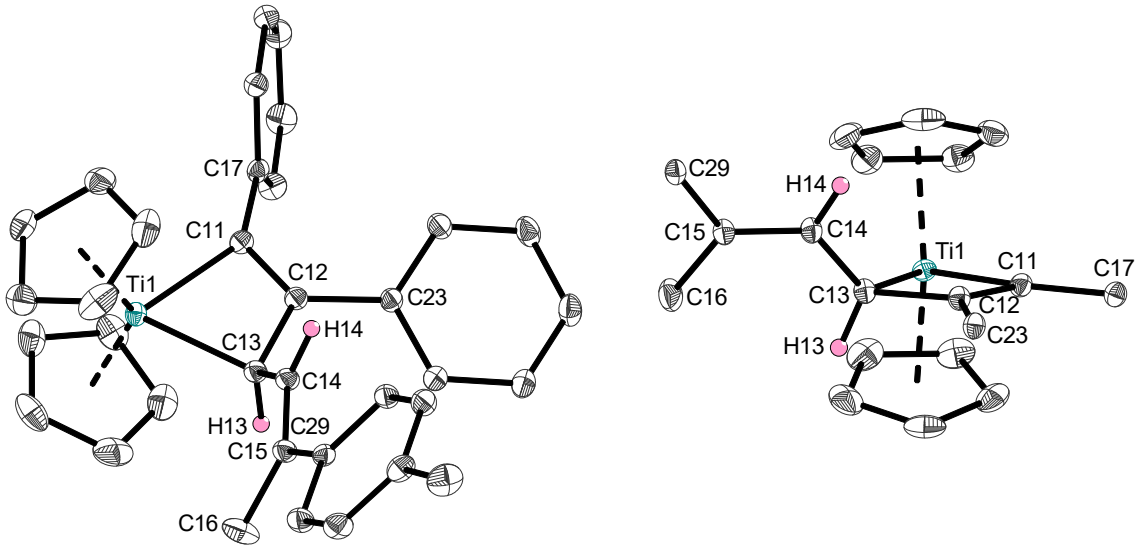

Figure S103: Molecular structure of complex **4c** (supine isomer). Hydrogen atoms are omitted for clarity. Thermal ellipsoids are drawn at the 50% probability level. Selected bond lengths (Å) and angles (deg): Ti1–C11 2.1104(8), Ti1–C13 2.1763(8), C11–C12 1.3511(11), C11–C17 1.4643(11), C12–C23 1.4935(11), C12–C13 1.5364(11), C13–C14 1.4736(11), C14–C15 1.3518(11), C15–C16 1.5067(12), C15–C29 1.4789(11); C11–Ti1–C13 69.97(3), Ti1–C11–C17 138.60(6), Ti1–C11–C12 90.20(5), Ti1–C13–C12 83.15(4), Ti1–C13–C14 128.14(6), C11–C12–C13 116.59(7), C12–C13–C14 114.54(6), C13–C14–C15 125.87(7), C14–C15–C29 122.45(7).

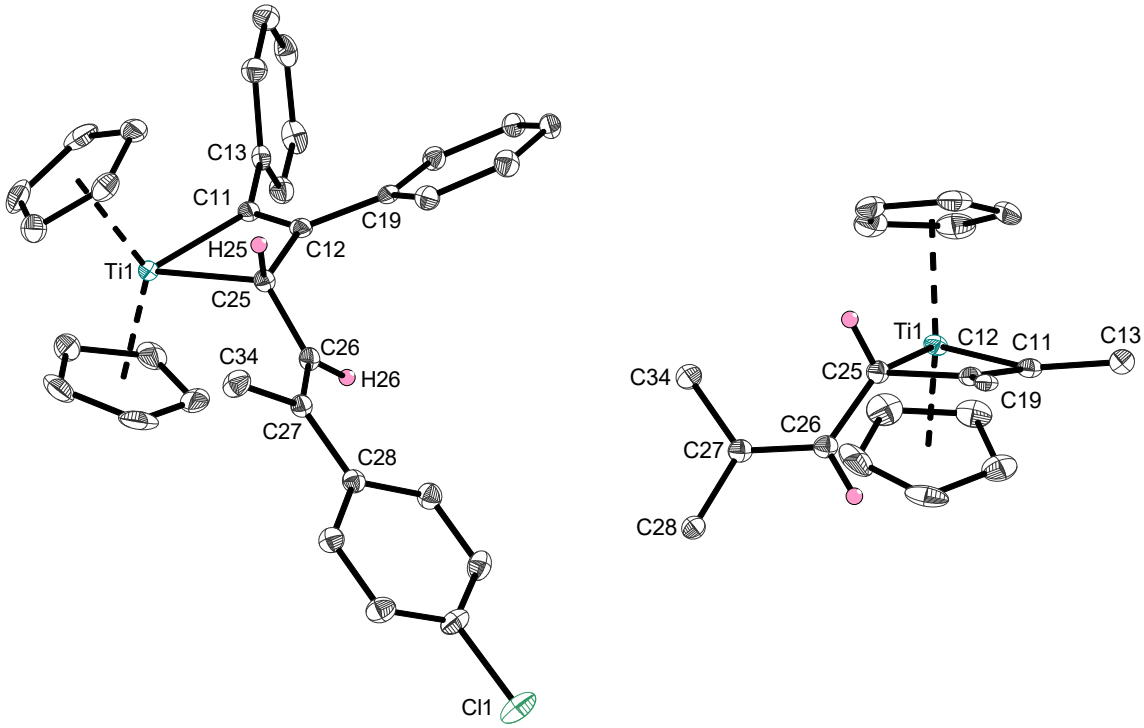

Figure S104: Molecular structure of complex **4d** (prone isomer). Hydrogen atoms are omitted for clarity. Thermal ellipsoids are drawn at the 50% probability level. Selected bond lengths (Å) and angles (deg): Ti1–C11 2.1099(13), Ti1–C25 2.1882(13), C11–C12 1.3476(19), C11–C13 1.4649(18), C12–C19 1.4981(17), C12–C25 1.5371(18), C25–C26 1.4729(18), C26–C27 1.3502(19), C27–C34 1.5126(18), C27–C28 1.4796(18); C11–Ti1–C25 69.32(5), Ti1–C11–C13 138.16(9), Ti1–C11–C12 91.22(9), Ti1–C25–C12 83.50(7), Ti1–C25–C26 125.65(9), C11–C12–C25 115.77(11), C12–C25–C26 115.32(11), C25–C26–C27 126.19(12), C26–C27–C28 121.91(12).

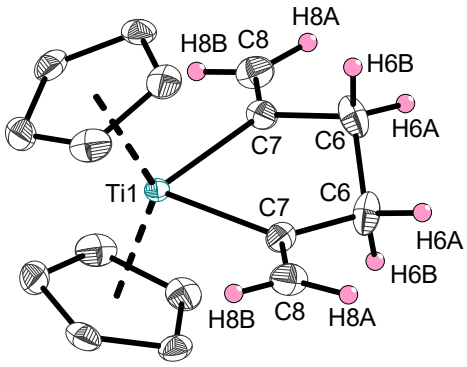

Figure S105: Molecular structure of complex **5a**. Most hydrogen atoms are omitted for clarity. Thermal ellipsoids are drawn at the 50% probability level. Selected bond lengths (Å) and angles (deg): Ti1–C7 2.1787(7), C7–C8 1.3386(10), C7–C6 1.5128(11); C7–Ti1–C7 81.74(4), Ti1–C7–C8 130.25(6), Ti1–C7–C6 108.61(5).

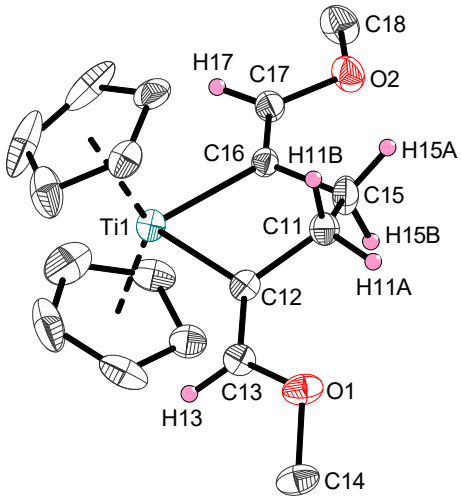

Figure S106: Molecular structure of complex **5b**. Most hydrogen atoms and disorders are omitted for clarity. Thermal ellipsoids are drawn at the 50% probability level. Selected bond lengths (Å) and angles (deg): Ti1–C12 2.1573(15), Ti1–C16 2.1687(16), C11–C12 1.516(2), C11–C15 1.541(3), C15–C16 1.524(2), C16–C17 1.329(2), C17–O2 1.398(2), C12–C13 1.336(2), C13–O1 1.395(2), O1–C14 1.426(2), O2–C18 1.417(2); C12–Ti1–C16 81.51(6), Ti1–C12–C13 128.83(13), Ti1–C12–C11 109.05(10), Ti1–C16–C17 127.61(12), Ti1–C16–C15 110.67(11), C16–C15–C11 111.40(14), C12–C11–C15 109.22(13), C13–O1–C14 112.75(15), C17–O2–C18 113.56(15).

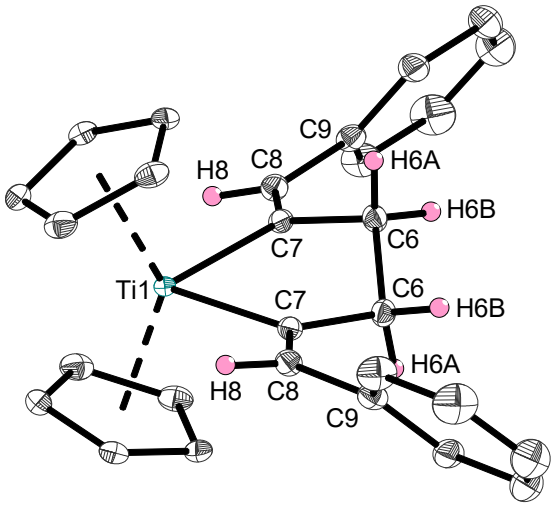

Figure S107: Molecular structure of complex **5e**. Most hydrogen atoms are omitted for clarity. Thermal ellipsoids are drawn at the 50% probability level. Selected bond lengths (Å) and angles (deg): Ti1–C7 2.1813(7), C7–C8 1.3490(10), C7–C6 1.5158(10), C6–C6 1.5380(14), C8–C9 1.4806(10); C7–Ti1–C7 81.04(4), Ti1–C7–C8 127.23(5), Ti1–C7–C6 109.43(4), C7–C8–C9 127.67(7).

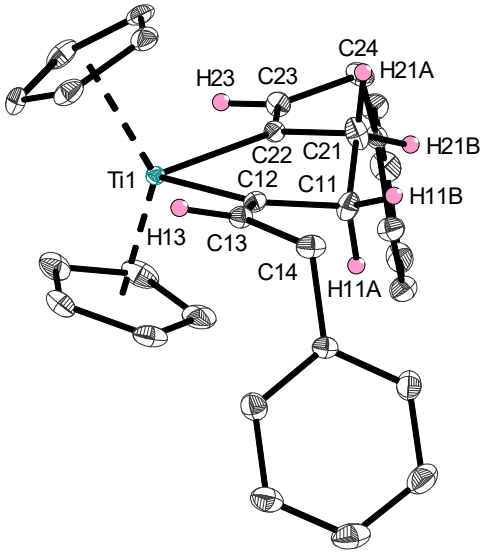

Figure S108: Molecular structure of complex **5f**. Most hydrogen atoms are omitted for clarity. Thermal ellipsoids are drawn at the 50% probability level. Selected bond lengths (Å) and angles (deg): Ti1–C12 2.166(3), Ti1–C22 2.173(3), C11–C12 1.522(4), C11–C21 1.536(5), C21–C22 1.519(4), C12–C13 1.343(4), C13–C14 1.519(4), C22–C23 1.339(4), C23–C24 1.512(4); C12–Ti1–C22 82.14(11), Ti1–C12–C13 128.3(2), Ti1–C12–C11 108.87(19), Ti1–C22–C23 127.0(2), Ti1–C22–C21 109.86(19), C22–C21–C11 111.9(2), C12–C11–C21 109.9(3), C12–C13–C14 126.4(3), C22–C23–C24 128.2(3).

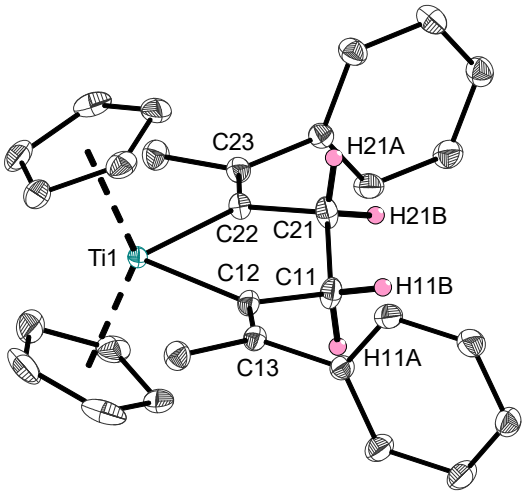

Figure S109: Molecular structure of complex **5i**. Most hydrogen atoms are omitted for clarity. Only one of the two crystallographically independent molecular structures is depicted. Thermal ellipsoids are drawn at the 50% probability level. Selected bond lengths (Å) and angles (deg): Ti1–C12 2.1857(6), Ti1–C22 2.1824(6), C11–C12 1.5251(9), C11–C21 1.5323(10), C21–C22 1.5250(9), C12–C13 1.3466(9), C22–C23 1.3471(9); C12–Ti1–C22 84.87(2), Ti1–C12–C13 133.71(5), Ti1–C12–C11 106.23(4), Ti1–C22–C23 133.73(5), Ti1–C22–C21 106.41(4), C22–C21–C11 112.78(5), C12–C11–C21 112.79(5).

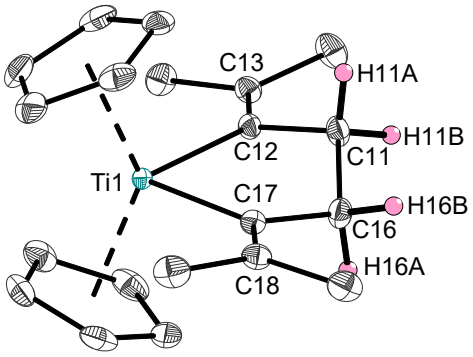

Figure S110: Molecular structure of complex **5j**. Most hydrogen atoms are omitted for clarity. Only one of the three crystallographically independent molecular structures is depicted. Thermal ellipsoids are drawn at the 50% probability level. Selected bond lengths (Å) and angles (deg): Ti1–C12 2.1790(12), Ti1–C17 2.1780(12), C11–C12 1.5256(17), C11–C16 1.5329(18), C16–C17 1.5261(17), C12–C13 1.3427(16), C17–C18 1.3439(17); C12–Ti1–C17 86.79(4), Ti1–C12–C13 133.19(9), Ti1–C12–C11 104.59(8), Ti1–C17–C18 134.61(9), Ti1–C17–C16 104.03(8), C17–C16–C11 113.79(10), C12–C11–C16 113.25(10).

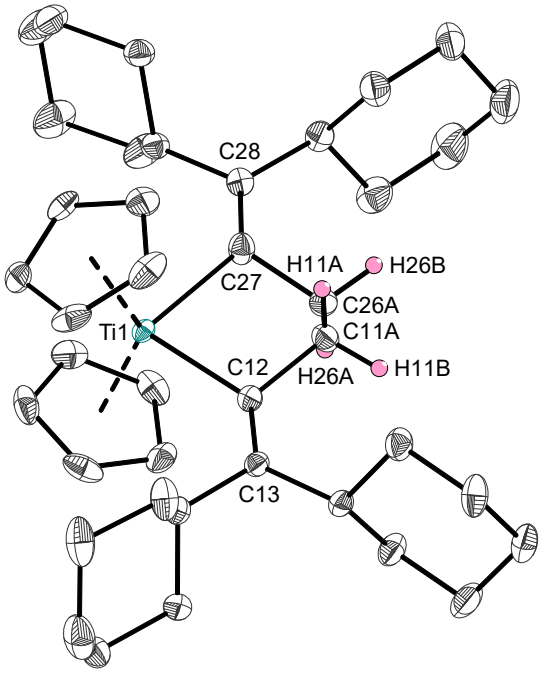

Figure S111: Molecular structure of complex **5k**. Most hydrogen atoms and disorders are omitted for clarity. Thermal ellipsoids are drawn at the 50% probability level. Selected bond lengths (Å) and angles (deg): Ti1–C12 2.2006(10), Ti1–C27 2.2112(11), C12–C13 1.3465(14), C11A–C12 1.525(2), C27–C28 1.3492(14), C27–C26A 1.546(2), C11A–C26A 1.517(3); C12–Ti1–C27 87.09(4), Ti1–C12–C13 135.50(8), Ti1–C12–C11A 102.00(9), Ti1–C27–C28 135.14(8), Ti1–C27–C26A 100.24(9), C12–C11A–C26A 111.43(17), C27–C26A–C11A 112.41(17).

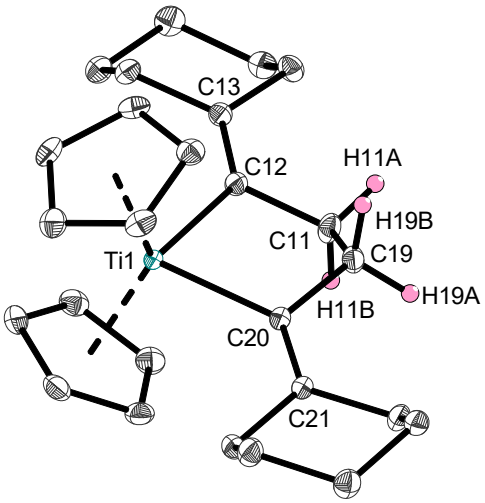

Figure S112: Molecular structure of complex **5n**. Most hydrogen atoms are omitted for clarity. Thermal ellipsoids are drawn at the 50% probability level. Selected bond lengths (Å) and angles (deg): Ti1–C12 2.1890(7), Ti1–C20 2.1888(6), C12–C13 1.3494(9), C20–C21 1.3488(9), C11–C12 1.5230(9), C19–C20 1.5252(9), C11–C19 1.5327(11); C12–Ti1–C20 86.79(2), Ti1–C12–C13 134.49(5), Ti1–C12–C11 103.98(4), Ti1–C20–C21 135.32(5), Ti1–C20–C19 103.54(4), C12–C11–C19 113.34(6), C20–C19–C11 113.80(6).

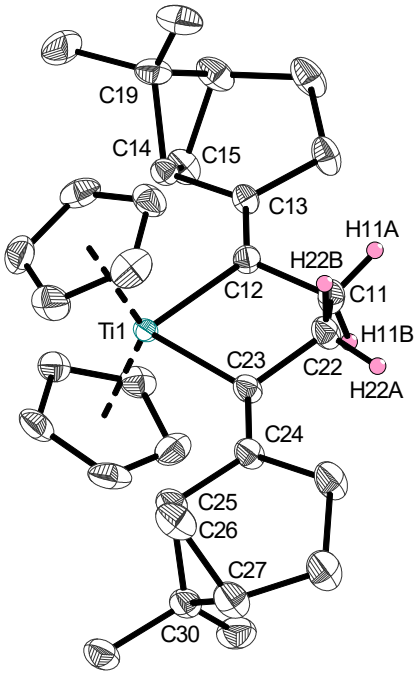

Figure S113: Molecular structures of complexes **5o-A, 5o-B**. Most hydrogen atoms are omitted for clarity. Only one of the two crystallographically independent molecules is shown. Thermal ellipsoids are drawn at the 50% probability level. Selected bond lengths (Å) and angles (deg): Ti1–C12 2.1715(14), Ti1–C23 2.1875(13), C12–C13 1.348(2), C23–C24 1.3439(19), C12–C11 1.5252(19), C11–C22 1.536(2), C23–C22 1.523(2), C23–C24 1.3439(19); C12–Ti1–C23 86.12(5), Ti1–C12–C13 132.33(10), Ti1–C12–C11 106.29(9), Ti1–C23–C24 133.45(10), Ti1–C23–C22 104.75(8), C12–C11–C22 113.84(12), C23–C22–C11 113.99(12).

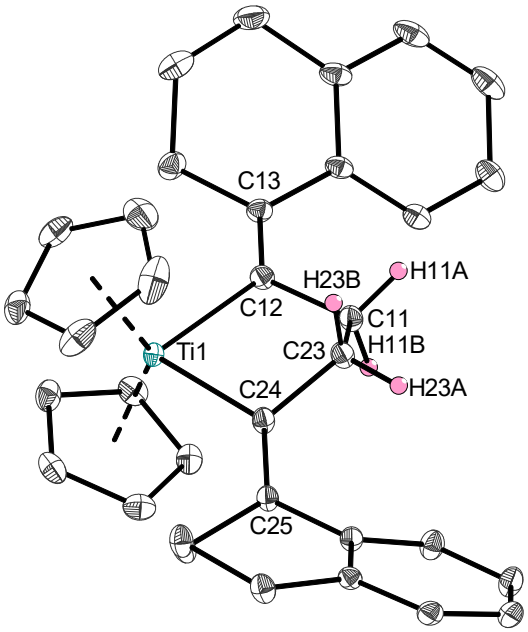

Figure S114: Molecular structure of complex **5p**. Most hydrogen atoms, solvent molecules and disorders are omitted for clarity. Only one of the four crystallographically independent molecules is shown. Thermal ellipsoids are drawn at the 50% probability level. Selected bond lengths (Å) and angles (deg): Ti1–C12 2.2047(6), Ti1–C24 2.1792(5), C12–C13 1.3552(8), C12–C11 1.5282(8), C24–C25 1.3535(8), C24–C23 1.5243(8), C11–C23 1.5314(9); C12–Ti1–C24 85.07(2), Ti1–C12–C13 131.57(4), Ti1–C12–C11 105.82(4), Ti1–C24–C25 132.44(4), Ti1–C24–C23 103.73(4), C12–C11–C23 111.88(5), C24–C23–C11 112.39(5).

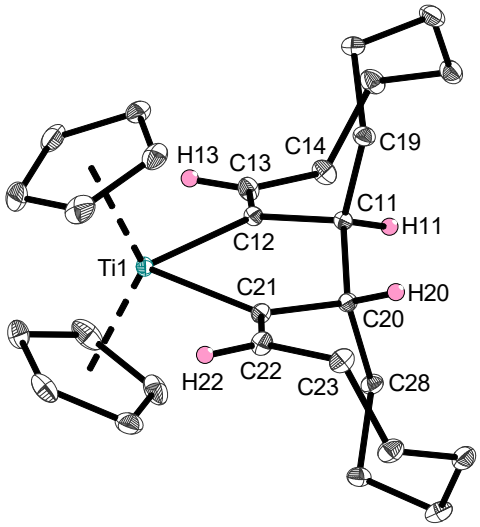

Figure S115: Molecular structure of complex **5r**. Most hydrogen atoms are omitted for clarity. Only one of the six crystallographically independent molecules is shown. Thermal ellipsoids are drawn at the 50% probability level. Selected bond lengths (Å) and angles (deg): Ti1–C12 2.2063(5), Ti1–C21 2.2047(5), C12–C13 1.3483(6), C12–C11 1.5236(6), C21–C22 1.3480(6), C21–C20 1.5228(6), C13–C14 1.5250(7), C22–C23 1.5229(7), C11–C20 1.5449(6), C11–C19 1.5465(6), C20–C28 1.5518(6); C12–Ti1–C21 79.110(18), Ti1–C12–C13 127.41(3), Ti1–C12–C11 112.52(3), Ti1–C21–C22 126.70(3), Ti1–C21–C20 112.91(3), C12–C11–C20 110.44(3), C12–C11–C19 112.72(4), C21–C20–C11 110.58(3), C21–C20–C28 113.55(4).

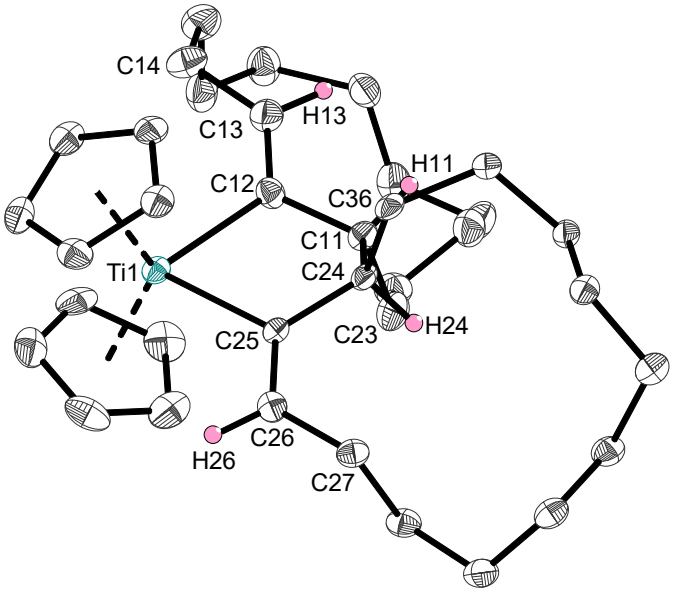

Figure S116: Molecular structure of complex **5t**. Most hydrogen atoms and disorders are omitted for clarity. Only one of the eight crystallographically independent molecules is shown. Thermal ellipsoids are drawn at the 25% probability level. Selected bond lengths (Å) and angles (deg): Ti1–C12 2.205(8), Ti1–C25 2.205(7), C12–C13 1.337(12), C13–C14 1.476(13), C25–C26 1.317(11), C26–C27 1.524(10), C12–C11 1.507(10), C25–C24 1.526(10), C11–C24 1.528(10), C24–C36 1.563(10), C11–C23 1.548(11); C12–Ti1–C25 78.4(3), Ti1–C12–C13 128.1(6), Ti1–C12–C11 112.9(5), Ti1–C25–C26 123.5(5), Ti1–C25–C24 112.4(4), C12–C11–C24 109.7(6), C12–C11–C23 115.6(7), C25–C24–C11 110.5(6), C25–C24–C36 114.5(6), C12–C13–C14 130.8(9), C25–C26–C27 125.8(7).

References

[1] V. V. Burlakov, A. V. Polyakov, A. I. Yanovsky, Y. T. Struchkov, V. B. Shur, M. E. Vol'pin, U. Rosenthal, H. Görls, *J. Organomet. Chem.* **1994**, *476*, *2*, 197-206.

[2] a) P. C. Young, M. S. Hadfield, L. Arrowsmith, K. M. Macleod, R. J. Mudd, J. A. Jordan-Hore, A.-L. Lee, *Org*. *Lett*. **2012**, *14*, *3*, 898-901; b) W. M. Sherrill, R. Kim, M. Rubin, *Tetrahedron* **2008**, *64*, 8610-8617.

[3] a) J. A. Cabezas, R. R. Poveda, J. A. Brenes, *Synthesis* **2018**, *50*, 3307-3321; b) J. Bielefeld, S. Mannhaupt, M. Schmidtmann, S. Doye, *Synlett* **2019**, *30*, 967-971; c) M. Rubin, V. Gevorgyan, *Synthesis* **2004**, *5*, 796-800; d) I. Erden, W. Cao, M. Price, M. Colton, *Tetrahedron* **2008**, *64*, 5497-5501; e) Z. Zhao, L. Racicot, G. K. Murphy, *Angew*. *Chem*. *Int*. *Ed*. **2017**, *56*, 11620-11623; *Angew*. *Chem*. **2017**, *129*, 11778-11781.

[4] L. Krause, R. Herbst-Irmer, G. M. Sheldrick, D. Stalke, *J. Appl. Cryst.* **2015**, *48*, 3-10.

[5] G. Sheldrick; A short history of SHELX. *Acta Cryst. A* **2008**, *64*, 112-122.

[6] G. Sheldrick; Crystal structure refinement with SHELXL. *Acta Cryst. C* **2015**, *71*, 3-8.

[7] O. V. Dolomanov, L. J. Bourhis, R. J. Gildea, J. A. K. Howard, H. Puschmann, *J. Appl. Cryst.* **2009**, *42*, 339-341.